Effects Of Initial Microbial Density On Disinfection Efficiency And Explanatory Mechanisms

A Thesis

Submitted to the Faculty

of

Drexel University

by

Barış Kaymak

in partial fulfillment of the

requirements for the degree

of

Doctor of Philosophy

July 2003

DEDICATIONS

To my Parents and My Brother

for Their Endless Support and Encouragement

ACKNOWLEDGEMENTS

I express my sincere gratitude to my research advisors, Dr. Charles N. Haas. I am very appreciative of his generous support and guidance that enabled me to complete this dissertation. I also thank Dr. Weilin Huang, Dr. Mehrdad Lordgooei, Dr. Joseph Martin and Gray Bulingame for serving on my Ph.D. Committee. In addition, I am grateful to Dr. Susan Kilham for her advice during proposal stage of this research. Finally, I am thankful to my fellow researchers Tim Bartrand, Dennis J. Greene, Lijie Li, Jason R. Marie and former SESEP faculty, students and staff who offered countless hours of assistance and companionship in my time at Drexel.

TABLE OF CONTENTS

LIST OF TABLES

LIST OF FIGURES

ABSTRACT

Effects of Initial Microbial Density on Disinfection
Efficiency and Explanatory Mechanisms
Barış Kaymak
Charles N. Haas, Ph.D.

Numerous water disinfection studies have reported deviations from the Chick-Watson Law, which was used to develop the *CT* tables provided by the USEPA's SWTR. Some of the modifications of the Chick-Watson Law incorporate explicit dependence on initial microbial density. In this study a series of inactivation experiments were conducted with a gram-negative (*E. coli*) and a gram-positive bacterium (*B. subtilis*) and a protozoan (*G. muris*) under various growth stages to investigate cell density effects on inactivation.

Cell density dependent inactivation was observed only during inactivation of continuous and batch cultures of *E. coli* at stationary growth phase and during inactivation of *G. muris* cysts. There was a statistically significant decrease in disinfection efficiency as the initial microbial density decreased. Inactivation of *E. coli* at exponential growth phase, vegetative cells of *B. subtilis* at exponential growth phase, and *B. subtilis* spores were independent of cell density.

Statistically significant effects of growth phase and culture growth technique on inactivation efficiency were observed in *E. coli* experiments. Exponentially growing cells of *E. coli* were more sensitive to monochloramine than stationary phase cells. Batch cultures of *E. coli* were more resistant to monochloramine than continuous cultures of *E. coli*. Similarly, spores of *B. subtilis* were more resistant than the vegetative cells at exponential growth phase.

The inactivation data of *B.* subtilis spores and *G. muris* cysts obtained in this study showed that *B. subtilis* spores can be used as a conservative surrogate to verify the removal efficiency of *G. muris* as they would overestimate CT requirement (over an order of magnitude) during the ozonation process. Comparison of survival data of *B. subtilis* spores from this study with survival data of *C. parvum* in the literature showed that *B. subtilis* spores were less resistant

at higher ozone CT. However, the relation between survivals of *C. parvum* oocysts and *B. subtilis* spores can be expressed precisely using multiple linear regression. Using inactivation data of *B. subtilis* spores, an approximately 2-log reduction of *C. parvum* by ozonation was verified. *B. subtilis* spores could be used as a simple and inexpensive surrogate for on-site disinfection process performance.

1. INTRODUCTION

Since the early history of water treatment, the primary purpose of potable water treatment has been to remove/reduce contaminants to a safe level. Among these contaminants are microbes, which caused over 500,000 diseases in 379 waterborne disease outbreaks between 1980 and 1994 in the USA (USEPA, 2001). Disinfection was one of the major advances in the drinking water industry as well as in other public health fields, to remove pathogens. The 1986 Amendments to the Safe Drinking Water Act (SDWA) required Environmental Protection Agency (EPA) to establish regulations to require disinfection of all public water supplies, within certain time frames. The requirements for microbial pathogen removal are relatively high compared to the other contaminants. Removal requirements for pathogens in all systems that use surface water or groundwater under direct influence (GWUDI) of surface water are currently regulated by the Surface Water Treatment Rule (SWTR) and the Interim Enhanced Surface Water Treatment Rule (IESWTR). SWTR and IESWTR require that all surface water treatment facilities provide a 2-log reduction of *Cryptosporidium*, 3-log reduction of *Giardia lamblia* and 4-log reduction of enteric viruses, where a 0.5-log and 2-log of inactivation of *Giardia lamblia* and enteric viruses was recommended to be achieved by disinfection, respectively. Maximum contaminant level goals (MCLGs) set for *Legionella, Giardia lamblia, Cryptosporidium,* viruses and total coliforms are zero. Unlike most other contaminants, any exposure to these pathogens, even a single viable organism, presents some level of health risk. Therefore, public water systems (PWSs) using surface water or GWUDI are required to practice disinfection profiling and benchmarking (USEPA, 2001).

The disinfection efficiency is usually expressed as log inactivation, defined as the base 10 logarithm of the ratio of viable microbial density at time T to initial viable microbial density $\left(\log(N_T/N_0)\right)$. The log inactivation of *Giardia* and enteric viruses achieved during water treatment are computed by the "*CT*" approach for disinfection profiling and benchmarking. "*CT*" is defined as the residual disinfectant concentration (C, mg/L) multiplied by the contact time (T,

minutes) between the point of disinfectant application and the point of residual measurement at the first customer (USEPA, 2001). Using the operating information (disinfectant type, temperature and pH) and the calculated daily peak hour's *CT* value, the corresponding removal rate (in log unit) can be determined for a specific organism from *CT* tables provided by the SWTR Guidance Manual (USEPA, 1990). These *CT* tables were developed using the Chick-Watson model with the parameters that give the best prediction of survival in laboratory inactivation experiments (Clark *et al*., 2002). In the Chick-Watson Model, which is used for predicting *CT*, the survival ratio of organisms is not a function of initial microbial density.

Other than exposure to pathogenic microorganism, there is another health risk associated with exposure to disinfection/disinfectant byproducts (DBPs). The disinfectants themselves may react with natural organic or inorganic materials in the source water and/or distribution systems and form harmful byproducts. The overall harm of DBPs can be smaller compared to the pathogens. However, because of the large population consuming disinfected water, the health risk due to DBPs should be taken seriously. The DBP standards are regulated under the Disinfection and Disinfectant Byproduct Rule (DBPR).

These two major concerns direct both suppliers and the regulators to ensure a proper balance between the reduction of microbial pathogens and the formation of DBPs in the drinking water. The use of appropriate design and operation criteria is important to balance the risks associated with microbial pathogens and DBPs. In this case, information on the effect of initial microbial density on disinfection efficiency becomes important.

Understanding how disinfectants inactivate microorganisms and the mechanisms of microbial resistance that can take place in the potable water environment are essential for the optimization of a disinfection process. The differences observed in disinfection kinetic studies show that more information is still needed for further understanding of the conditions that control the disinfectant-microorganism interaction. The study of the complex effects of modifying environmental factors such as density of microorganisms on disinfection kinetics is

necessary to optimize the disinfection process. This information will help to improve modeling disinfection kinetics.

The most commonly used kinetic models for estimating the rate of inactivation in drinking water are the Chick-Watson Law and Hom Model. The fundamental variables considered in the Chick-Watson Law and Hom Model are concentration of disinfectant and contact time with disinfectant for a specific organism and oxidant under constant ancillary parameters such as pH, temperature, etc. However, other than these variables, there are complex effects of other modifying environmental factors for an organism that affects the kinetics of inactivation such as growth conditions, development of resistance and so on (Barbeau *et al*., 1999; Driedger *et al*., 2001; Facile *et al*., 2000; Sommer *et al*., 1995). Due to the development of and/or changes in microbial resistance, the rate and the extent of disinfectant damage on an organism may show variations even within the same species with the same disinfectant.

Bacteria obtain a wide range of information from their surroundings to adapt themselves. They can even communicate with each other by a process called quorum sensing using diffusible non-peptide pheromones. With the help of these non-peptide pheromones they control their gene expression and regulate a variety of physiological functions in response to cell density (Decho, 1999). Also, microorganisms adapt to external stresses with different stress response mechanisms. The external stress may force the organisms to develop resistance by changing the cellular morphology, physiology and structure. As a result of these changes, alteration of the target in the cell affected by the external stress, reduction in the target access, adaptation to the environment and/or inactivation of the inhibitor may occur (Chapman, 1998). All these alterations may directly or indirectly help organisms to gain resistance to biocides. The bacteria develop several complex mechanisms of resistance, with a considerable degree of overlap, to allow them to cope with potential external stresses (Dukan *et al*., 1996). For example, the organisms in stationary phase are more resistant to disinfectants than in

exponential growth phase. The resistance is not developed in response to disinfectants, but the organism gains resistance indirectly against disinfectants as a result of adjusting to starvation.

Studies on the development of resistance to external stress as discussed above and on quorum sensing do not address the presence of any direct or indirect effects of cell population on disinfectant resistance or sensitivity. Therefore, it is important to investigate the effects of initial microbial density on disinfection efficiency for a better understanding of the disinfection kinetics. Improvement in modeling disinfection kinetics will help to balance the risks from pathogens and DBP exposure through drinking water.

2. OBJECTIVES

The "*CT*" tables provided in the SWTR Guidance Manual were based on laboratory experiments. These experiments were performed at relatively high initial microbial densities (N_o>1000 organisms/mL) with the unstated fundamental assumption that survival ratio (N/N_o) is not a function of initial microbial density (N_o) as predicted by theChick-Watson Law. Inactivation of organisms in batch experiments does not always follow the exponential decay pattern predicted by the Chick-Watson Model. There are alternative kinetic inactivation models that incorporate explicit dependence on N_o.

Microorganisms can develop microbial resistance in different ways under stressed conditions.The regulation of cell activities in bacteria in response to cell density is discussed in the later sections. There has been no study in biocide resistance and quorum sensing focusing on cell density dependent disinfection resistance. The driving mechanisms and the extent of the cell density dependence of inactivation efficiency are not known. These questions motivated the investigations of this study.

The primary objective of this study was to investigate:

- The dependency of disinfection efficiency on microbial density
    - If this dependency is valid for both bacteria (both gram-negative and gram-positive) and protozoa;
    - If this dependency is valid for organisms in dormant, stationary and exponential growth phases;
    - If this dependency is affected by culturing techniques;
- If this dependency is driven by external substances released by cells:
- Investigation of the use of bacterial spores as a surrogate for determining the hydrodynamic inactivation efficiency of ozonation of *Cryptosporidium*.

The survival data obtained in this study would also become part of the database for the inactivation of the organisms studied and the disinfectants used.

3. LITERATURE REVIEW

3.1. Mechanisms of Disinfection and Bacterial Resistance to Disinfectants

Generally, disinfectants interact with three broad regions of the bacteria cell: the cell wall, cytoplasmic membrane and cytoplasm (Denyer and Stewart, 1998). The type and mechanism of the interaction between microorganisms and disinfectants plays an important role in the kinetics of inactivation. Understanding these interactions also helps to understand the linear, concave, convex or combined behavior in semi-log inactivation curves, and therefore the kinetics of inactivation (Stewart and Olson, 1996).

3.1.1. Mechanisms of Action of Disinfectants

Cellular morphology, cellular chemical composition, extra-cellular materials and chemical properties of disinfectants are the most important factors that affect the access of biocide to cell wall, cytoplasmic membrane and cytoplasm. Sorption and partitioning at the target site are the main mechanisms of interaction. These processes can be influenced by factors such as biocide concentration, type of organism, external conditions (such as temperature, pH, humidity, etc). The target sites are generally located at the cell envelope or within the cytoplasmic region of the cell. However, the cytoplasmic membrane has a richer matrix where there are balanced interactions between phospholipid and enzymic/structural protein. The control of impermeability and the maintenance of intracellular homeostasis and vectorial transport/metabolism are ensured by cytoplasmic membrane. These critically sensitive functions and the large expanse for interaction make the cytoplasmic membrane more vulnerable to biocide attack (Denyer and Stewart, 1998). Other than cell membrane, maintenance of the folding proteins and the integrity of DNA are important for cell survival (Booth, 2002). Biocide chemistry also affects the magnitude or rate of penetration of biocide through the cell envelope and damage to the cell (Denyer and Stewart, 1998; Stewart and Olson, 1996).

Biocides from different chemical classes exist, however, the final damaging outcomes may show similarity (Denyer and Stewart, 1998). The main observed damages are:

- Uncoupling of oxidative phosphorylation and inhibition of active transport across the membrane by disruption of the transmembrane proton motive force;
- Inhibition of respiration or catabolic/anabolic reactions;
- Disruption of replication;
- Lysis;
- Coagulation of intracellular material;
- Impairment of membrane functions and resulting leakage of essential cell constituents.

The following injuries occur in microorganisms due to the action of chlorine; (1) alteration of outer membrane and leaking of critical cell components, (2) alteration of cell membrane functions, (3) destruction of enzymes and proteins by binding of sulfhydryl groups, and (4) denaturation of nucleic acid. The primary damage to the cell by chlorine is impairment of physiological functions associated with the cell membrane (Stewart and Olson, 1996).

The main actions of monochloramine on bacteria are the irreversible denaturation of proteins and nucleic acid. Unlike chlorine, there are no existing data on the modification of permeability of the cell by monochloramine (Stewart and Olson, 1996).

Similar to chlorine, ozone inactivates the microorganisms by impairment of cell permeability, destruction of protein integrity, and denaturation of nucleic acids (Stewart and Olson, 1996).

3.1.2. Bacterial Resistance to Biocides

Three general classes of resistance mechanisms are seen in bacteria: alteration of the target (either its binding site or of its relevance to the cell's metabolism), reduction in target access, and inactivation of the inhibitor (Chapman, 1998). For example, the damage to mRNA might be significant, however, the cells can easily escape consequences of damage simply by the natural process of turnover (Booth, 2002). In addition, cells can use a variety of mechanisms, including export systems, detoxification enzymes and basal expression of repair systems to limit

the damage to nucleic acids and proteins that would arise from chemical stresses (Booth, 2002). Some bacteria can reduce the target access by changing the structure of the cell such as forming endospores (Russell, 1995).

In potable water, microorganisms may show intrinsic, acquired or both type of resistances (Bower and Daeschel, 1999; Russell, 1995; Stewart and Olson, 1996). Intrinsic resistance is the natural chromosomally controlled property of the organisms that prevents or reduces the action of the biocide. Acquired (i.e., cell-mediated) resistance arises from changes in the genetic material and/or physiological characteristics of the cell to survive under external stress conditions (Russell, 1995; Stewart and Olson, 1996). This type of resistance, resistance as result of change in the genetics of the cell, will be effective on young and exponentially growing cells, therefore it will not be described in detail here.

3.1.2.1. Intrinsic Resistance

The intrinsic resistance of the microorganisms is due to the natural structure of the cell (Russell, 1995; Russell, 1999). Before reaching the target site, the biocide must first pass through the outer layers of the cell. These natural barriers control the permeability, therefore, the uptake of biocide. The structure, nature and composition of the outer layer depends upon the organism in question (Russell, 1995). For example, gram-negative organisms are generally more resistant to disinfectants than gram-positive organisms (Russell, 1999). Bacterial spores are the most disinfectant resistant types of bacteria and require a higher concentration of biocide for inactivation (Russell, 1995).

In general, the basic material of cell walls of nonsporulating gram-positive bacteria is peptidoglycan, which forms a thick, fibrous layer. The peptidoglycan layer is not homogenous and contains other molecules such as teichoic and teichuronic acids and lipids. The wall of gram-positive bacteria may not necessarily form a barrier to entry of antibacterial substances as does the cell wall of gram-negative bacteria. This is probably the main reason for the difference in biocide resistance of these two types of bacteria. An increase in the lipid content of the cell

wall enhances the resistance in gram-positive bacteria to antibacterial agents (Russell *et al*., 1999).

Gram-negative bacteria are of considerably different composition than gram-positive bacteria, mainly on the lipid content of the cell envelope. Gram-negative bacteria have an additional lipopolysaccharide (LPS) over-layer compared to gram-positive bacteria (Russell, 1995; Russell, 1999). The cell surface of gram-negative bacteria is hydrophilic. Low molecular weight hydrophilic molecules may readily pass through the cell envelope via the aqueous porins, but LPS molecules in the outer membrane of gram-negative bacteria inhibit the access of hydrophobic molecules to the cell interior. Also, differences in LPS composition and cation content of the higher membrane are related to the resistance of bacteria to some biocides (Russell, 1995).

Bacterial spores are invariably the most resistant of all types of bacteria. They have an additional spore coat, which makes them more resistant to the action of some agents. A schematic diagram of a 'typical' bacteria spore is given in Figure 3.1 (Russell, 1995). The outer and the inner spore coats are mainly composed of protein with small amounts of complex carbohydrates and lipid. The cortex is composed principally of peptidoglycan and the core of bacterial spore contains protein, DNA, RNA, dipicolinic acid and divalent cations (Russell, 1995). The resistance of spores may depend on the bacterial species and strain, on the method of production, preparation and storage, on the conditions used during a study and on the cellular stage of development.

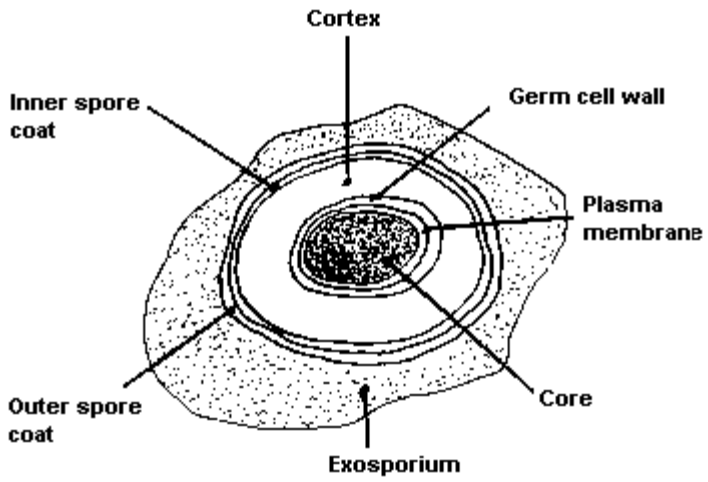

Figure 3.1: A typical bacterial spore (not drawn to scale, www.bmb.leeds.ac.uk/.../ icu8/ introduction/bacteria.html).

3.2. Microbiology of the Organisms Studied

3.2.1. Microbiology of *Giardia muris*

Giardia muris is a flagellated intestinal protozoan. Protozoa are unicellular eukaryotes that have characteristic organelles (Maier *et al*., 2000). The source of the *muris* group is rodents and birds and they transfer to the environment through fecal contamination. They exist in two forms in their life cycle. They exist either in environmentally resistant cyst form or in active trophozoite form. The life cycle of *Giardia* is given in Figure 3.2. The cyst formation takes place as the organism move down through the colon. During cyst formation the cytoplasm becomes condensed and cyst wall is secreted. The cyst wall allows them to survive outside the host and in the environment for long periods of time at reduced temperatures and reduced available nutrient sources. During maturation of the cyst, the internal structures of the cyst are also doubled. That is why two trophozoites are produced from the excystation of a single cyst. The cyst starts excystation following ingestion and produces trophozoites again. The excystation can also occur in appropriate culture medium (Garcia, 2001).

The trophozoites are teardrop shaped, usually 10 to 20 µm in length and 5 to 15µm in width. They have four pairs of flagella, two nuclei, two axonemes and two slightly curved bodies called the medians (Garcia, 2001).

The cysts are usually round or oval in shape and measure 11 to 14 µm in length and 7 to 10 µm in width. They contain four nuclei, axonemes and median bodies (Garcia, 2001).

G. muris is non-pathogenic to humans and it has been successfully used in disinfection studies (Haas *et al*., 1995; Owens *et al*., 2000).

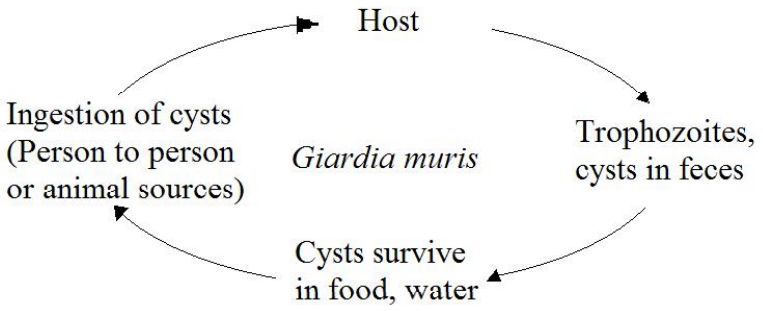

Figure 3.2: The life cycle of *Giardia* (Garcia, 2001).

3.2.2. Microbiology of *Escherichia coli*

Escherichia coli is a short gram-negative, non-sporing and usually peritrichous and fimbriate bacillus. *E. coli* can have a capsule or a microcapsule. Few strains of *E. coli* produce profuse polysaccharide slimes (Sussman, 1985). *E. coli* belongs to the family Enterobacteriaceae and it is the only member of genus *Escherichia*. *E. coli* is a facultative anaerobe and it grows readily on simple culture media and synthetic media with glycerol or glucose as the energy and carbon source. The optimum growth temperature for *E. coli* is 37ºC . *E. coli* is found in the gastro-intestinal tract, and principally the bowel, of mammals and birds. They can also be found in nature as a result of fecal contamination (Sussman, 1985).

Non-pathogenic strains of *Escherichia coli* have been used by biochemists and geneticists for elucidating general biological phenomena such as metabolic pathways, protein and nucleic acid synthesis, enzyme induction and repression, and so on. It a well studied microorganism. The strain of *E. coli* used (ATCC 13706) in this study is a non-pathogenic organism. It has been successfully used in disinfection studies (Haas *et al*., 1995; Hunt and Mariñas, 1999; Kouame and Haas, 1991). Also, control of gene expression in response to cell density (quorum sensing mechanism) has been observed in this organism (Gruenheid and Finlay, 2000).

3.2.3. Microbiology of *Bacillus subtilis*

Bacillus subtilis has been highly studied compared to other prokaryotic organisms. *B. subtilis* belongs to the family *Bacillaceae*, spore-forming bacteria. It is a gram-positive, rod shaped, aerobic endospore-forming bacteria. The primary habitat of *Bacillus* species is soil or rotting plant materials. They are transferred to foods, animals, marine and fresh water habitats and other associated environments (Sonenshein *et al*., 1993).

This organism undergoes a differentiation process to form resistant structures called endospores or simply spores, when nutrients are exhausted, and/or environmental stress exists (Edward, 2001). Spores are complex multi-layered structures that contain a spore coat and a cortex. The spore coat possesses barriers that limit biocide penetration into the cortex. The cortex contains calcium dipicolinate, but little water, which contributes to its ability to survive under adverse conditions. Inside the spore (in the core) there exists protein, DNA, RNA, dipicolinic acid and divalent cations (Russell, 1995). The development of bacterial spores from vegetative cells can be divided into 7 stages (Table 3.1).

Table 3.1: Stages of sporulation process.

Stage	Event
0	Vegetative cell
1	Pre-sporulation phase: DNA as an axial filament
2	Septation:asymmetric cell formation
3	Engulfment (encystment) of fore spores
4	Cortex formation between inner and outer forespore membranes commences
5	Synthesis of spore coats and DPA: uptake of Ca^{2+}
6	Spore maturation: coat material becomes more dense, refractility increases
7	Lysis of mother cell and liberation of mature spore

Stages from 4 to 7 are the most important in terms of development of biocide resistance. The resistance development stages may be different for different types of biocides. For example, development of resistance to toluene is an early event whereas lysozyme resistance development is a later event (Russell, 1995). The biocide resistance process is reversible. Despite extreme dormancy, spores maintain alert sensory mechanisms (Atrih and Foster, 2002). When the external environment becomes favorable again, the protective layers break down and the spores germinate back to vegetative cells (Edward, 2001; Russell, 1995).

B. subtilis is considered to be non-pathogenic (Sonenshein *et al*., 1993) and it has been successfully used in disinfection studies (Barbeau *et al*., 1999; Driedger *et al*., 2001; Facile *et al*., 2000; Sommer *et al*., 1995).

3.3. Cell Density Related Cellular Activities

3.3.1. Regulation of Gene Expression by Cell-to-cell Signaling

Bacteria obtain a wide range of information including physical cues such as temperature and viscosity, inorganic cues such as pH, oxygen and ionic concentrations, and various organic chemical cues from their surroundings to successfully adapt to changing natural conditions. In this way, organisms can respond to the external environment and modulate gene expression accordingly (Decho, 1999). Many bacterial genera within the proteobacteria communicate with each other and other organisms by diffusible non-peptide pheromones called autoinducers. These extra-cellular autoinducers are mainly comprised of homoserine lactone (HSL) rings

conjugated to acyl side chains of variable length, oxidation state, and saturation (Winans and Zhu, 2000; Zambrano and Kolter, 1996). Numerous gram-negative bacteria produce one or more *N*-acyl-homoserine lactones (acyl-HSLs) to control their gene expression and to regulate a variety of physiological functions in response to cell density (Bassler, 1999; Gray, 1997; Gruenheid and Finlay, 2000; Kaprelyants and Kell, 1996; Lazazzera, 2000; Mah and O'Toole, 2001). This population density-dependent mechanism is known as quorum sensing. Many of the quorum sensing systems are composed of two proteins, one encodes the autoinducer synthase and the other encodes a transcriptional activator protein that is responsible for detecting the autoinducer and induction of the expression of the appropriate output (Bassler, 1999; Winans and Zhu, 2000).

The acyl-HSL regulatory system was first identified in the marine symbiont *Vibrio fischeri* (Engebrecht *et al*., 1983). The LuxI protein in this organism synthesizes the autoinducer (3-oxo-C6-HSL). The second protein LuxR is a positive regulator of the operon, which is responsible for encoding the autoinducer synthase (*luxI*), the luciferase proteins and the other proteins that synthesize luciferase substrates. The autoinducer is a low molecular weight, often diffusible small signal molecule. It is generally thought to diffuse readily across the cell envelope causing intracellular concentrations similar to extra-cellular concentrations These molecules accumulate in their surroundings as the cell density increases. At low cell density, therefore, low autoinducer concentration, the bioluminescence operon is weakly expressed. However, when the concentration of the autoinducers exceeds a threshold level, they start to bind the LuxR and the bioluminescence operon is strongly expressed (Bassler, 1999; Coulthurst *et al*., 2002; Gray, 1997). Under this condition, bacteria also synthesize a greatly increased level of autoinducer, resulting in a positive feedback loop (Winans and Zhu, 2000).

The families of proteins, which synthesize autoinducer type pheromones (e.g. LuxI *in V. fisheri*, RhlI in *Pseudomonas aeruginosa*) appear to carry out two reactions: formation of HSL ring and acylation of amine of HSL (Winans and Zhu, 2000). LuxR type proteins serve as an

autoinducer receptor and an autoinducer-dependent transcriptional regulator as mentioned before. It is thought that these proteins have two modules for these two functions. The amino terminal module binds the autoinducers and mediates multimerization. The second module, carboxyl terminal module binds particular DNA sites near target promoters and also makes stimulatory contacts with RNA polymerase (Winans and Zhu, 2000). In some of the gram-negative organisms this mechanism may have additional and/or different components and may be more complex. For example, in *Pseudomonas aeruginosa,* the quorum sensing system has a third protein RsaL which inhibits the transcription of *lasI* (autoinducer synthase). This organism expresses a second pair of LuxR-LuxI type proteins consisting of the RhlI and RhlR proteins and the pheromone C4-HSL. These protein systems regulate production of rhamnolipid surfactant and the *rpoS* stationary phase sigma factor (Winans and Zhu, 2000). These two protein systems function in tandem to control the expression of virulence factors (Bassler, 1999). Davies *et al*., (1998) studied the involvement of these cell-to-cell signals on bacterial biofilm development and the *lasI-rhlI* mutant *P. aeruginosa*, which can make neither of the quorum sensing signals, failed to form normal biofilms.

In some organisms a second quorum sensing system has been identified that functions in parallel with signaling system-1 to control cell density dependent expression. In *Vibrio harveyi*, a gram-negative bioluminescent marine bacterium, the quorum sensing system-1 is composed of sensor-1 and it responds to autoinducer-1. Autoinducer-1 is an HSL produced by most gram-negative bacteria. The second system is composed of a sensor and a cognate autoinducer (autoinducer-2), but it is a non-species-specific system. The structure of autoinducer-2 is not known, however, it is known that autoinducer-2 is a unique "universal" signal that can be used by a variety of bacteria for communication among and between species (Anand and Griffiths, 2002).

Quorum sensing is also an important step in starvation sensing. Both processes co-regulate each other. In one study, mutants blocked in steps prior to synthesis of homoserine (HS)

did not induce σ^s, a sigma factor that is maximally active under conditions of starvation, unless they were provided with HS or HSL (Zambrano and Kolter, 1996). Similarly, *Pseudomonas aeruginosa, Rhizobium leguminosarum* and *Vibrio* sp. Strain S14 stationary phase transcription factors were regulated by quorum sensing. On the other hand in *Vibrio fischeri, Ralstonia solanacearum* and *Myxococcus xanthus,* it has been observed that the production of quorum sensing signaling molecule requires σ^s, a sigma factor that is maximally active under conditions of starvation. In these organisms, cell-to-cell signaling molecules are regulated by starvation (Lazazzera, 2000). Co-regulation of quorum sensing and starvation sensing pathways are important since transition to stationary growth phase results in increased resistance to a number of environmental stresses.

Some of the other observed behavioral and physiological cell functions regulated by quorum sensing signals are luminescence, conjugation, production of secondary metabolites (including antibiotics), virulence, and mating (Coulthurst *et al*., 2002; Gray, 1997).

There also exist a number of processes in gram-positive bacteria in response to cell population density (Bassler, 1999). In the past decade, many of the studies have shown that some of the bacterial activities such as formation of endospores, release of diverse antibiotics, transition to stationary phase, competence for DNA uptake, virulence and microcin production occur preferentially at high population densities and are simulated by the exchange of chemical signals between bacteria (Winans and Zhu, 2000).

Gram-positive bacteria have neither HSL nor LuxI/LuxR type signaling circuits. Gram-positive bacteria have a two component common signaling substructure similar to gram-negative LuxI/LuxR signaling. Also, as in the case of gram-negative organisms, signaling mechanisms of gram-positive bacteria may have variations in type and complexity of additional regulatory factors. For example, *Bacillus subtilis* imports naked DNA during the transition from logarithmic phase to stationary phase which requires expression of approximately 40 genes. The regulation of these genes is controlled by two different peptide pheromones, CSF (competence

and sporulation factor) and ComX. Both of the peptides influence the phosphorylation state of the response regulator ComA which regulates several operons including encoding of the key regulator of competence genes (Winans and Zhu, 2000). These two processed peptide signals help bacteria to choose between competence for DNA uptake and sporulation. The extra-cellular peptide ComX, activates the two component system ComA~P to allow the transition to the transformable state. The other peptide signal, CSF promotes competence development when it is at low densities. At high densities of CSF competence is inhibited and sporulation is induced (Bassler, 1999).

The cell-to-cell signaling mechanism in bacteria helps bacteria to adapt and respond to external stresses resulting from a certain cell population of its own kind or possibly some other species (Surette and Bassler, 1998). For example, *B. subtilis* has two classes of genes regulated by quorum sensing, where one of them is more effective when its own concentration is high and the other one is less effective at high cell densities. These genes are involved in utilization of alternate carbon and energy sources and modification of the cell surface. As these genes are maximally expressed under conditions of high cell density and starvation, these genes play a role in transition stationary phase (Lazazzera, 2000).

There are studies suggesting that living cells of protozoan ciliates excrete signaling substances. Ekelund *et al*., (2002) suggest that encystment is a cell density dependent process driven by a signaling substance excreted by the ciliates. The study of Christensen *et al*. (2001) indicates that *Tetrahymena thermophila* has receptor and signaling transduction systems which when activated, prevent cell death and support poliferation in low-density cultures. However, neither of these studies investigated the mechanisms of any cell density dependent activity. In addition, there does not appear to be any previous work that looked at on density effects on inactivation kinetics.

3.4. Growth Condition and Medium Effects on Microbial Resistance

Bacteria have evolved adaptation mechanisms to protect themselves against challenges of changing environment and to facilitate survival under conditions of stress (Abee and Wouters, 1999). Any deviation from optimal growth condition that results in a reduced growth rate can be defined as a stress (Booth, 2002; Storz, 2000). In nature, organisms are rarely in optimal growth conditions. Therefore, it is important to study the effects of a changing environment on efficiencies of inactivation.

Studies have observed that organisms grown under nutrient limited conditions are phenotypically different than the ones grown in nutrient rich environments (Hengge-Aronis, 2000; Ishihama, 1997; Russell *et al*., 1999; Sterkenurg *et al*., 1984). Sterkenurg *et al*., (1984) observed changes in protein structure of the envelope of *Klebsiella aerogenes* when grown under potassium-, carbon-, sulfur- and phosphorous-limited conditions. Also, other nutrient limitations may lead to alterations of capsule presence or composition (Russell, 1995), lipopolysaccharide components, cell membrane lipids or cell wall components (Stewart and Olson, 1996). In most of the cases, nutrient limitation affected the growth rate. Therefore, nutrient limitation is also a stress condition for cells. When a bacterial culture becomes starved for a particular nutrient, it slows down its growth, or stops growing (Mah and O'Toole, 2001). This is almost a universal survival strategy (Booth, 2002). The survival strategy for some gram-positive organisms, such as *Bacillus subtilis*, is differentiation to spores without reproduction, whereas other bacteria such as *E. coli* enter into stationary phase (Abee and Wouters, 1999).

It has been observed that in some organisms the sensitivity to antibacterial agents increases as growth rate increases (Gilbert and Brown, 1980). Some of the stationary phase organisms, where the net growth rate is approximately zero, are more resistant than the ones at exponential phase to some of the antibacterial agents (Datta and Benjamin, 1999; Gilbert and Brown, 1980; Jørgensen *et al*., 1999; Lazazzera, 2000; Mah and O'Toole, 2001; Stewart and Olson, 1996). It was observed that some of the organisms have higher resistance to antimicrobial

agents at stationary phase (Table 3.2). It has been known for a long time that stationary phase cells are morphologically and physiologically distinct from rapidly growing cells (Hengge-Aronis, 2000; Ishihama, 1997). Numerous alterations in cellular physiology and morphology to enhance survival under cellular stress, other than starvation, have been observed in bacteria. Many of these changes occur in cell-wall components, cell-membrane lipids, outer-membrane proteins and fimbriae. Cell surface changes usually alter the permeability. Changes in the permeability of the membrane seem to be a common result of many of these studies. Permeability of the cell envelope is an important factor in antibacterial resistance (Gilbert and Brown, 1980; Sterkenurg *et al*., 1984; Stewart and Olson, 1996). The transport of the chemicals into the cell is controlled by the cell envelope. It is known that changes in permeability limit the influx of chemicals including disinfectants through the cell membrane. This way, the access of disinfectants to target sites is limited and this results in higher resistance relative to those grown in a nutrient rich environment where the organism has a higher growth rate. When the permeability of organism cells is increased, they become more sensitive to anti-microbial agents (Stewart and Olson, 1996). Also, if a bacterium changes from its rod shape into a smaller spherical shape to reduce the cell surface area to volume ratio, which favors the organism in nutrient limited conditions, this reduces the contact area for biocides.

Table 3.2: List of some of the organisms that show higher resistance to antimicrobial agents at stationary phase.

Organism	Anti-microbial Agent	Source
E. coli	Antibiotics (CGP 17520 or cefonicid)	Tuomanen *et al*., 1986
E. coli	HCl (pH 2-3)	Arnold and Kasper, 1995; Benjamin and Datta, 1995; Datta and Benjamin, 1999
E. coli	Chlorine	Saby *et al*., 1999
Listeria monocytogenes	Lactic acid (pH 3.5)	O'Driscoll *et al*., 1996
Mycobacterium avium	Chlorine	Taylor *et al*., 2000
Pseudomonas aeruginosa	Acetic Acid and Glutaraldehyde	Carson *et al*., 1972
Pseudomonas syringae	H_2O_2	Klotz and Hutcheson, 1992
Pseudomonas putida	H_2O_2	Givskov *et al*., 1994

The alterations in cellular physiology and/or morphology can be due to either lack of nutrients in the environment for synthesis of certain cellular materials or as an adaptation to external conditions (Hengge-Aronis, 2000). For example, under Mg limited conditions, the normal outer membrane of cells stabilizing Mg^{+2} bridges are likely to be replaced by polyamides, resulting in reduced sensitivity to ion chelators and inhibition of biocide uptake by cations (Russell *et al*., 1999). Resistant strains can be developed due to other environmental stress conditions such as pH and temperature. It has been observed that naturally occurring *Pseudonomas aeruginosa* cells grown at 25^0C were more resistant then the ones grown at 37ºC . Similarly, in the study of Berg *et al*., (1982), *E. coli* cultures grown at 37ºC showed higher sensitivity to chlorine dioxide than those grown at 25^0C. *Bacillus subtilis* sporulated at 50^0C was observed to be more resistant than the spores produced at 37ºC (Russell *et al*., 1999).

The cellular stresses including high osmolarity, high or low temperature, acidic pH and oxidative stress result in accumulation of σ^s, a sigma subunit of RNA polymerase, which acts as the master regulator of this response (Dukan *et al*., 1996; Eisenstark, 1998; Hengge-Aronis, 2000; Jørgensen *et al*., 1999). There are more than 50 σ^s-controlled genes conferring stress tolerance, mediating structural and morphological rearrangements, and redirecting metabolism, such as *dps* (protecting DNA), *katE* (catalase), *otsA/otsB* (general stress protectant and *xthA* (DNA repair) (Hengge-Aronis, 2000; Jørgensen *et al*., 1999). It has been reported that the *rpoS* gene, which codes for a homologue of an *Escherichia coli* stationary phase σ factor is controlled by quorum sensing (Jørgensen *et al*., 1999; Whiteley *et al*., 2000; Yamada *et al*., 1999; Zambrano and Kolter, 1996). The coregulation between quorum sensing mechanism and induction of a sigma factor was already discussed for some strains of organisms in Section 3.3.1.

The genes and cellular activities that are regulated by RpoS include: (a) anti-oxidant enzymes, (b) DNA repair enzymes, (c) DNA binding proteins, (d) DNA bending proteins, (e)

cell morphology, (f) response to antibiotics, (g) virulence in interaction with foreign cells, (h) synthesis of a number of additional components, especially those needed for survival during long and harsh periods of dormancy, (i) membrane transport functions (Eisenstark, 1998). As mentioned before the *rpoS* gene is controlled by quorum sensing in some organisms (Jørgensen *et al*., 1999; Whiteley *et al*., 2000; Yamada *et al*., 1999; Zambrano and Kolter, 1996) and all of the above gene regulations may be directly or indirectly affected by cell density.

Another important aspect concerns growth medium and/or the condition in laboratory experiments that are used for growing bacteria. Generally, continuous and batch culture techniques are both used for growing bacteria (Russell *et al*., 1999). Although the batch culture technique is the predominantly used method in disinfection studies, it produces a heterogeneous population of cells with different physiological ages. Batch cultures are closed systems where the metabolic activities of bacterial populations change as the nutrients are utilized. In batch culture, the cells grow rapidly at the beginning and slow down as the nutrient concentration within the culture is depleted. However, in a chemostat, constant growth rate can be achieved and the growth rate can be controlled by dilution rate (Whiteley *et al*., 1997).

Even with the above mentioned disadvantages of batch cultures, far more extensive investigations have been undertaken with batch-grown cultures. Batch techniques are relatively easier and inexpensive compared to continuous culture techniques. In disinfection studies, the batch culture-grown organisms are commonly used (Barbeau *et al*., 1999; Gyürèk and Finch, 1998; Haas *et al*., 1995; Kouame and Haas, 1991).

3.5. Disinfection Kinetics

Five commonly observed curves on semilog plots of survival during the inactivation of microorganisms are linear curves, curves with a shoulder (convex), curves with a tailing (concave), S shape (tailing-off + shoulder) and inverted S shape (shoulder + tailing-off) (Anotai, 1996; Haas and Finch, 1999; Stewart and Olson, 1996; Xiong *et al*., 1999). Initial studies on kinetics of inactivation have considered: (1) chemical species and concentration of disinfectant,

(2) contact time with the residual disinfectant, (3) temperature and pH, (4) type of microorganisms, as fundamental variables of inactivation kinetic models (Stewart and Olson, 1996). Later studies have been proposed to describe the nonlinear inactivation behavior. Some of these models were based on a best-fit mathematical model whereas some of them were based on assumed inactivation mechanisms (Haas and Finch, 1999; Stewart and Olson, 1996).

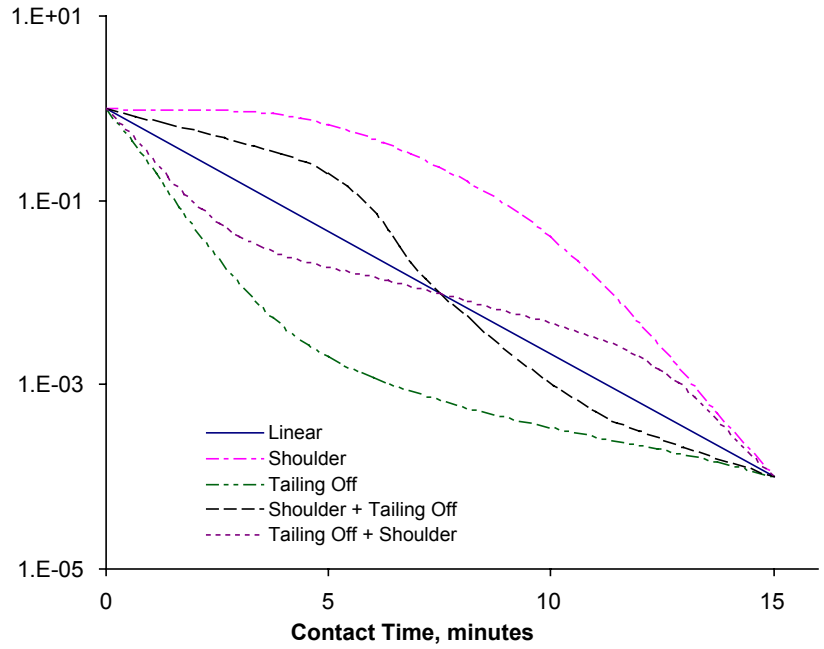

Figure 3.3: Typical microbial survival curves.

The major assumptions used in derivation of a kinetics inactivation model are: (1) no back mixing; (2) uniform dispersion of organisms and disinfectant molecules; (3) sufficient mixture to ensure liquid diffusion is not rate limiting; (4) constant temperature and pH during the contact time (Gyürèk and Finch, 1998).

3.5.1. Chick's Law

The earliest inactivation kinetic approach was used by Chick (1908) who defined inactivation kinetics as first order.

$$r_d = \frac{dN}{dt} = -kN \tag{1.1}$$

In Equation 1.1, r_d is the disinfection rate (number of organisms inactivated per unit volume per unit time) and N is the concentration of viable organisms. In a batch system, this results in an exponential decay in organisms, because the rate of inactivation equals $\partial N/\partial t$, assuming that the rate constant, k, is actually constant.

Under constant disinfectant concentration (i.e., when there is no disinfectant decay and demand), Equation 1.1 can be integrated to obtain the relationship in batch systems.

$$\ln S = \ln \frac{N}{N_o} = -kCt$$

3.5.2. Chick-Watson Law

Watson (1908) proposed Equation 1.2 where the pseudo-first-order reaction rate assumption is not used but related the rate constant of inactivation, k, to the disinfectant concentration, C:

$$k=k`C^n \tag{1.2}$$

In Equation 1.2, n is termed the coefficient of dilution, and $k`$ is presumed independent of disinfectant and microorganism concentration. The Chick-Watson Law defines inactivation as a function of disinfectant concentration and contact time. The rate equation for the Chick-Watson Law is

$$r_d = \frac{dN}{dt} = -k' C^n N \tag{1.3}$$

From the Chick-Watson Law, when C, n, and k are constant (i.e., there is no disinfectant demand and decay), the above rate law may be integrated so that in a batch system the following relationship arises:

$$\ln S = \ln \frac{N}{N_o} = -k'C^n t \tag{1.4}$$

In Equation 1.4, *S, N* and N_o are the survival ratio, the concentrations of viable microorganisms at time t and time 0, respectively. When disinfectant composition changes with time, or when a configuration other than a batch (or plug flow) system is used, the appropriate rate laws characterizing disinfectant transformation along with the applicable mass balances must be used to obtain the relationship between microbial inactivation and concentration and time (Haas and Karra, 1984).

This model is currently used in the SWTR to calculate the disinfection credit, where the parameters are estimated according to laboratory experiments (Clark *et al*., 2002).

3.5.3. Hom Model

One flexible model for describing complex inactivation kinetics was originally developed by Hom (1972), although a simplified version was in use much earlier (Fair *et al*., 1948). In earlier work, Fair *et al*., (1948) used a model of the form of Equation 1.5 with $m = 2$ to analyze *E. coli* inactivation by free and combined chlorine. In the original presentation, for a batch system in which disinfection residual was held constant, inactivation was a nonlinear function of *C* and *t*. The Hom equation can be derived from the following differential rate expression (Haas and Joffe, 1994):

$$r_d = \frac{dN}{dt} = -mN(kC^n)^{1/m}\left[-\ln\left(\frac{N}{N_0}\right)\right]^{(1-1/m)}$$

The following equation describes the survival ratio, *S*, versus time, *t*, with parameters *k*, *n*, and *m* in a batch system with constant *C*:

$$\ln S = \ln\left(\frac{N}{N_o}\right) = -kC^n t^m \qquad (1.5)$$

If $m = 1$, Equation 1.5 becomes the Chick-Watson relationship (Equation 1.4). Concave and convex curves are obtained in semi-log plots of survival against time and/or CT product when $m > 1$ and when $m < 1$, respectively (Haas and Karra, 1984). This relationship was found to give satisfactory results when applied to prior studies on inactivation of *Giardia*

(Anmangandla, 1993), *Cryptosporidium* (Driedger *et al*., 2000), aerobic spore-forming bacteria (Barbeau *et al*., 1999), and HPC bacteria (Pernitsky *et al*., 1995).

3.5.4. Rational Model (Power Law)

This model is a generalized power law kinetic formulation. This model was apparently first used to describe ozone inactivation of virus by Majumdar *et al*., (1973) and is written as:

$$r_d = \frac{dN}{dt} = -kC^n N^x \tag{1.6}$$

Equation 1.6 can be integrated to yield

$$\ln S = \ln\left(\frac{N}{N_o}\right) = \frac{-1}{x-1}\ln[1+(x-1)kC^n t N_o^{x-1}]$$

Unlike the previously described models, this model has an additional independent variable N_0, in addition to time and disinfectant concentration, which represents the viable microbial concentration dependency of survival.

An example of the use of the Rational Model is that of Roy *et al*., (1981). They applied this model to continuously stirred tank reactor studies on the inactivation of poliovirus 1 with ozone in demand-free systems. This study obtained a best-fit "*x*" value of 0.69, which shows a non-linear dependency of inactivation efficiency on viable microbial density. This model is capable of describing shoulders ($x < 1$) or tailing-off ($x > 1$) behavior. It reduces to the Chick-Watson model when *x* is equal to 1.

3.5.5. Hom Power Law (HPL)

This kinetic model was developed by Anotai (1996). This model includes subsets of both the Hom and Rational models and incorporates the parameters of both models (*k, m, n,* and *x*). This model also includes viable microbial density as an independent variable. In a differential form, the rate of inactivation can be defined as:

$$r_d = \frac{dN}{dt} = mkC^n N^x \left[\frac{\left\{ \left(\frac{N^{1-x}}{N_0^{1-x}} - 1 \right) N_0^{1-x} \right\}^{1-\frac{1}{m}}}{(x-1)^{1-\frac{1}{m}} (kC^n)^{1-\frac{1}{m}}} \right] \tag{1.7}$$

Under demand-free conditions in a batch system, survival can be written as:

$$\ln S = \ln \frac{N}{N_0} = -\frac{\ln\left[1 + N_o^{(x-1)}(x-1)kC^n t^m\right]}{(x-1)}$$

where the parameters *k, m, n* and *x* are the same parameters as those from the Hom and Rational models. This model is a more generalized form of the previous models discussed before. Equation 1.7 can be reduced to Equation 1.1, the simplest model, by setting *x, n* and *m* to 1 (Haas and Finch, 1999).

3.5.6. Series Event Model

This model depicts inactivation as series of events occurring in a discrete stepwise fashion. The rate of passing from one event to another is first order with respect to disinfectant concentration. An organism survives until it reaches an event level smaller than the threshold and is completely inactivated when an event level exceeds the threshold (Gyürèk and Finch, 1998; Severin *et al*., 1984). The rate of destruction of κ^{th} site in an organism is given by

$$\frac{dN_\kappa}{dt} = kCN_{\kappa-1} - kCN_\kappa$$

Solving for $\kappa=0$ to $\kappa=l$-1 gives the log fraction of organisms surviving, those not exceeding the threshold event *l*-1 at the end of the contact time.

$$\ln \frac{N}{N_o} = -kCt + \ln\left(\sum_{\kappa=0}^{l-1} \frac{(kCt)^\kappa}{\kappa!} \right)$$

Where κ is the event level, *l* is the threshold event

3.5.7. Multiple-target Model

This model was developed for inactivation by radiation other than ultraviolet and current knowledge on ultraviolet radiation does not support this model. However, this model is still used due to its simple logic, mathematics and ability to fit batch data (Severin *et al*., 1983). This model is based on the assumption that a particle contains a finite number (n_c) of discrete critical targets, all of which must be hit once for complete destruction of the particle. The destruction rate of the target is described by first order kinetics:

$$\frac{dq}{dt} = -kCq$$

where, q is concentration of targets (#/mL).

Since the number of particles is finite, the number of available targets decreases as inactivation progresses. Therefore, the probability of hitting the next target decreases as the reaction proceeds. A binomial probability of zero gives the probability of a specific target surviving,

$$P(0) = \frac{q}{q_c}$$

where, q and q_c are the concentrations of targets at time t and critical concentration of targets, respectively (#/mL). The probability of a particle to survive with n_c critical targets would be

$$\frac{N}{N_0} = \left[1 - \left(1 - P(0)\right)^{n_c}\right]$$

The term particle is used because the targets to be hit may be on a single organism or on a clump of organisms, but due to enumeration methods used, it is not possible to differentiate whether the particle is a “clump” or an “organism” (Severin *et al*., 1983).

The probability of survival of a particle with n_c critical targets is given by (Gyürèk *et al*., 1999):

$$\log\frac{N}{N_o} = \log(P_i) = \log\left[1-\left(1-e^{-kCT}\right)^{n_c}\right]$$

where, k in this model, unlike the previous models, has units of L/(mg.min).

3.5.8. Modified Multiple-target

This model has the same basic assumptions as the Multiple-target Model. The only modification is that, in the Modified Multiple-target Model the destruction rate of particles is described by non-first order kinetics whereas in the Multiple-target Model it was described by first order kinetics:

$$\frac{dq}{dt} = -kC^n q$$

To the authors' knowledge, the Modified Multiple-target Model has never been applied to describe disinfection kinetics. The commonly used kinetic models such as Chick-Watson, Hom Model and Power Law all incorporate non-first order dependence on disinfectant concentration. Therefore, it is assumed this addition will improve the ability of the model to describe inactivation kinetics more efficiently.

The probability of survival of a particle with n_c critical targets under disinfectant demand-free conditions is,

$$\log\frac{N}{N_o} = \log(P_i) = \log\left\{1-\left[1-\left(e^{-kC^n t}\right)\right]^{n_c}\right\} \qquad (1.8)$$

This model reduces to the Multiple-target Model when "*n*" is equal to 1.

The models presented here are the most commonly used inactivation models in the literature except Modified Multiple-target model. The first five models presented (Chick's Law, Chick-Watson Law, Hom Model, Power Law and Hom Power Law) are nested sets that the first four models are the special cases of the Hom Power Law. Pairwise comparison of the success of describing observed inactivation of each model, will be helpful to see the significance of improvement in fit by addition of the parameter. Multiple-target and Series Event models are

probabilistic models were the models were developed based on action of disinfectants. Modified Multiple-target was developed using the same probabilistic method where the rate of destruction of the target was described by non-first order kinetics. Use of these models would facilitate to perceive the validity of the assumed action of disinfectants.

In all the inactivation models described here, the predicted surviving organisms concentration was dependent on initial boundary conditions including initial microbial density (N_o). However, in the regulations (SWTR and IESWTR), the efficiency of disinfection is measured as log removal, percent removal or survival ratio. As seen in the integrated form of these models, except Power Law and Hom Power Law, the survival ratio (N/N_o) was dependent only on disinfectant concentration and contact time. In Power Law and Hom Power Law, the survival ratio was also a function of initial microbial density. Therefore, evaluation of the inactivation models was essential to investigate the effects of initial microbial density on disinfection efficiency.

3.6. Cell Density Effects on Inactivation Efficiency

In studies on kinetics of chemical disinfection, the inactivation of organisms has been described by different kinetic models. Some of the most commonly used kinetic inactivation models in water disinfection were described in Section 3.5. Most of the kinetic inactivation models have disinfectant concentration and contact time as independent variables. Therefore most of the studies conducted on disinfection kinetics have been focused on inactivation efficiencies of different chemical disinfectants on different organisms under different conditions such as pH, temperature, turbidity or presence of other chemicals or disinfectants. However, the disinfection efficiency over a wide range of initial microbial densities has not been studied.

In the early study of Majumdar *et al*. (1973), the inactivation of poliovirus with ozone was described by Rational Model and a non-first order dependency on initial poliovirus density was observed. The experiments were conducted at a constant residual ozone concentration (±7.2%), where the initial poliovirus density ranged only five fold (from 1.5×10^4 to 7.5×10^4

PFU/mL). Another example of the use of the Rational Model is the study of Roy (1981) who used the Rational Model to describe the inactivation of poliovirus 1 in a continuously stirred tank reactor with ozone, in demand-free systems. A non-linear dependency of inactivation efficiency on viable organism density was observed. In a recent study by Gyürèk and Finch (1998), inactivation of heterotrophic plate count bacteria with ozone was best described by the Hom model. The study found no statistically significant improvement in the fit to the Hom Power Law, which means that the accounting of microbial density effects on the model did not improve the goodness of fit. However, it may not be reliable to conclude whether the initial microbial density has any effects on the disinfection efficiency using survival data at constant initial microbial density.

In a study conducted by Datta and Benjamin (1999) on the acid sensitivity of enterohemorrhagic *E. coli*, cell density dependent acid resistance was observed in *E. coli* cultures at stationary phase (Datta and Benjamin, 1999). Datta and Benjamin (1999) carried out a series of experiments with *E. coli* cultures both in stationary and in exponential growth phases. The experiments were conducted at an initial microbial density of $2\text{-}5\times10^{9}$ cells/mL and decimal dilutions (1/10, 1/100 and 1/1000) in Luria Broth with culture supernatant. Both of the media were acidified by HCl to pH 2.5. In both of the media, survival ratios after 60 minutes exposure to acidified medium were higher at decimal dilutions. Cell density dependent acid sensitivity was not observed in cultures under exponential growth phase and in *rpoS* mutant strains which lack the gene that encodes alternate sigma factor, σ^{s}, responsible for stationary phase stress response. This study found that some strains of *Shigella* and *E. coli* were more acid sensitive at higher cell densities, whereas some of the strains showed no sensitivity variation due to changes in cell density (Figure 3.4) (Datta and Benjamin, 1999).

A recent study by Cui *et al*., (2001) confirmed that cell density dependent acid survival of *E. coli.* The relation observed between cell density and acid survival was same as findings of Datta and Benjamin, (1999). The survival of *E. coli* was higher at lower initial microbial

densities. 2×10^6 to 2×10^9 cells/mL were exposed to pH 2.5 for 2 hours and a clear dose response relationship between available arginine and/or glutamate, cell density and cell survival was observed (Cui *et al*., 2001).

Walker *et al*., (1995) observed cell density dependent resistance to five minutes nitric oxide exposure in Chinese hamster fibroblasts (HA1) and H_2O_2 resistant variants derived from HA1 cells. However, in this study, higher survival was observed at higher cell densities. The cell plating density ranged from 2×10^6 to 6×10^6 in this study.

Although cell density dependent acid sensitivity was confirmed for some bacteria, the mechanisms of action of acidic conditions and disinfectants are different. Also, the initial microbial density range studied in acid sensitivity studies are far from what is observed in raw source water. The previous studies on disinfection kinetics lack survival data on a deliberately broad range of initial microbial densities to draw a clear conclusion on the effect and magnitude of cell density on inactivation efficiency. The literature on cell density dependent activities, quorum sensing, do not address any relation between cell density and disinfection efficiency. Therefore, there is a big necessity of a more detailed study on the effects of cell density of various organisms such as bacteria and protozoa at various cellular physiology/morphology stages such as endospores, stationary growth phase, exponential growth phase.

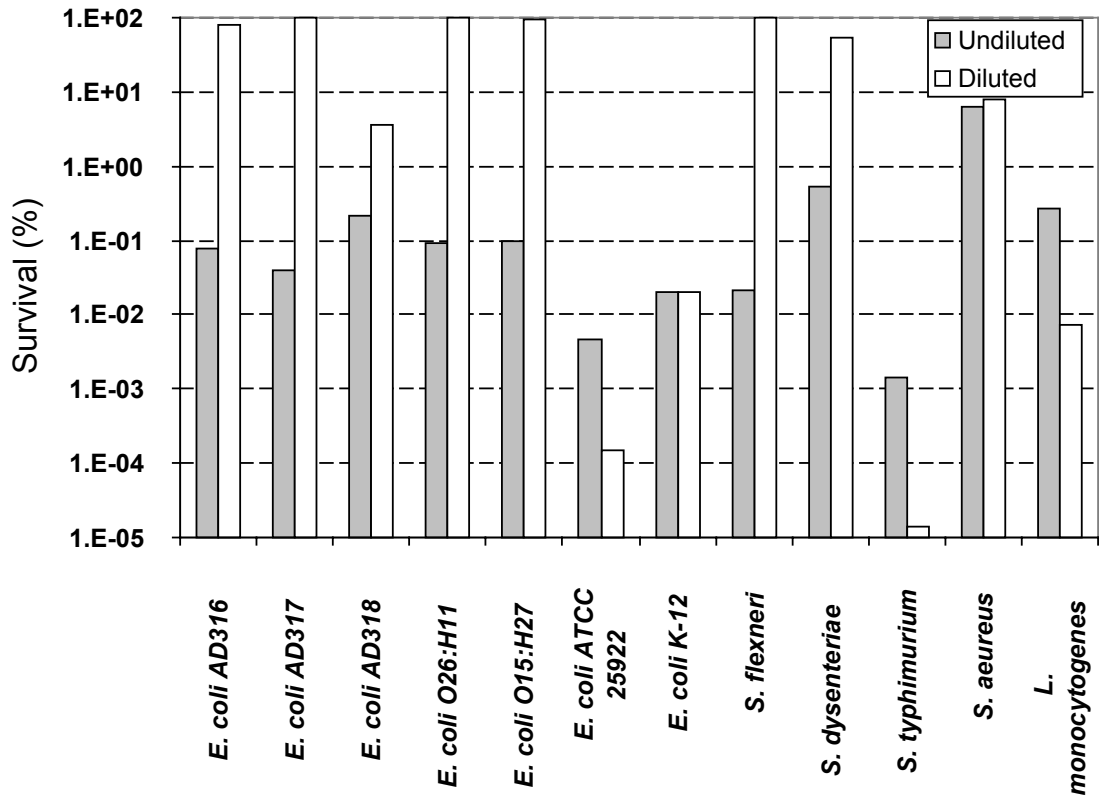

Figure 3.4: Effects of cell density on acid sensitivity of various bacterial strains. The density of undiluted cultures are 2-5x10^9 ml^{-1}, and the density of the diluted cultures are 2-5×10^6 ml^{-1} (Datta and Benjamin, 1999).

3.7. Surrogate Studies for Protozoan

Even though recent advances in water treatment allow us to produce better quality drinking water, disinfectant resistant pathogens are still a major concern. Waterborne diarrhea caused by persistent pathogenic protozoa is one of the most frequently identified waterborne disease in developed countries (Craun *et al*., 1998; Hijnen *et al*., 2000). *Giardia lamblia* and *Cryptosporidium parvum* have caused 32 percent of all the reported outbreaks from 1991 through 1998, including a single outbreak in Milwaukee, Wis., in 1993 causing an estimated 400,000 illnesses and 4,400 hospitalizations. Low dosages of both *G. lamblia* and *C. parvum* can cause infection (Craun *et al*., 1998). There are several methods proposed for the direct detection of this organisms, however, these methods have limitations. The current enumeration techniques

for routine monitoring of *Giardia* cysts and *Cryptosporidium* oocysts have relatively poor recovery and sensitivity. In addition, these methods are cumbersome, expensive, time consuming and are therefore not appropriate for routine monitoring in public water treatment systems (Radziminski *et al*., 2002).

The protozoan (oo)cysts occur unpredictably in ambient waters and there are constraints in monitoring recovery sensitivity and accuracy. Currently, there are no perfectly reliable indicators of the presence of protozoan parasites. In a study by Payment and Franco (1993), the correlations of occurrence of *Giardia lamblia* and *Cryptosporidium parvum* with somatic coliphages, male-specific coliphages and *Clostridium perfringens* spores were studied. None of these organisms qualified to serve as an indicator of the protozoan parasites.

Currently, the IESWTR requires systems to measure turbidity to indicate water quality and efficiency of filtration. Higher turbidity levels are often associated with more disease-causing microorganisms such as viruses, protozoa, and some bacteria (USEPA, 2001). However, turbidity appears to be an inadequate predictor of the removal of particles that are similar to oocysts in size when source water turbidity is less than 5 NTU (Rice *et al*., 1996). Also, turbidity monitoring cannot reliably distinguish between oocysts that are viable or infective and those that are not. Another predictor of (oo)cysts and other cyst-sized particles removal is particle counting (Rice *et al*., 1996). However, this method also fails to give information about the viability or infectivity of the (oo)cysts.

In addition, due to methodological constraints, detection of higher inactivation ratio and routine monitoring of the finished drinking water are limited (Payment and Franco, 1993). The densities of protozoa in raw water are generally too low to directly measure the inactivation capability of a treatment plant. Since they are pathogens, seeding studies in any water treatment utility would cause unacceptable health risks to consumers (Craik *et al*., 2002). Therefore, it is hard to demonstrate the actual *Cryptosporidium* and *Giardia* removal efficiency of the treatment system. The seeding studies can be conducted in pilot plants, but this would be expensive.

Due to the great concern for waterborne outbreaks associated with protozoan parasites, it is necessary to investigate an accurate, reliable, inexpensive and simple way of monitoring the treatment performance. The ideal surrogate should have similar resistance to disinfectants as *Cryptosporidium* and/or *Giardia* and similar particle characteristics in order to estimate its removal efficiency during the disinfection process, filtration and other treatment processes. Bacterial spores have been proposed as an indicator of disinfection process efficiency in many studies (Barbeau *et al*., 1999; Driedger *et al*., 2001; Facile *et al*., 2000; Owens *et al*., 2000; Radziminski *et al*., 2002; Rice *et al*., 1996). The use of spore removal, coupled with monitoring for turbidity and particle counts could help utilities optimize unit operations (Rice *et al*., 1996).

Aerobic spores originate primarily in soil and into most source waters (Nieminski *et al*., 2000). They are generally at relatively higher concentrations than *Giardia* and *Cryptosporidium* (Payment and Franco, 1993; Rice *et al*., 1996). They can be easily detected in smaller volumes of samples, which allows water utilities to detect higher removal rates in the treatment system. Most of these organisms are not pathogenic and, therefore, they do not present a public health risk. Hence, they can be used in seeding studies to evaluate the disinfection performance of full-scale or pilot-scale treatment plants.

There have been studies comparing the resistance of different species of aerobic and/or anaerobic bacterial spores with *Cryptosporidium* and *Giardia*. Some studies observed similar inactivation ratios of bacterial spores and *Cryptosporidium* (Facile *et al*., 2000; Hijnen *et al*., 2000; Owens *et al*., 2000; Radziminski *et al*., 2002; Venczel *et al*., 1997), whereas other studies observed that bacterial spores were significantly less resistant than *Cryptosporidium* (Barbeau *et al*., 1999; Chauret *et al*., 2001; Craik *et al*., 2002; Payment and Franco, 1993). In a study by Hijnen *et al*., (2000), the sulphite-reducing *Clostridia* spores showed comparable resistance to ozone as *Cryptosporidium* in lab-scale experiments. In studies by Payment and Franco (1993) and Venczel *et al*., (1997), the inactivation of *Clostridium perfringens* was compared with *Cryptosporidium*. Payment and Franco (1993) compared the inactivation of both of the

organisms in three treatment plants where one of them used ozone disinfection and the other two applied chlorine dioxide. Payment and Franco's (1993) study showed that *C. perfringens* were too sensitive to be a surrogate for disinfection of oocysts, whereas Venczel *et al*., (1997) observed similar inactivation ratios with both of the bacterial spores. In lab-scale inactivation studies conducted by Radziminski *et al*., (2002) and Facile *et al*., (2000) similar levels of inactivation of *B. subtilis* spores and *C. parvum* were observed with chlorine dioxide and ozone, respectively.

Owens *et al*., (2000) conducted a pilot scale study on the inactivation of *B. subtilis* spores with ozone using Ohio River water. Their results showed higher resistance of endospores of aerobic spore-forming bacteria to ozone with respect to *Cryptosporidium.* In the inactivation studies conducted by Craik *et al*., (2002) ozone inactivation of *B. subtilis* spores were investigated with bench scale experiments. They observed substantial differences between their study and *C. parvum* oocyst inactivation predicted by a previously published kinetic model. In the study of Nieminski *et al*., (2000) both anaerobic and aerobic spore formers, *C. perfringens* and *B. subtilis,* were less resistant than *Cryptosporidium* and failed to serve as surrogates for the inactivation of oocysts.

Sporulation techniques and conditions affect the resistance of pure cultures of bacterial spores (Rice *et al*., 1996). The indigenous spores may exist in different stages of maturity and metabolic dormancy under natural conditions. As a result of these factors, different responses of bacterial spores to oxidative stress were observed (Rice *et al*., 1996).

Although some of the studies do not agree with each other in conclusion on the use of bacterial spores as a surrogate for disinfection efficiency of oocysts, they mostly agree on the requirement for more research in this topic. Bacterial spores are readily available in most source waters and they are non-pathogenic, very resistant to the disinfection process, easy and inexpensive to work with. Currently, they are one of the best candidate surrogates for the disinfection efficiency of oocysts.

4. SCOPE OF EXPERIMENTS

The main objective of this study was to investigate whether the disinfection process of waterborne microorganisms is dependent on the microbial population density. To satisfy this objective, a series of bench-scale inactivation experiments were conducted using three different species of microorganisms (*G. muris, E. coli* and *B. subtilis*) with two different types of disinfectants (ozone and monochloramine).

Giardia muris is a flagellated intestinal protozoan. This parasite forms environmentally resistant cysts, which are passed in the feces. Pathogenic protozoa are one of the major concerns in drinking water. Therefore, it is necessary to investigate whether inactivation of this organism is cell-density dependent or not. This strain of *Giardia* is non-pathogenic and it has been successfully used in inactivation studies (Haas *et al*., 1995; Owens *et al*., 2000).

Escherichia coli is a short gram-negative, non-sporulating bacterium. *E. coli* is found in the gastro-intestinal tract, and principally the bowel of mammals and birds. They can also be found in nature as a result of fecal contamination (Sussman, 1985). *E. coli* is found in the source water over a wide range of densities (Payment and Franco, 1993). The MCLG for total coliforms is zero under the IESWTR. The strain of *E. coli* studied (ATCC 13706) is a non-pathogenic organism and easy to work with. It has been successfully used in disinfection studies (Haas *et al*., 1995; Hunt and Mariñas, 1999; Kouame and Haas, 1991). In addition, control of gene expression in response to cell density (quorum sensing mechanism) has been observed in this organism (Gruenheid and Finlay, 2000).

Bacillus subtilis is a gram-positive, rod shaped, aerobic endospore-forming bacterium. The primary habitats of *Bacillus* species are soil or rotting plant materials. It has been found in the source water (Payment and Franco, 1993; Rice *et al*., 1996). *B. subtilis* is considered to be non-pathogenic (Sonenshein *et al*., 1993) and it has been successfully used in disinfection studies (Barbeau *et al*., 1999; Driedger *et al*., 2001; Facile *et al*., 2000; Sommer *et al*., 1995). It is known that the cellular morphology and activity of gram-negative and gram-positive bacteria

have differences. Conducting experiments with both gram-negative and gram-positive bacteria will give the opportunity to compare the effect of cell density on disinfectant resistance/sensitivity for both types. Spores of *B. subtilis* are very resistant to chemical agents. Similar CT values of *B. subtilis* spores and *C. parvum* have been reported in the literature (Chauret *et al*., 2001; Facile *et al*., 2000). Studies of the inactivation of spores of *B. subtilis* will also help to investigate the potential use of this organism as a surrogate for disinfection efficiency of protozoa.

Monochloramine is a relatively stable oxidant. More and more water utilities are using chloramines instead of, or in addition to, free chlorine. Chloramines act more slowly than free chlorine, but chloramines reduce the formation of trihalomethanes (THMs). Chloramines are safe and effective in water treatment (Spellman, 1999). Therefore, monochloramine was picked for inactivation experiments of *E. coli* and vegetative cells of *B. subtilis*. In these experiments, the initial monochloramine dose was 0.75, 1.0 and 1.5 mg/L.

Ozone has the highest oxidation power compared with the chemical oxidants used in drinking water treatment. It is very effective against resistant organisms, such as protozoa. There is an increasing trend in the use of ozone as an alternative disinfectant in water treatment facilities. Since ozone is highly efficient, it was used for the inactivation of *G. muris* and *B. subtilis* spores. The initial ozone dose was 0.25, 0.40, 0.50 and 0.75 mg/L in *G. muris* experiments and 1.0, 1.5 and 2.0 mg/L in *B. subtilis* spores experiments.

All the experiments were conducted using demand-free Milli-Q^{TM} water buffered at 15ºC. The *E. coli* experiments were conducted at pH 7, whereas the of *B. subtilis* and *G. muris* experiments were conducted at pH 8.

To satisfy the objective of investigating the dependency of disinfection efficiency on microbial density, the experiments were conducted by deliberately varying initial microbial densities. The initial microbial densities in inactivation experiments with bacteria (*E. coli* and *B. subtilis*) ranged approximately from 10^3 CFU/mL to 10^5 CFU/mL. The initial trophozoite

density in inactivation experiments of *G. muris* ranged approximately from 6,250 trop/mL to 50,000 trop/mL. The other two variables in these experiments were the time and applied disinfectant dose. Each experimental series were conducted at constant temperature (15ºC) and pH (7-8).

The inactivation experiments were conducted with the above organisms under different growth stages. First of all, inactivation of each organism was studied under conditions that exist in nature. The inactivation *G. muris* and *B. subtilis* experiments were conducted when the cells were in the cyst and spore forms, respectively. Two separate series of inactivation experiments were conducted using *E. coli* when the cells were at stationary growth phase. The stationary phase organisms were obtained from batch and continuous cultures. Although the incubation period and conditions were identical in each experiment, the batch cultures were closed systems that were continually changing due to metabolic activities of the bacterial population (Whiteley *et al*., 1997). This helped us to investigate and validate that the dynamic conditions and heterogeneity in the batch cultures were not the reasons for cell density dependent inactivation. In addition, the agreement between these two series would show the reproducibility of the data.

Cellular activities and structure also change within a strain due to growth conditions (See Section 3.4). Approximately, 1000 genes highly expressed in the exponentially growing *E. coli* cells are mostly turned off or markedly repressed in the stationary phase cells (Ishihama, 1997). Inactivation of bacteria (*E. coli* and *B. subtilis*) was also studied during the exponential growth phase to understand under which phase(s) the mechanism responsible for cell density effects is active. Also, conducting the experiments at two different growth phases allowed the determination of the degree of change in biocide resistance due to growth phase.

As described in Section 3.3, there are cell density dependent activities called quorum sensing, which are mediated by extra-cellular substances. It is not known whether the presence of these extra-cellular substances have any effect on the cell density dependency of inactivation efficiency. The answer to this question was investigated by supplying an excess of these extra-

cellular materials. Disinfected microorganism suspension (DMS) was used for this purpose, where the preparation of this suspension is explained in more detail in later sections (Section 5.2.2). When these extra-cellular substances are supplied in excess in the experimental water, the contribution of the extra-cellular substances within the microbial suspension would be too diluted to have any significant effects. Based on this assumption, the answer to the question, "Is the cell density dependence of inactivation efficiency driven by external chemicals released by cells?" was investigated by conducting inactivation experiments in the presence of DMS.

Disinfection of any of organism has not been studied over a wide range of initial microbial density intentionally. Although cell density dependent acid sensitivity was studied for some bacteria, the initial microbial density range studied in acid sensitivity studies were far from what is observed in raw source water. The previous studies on disinfection kinetics lack survival data on a deliberately broad range of initial microbial densities to draw a clear conclusion on the effect and magnitude of cell density on inactivation efficiency. The literature on cell density dependent activities, quorum sensing, do not address any relation between cell density and disinfection efficiency. Therefore, in this study, effects of initial microbial density were studied on three different organisms under different conditions. Effects of initial microbial density on the inactivation of *E. coli* were studied at stationary growth phase, at stationary growth phase in the presence of DMS, and at exponential growth phase. Effects of initial microbial density on the inactivation of *B. subtilis* were studied using the organisms in spore and exponentially growing vegetative cell forms. Effects of initial microbial density on inactivation of *G. muris* were studied using the organisms in cyst form. The survival of each organism under the conditions described above was measured at various initial microbial densities, time and applied disinfectant doses.

5. EXPERIMENTAL MATERIALS AND METHODOLOGY

5.1. Chemical Solutions

5.1.1. Laboratory Water

The reagent-grade water used in the laboratory was processed by a Milli-Q™ water system (Millipore Intertech., Bedford, MA), which was comprised of distillation, ion exchange, activated carbon adsorption and membrane filtration.

5.1.2. Stock Chlorine Solution

Preparation: The stock chlorine solution was prepared by bubbling chlorine gas into a weak alkaline solution to obtain a concentration equal to 150 ± 10 mg /L. The weak alkaline solution was prepared by addition of sufficient 0.1 molar NaOH to bring the distilled water to a final pH of 8.

Analysis of residual: Chlorine levels were determined by the colorimetric DPD method (APHA *et al*., 1995).

Storage: The stock chlorine solution was stored in a brown glass bottle in dark refrigerated conditions and was discarded when the concentration decreased to less than 140 mg/L.

5.1.3. Ammonium Chloride

The stock ammonium chloride solution was prepared by the addition of 150 mg of NH_4CI to one liter of stock phosphate buffer solution. Stock phosphate buffer solution was prepared by dissolving 34.0 g of potassium phosphate in 500 mL of distilled water and then the pH was adjusted to 8.0 with 1N of sodium hydroxide (NaOH). Next, it was diluted to 1L with Milli-Q™ water to form a solution of 150 mg/L NH_4CI. The solution was stored in a brown glass bottle in dark refrigerated conditions. The stock ammonium chloride solution was prepared and discarded at the same time as the stock chlorine solution.

5.1.4. Stock Monochloramine Solution

Preparation: Preformed monochloramine was prepared on the day it was used, by mixing equal volumes of chlorine and ammonium chloride solution at a 3:1 (Cl_2:N) weight ratio, yielding a 150 ± 10 mg/L (as Cl_2) solution. Each solution was prepared in a pH 8 phosphate buffer.

Analysis for Residual: After the combined solution was stirred for over 30 minutes, the resultant solution was checked for free chlorine and monochloramine using the DPD colorimetric method. There are studies that give the results of this method used to analyze synthetic water samples without interferences (APHA *et al*., 1995). The residual in the aqueous stock monochloramine was measured within 10 minutes before dosing to reactors.

Storage: The stock monochloramine solution was stored at room temperature until use in experiments. The stock solution was used within an hour after it was prepared.

5.1.5. Stock Ozone Solution

Preparation: Oxygen carrier gas containing approximately 5 percent ozone was bubbled by means of a Polymetrics ozone generator Model T408 (Polymetrics, Inc., Colorado Springs, Colo.) for 10 minutes at 20ºC through 400 mL of Milli-Q™ water in a 500 mL gas adsorption flask. Ozone concentration in the stock solution was between 10 and 20 mg/L

Effluent gas was neutralized by passage through a solution containing 132 g/L of sodium thiosulfate and 3 g/L of potassium iodide to remove the excess ozone.

Analysis for Residual: Ozone residuals were measured by the indigo colorimetric procedure. The relative error of this method is less than 5% in the absence of interference. This may be reduced to 1% underlaboratory conditions (APHA *et al*., 1995). The residual in the aqueous stock solution was measured at most 5 minutes before dosing to reactors.

Storage: The aqueous ozone solution was stored in the refrigerator at 4ºC and used within an hour of generation.

5.1.6. Sodium Hydroxide

A 0.1 M sodium hydroxide solution was prepared by dissolving 4.0 g of NaOH in 1 L of Milli-Q™ water. The solution was kept in a glass bottle at room temperature.

5.1.7. Sodium Thiosulfate

10% sodium thiosulfate solution was prepared by adding 100 mg of sodium thiosulfate to 1L of water. 1 ml of this solution was added to each sampling tube and then autoclaved at 15 psi for 15 minutes before use.

5.1.8. Dilution Water

In order to prepare decimal dilutions of organisms prior to enumeration, phosphate buffered dilution water was prepared according to Standard Methods (APHA *et al*., 1995). Bacteria were suspended in dilution water no more than 30 minutes at room temperature to avoid death or multiplication (APHA *et al*., 1995).

Stock phosphate buffer solution was prepared by dissolving 34.0 g of potassium phosphate in 500 mL of distilled water, adjusting the water to pH 7.2 ± 0.5 with 1N sodium hydroxide (NaOH) and diluting it to 1 L with Milli-Q™ water. Then 1.25 mL of stock phosphate buffer solution and 5.0 mL of magnesium chloride solution (81.9 g/L $MgCl_2.6\ H_2O$ distilled water) was diluted to 1 L of distilled Milli-Q™ water.

5.1.9. Experimental Buffered Water

The experimental buffered water was used to fill the reactors. It was prepared by addition of 0.54 g/L of Na_2HPO_4 and 0.884 g/L of KH_2PO_4 to Milli-Q™ water. This water was buffered to a pH of 7.0 for experiments with *E. coli* and 8.0 for experiments with *B. subtilis* and *G. muris*.

5.1.10. Phosphate Buffered Saline Solution (PBS)

A 10× Phosphate Buffered Saline solution was prepared by dissolving 80 g of NaCI, 2 g of potassium dihydrogen phosphate (KH_2PO_4), 29 g of hydrated disodium hydrogen phosphate

($Na_2HPO_4 \cdot 12H_2O$) and 2 g of potassium chloride (KCI) in Milli-Q™ water to a final volume of 1 L. 1X PBS was formed by mixing 100 mL of 10X PBS with 900 mL of Milli-Q™ water.

5.1.11. Demand-free Water

The Milli-Q™ water was tested for monochloramine demand and it was observed that there was no significant demand of monochloramine.

Ozone demand-free water was prepared by ozonating Milli-Q™ water for 10 minutes to obtain an ozone dose of 10 mg/L or more. The ozonated water was kept in the refrigerator for 1 hour or more. The remaining ozone residual was neutralized by boiling or autoclaving the demand-free water for 15 minutes or more.

5.1.12. Eluting Solution

The eluting solution was prepared by addition of 100 mL 10X PBS, 100 mL 1% sodium dodecyl sulfate (SDS), 100 mL 1% Tween 80 and 0.1 mL of Sigma Antifoam A (Cat. No. A-5758) and sufficient amount of 0.01 M NaOH to adjust the pH.

1% SDS was made by addition of 1g sodium dodecyl sulfate in a Milli-Q™ water to final volume of 100 mL. 1% Tween 80 stock solution was made by addition of 1 mL of polyoxyethylenesorbitan monooleate (Tween 80) to 99 mL of Milli-Q™ water.

The eluting solution was formed by addition of 100 mL 10X PBS, 100 mL 1% SDS, 100 mL 1% Tween 80. 0.1 mL of Sigma Antifoam A (Cat. No. A-5758) was added to control foam formation. The pH of the solution was adjusted to approximately 7.4 by addition of sufficient amount of 0.01 NaOH. Later the solution was diluted to final volume of 1L by Milli-Q™ water. The solution was stored at room temperature and used within a week of preparation.

5.1.13. Reducing Solution

Reducing solution was formed by addition of 1.958 g of Hank's Balanced Salts, 1.9 g of glutathione, and 2.002 g of L-cysteine to 200 mL of Milli-Q™ water. The solution was filter sterilized using a 0.1µm syringe filter (Millex cat. No. SLVVR25LS, Millipore Corp., Bedford, MA, 01730) prior to use. It was prepared the day prior to use.

5.1.14. Proteose Peptone Solution

Stock (5%) proteose peptone solution was made by the addition of 5 g of proteose peptone to 100 mL of Milli-Q™ water. The solution was boiled gently for 10 to 15 minutes. The solution was filter sterilized using a 0.1µm syringe filter (Millex cat. No. SLVVR25LS, Millipore Corp., Bedford, MA, 01730) and refrigerated until use. This was usually prepared one day prior to use. Upon the day of use a solution of 0.5% proteose peptone was made by dilution of 10 mL of 5% stock with 90 mL of 1X PBS

5.1.15. Excystation Medium

Exystation medium was formed by mixing 10 mL of 5% proteose peptone solution, 10 mL of 10X PBS and 80 mL of Milli-Q™ water. It was prepared the day of use.

5.1.16. Sterile Growth Medium

Nutrient Broth: (Difco™ no. 0003-01-6, Difco Laboratories, Detroit, Mich.). It was prepared according to the manufacturer's specifications. 8 g of powdered nutrient broth was suspended in 1 L Milli-Q™ water. Then the suspension was dispersed into either 16 mm x 150 mm glass tubes with plastic caps or 8-oz wide mouth HDPE bottles and sterilized by autoclaving for 15 minutes or more.

Nutrient Agar: (Difco™ No. 0001-17). It was prepared according to the manufacturer's specification. 23 g of powdered nutrient agar was suspended in 1 L Milli-Q™ water and then boiled to dissolve completely. Then the suspension was sterilized by autoclaving for 15 minutes or more. Next, the agar was dispersed onto Petri dishes to prepare culture dishes or 16 mm × 150 mm glass tubes with plastic caps to prepare slants under aseptic conditions.

R2A Agar: (Difco No. 1826-17-1). The sterile media was prepared according to the manufacturer's specifications. 18.2 g of the powder R2A agar was suspended in 1 L of Milli-Q™ water. Then, it was mixed well and boiled for 1 minutes to completely dissolve the powder. The suspension was sterilized by autoclaving for 15 minutes or more. Next, the agar was

dispersed onto Petri dishes to prepare culture dishes or 16 mm × 150 mm glass tubes with plastic caps to prepare slants under aseptic conditions.

Trypticase Soy Broth (TSB): (BBL No. 211768, Becton Dickinson Microbiology Systems, Sparks, MD). The sterile media was prepared according to the manufacturer's specifications. 30 g of powdered TSB was suspended in 1 L Milli-Q™ water, mixed thoroughly and then warmed gently until solution is complete. Then the suspension was sterilized by autoclaving for 15 minutes or more. Next, the broth was dispersed onto Petri dishes with pads using aseptic technique.

5.2. Microbial Preparation

5.2.1. Preparation of *Giardia muris*

All *Giardia muris* cysts were obtained from the Oregon Health Sciences University, Portland, Oregon. This strain of *G. muris* was obtained from specific pathogen-free mice (e.g., Swiss albino mice, CF-1). For the production of highly purified cysts, feces were collected from the host and the cysts were isolated from the fecal material by a sucrose gradient technique.

The final cyst preparation was stored at 4°C in 0.01% TWEEN 20 with distilled water containing 50 to 100 units of penicillin/mL and 50 to 100 µg of streptomycin/mL. The final cyst preparation was re-suspended to the desired concentration (determined by hemocytometer count) using oxidant demand-free water and shipped to Drexel University overnight in an insulated box with coolants. Cysts were stored at 4°C and used within 7 days of preparation.

Cysts were washed three times (each wash consisted of centrifugation at 5,000×g for 5 minutes, decanted, and resuspended) and re-suspended in disinfectant demand-free buffer immediately prior to experimental use, and then diluted to 10 mL with disinfectant demand-free buffer for inoculation into reactor vessels.

5.2.2. Preparation of *Escherichia coli*

The working stock cultures were prepared according to the procedures of (Kouame and Haas, 1991). Under aseptic conditions, a loopful of permanent stock culture (*E. coli* ATCC

catalog no. 13706) was transferred to Petri dishes containing sterile nutrient agar. These plates were placed into the incubator at 37°C overnight. Then these plates were stored at 4°C. These working stock cultures were used for a three to four week period. The contents of the last two plates were used to prepare a new set of working stock cultures.

To prepare the microorganisms for the inactivation experiments (experimental cultures), assay tubes containing sterile nutrient agar were inoculated with microorganisms from the working stock culture. These assay tubes were incubated at 37°C overnight. Then the microorganisms were harvested by washing with 10 mL of buffered demand-free water, centrifuging with IEC Clinical Centrifuge (rotor# 215, r = 14.1 cm) at 5000 rpm for 10 minutes, and then washed two times with 10 mL of buffered demand-free water. The microbial suspension was mixed using a vortex mixer at all stages. An appropriate amount of the final suspension was dosed to the buffered experimental water for the experiment run.

E. coli suspended in DMS: The DMS was prepared as follows. The experimental *E. coli* cultures were prepared in the same way as above. Additionally, cell free culture fluid was added to reactors before the experiment run. To prepare the cell free culture fluid, the same procedures were followed as in the preparation of the microorganism suspensions. However, this time approximately 40 mL of this suspension was first treated with approximately 2.5 mg/L of monochloramine residual to inactivate the cells. 2.5 mg/L of monochloramine residual achieved more than 6-log removal in 10 minutes. The success of this process was checked by enumeration of *E. coli* in the disinfected suspension and no growth of colonies was observed. Unlike the *E. coli* suspension, the dose of cell free suspension was the same for each experiment. The criterion for the dose was its optical density at 660 nm and the dose was constant in each experiment. The dose of DMS was equivalent to 10^6 CFU/mL.

E. coli in exponential growth phase: The *E. coli* cultures in exponential growth phase were prepared according to procedures used by Datta and Benjamin (1999). To prepare *E. coli* in exponential growth phase, a loopful of the overnight culture suspension at stationary phase was

inoculated in 8 oz wide-mouth HDPE bottles containing 50 mL of nutrient broth. Next, these bottles are incubated in a temperature-controlled shaker (Lab-Line Instruments Inc. Model No. 3527) at 37 ^{0}C and at 160 rpm. Exponential growth occurred only for very brief periods of time following inoculation. The growth curve of *E. coli* was developed by monitoring the optical density of the microbial suspension during the incubation, once (Figure 5.1). According to this figure, *E. coli* grew exponentially with optical densities of 0.450 to 0.550 at 660 nm. Therefore, the cultures were incubated at 37ºC with shaking until the absorbance was about 0.500 at 660 nm. Next, the organisms were harvested by centrifuging at 5000 rpm for 10 min and washed with 10 mL buffered demand-free water twice. The final suspension was ready to be dosed to experimental water.

Continuous cultures of *E. coli:* The chemostat (Figure 5.6 and Figure 5.7) was inoculated with a loopful of working stock culture of *E. coli*. After inoculation, samples were periodically taken from the waste outlet to measure the microbial concentration in the chemostat using membrane filtration method (Figure 5.2). Under typical laboratory conditions, *E. coli* starves at approximately 1×10^7 - 5×10^9 cells/mL (Huisman and Kolter, 1994). In this study, the steady state conditions were reached around 10^9 cells/mL in 4 days at a dilution rate of 9.1×10^{-3} hour^{-1}. After steady state was reached, 2-3 mL of microbial culture was drawn from the chemostat in the day of an experimental run. Next, this culture was diluted to 10 mL and the organisms were harvested by centrifuging at 5000 rpm for 10 minutes and washing with 10 mL buffered demand-free water twice. The final suspension was ready to be dosed in experimental water.

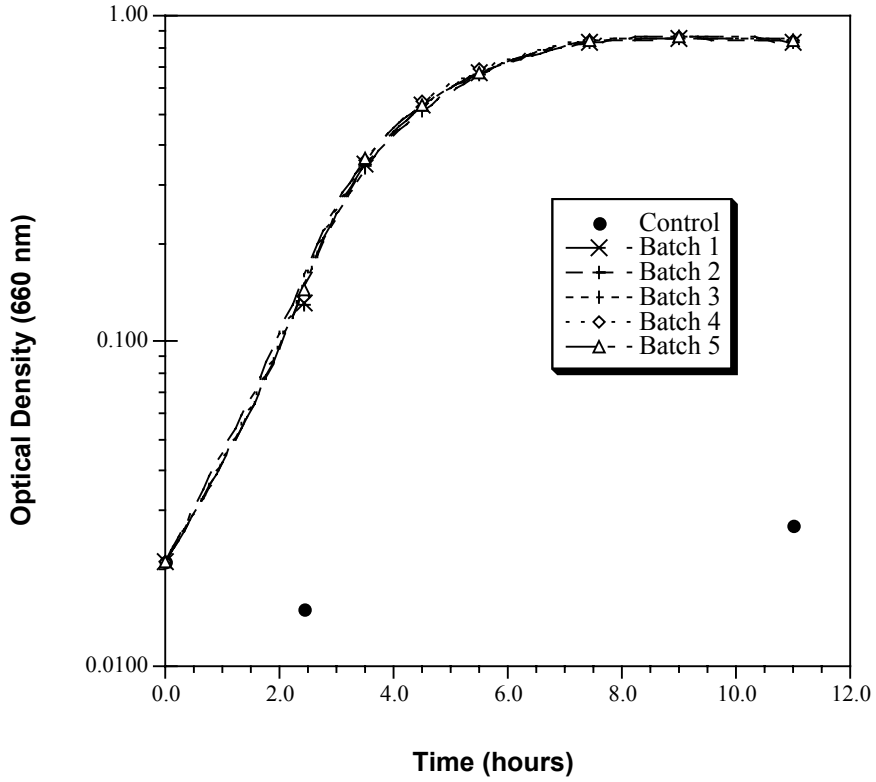

Figure 5.1: Growth curve of *E. coli* at 37ºC, 160 rpm, in nutrient broth.

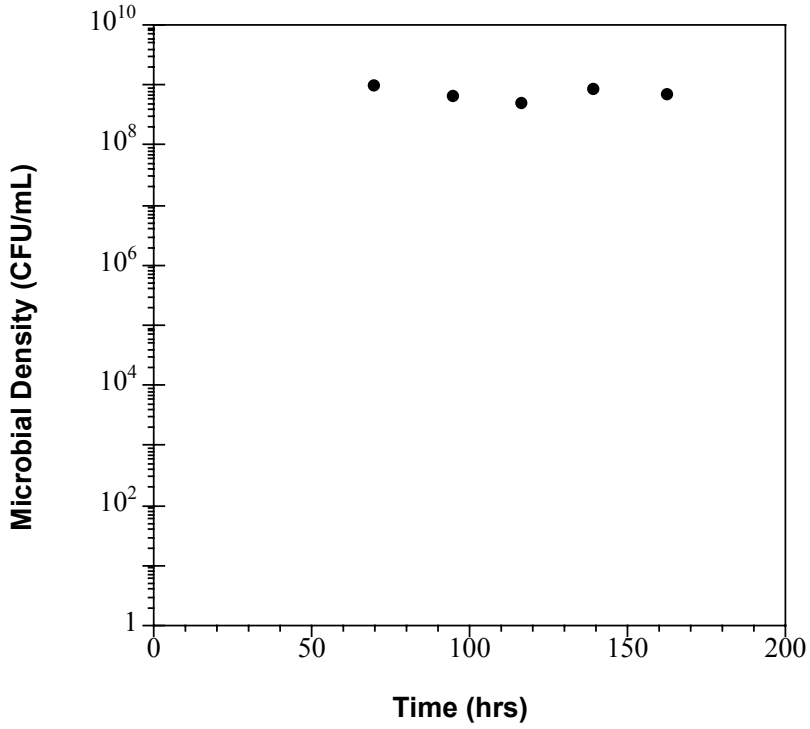

Figure 5.2: Start-up microbial density of the chemostat.

To have a certain initial microbial density in the reactors, the approximate density of organisms in the final suspension needs to be known. The density of organisms in the suspension was roughly calculated by the standard curve of OD_{660} versus microbial density. The standard curves for *E. coli* at stationary and exponential growth phases were prepared by measuring optical densities of dilutions of a microbial suspension at 660 nm and microbial density (Figure 5.3).

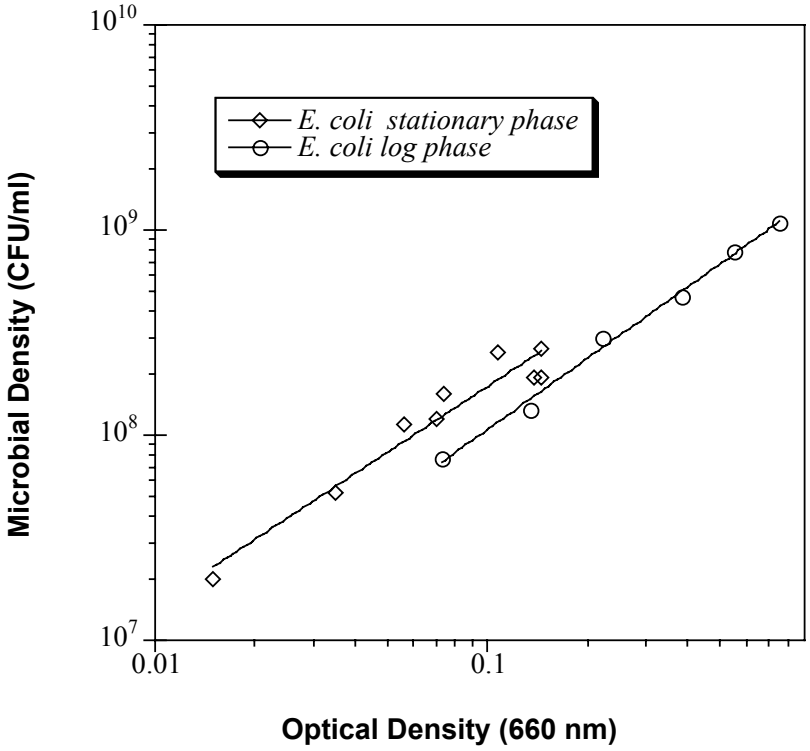

Figure 5.3: Standard curve of optical density (660 nm) versus cell count of *E. coli* at stationary growth phase and *E. coli* at exponential growth phase.

With the use of this standard curve of optical density (660 nm) versus cell count, an approximate initial cell concentration was calculated using the following relationship:

Microbial Density of *E. coli* at stationary growth phase (CFU/mL):

$$N = 2.01\times10^{9}\times\left(OD_{660}\right)^{1.06}$$

Microbial Density of *E. coli* at logarithmic growth phase (CFU/mL):

$$N = 1.52\times10^{9}\times\left(OD_{660}\right)^{1.16}$$

where OD_{660} is optical density at 660 nm.

The experiments were done within the 2 hours of preparation of the *E. coli* suspension.

5.2.3. Preparation of *Bacillus subtilis*

The working stock cultures of *B. subtilis* were prepared according to the procedures of Kouame and Haas (1991), Barbeau *et al*., (1996) and Barbeau *et al*., (1999). The *Bacillus subtilis* strain was purchased from ATCC (ATCC No. 6633). The culture was shipped as freeze-dried and the first incubation was done according to supplier's instructions.

The working stock spore cultures were prepared by transferring a loopful of *B. subtilis* culture to Petri dishes containing R2A media under sterile conditions. The R2A plates were incubated at 35ºC for 10 days to sporulate. After sporulation, the spore cultures were stored in the refrigerator at 4ºC during the project period. When more stock cultures were required, they were reproduced by transferring onto new plates, and then incubating at 35ºC for 10 days (Barbeau *et al*., 1996; Barbeau *et al*., 1999).

To prepare the spore cultures to be dosed into the reactors, a loopful of *B. subtilis* spores from stock culture was inoculated onto R2A slants and then incubated at 35ºC for 10 days to sporulate. After sporulation was complete, spores were collected by rinsing the agar with sterile phosphate buffer. Then, they were harvested by centrifugation at 6,000 rpm for 10 minutes and washed twice with sterile phosphate buffer. The final spore suspension was heated at 75^0C for 15 minutes to isolate spores from vegetative cells and subsequently maintained at 4ºC (Barbeau *et al*., 1996; Barbeau *et al*., 1999). The spore suspensions were used within a week.

The vegetative cells of *B. subtilis* at exponential growth phase were prepared according to procedures used by Datta and Benjamin (1999). Experimental vegetative *B. subtilis* cultures at exponential growth phase were also prepared from the stock culture. This time the organisms were incubated only overnight on R2A medium. After collecting the organisms from the medium by rinsing with sterile phosphate buffer and washing for two times, the culture was then incubated at 35ºC with shaking at 160 rpm. The growth curve of vegetative cells of *B. subtilis* was developed by monitoring the optical density of the microbial suspension during the incubation (Figure 5.4). According to this figure, *B. subtilis* grew exponentially between optical

densities of 0.250 to 0.350 at 660 nm. Therefore, the cultures were incubated at 35ºC with shaking until the absorbance was about 0.300 at 660 nm. Next, the organisms were harvested by centrifuging at 6000 rpm for 10 minutes and washing with 10 mL buffered demand-free water twice. The final suspension was ready to be dosed to experimental water.

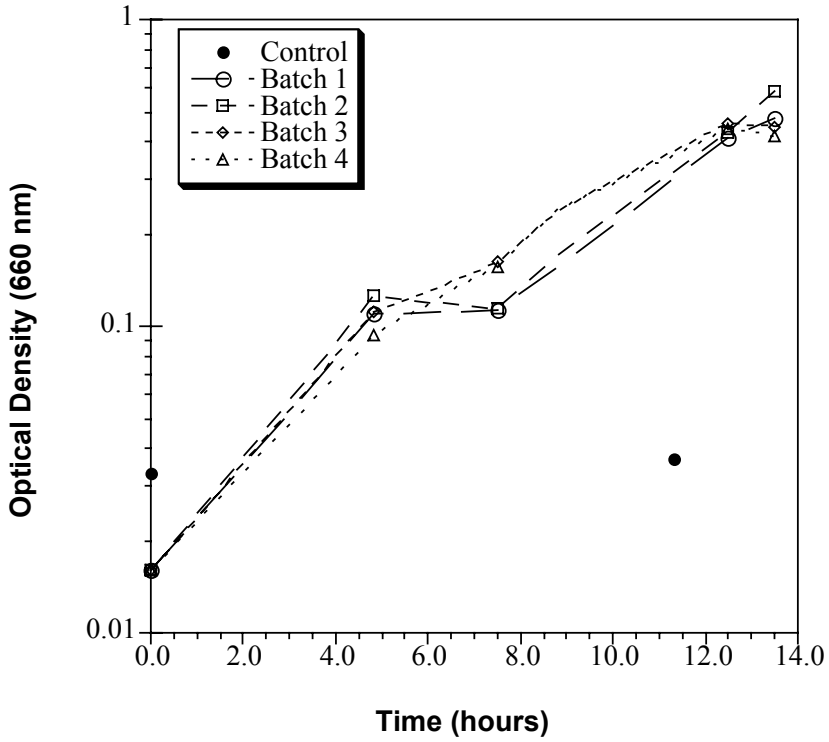

Figure 5.4: Growth curve of *B. subtilis* vegetative cells at 35ºC 160 rpm in nutrient broth.

To estimate the initial microbial density in the working stock culture, a standard curve was also prepared for *B. subtilis* spores and vegetative cells at exponential growth phase (Figure 5.5). The relation between optical density at 660 nm and microbial density was as follows;

Microbial Density of *B. subtilis* spores (CFU/mL):

$$N = 6.97 \times 10^{8} \times (OD_{660})^{1.44}$$

Microbial Density of *B. subtilis* vegetative cells at exponential phase (CFU/mL):

$$N = 9.13 \times 10^7 \times \left(OD_{660}\right)^{1.30}$$

where OD_{660} is optical density at 660 nm.

The experiments were done within 2 hours of preparation of the *B. subtilis* suspension.

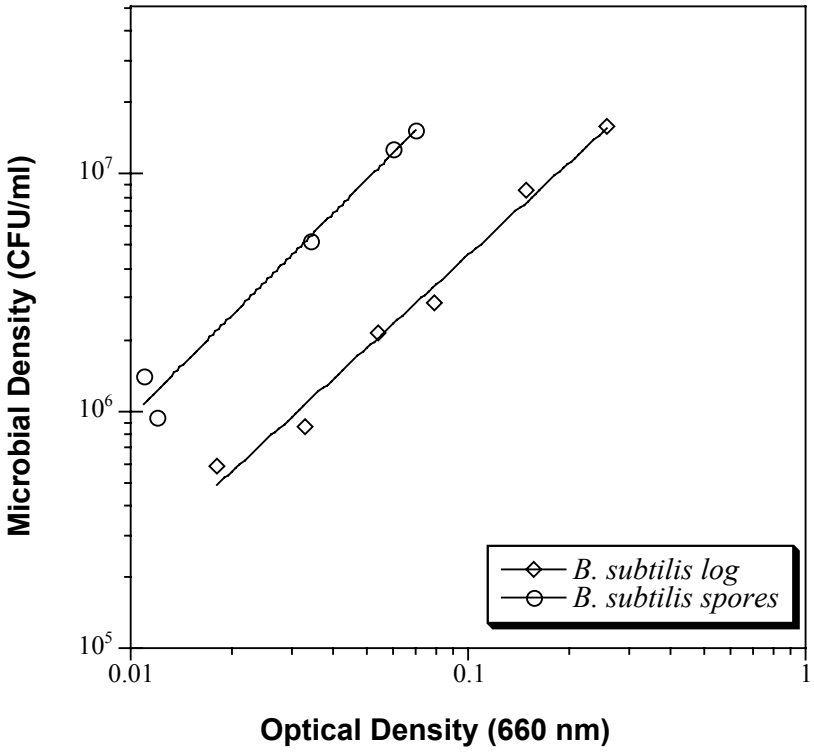

Figure 5.5: Standard curve of optical density (660 nm) versus cell count of *B. subtilis* vegetative cells at exponential growth phase and *B. subtilis* spores.

5.3. Equipment Setup

5.3.1. Chemostat

For continuous cultures of *E. coli,* a chemostat apparatus was set up in the laboratory similar to that of Whiteley *et al*. (1997). A 1000 mL Pyrex Erlenmeyer flask was modified to include a waste outlet. The final working volume of the chemostat was approximately 900 mL.

Three holes were drilled in a rubber stopper that fit tightly into the top of the modified Erlenmeyer flask (chemostat). Three glass tubes with outer diameters of 8 mm, 6 mm and 4 mm were placed into these holes as shown in Figure 5.6. The insert with a 6 mm diameter was used to deliver air into the chemostat. The atmospheric air was supplied by an air compressor at constant rate. The air was first bubbled into 500 mL of water in a flask to increase the humidity and to remove oils and/or particulates (Whiteley *et al*., 1997). This air was then sterilized through a 0.1 μm filter (Millex Cat. No. SLVVR25LS, Millipore Corp., Bedford, MA, 01730) before entering the chemostat. The 8 mm diameter tubing was used as an air outlet. This tube was plugged with cotton to prevent contamination. The 4 mm diameter tubing was used to supply nutrient broth into the chemostat. The 0.8 mm inner diameter capillary tubing (Tygon Sanitary Silicone Tubing, Akron, OH. Cat. No. ABW00001) was placed into this 4 mm tube and sealed with heat resistant silicon sealant to protect the media from contamination. Sterile nutrient broth was pumped with a peristaltic pump (Fisher Scientific, Cat. No. 13-876-4) into the chemostat through this capillary tubing at a rate of 8.2 mL/hr. The hydraulic residence time of the chemostat was approximately 110 hours. The media in the chemostat was continuously stirred with a 5 cm long magnetic stir bar. The waste was discharged by gravity through the added port (outlet) on the Erlenmeyer flask. This port was also used to collect the organisms for inactivation experiments (2-3 mL for each experiment). The waste was collected in a separate flask. Chemostat, fresh medium, waste collection flask, magnetic stirrer and peristaltic pump were set up in an incubator (Figure 5.7) to keep the temperature constant at 37ºC. All these parts were run under aseptic conditions. To check if there was any source of contamination in the chemostat, the chemostat was run for two days without inoculating any microorganisms. At the end of two days, no organisms were detected in the media in the chemostat, showing that the air was properly sterilized by the filter and the seals were tight enough to protect the media from environmental contamination.

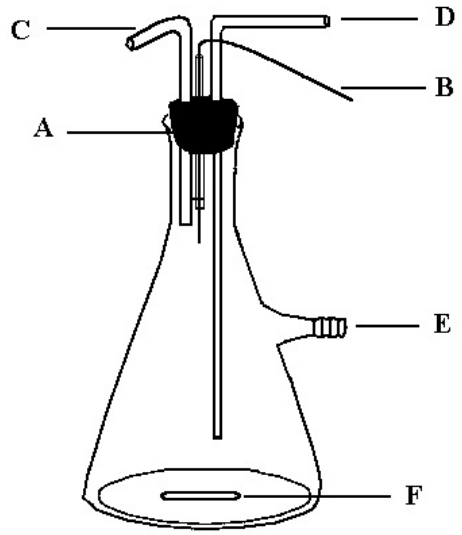

Figure 5.6: Chemostat apparatus for growing *E. coli*. (A) Rubber stopper, (B) Capillary tubing, (C) Air outlet, (D) Air inlet, (E) Waste outlet, (F) Magnetic stir bar.

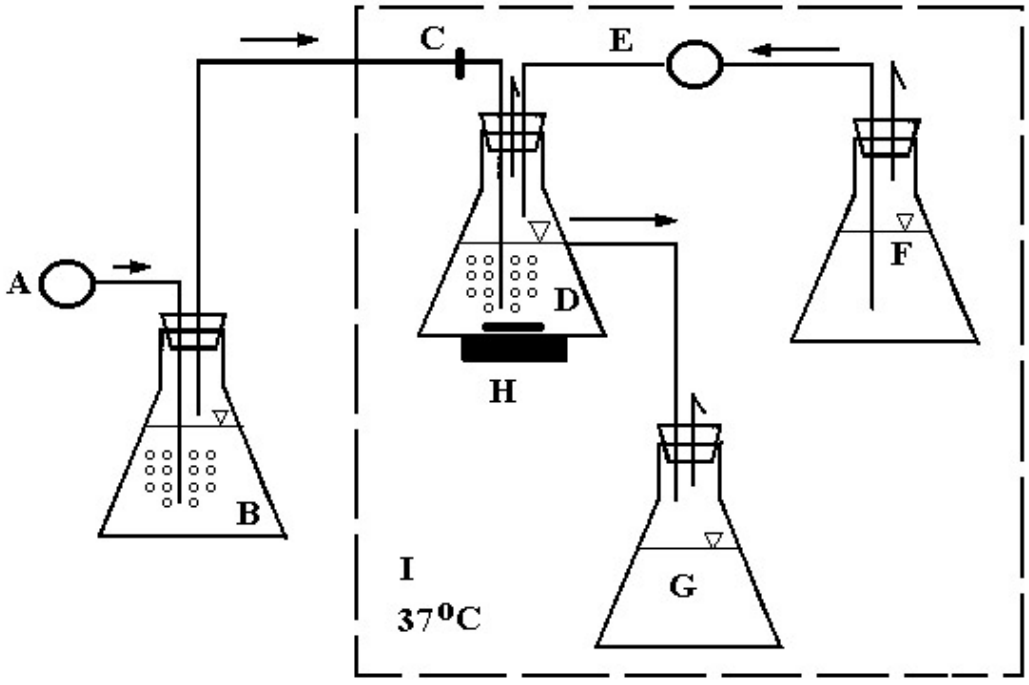

Figure 5.7: Schematic set up of continuous culture system. The items inside the dashed lines are placed in an incubator at 37^{o}C: (A) Air compressor, (B) Air bubbling flask, (C) Filter, (D) Chemostat, (E) Peristaltic pump, (F) Fresh media, (G) Waste collection flask, (H) Magnetic stirrer and (I) Incubator.

5.3.2. Reactor Vessel

Three to seven 1L heat resistant glass beakers were used as reaction vessels (Figure 5.8). Each reactor vessel was sufficiently mixed by a large star shaped stir bar (32 × 32 mm; catalog no. 14-511-96D, Fisher Scientific, Pittsburgh, PA). The temperatures of the reactor vessels were held constant at 15^{o}C using a circulating refrigerated water bath (VWR Scientific, model no. 1186, Plainfield, NJ). Before the experiment, the stir bars were placed into the reactor vessels and then the reactor vessels were covered with aluminum foil and autoclaved at 121^{0}C for 15 minutes or more. The reactor vessels used in the *G. muris* experiments were rinsed with eluting solution before the experiment was run to prevent adsorption of cysts to the reactor wall.

Reactors A and B: Microbial viability control reactors. These reactors contained organisms plus the buffered water, but no disinfectant. The initial microbial density was measured in these reactors.

Reactors C and D: Disinfectant residual control reactors. These reactors contained organisms plus the experimental water and disinfectant. These reactors were used to determine the residual disinfectant concentration, pH and temperature during the experimental run.

Reactors E and F: Test reactors. These reactors contained the same materials as Reactors C and D. These reactors were used to determine the inactivation due to the disinfectant.

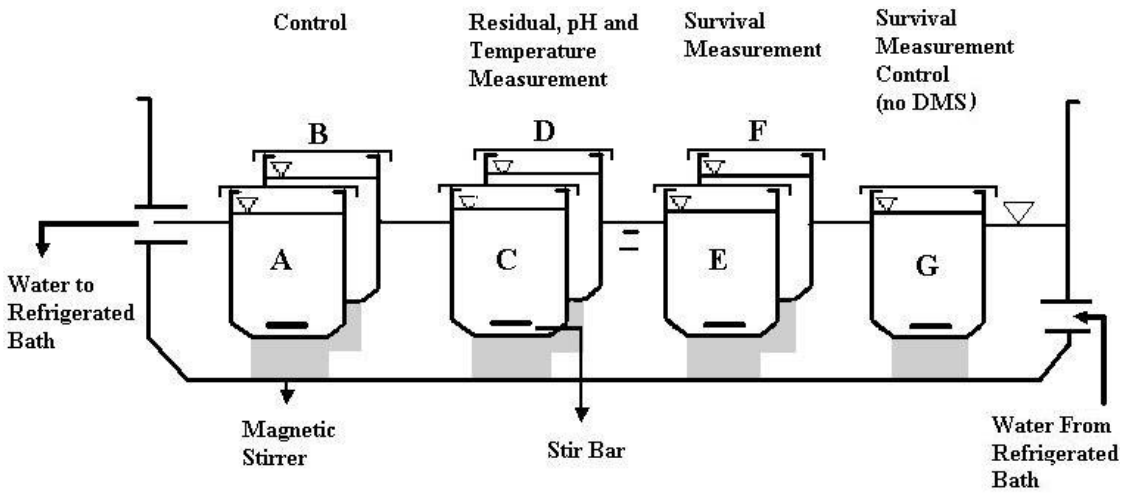

Figure 5.8: The configuration of batch reactors.

Reactor G. Disinfection control reactor for DMS experiments. This reactor was used only in DMS experiments. This rector was used to determine inactivation due to disinfectant in the absence of DMS.

5.3.3. Glassware and Utensil Preparation

All glassware was cleaned with liquid laboratory glassware cleaning solution (Alconox Powder Detergent; catalog no. 04-522-5, Fisher Scientific, Pittsburgh, PA) and rinsed with Milli-Q™ water. All glassware and utensils were sterilized by autoclaving at 121^0C for 15 minutes or more before and after they are in contact with microorganisms.

5.3.4. Demand-free Glassware Preparation

Ozone Demand-free: All glassware was soaked in 2 mg/L or more of ozone solution for 30 minutes or more and then dried at 110^0C for 5 hours to satisfy ozone demand.

Chlorine Demand-free: No significant chlorine demand by the glassware was observed.

5.4. Performance of Experiments

First, disinfectant demand-free experimental buffered solution was prepared and autoclaved the day before the experiment. On the day of the experimental run, certain amounts

of microbial suspensions of *G. muris*, *E. coli* or *B. subtilis* were added to the experimental buffered solution to obtain the desired initial microbial density. After mixing for 10 to 15 minutes, equal aliquots of experimental water (microbial suspension) were dispersed into batch reactors. In the inactivation of *E. coli* with monochloramine, the reactor volume was 1000 mL and in the rest of the experiments the reactor volume was 500 mL. In the inactivation of *E. coli* with monochloramine and *G. muris* with ozone, 3 reactors were used (A, C and E). In inactivation of *E. coli* with monochloramine in the presence of DMS experiments, 7 reactors were used (A through G). In the rest of the experiments, six reactors were used (A through F). In the DMS experiments, only 500 mL of this experimental water was added to reactor G. Then, 10^6 cell/mL equivalent of DMS was dosed to the remaining experimental water. After mixing for another 10 to 15 minutes, this experimental water was dispersed into the rest of the batch reactors, A through F. Next, the reactors were placed in the water bath on the submersible stirrers. The temperatures of the reactors were held constant at 15ºC in a circulating refrigerated water bath.

The stirrers were set to produce minimum vortex with appropriate mixing, and all the reactors were mixed at the same magnitude. Tracer tests showed that steady state conditions were reached in a reactor within 10 seconds of addition of 0.1 N NaCl.

At time zero (t = 0 minute), stock oxidant solution was added to reactors C, D, E, F and G to maintain the required disinfectant concentrations and the same amount of chlorine demand-free buffer was added to reactors A and B. The working monochloramine concentrations for disinfection of *E. coli* experiments and vegetative cells of *B. subtilis* were 0.75 mg/L, 1.0 mg/L and 1.5 mg/L. The applied ozone concentrations for disinfection of *B. subtilis* spore experiments were 1.5 mg/L, 2.0 mg/L and 2.5 mg/. In the disinfection of *G. muris* experiments, the applied ozone doses were 0.25 mg/L, 0.40 mg/L, 0.50 mg/L and 0.75 mg/L.

The *E. coli* and *B. subtilis* samples were removed from the reactor vessels by means of a 10-mL polystyrene sterile pipette and *G. muris* samples were removed by means of a 60 mL sterile HDPE syringe.

From reactors A and B, two samples (at the beginning and at the end of the experiment) were taken for control of microbial concentration and determination of initial microbial density during the course of the experiment. The sample size from these reactors was 10 mL in the experiments with bacteria (*E. coli* and *B. subtilis*) and each was taken into 16mm × 150mm glass tubes. The size of the samples in the *G. muris* experiments were 20 mL to 35 mL and they were taken into 35 mL centrifuge tubes which were already rinsed with eluting solution. The samples taken from reactors A and B were subjected to enumeration of viable organisms using the techniques described in Section 5.5.

From reactors C and D, three or more samples were taken to measure the residual disinfectant concentration and pH depending on the duration of the experimental run. A sample size of 30 mL was sufficient to make duplicate monochloramine measurements and pH measurements. In the ozone experiments, each sample size ranged from 30 mL to 60 mL to make triple ozone measurement. Since the ozone experiments were shorter, only one additional 10 mL sample was taken for pH measurement. Also a pre-sterilized thermometer was immersed into one of these reactors to monitor the temperature throughout the experiment.

From reactors E and F, five or more samples were taken at predetermined times, to determine the viability of organisms in the presence of the disinfectant. The volume of samples taken from these reactors was 9 mL. The disinfectant residuals in these samples were immediately quenched with excess sterile sodium thiosulfate (1 mL). Next, the samples were analyzed for viable organisms.

From reactor G, five or more samples were taken to determine the viability of organisms in the presence of disinfectant and in absence of DMS. The volume of the reactor and sampling time from the reactor were identical to reactors E and F. The disinfectant residuals in these

samples were immediately quenched with excess sterile 10% sodium thiosulfate (1 mL). Next, the samples were analyzed for viable organisms.

5.5. Microbial Enumeration

5.5.1. In vitro Excystation

5.5.1.1. Laboratory Apparatus

Sample tubes: 35 mL centrifuge tubes with conical bottom (Nalgene Inc International, catalog no. 3146-0050) were used to store the samples. The tubes were rinsed with eluting solution before the experiment. Then 0.2 mL of 0.5 M sodium thiosulfate was added to each sample tube.

Pipettes and Syringes: The samples were drawn from the reactors by means of a 60 mL sterile HDPE syringe (Becton Dickinson, Catalog No. 309664, Franklin Lakes, NJ). Also in the experiments 5, 10 and 25mL polystyrene sterile pipettes were used for washing samples, and for dosing proteose peptone, reducing solution and sodium bicarbonate. All the syringes and the pipettes in contact with cysts were rinsed with eluting solution in advance.

Glassware: All the glassware (reactors and graduated cylinder) was made demand-free before the experiment as described in Section 5.3.4. Also, they were rinsed with eluting solution before the experiments. The reactors were kept covered with aluminum foil throughout the experiments.

Incubator: A Precision® stainless steel water bath (Precision Scientific, Model No. 185, Chicago, IL) was used at a temperature setting of 37 ± 1ºC.

Microscope: A Phase contrast microscope was used to examine the *G. muris* cysts and trophozoites (Leica Microsystems Wetzlar GmbH, Model: Leitz Diaplan, Wetzlar, Germany).

5.5.1.2. Enumeration Procedures

Each 20 - 35 mL sample was centrifuged for 5 minutes at 5000 rpm (setting 5) in an lEC clinical centrifuge (rotor #215, r = 14.1 cm). After centrifugation, each sample was aspirated down to 1 mL. This remaining 1 mL of sample was used for the excystation procedure to

determine cyst viability in each sample. *In vitro* excystation were performed by using a modified excystation procedure (Sauch, 1988). 10 mL of reducing solution was added to the 1 mL sample, and approximately 7-10 mL of 0.1 N sodium bicarbonate was added to bring the sample to a final pH of 4.7. The suspension was then vortexed and placed into a heated water bath to incubate for 30 minutes at 37^{o}C. The sample was then removed and again centrifuged for two minutes at 6000 rpm (setting 6). After this centrifugation, the sample was again aspirated down to 1 mL and then it was washed by the addition of 20 mL of excystation medium. Next, the sample was centrifuged at 6000 rpm for two minutes. After aspiration down to 1 mL again, 1 to 11 mL of 0.5 % prewarmed proteose peptone in PBS (instead of distilled water) was added to the sample. The amount of 0.5% prewarmed proteose peptone was governed by the expected cyst density. Next, the sample was incubated for 45 minutes at 37ºC, after which time it was removed, vortexed, and counted.

5.5.1.3. Volumetric Method

Each sample was examined using phase contrast microscopy and quantified by hemocytometer count. The *G. muris* cysts and trophozoites were examined by a phase contrast microscope (Leica Microsystems Wetzlar GmbH, Model: Leitz Diaplan, Wetzlar, Germany) at 400 magnification. For each of these samples, a count of the partially and fully excysted trophozoites present were recorded along with the corresponding volume of sample scored by the hemocytometer (Hausser Scientific Company, Catalog No. 3100, Horsham, PA) (Haas *et al*., 1994).

The volume of sample examined in each hemocytometer slide (Figure 5.9) was 1.8µl (two 3mm × 3mm cells). The trophozoite density in the sample was calculated by the following relationship:

$$\#\ \text{of organism/mL} = \frac{\sum N}{n \times 1.8 \times 10^{-3}\, ml} \times \frac{V_{final}}{V_{sample}}$$

where, n is the number of slides counted

ΣN is the total number of trophozoites in "n" slides

V_{sample} is the volume of sample taken from the rector (mL).

V_{final} is the final volume of sample after excystation (mL).

For each sample at least two slides were counted, which corresponds to a detection limit of 16 trophozoites/mL.

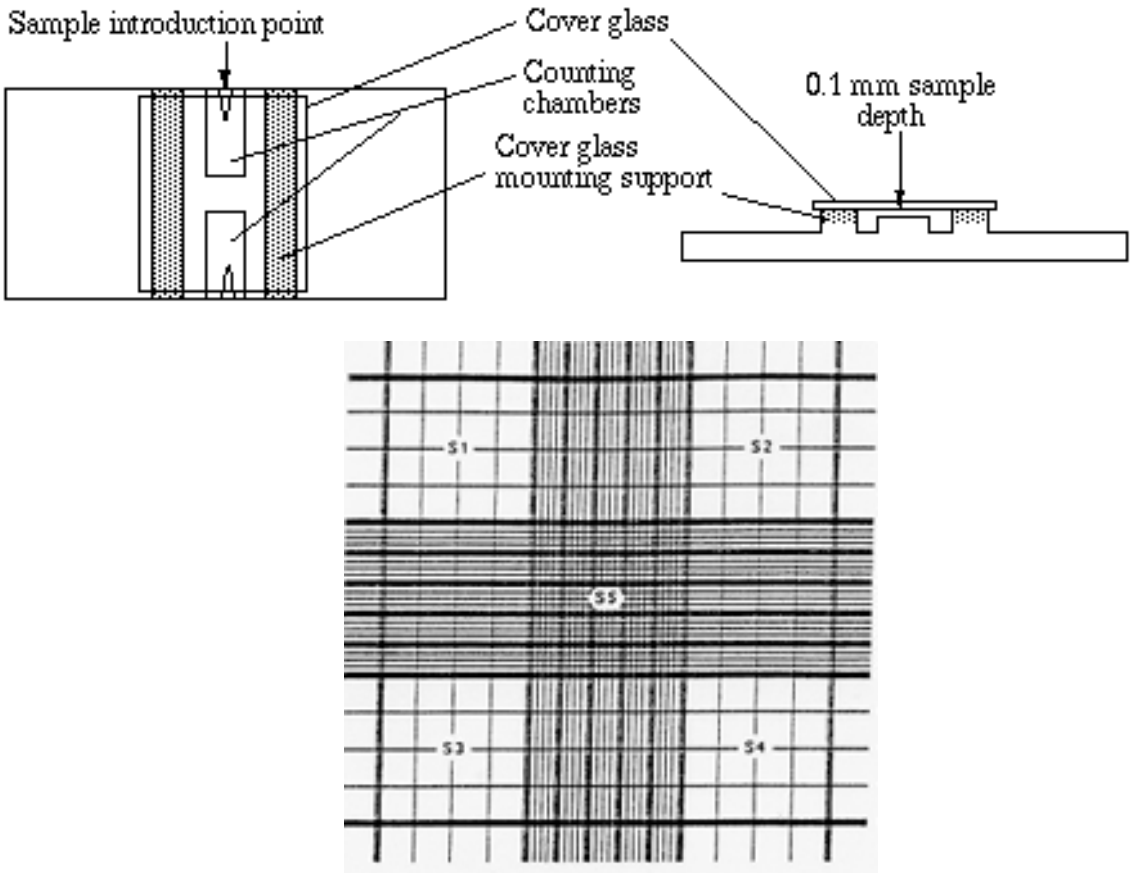

Figure 5.9: Hemocytometer. Top panel shows the complete hemocytometer and the bottom panel shows a single counting chamber of a hemocytometer. (*Source:* http://www.ruf.rice.edu/ ~bioslabs/methods/microscopy/countgrid.gif).

5.5.2. Membrane Filtration

5.5.2.1. Laboratory Apparatus and Media

Growth Medium: Bacto nutrient agar (Difco™ catalog number 0001-17) was used for the maintenance of *E. coli* cultures and the incubation of *E. coli* samples. R2A medium (Difco Cat. No. 1826-17-1) was used for the maintenance and sporulation of *B. subtilis*. Nutrient rich TSB (BBL Cat. No. 211768) was used in overnight growth of the *B. subtilis* samples during the enumeration process. Nutrient broth (Difco™ Cat. No. 00003-01) was used for the preparation of exponential phase cultures. They were prepared according to manufacturer's specifications. Nutrient agar and R2A agar were dispersed to disposable, sterile, plastic, 50mm x 11mm size Petri dishes (culture dishes) and 16 mm × 150 mm size autoclavable plastic capped glass tubes (slants) using aseptic procedures. TSB was added to 50 mm × 11 mm size Petri dish pads until the pad was saturated with TSB (1.5 mL) using aseptic procedures. 50 mL of nutrient broth was distributed to 8 oz wide mouth HDPE bottles and autoclaved for 15 minutes.

Glassware: Sterility and aseptic technique were key elements in successful membrane filtration analyses. All the glassware in contact with *E. coli* and *B. subtilis* were autoclaved for 15 minutes or more before the experiment. The glass beakers were covered with aluminum foil before autoclaving.

16 mm × 150mm size autoclavable glass tubes were used for dilution and sampling. Before the experiment, 9 mL of dilution water and 1 mL of 0.5 M sodium thiosulfate were added to each dilution and sampling tubes, respectively. Next, these tubes were covered with plastic caps and autoclaved for 15 minutes or more.

Pipettes: In the experiments 10 mL polystyrene sterile pipettes were used for taking samples from reactors A, B, E, F and G. 1 mL borosilicate sterile pipettes were used for dilution and 2 and 5 mL polystyrene sterile pipettes were used for dispersing the decimal dilution to membrane filters.

Culture dishes: Disposable, sterile, plastic 50 mm × 11 mm sterile Petri dishes and Petri dish pads with tight fittings were used. These dishes were stored in plastic sealed boxes.

Filtration units: The filter holding assembly (constructed of autoclavable plastic) that was used in these experiments consisted of a seamless funnel fastened to a base by magnetic force. The design permitted the membrane filter to be held securely on the porous plate of the receptacle without mechanical damage and allowed all fluid to pass through the membrane during filtration. The top open portion of the assembly was covered tightly with aluminum foil and the assembly was sterilized in autoclavable pouches for 15 minutes or more before an experiment.

Membrane filter: Pre-sterilized, individually wrapped, 47 mm GN-6 grid with 0.45 µm pore size membrane filters (Gelman Sciences, Cat. No. 66068, Ann Arbor, MI) were used in the experiments.

Forceps: Smooth-tipped forceps without corrugation on the inner sides of the tips was used. They were sterilized before use by dipping in 95 percent ethyl alcohol and then flaming (APHA *et al*., 1995).

Incubator: A Precision® mechanical convection (Precision Scientific, model no. 4EM, Chicago, IL) type incubator was used to provide a temperature of 37 ± 0.5ºC for incubation of *E. coli* and 35 ± 0.5ºC for incubation of *B. subtilis* at a high level of humidity (approximately 90 percent relative humidity) (APHA *et al*., 1995).

Milli-Q™ water: 500 mL autoclavable squeeze bottles were filled with Milli-Q™ water and the tips of the bottles were covered with aluminum foil and autoclaved for 15 minutes or more. This water was used to rinse the filter holding assembly after the filtration of each sample. Also, at each filtration, at least 10 mL of this water was added to the membrane filter holder to ensure a uniform distribution of microorganisms over the membrane filter.

Water bath*:* A water bath (Precision Scientific, model no. 185, Chicago, IL) at 75ºC was used to kill vegetative cells and activate spore germination. The spore suspension and the samples were placed in the water bath for 15 minutes for pasteurization.

5.5.2.2. Enumeration procedure

Escherichia coli:

The membrane filtration procedure was used to analyze the samples for *E. coli* (APHA *et al*., 1995). Lower equivalent volumes of sample sizes were achieved by dilution. The decimal dilutions of samples were prepared by the addition of 1 mL sample to pre-sterilized dilution tubes containing 9 mL dilution water. The resulting dilution tube contained 10^{-1} mL equivalent volume of sample per mL of diluted sample. In a similar method, further decimal dilutions were prepared using aseptic technique. The dilution tubes were vortexed at each step. The dilution tubes were stored in the refrigerator until the filtration step. The dilution tubes were kept at room temperature for not more than 30 minutes.

Before starting filtration, the nutrient agar or TSB plates were labeled according to sampling time (e.g., 1 minute, 2 minutes, etc.), sample ID (e.g., Reactor A, Reactor B) and equivalent sample volume (e.g., 10^{-2} mL, 10^{-3} mL, etc.). Then, 1 mL of each diluted sample was added to a membrane filter holder using aseptic technique. Also, at least 10 mL of autoclaved Milli-Q™ water was added to the membrane filter holder to ensure a uniform distribution over the membrane filter. In the inactivation of stationary phase *E. coli,* three replicates of each dilution were filtered. In the rest of the experiments, due to a higher number of samples, two replicates of each dilution were filtered. The filters were removed from the filter holding assembly by sterilized forceps and placed on the culture dishes. The dishes were next placed into the incubator. The membrane filter holders were rinsed with sterilized Milli-Q™ water before a new membrane filter was placed on the membrane filter holder for filtration of the next sample. The membrane filters with no growth at the end of incubation showed that there was no carryover of cells between filtration of each sample.

Incubation: The culture dishes were incubated for 24 to 25 hours at 37 ± 0.5ºC. At the end of the incubation period, the number of colonies were counted using a Quebec® colony counter.

The concentration of the organisms was computed by

$$N = \frac{\sum_i Nc_i}{\sum_i V_i} \tag{5.1}$$

where the summation is taken over all replicates of the particular sample. Nc_i and V_i are the number of colonies in each culture dish and equivalent volume (mL) of sample in a particular replicate analysis, respectively. The results were tabulated as colony forming units (CFU) per mL and recorded in spreadsheet files.

Bacillus subtilis:

The viability of spores was determined by a modified membrane filtration method (Barbeau *et al*., 1999). Prior to filtration, the samples were pasteurized at 75ºC for 15 minutes to kill all the vegetative cells and to activate spore germination. Next, the decimal dilutions of samples were prepared as described above. The dilution tubes were stored in the refrigerator until the filtration step. The dilution tubes were kept at room temperature for not more than 30 minutes.

The same procedures as used for the filtration of *E. coli* samples were followed for *B. subtilis* samples with the exception that the filters were placed on TSB Petri dish pads.

Incubation: The culture dishes were incubated for 24 to 25 hours at 35 ± 0.5ºC. At the end of incubation period the number colonies were counted by using a Quebec® colony counter.

The microbial concentrations of the organisms were computed by the same formula as for the *E. coli* experiments (Equation 5.1).

The aseptic techniques described here and used in the experimental procedure were verified by conducting the complete disinfection experiment using sterilized buffered water

instead of a microbial suspension at the beginning. All the steps were identical to disinfection experiments conducted in this study. At the end, after incubation of membrane filters at 37ºC for 24 hours, no growth was observed in any of the 35 membranes. This verifies the aseptic conditions and techniques during disinfection experiments in this study.

6. EXPERIMENTAL INVESTIGATION OF CELL DENSITY EFFECT ON DISINFECTION EFFICIENCY

The main objective of this study was to investigate whether the process of disinfection of microorganisms in water is dependent on the initial cell population. To satisfy this objective, a series of disinfection experiments were conducted as described in Chapter 4 using the methods described in Chapter 5. In these experiments, the survival of organisms was measured at various applied disinfectant doses, times and initial microbial densities. The results of these experiments were analyzed using multiple linear regression and nonlinear regression in order to investigate the best regression model with the subset of predictors that have statistically significant effects on the response variable (survival of organisms).

6.1. Results

A total of 7 series of disinfection experiments were conducted using three different microorganisms and two different disinfectants. These series can be summarized as follow:

- *B. subtilis* spores experiments: Batch cultures of *Bacillus subtilis* spores were inactivated with ozone.
- *B. subtilis* log experiments: Batch cultures of *Bacillus subtilis* vegetative cells in exponential (logarithmic) growth phase were inactivated with preformed monochloramine.
- *G. muris* experiments: *Giardia muris* cysts were inactivated with ozone.
- *E. coli* (batch) experiments: Batch cultures of *Escherichia coli* in stationary growth phase were inactivated with preformed monochloramine.
- *E. coli* chemostat experiments: Continuous cultures of *Escherichia coli* at stationary growth phase were inactivated with preformed monochloramine.
- *E. coli* log experiments: Batch cultures of *Escherichia coli* in exponential (logarithmic) growth phase were inactivated with preformed monochloramine.

- *E. coli* DMS experiments: Batch cultures of *Escherichia coli* in stationary growth phase were inactivated with preformed monochloramine in the presence of disinfected microbial suspension (DMS).
- *E. coli* DMS control data: Batch cultures of *Escherichia coli* in stationary growth phase were inactivated with preformed monochloramine in the absence of disinfected microbial suspension (conducted simultaneously with *E. coli* DMS experiments).

The summary of temperature and pH of each experimental series is given in Table 6.1 and Table 6.2, respectively.

Table 6.1: Summary of temperatures in each experimental series.

Experiments	Number of Experiments	Temperature (ºC)			
		Mean	Minimum	Maximum	St Dev
G. muris	19	15.0	14.0	16.0	0.37
E. coli batch	21	15.0	13.0	16.0	0.78
E. coli log	24	14.8	14.0	15.0	0.33
E. coli DMS	24	14.8	14.5	15.0	0.24
E. coli chemostat	24	14.7	14.0	15.0	0.39
B. subtilis spores	24	14.6	14.0	15.5	0.46
B. subtilis log	18	14.9	14.5	15.0	0.16

Table 6.2: Summary of pH in each experimental series.

Experiments	Number of Experiments	pH			
		Mean	Minimum	Maximum	St Dev
G. muris	19	8.03	7.94	8.17	0.06
E. coli batch	21	7.02	6.91	7.11	0.05
E. coli log	24	6.99	6.82	7.09	0.07
E. coli DMS	24	7.04	6.99	7.12	0.04
E. coli chemostat	24	7.00	6.89	7.15	0.07
B. subtilis spores	24	7.96	7.87	8.07	0.06
B. subtilis log	18	7.95	7.88	8.03	0.04

All the raw data obtained from seven of the experimental series are given in Appendix A. The plots of initial microbial doses against the applied disinfectant doses of each experiment

are also given in Figure 6.1 through Figure 6.7. As seen in these plots the proposed initial microbial density range have been covered in all the experiment series except *B. subtilis* log experiment series. In these series of experiments due to slow growth rate of *B. subtilis,* it was not feasible to conduct inactivation experiments at higher initial microbial densities. However, the initial microbial density in these series of inactivation experiments ranged over 20 fold. Inactivation of this organism has not been studied over a deliberately this much wide range of N_o.

The experimental inactivation data from each series was analyzed separately, using multiple linear regression and nonlinear regression methods. The basic purpose of these methods was to investigate the independent variables and the significance of their effect on disinfection efficiency. Before analyzing the inactivation data, the kinetics of the disinfectant residuals were analyzed.

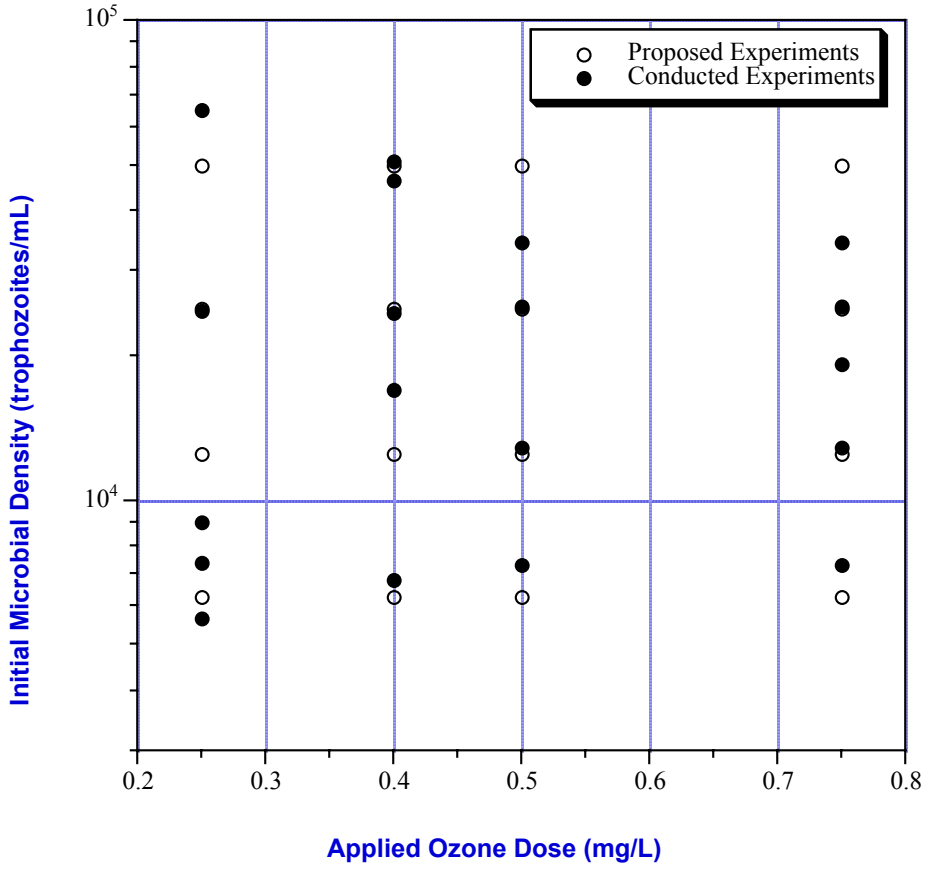

Figure 6.1: Comparison of the designed and performed disinfection of *G. muris* experiments.

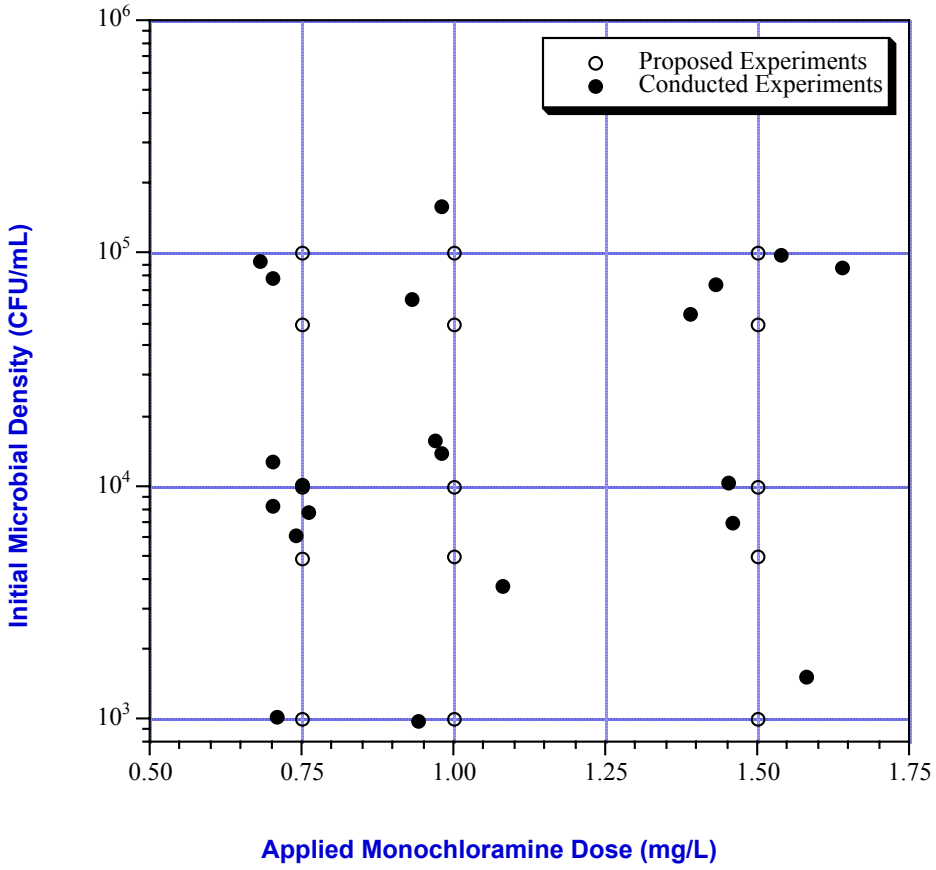

Figure 6.2: Comparison of the designed and performed disinfection of *E. coli* batch experiments.

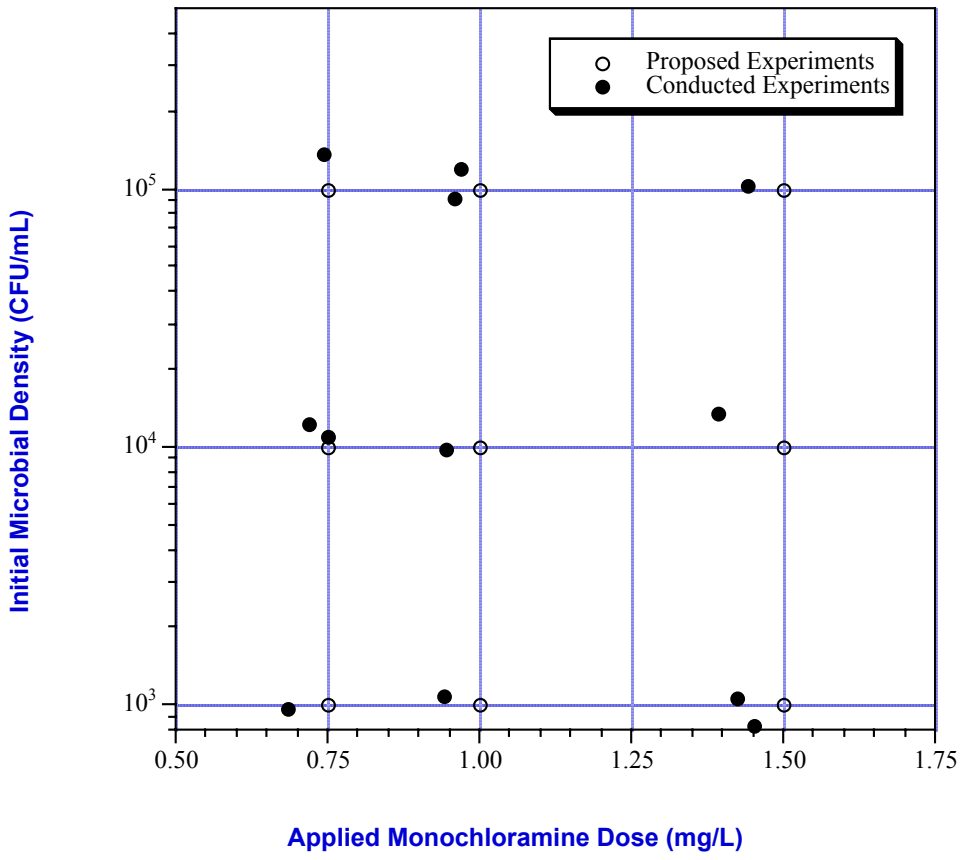

Figure 6.3: Comparison of the designed and performed disinfection of *E. coli* log phase experiments.

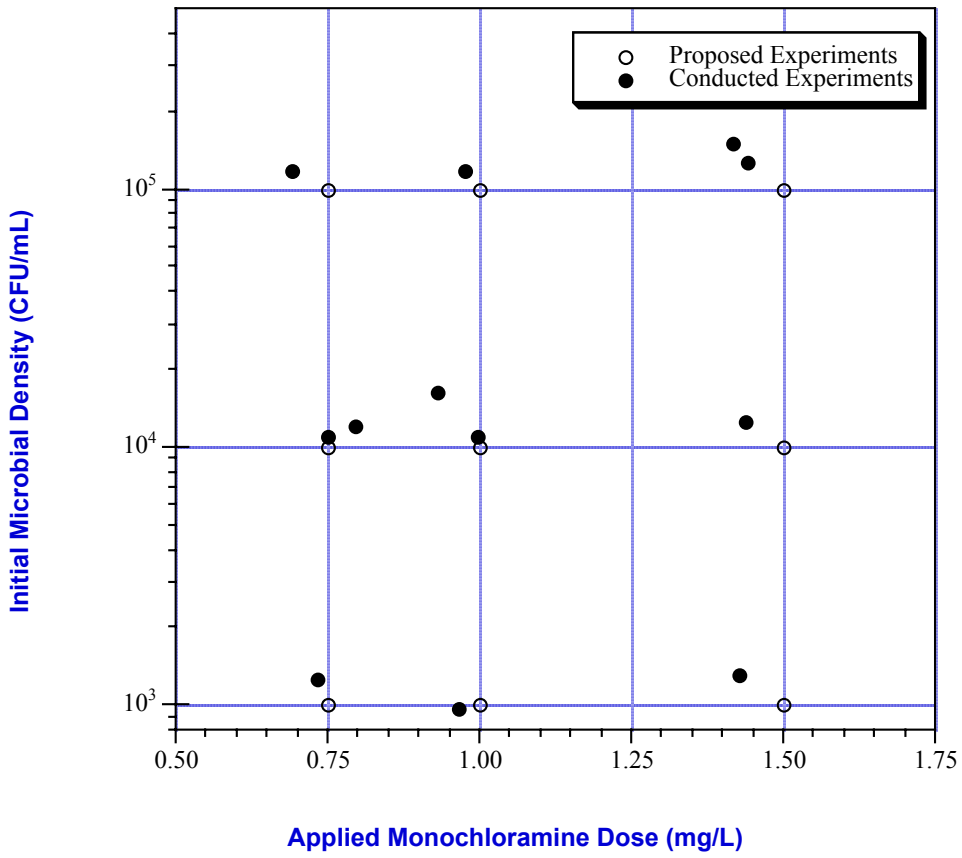

Figure 6.4: Comparison of the designed and performed disinfection of *E. coli* DMS experiments.

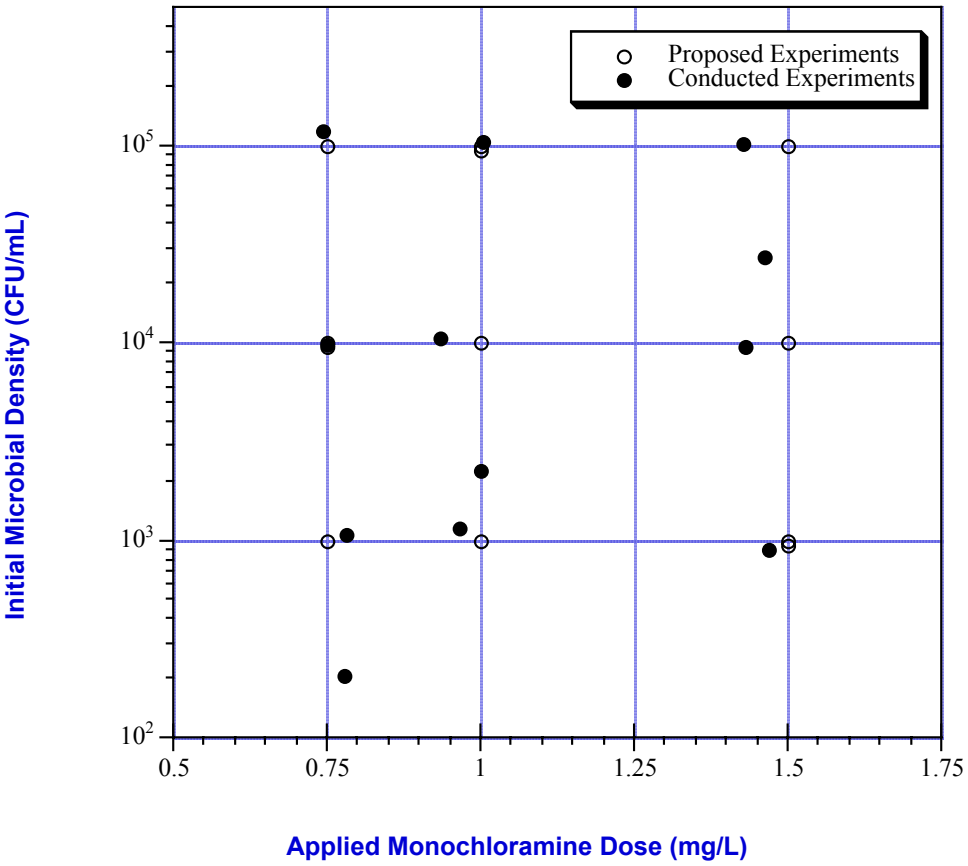

Figure 6.5: Comparison of the designed and performed disinfection of *E. coli* chemostat experiments.

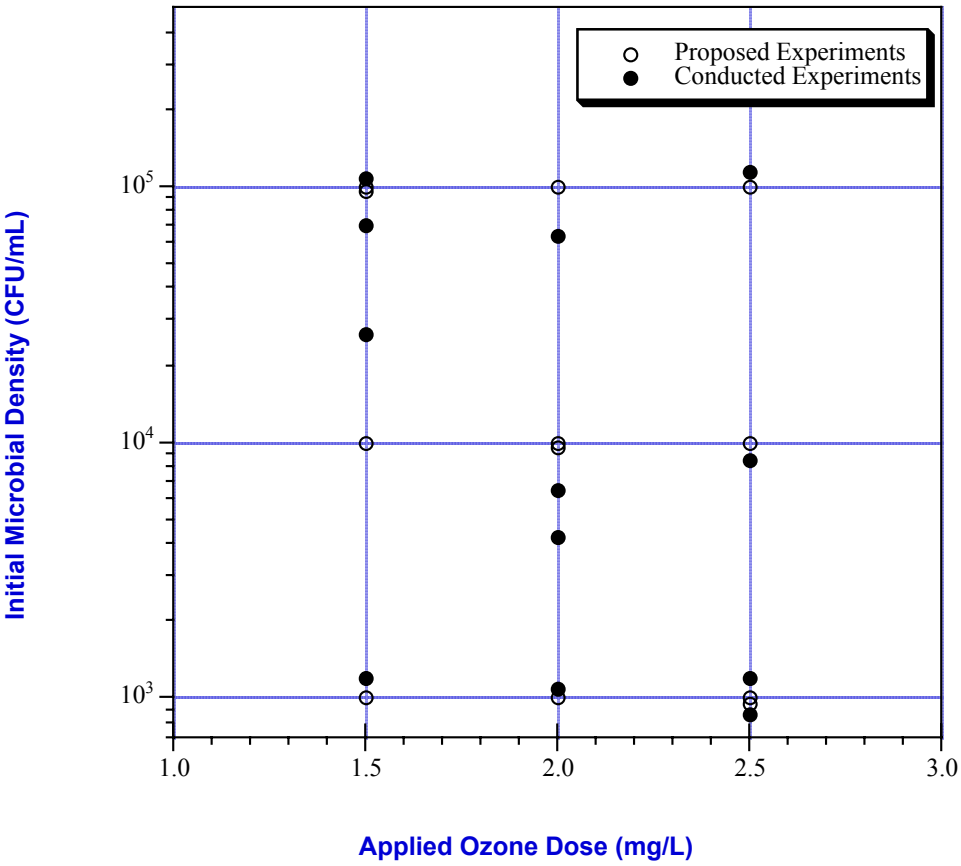

Figure 6.6: Comparison of the designed and performed disinfection of *B. subtilis* experiments.

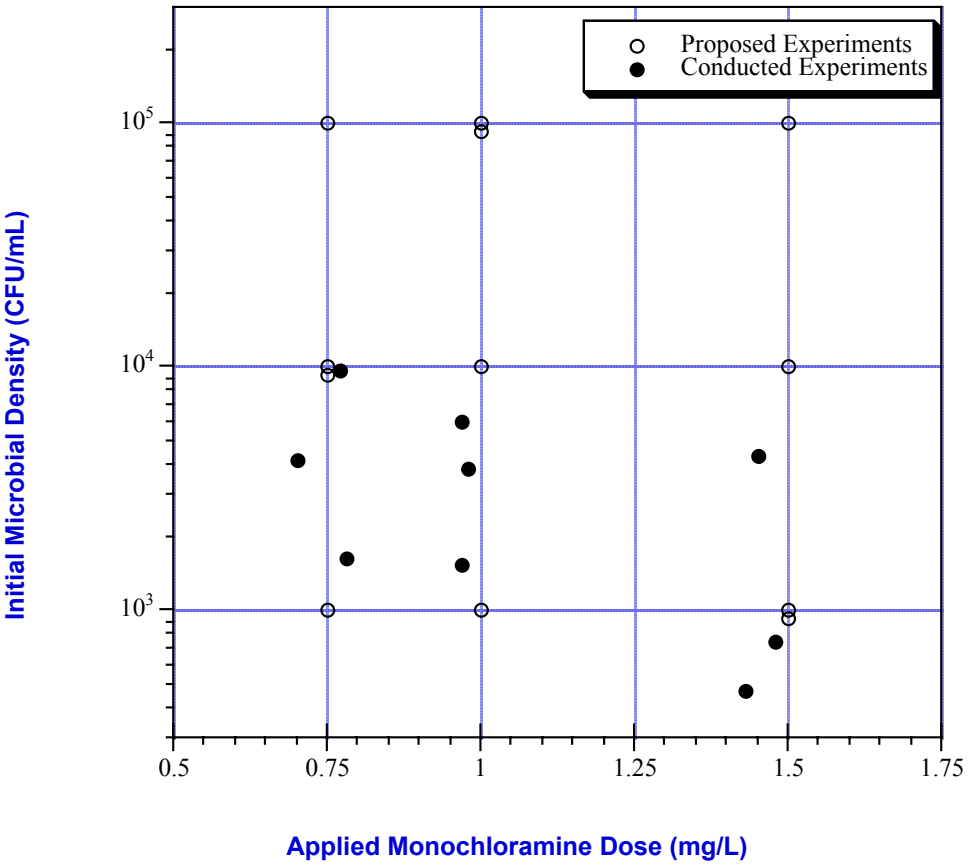

Figure 6.7: Comparison of the designed and performed disinfection of *B. subtilis* log phase experiments.

6.2. Kinetic Analysis of Disinfectant Residual

The disinfectant concentration is likely to decrease during the contact time. Disinfectant demand-free conditions are unlikely for most oxidants. Decreases in disinfectant residuals are attributed to demand caused by particulate, reduced inorganic species, organic matter, microorganisms, volatilization, and reaction of the disinfectant with water (Haas and Finch,

1999). Although the microbial cultures were washed with sterile Milli-Q™ water, some instantaneous demand of ozone was observed in the experimental water.

In many cases, following any initial disinfectant demand being satisfied, the rate of disappearance of chlorine species, and ozone in aqueous solution can generally be described by first-order kinetics (Haas and Karra, 1984). In other words, if the applied dose of disinfectant is equal to C_a, then the residual at time t (C_t, in batch systems) can be written as:

$$C_t=(C_a-D)\exp(-k^*t) \qquad (6.1)$$

where C_a is the applied disinfectant dose (mg/L), D is the instantaneous disinfectant demand (mg/L), k^* is the first order disinfectant decay rate ($time^{-1}$) and t is time. The term initial residual (C_0) is used for disinfectant concentration right after the instantaneous demand being satisfied (C_a-D).

In the inactivation with ozone experiments, significant instantaneous demand was observed. The ozone residual data were fit to first order decay using instantaneous demand model (Equation 6.1). In the inactivation with monochloramine experiments, there was no significant demand and the instantaneous demand model predicted a negative decay rate (k^*) in some cases. Therefore, the first order decay without instantaneous demand model was used for the monochloramine data. In these cases, the parameter D was set to zero in Equation 6.1. In other words, the initial residual (C_o) was equal to the applied dose (C_a).

The values of the first order disinfectant decay rate (k^*) and the instantaneous demand (D) were determined by nonlinear least-squares regression. In this approach, the best-fit values of k^* and D were estimated as the values that minimized the sum of squares of the difference between predicted and observed disinfectant residuals;

$$\text{RSS} = \text{minimum}\sum\left[C_{predicted} - C_{observed}\right]^2$$

where, $C_{observed}$ is the actual disinfectant concentration measured (mg/L) and $C_{predicted}$ is the corresponding concentration (mg/L) predicted using Equation 6.1.

The values of k^* and D were estimated for each experiment separately. All the non-linear least squares in this study were done using non-linear optimization in MATLAB® (The Math Work, Inc., 1984-1996).

The summary of the disinfectant kinetic analysis for each experiment with monochloramine and ozone are given Table 6.3 and Table 6.4, respectively. In these tables, the adjusted coefficients of determination (adjusted r^2) of each model fit were calculated using Equation 6.2.

$$\text{Adjusted } r^2 = 1 - \frac{RSS/(n-p)}{TSS/(n-1)} \tag{6.2}$$

where, n is the number of observations, p is the number of parameters where separate parameters were used for each experiment, RSS is residual sum of squares, and TSS is total sum of squares.

In addition, the regression plots for each of the experimental series are given in Figure 6.8 through Figure 6.14. The estimated disinfectant decay rate (k^*) and instantaneous demands (D) for each experiment are presented in Appendix B.

Table 6.3: Summary of monochloramine decay rates in each experimental series.

	Decay Rate (minutes^{-1})		
Experiments	Average	Standard Deviation	Adjusted r^2
E. coli batch	1.71×10^{-3}	2.39×10^{-3}	0.9997
E. coli Log	1.71×10^{-3}	1.68×10^{-3}	0.9999
E. coli Chemostat	6.41×10^{-4}	4.91×10^{-4}	0.9999
E. coli DMS	2.07×10^{-3}	1.75×10^{-3}	0.9999
B. subtilis Log	2.01×10^{-4}	1.71×10^{-4}	0.9999
All	1.37×10^{-3}	1.80×10^{-3}	-

The kinetic analysis of disinfectant residuals showed that there was a substantial decay of ozone (average decay rate of 0.296 minutes^{-1}), whereas monochloramine was more stable (average decay rate of 1.37×10^{-3} minutes^{-1}) throughout the experiment runs.

Any correlation between initial microbial density and disinfectant decay and demand was also tested (Table 6.5). A significant correlation ($P < 0.05$) was observed only between ozone demand and initial *G. muris* density. The demand of ozone in *B. subtilis* spore experiments did not show any significant correlation with the initial density of spores. In neither of the experimental series disinfectant decay was correlated with initial microbial density.

Table 6.4: Summary of ozone demand and decay rates in each experimental series.

Experiments	Demand (mg/L)		Decay Rate ($minutes^{-1}$)		Adjusted r^2
	Average	Standard Deviation	Average	Standard Deviation	
G. muris	0.240	0.075	0.505	0.404	0.9882
B. subtilis spores	0.930	0.295	0.156	0.060	0.9968
All	0.654	0.412	0.296	0.308	-

Table 6.5: Pairwise correlation coefficient significance level and correlation coefficients between initial microbial density and disinfectant demand and decay rates.

Experiment-Model		Decay Rate	Demand
G. muris	Correlation Coefficient	0.2800	0.5834
	Probability	0.2935	0.0177
E. coli	Correlation Coefficient	-0.2279	N/A
	Probability	0.3204	N/A
E. coli Log	Correlation Coefficient	0.0152	N/A
	Probability	0.9627	N/A
E. coli DMS	Correlation Coefficient	-0.4114	N/A
	Probability	0.1839	N/A
E. coli Chemostat	Correlation Coefficient	0.1914	N/A
	Probability	0.5513	N/A
B. subtilis Spores	Correlation Coefficient	0.1588	-0.1623
	Probability	0.4587	0.4487
B. subtilis Log	Correlation Coefficient	0.0084	N/A
	Probability	0.9828	N/A

N/A: Not Applicable

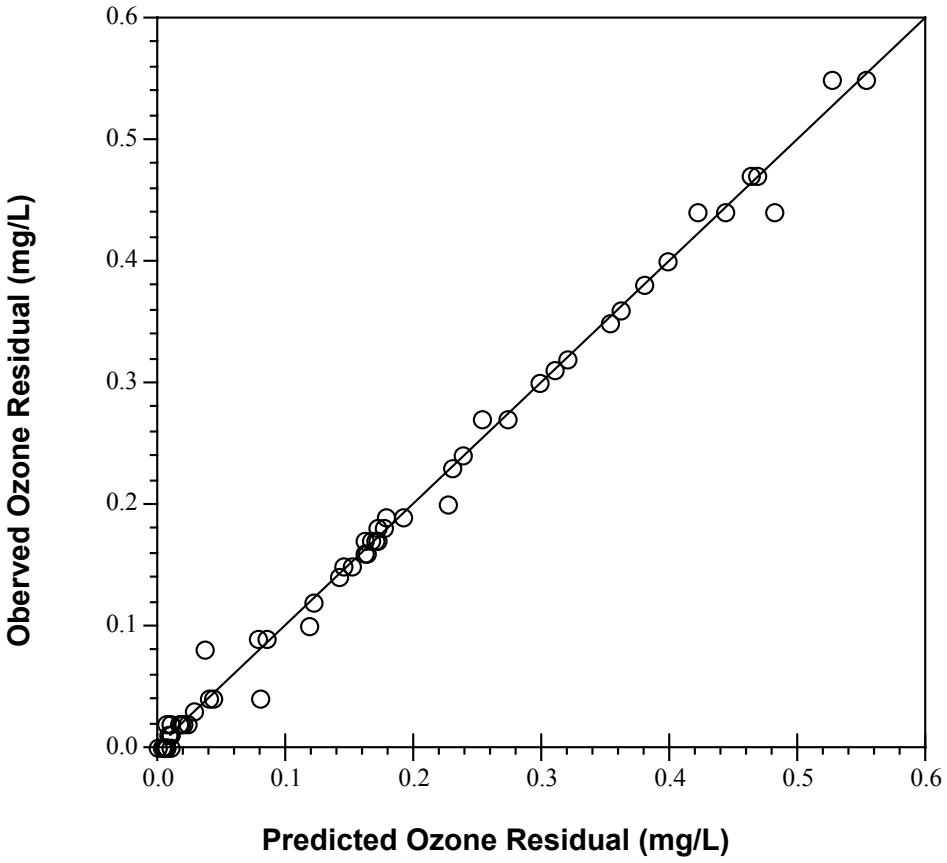

Figure 6.8: Plot of observed and fitted ozone residuals in *G. muris* experiments.

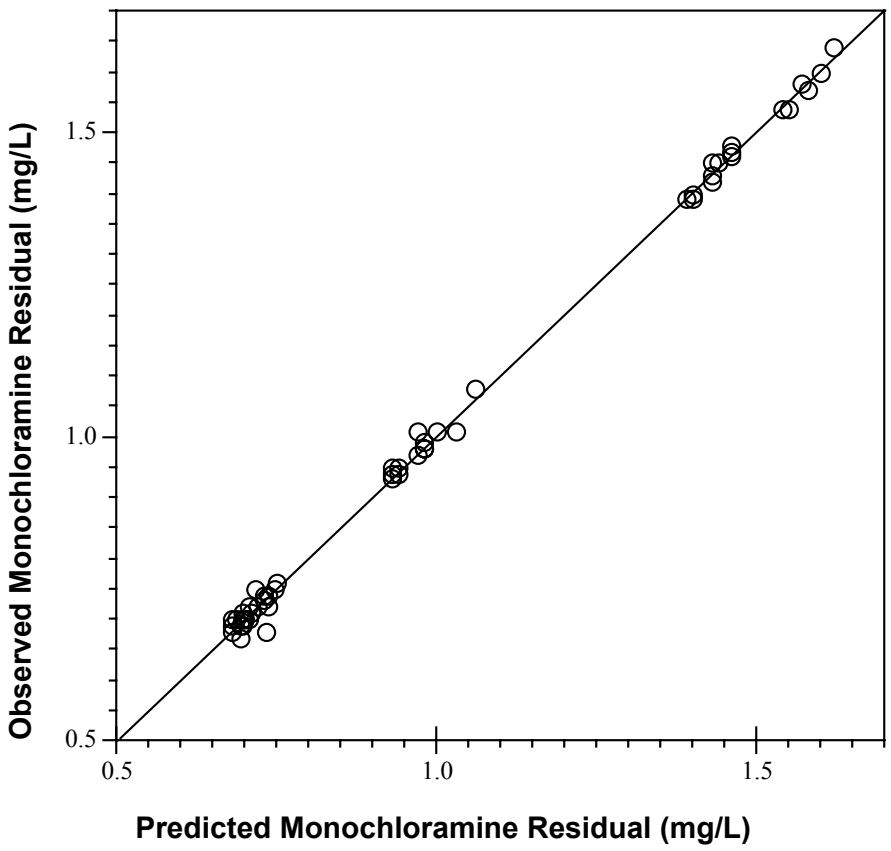

Figure 6.9: Plot of observed and fitted monochloramine residuals in *E. coli* batch experiments.

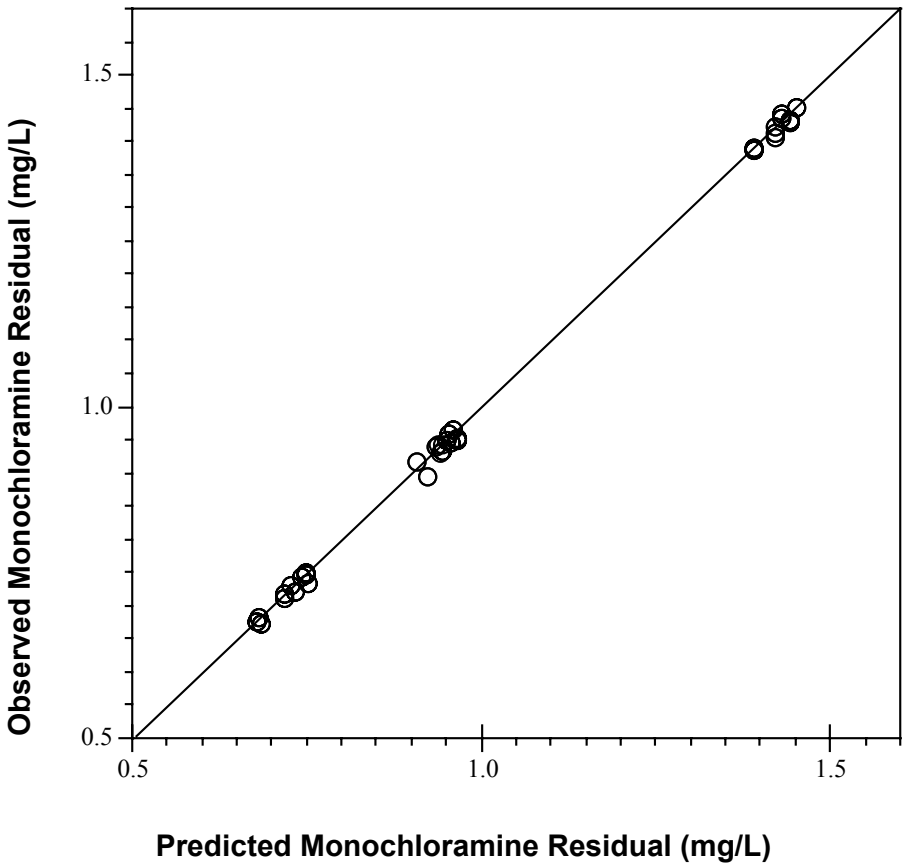

Figure 6.10: Plot of observed and fitted monochloramine residuals in *E. coli* log experiments.

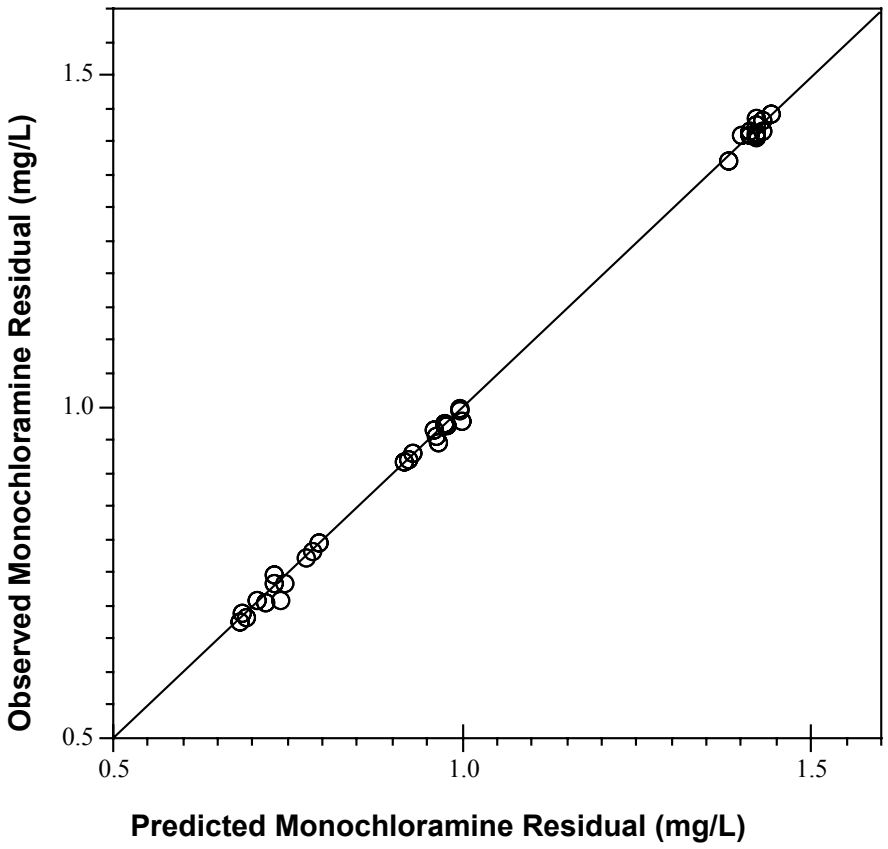

Figure 6.11: Plot of observed and fitted monochloramine residuals in *E. coli* DMS experiments.

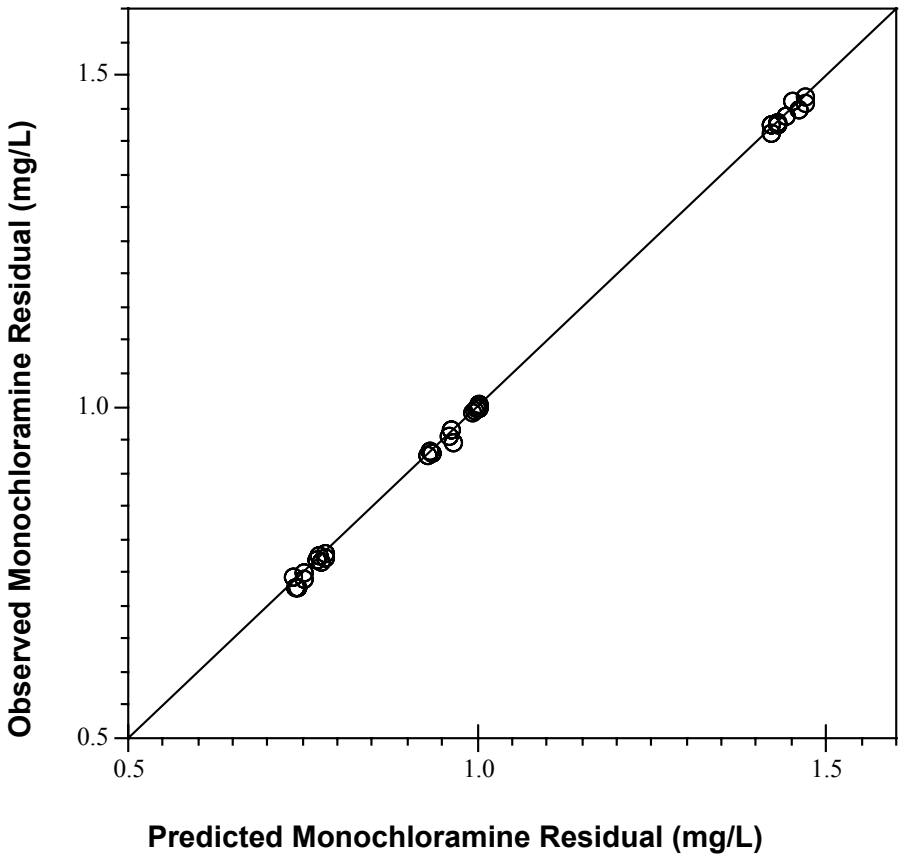

Figure 6.12: Plot of observed and fitted monochloramine residuals in *E. coli* chemostat experiments.

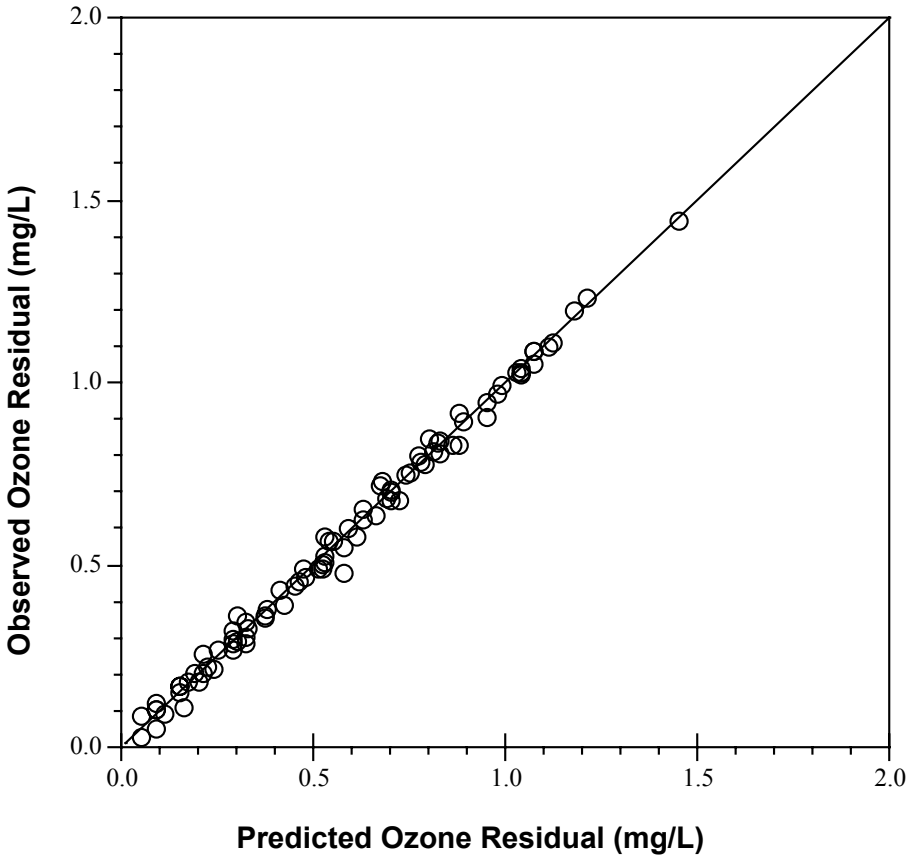

Figure 6.13: Plot of observed and fitted ozone residuals in *B. subtilis* spore experiments.

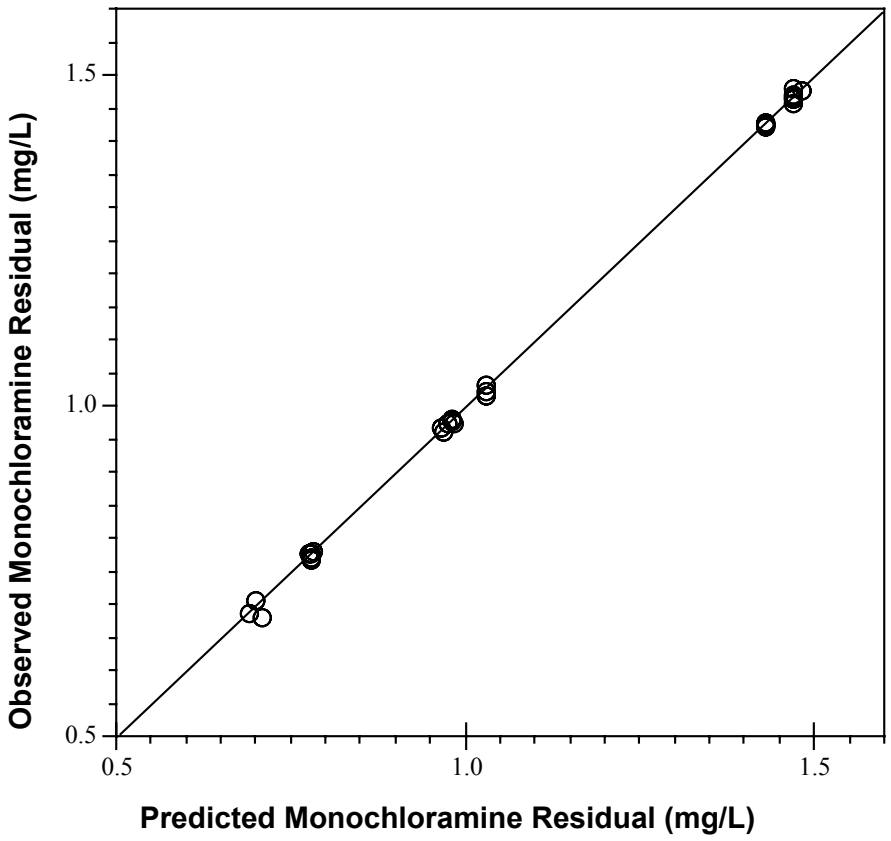

Figure 6.14: Plot of observed and fitted monochloramine residuals in *B. subtilis* log experiments.

6.3. Regression Analysis of Microbial Survival Data

The experimental inactivation data from each series of experiments were analyzed separately, using multiple linear regression and nonlinear regression methods. The basic purpose of the use of regression analysis was to express the nature of the relations between the independent variables and the response variable more precisely. In multiple linear regression and non-linear regression analyses, the relationship of survival with the experimental variables (time

(t), applied disinfectant doses (C_a) and initial microbial densities (N_o)) was estimated by expressing survival as a linear and a non-linear function of experimental variables, respectively. In addition, the regression was used to predict the survival in terms of time (t), applied disinfectant doses (C_a) and/or initial microbial densities (N_o).

6.3.1. Multiple Linear Regression

The main purpose for conducting a regression analysis was to determine the quantitative relation between the experimental variables (time (t), applied disinfectant doses (C_a) and initial microbial densities (N_o)), and the response variable (survival ratio (S)). With use of multiple linear regression (MLR), the mathematical form of equation relating survival ratio with time, applied disinfectant dose and initial microbial density, was developed.

During MLR analysis, time, disinfectant dose, N_0 and integrated CT product or simply CT were used as predictors. Integrated CT products were calculated using the estimated demand and decay rates in the previous section:

$$CT = \int_{t=0}^{t=t} (C_a - D)e^{(-k*t)}\, dt$$

Use of CT as an independent predictor takes disinfectant decay and demand terms into account in the developed model. In addition, use of logarithmic transformation of CT as a predictor would help to describe any nonlinear relation. To include the nonlinear relationships between survival ratio and initial microbial density, linear, quadratic and cubic logarithmic transformations of initial microbial density were used as independent predictors.

A total of 8 predictors (contact time, disinfectant dose, initial microbial density, CT, $\ln CT$, $\ln(N_0)$, $\ln^2(N_0)$, $\ln^3(N_0)$) were used to find the best combination of predictors that describe the inactivation data. With 8 predictors, there were 256 possible models for each data set. Therefore, it was not feasible to fit the data to each possible multiple linear model. Stepwise procedures were used to develop the model that included the predictors that had statistically significant ($P < 0.05$) effects on the dependent variable. The logarithmic transformation of

survival ratio was the response variable in the regression process. Only the data with non-zero survival was used in the regression analysis. A stepwise forward selection was conducted using statistical software, STATA 7™ (STATA Corp., 1985 - 2001). Forward selection starts with a model only with a constant, without any predictors, and adds the one with greatest *F* statistics. If the addition of the parameter makes significant improvement in the fit ($P < 0.05$), then the model with that variable is accepted. The process continues by adding one more predictor until a predictor with a non-significant ($P < 0.05$) partial regression slope is reached or all predictors are included (Quinn and Keough, 2002).

The predictors that had significant effects on logarithmic transformation of survival ratio are given in Table 6.6. The STATA 7™ output, including detailed statistics of stepwise regression of each data set is presented in Appendix C. Since stepwise regression starts with a constant without any predictors, the constant was included in the stepwise regression model whether it is significant or not. A nonsignificant constant was only observed in the stepwise regression of *B. subtilis* at exponential growth phase. Therefore, only for this set, MLR was conducted using the significant predictors in stepwise regression and without the constant.

The next step involved checking the normality of errors and the significance of correlation between errors and the predictors.

Based on the Shapiro-Wilk test for normal distribution of regression residuals, only the errors of regression of *E. coli* chemostat data were normally distributed. The residuals of the rest of the MLR were not normally distributed. Only the *E. coli* and *E. coli* log experiments had symmetrical regression residuals. The histograms of regression residuals are given in Figure 6.15 through Figure 6.22. In these plots, the solid line represents the normal distribution. None of the predictors had any significant ($P < 0.05$) correlation with regression residuals. The multiple linear models developed for each data set by stepwise regression are given in Table 6.8.

Table 6.6: Subsets of the predictors in the best-fit multiple linear model.

Experiment - Disinfectant	adj r^2	RSS	Predictors: Time	*Co*	*CT*	ln*CT*	N_o	lnN_o	ln^3N_o
G. muris – Ozone	0.54	91.33	√			√			
E. coli - Monochloramine	0.72	290.14			√	√		√	
E. coli log – Monochloramine	0.66	244.29			√	√			
E. coli DMS – Monochloramine	0.41	304.97			√		√	√	√
E. coli DMS Ctrl – Monochloramine	0.59	125.39			√				
E. coli chemostat – Monochloramine	0.85	131.10		√	√	√	√		
B. subtilis spores – Ozone	0.83	212.19	√	√	√				
B. subtilis log - Monochloramine	0.90	127.76		√		√			

Table 6.7: Significance of pairwise correlation of MLR residual with predictors and Shapiro-Wilk test for normal regression residuals.

Experiment	Probability of Predictors: Time	C_o	*CT*	ln*CT*	N_o	lnN_o	ln^3N_o	Normality *P*	Skewness *P*
G. muris	1.00			1.00				0.0229	0.013
E. coli			1.00	1.00		1.00		0.0007	0.202
E. coli log			1.00	1.00				0.0060	0.435
E. coli DMS			1.00		1.00	1.00	1.00	<0.0001	<0.001
E. coli DMS *Ctrl*			1.00					0.0138	0.012
E. coli chemostat		1.00	1.00	1.00	1.00			0.1057	0.021
B. subtilis spores	1.00	1.00	1.00					0.0113	0.019
B. subtilis log		0.60		0.62				<0.0001	<0.001

Table 6.8: MLR models for each inactivation data set developed using stepwise regression.

Experiment	
G. muris	$\ln S=-8.593843-1.787748\times \ln CT+0.9508017\times Time$
E. coli	$\ln S =6.152156-1.8085\times CT-0.506256\times \ln N_o+2.868479\times \ln CT$
E. coli log	$\ln S =2.716801-3.368067\times CT+5.5364\times \ln CT$
E. coli DMS	$\ln S =42.68778-0.6515395\times CT-8.44915\times \ln N_o-0.0001522\times N_o+ 0.0475057\times \ln^3 N_o$
E. coli DMS Ctrl	$\ln S =1.837306-0.9573994\times CT$
E. coli chemostat	$\ln S =2.753049-2.024963\times CT-1.560671\times C_o+2.917124\times \ln CT- 6.47\times 10^{-6}\times N_o$
B. subtilis spores	$\ln S =3.075749-0.9284106\times CT-0.3894717\times Time-1.635658\times C_o$
B. subtilis log	$\ln S =-1.85155\times \ln CT+1.222736\times C_o$

$\ln S = \ln(N/N_0)$

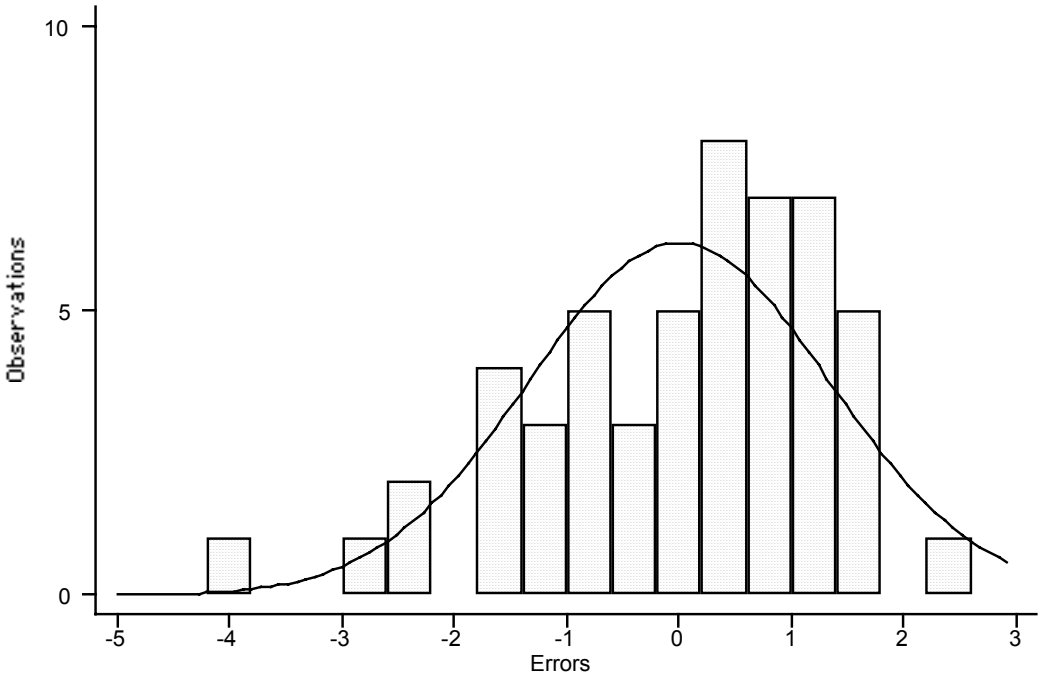

Figure 6.15: Distribution of MLR residuals of *G. muris* experiments.

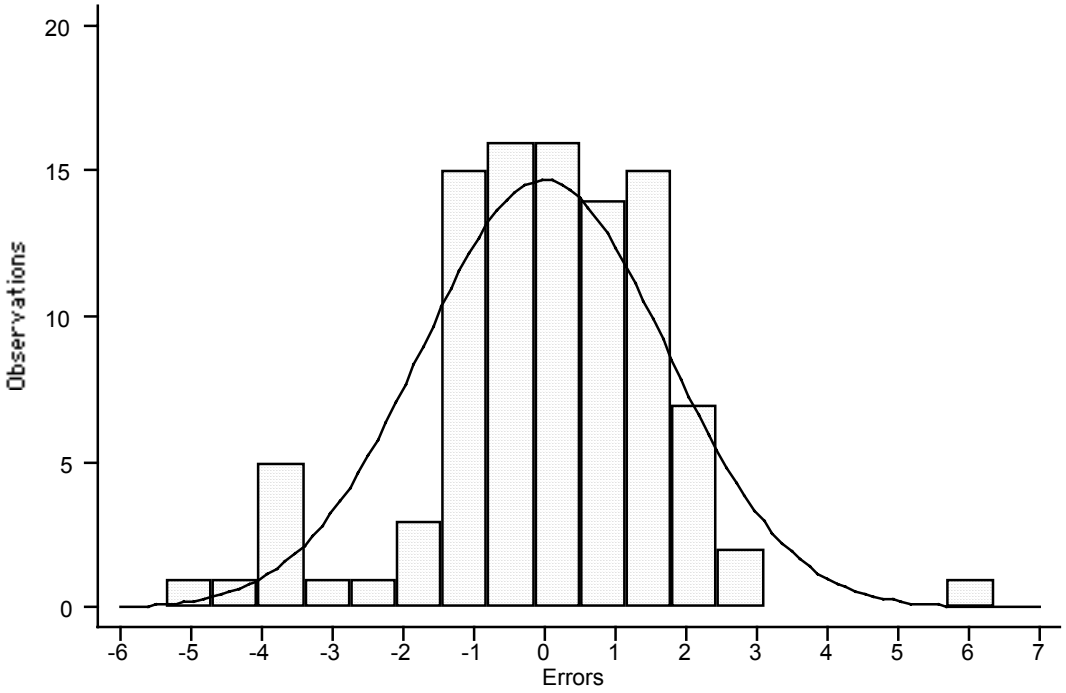

Figure 6.16: Distribution of MLR residuals of *E. coli* batch experiments.

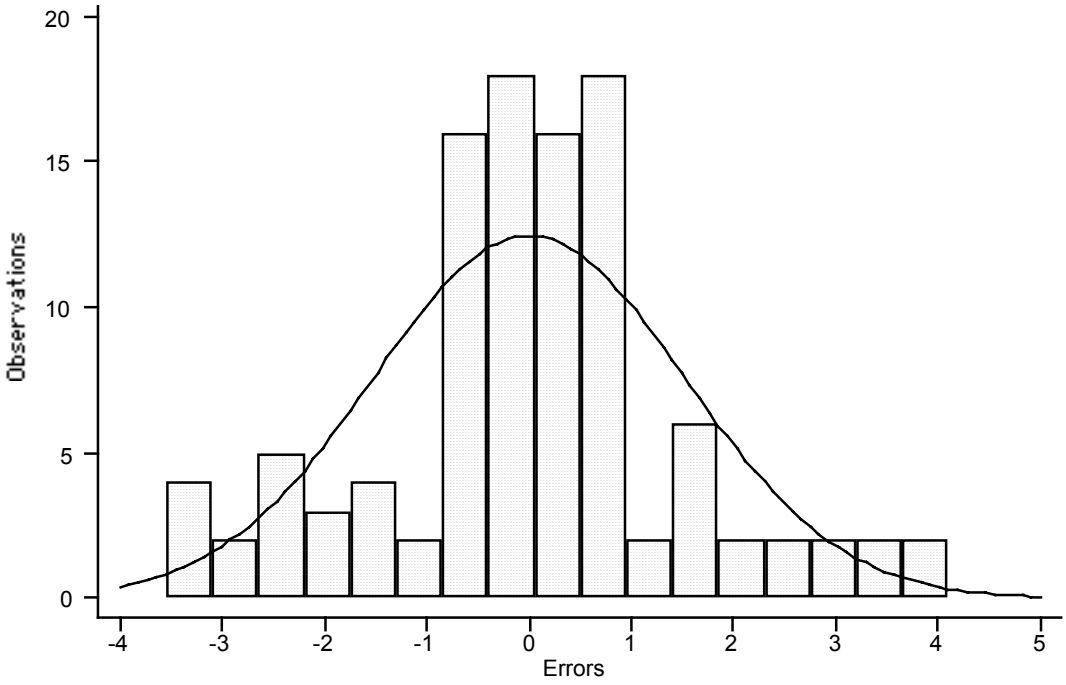

Figure 6.17: Distribution of MLR residuals of *E. coli* log experiments.

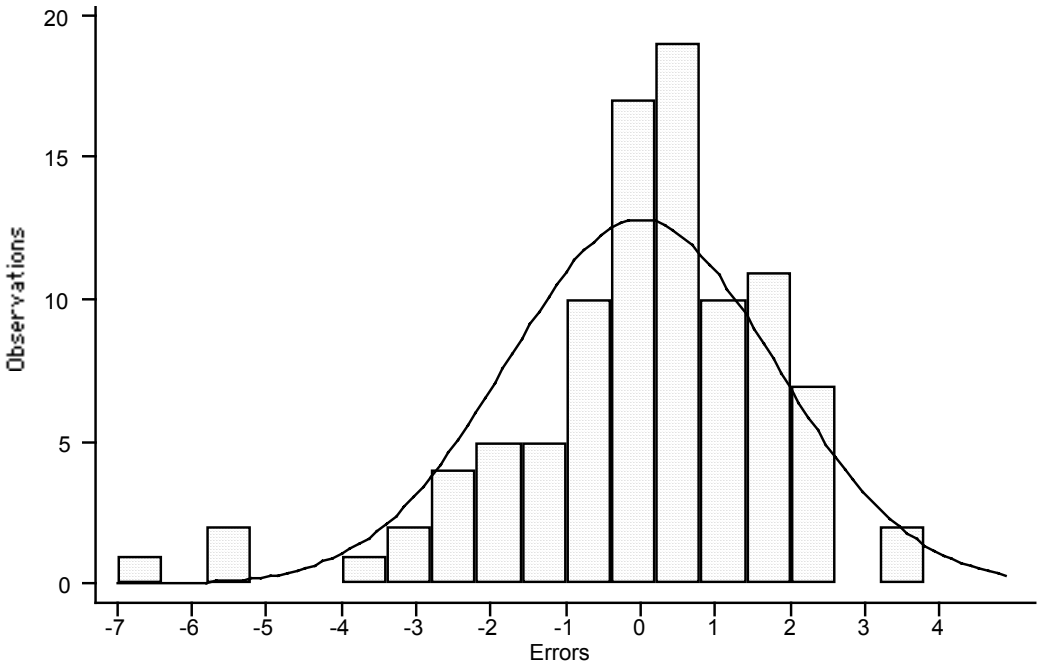

Figure 6.18: Distribution of MLR residuals of *E. coli* DMS experiments.

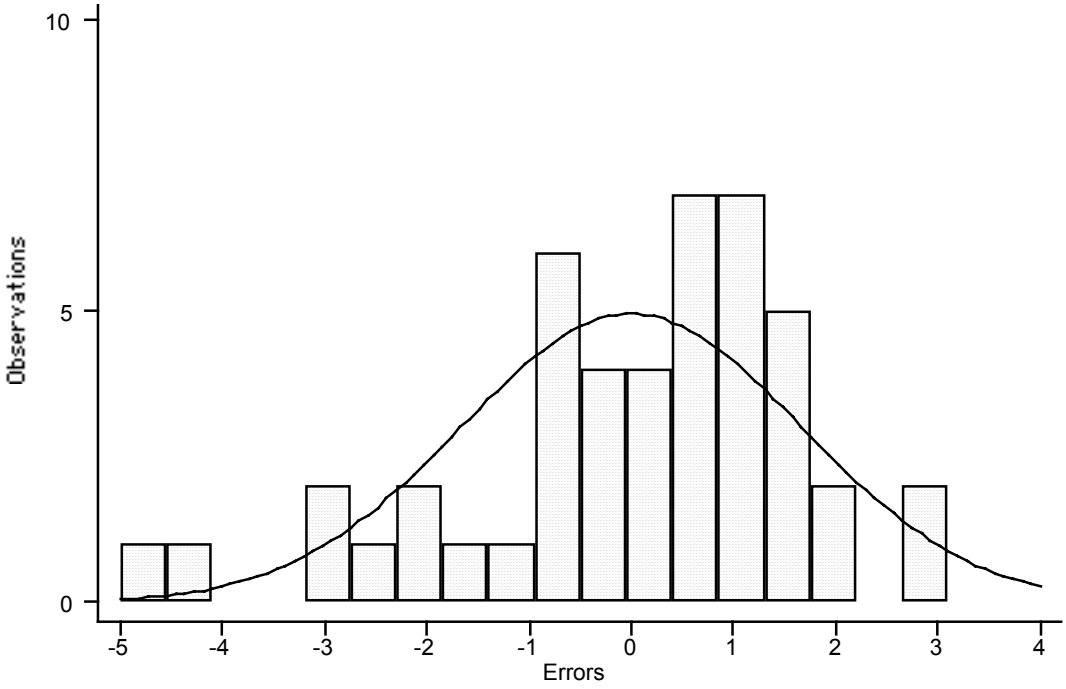

Figure 6.19: Distribution of MLR residuals of *E. coli* DMS control experiments.

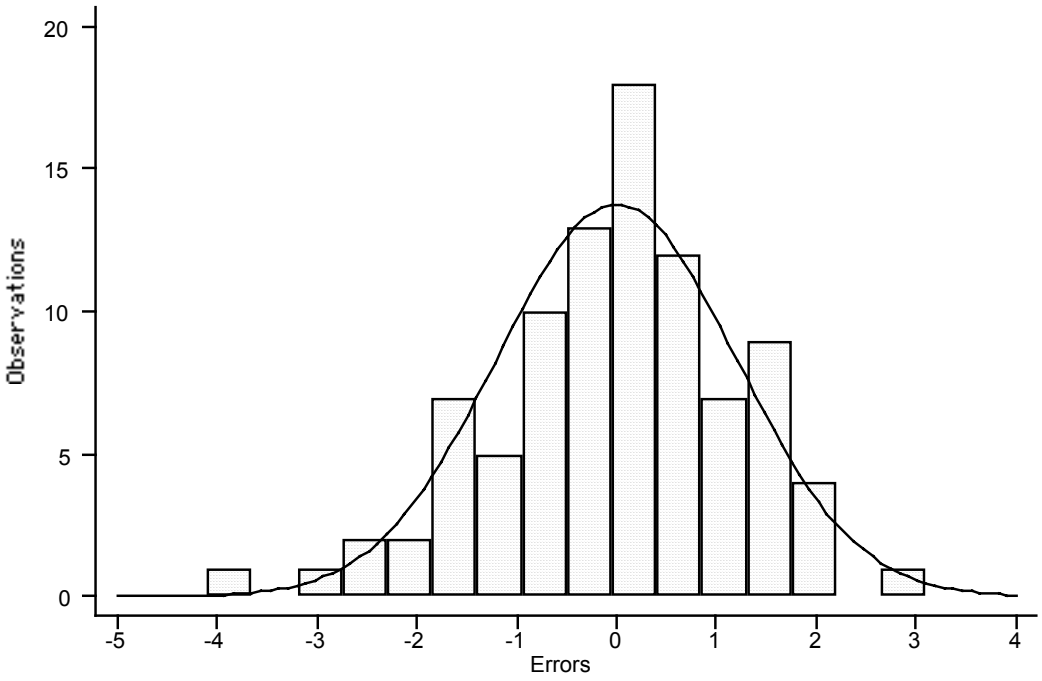

Figure 6.20: Distribution of MLR residuals of *E. coli* chemostat experiments.

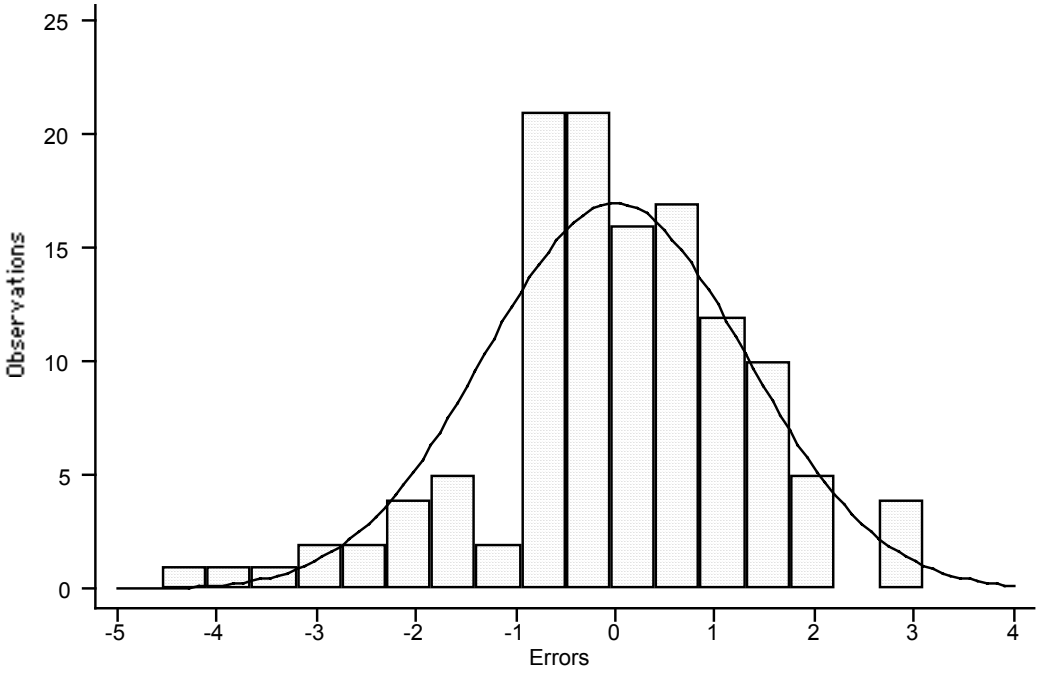

Figure 6.21: Distribution of MLR residuals of *B. subtilis* spores experiments.

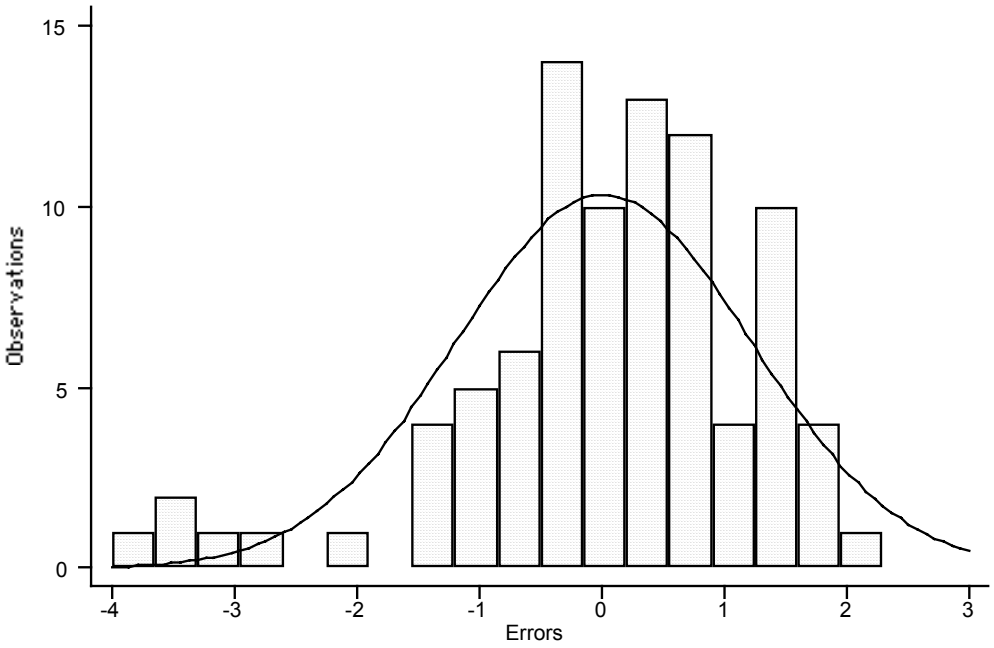

Figure 6.22: Distribution of MLR residuals of *B. subtilis* log experiments.

The objective of MLR was to determine the subset of predictors that provided the best-fit to the observed survival ratio data. The survival ratios predicted by the models given in Table 6.8 and the observed survival ratios are plotted in Figure 6.24 through Figure 6.31. These plots show visually how well the model fits the observed data. The solid line shows equal observed and predicted density of surviving organisms. In a perfect fit, all observations should be on this line, i.e., all the predicted data would be equal to observed data.

In the MLR residual plot of *B. subtilis* at exponential growth phase survival data, 5 data points were observed to have unusually large residuals (Figure 6.31). These 5 points were the survival data from experiments 411 and 412, which were conducted the same day using the same batch of *B. subtilis* cultures at exponential growth phase. These five data are marked in the raw data tables in Appendix C (Table A.15). These 5 observations can also be noticed in the histogram plot of the MLR residual (Figure 6.22). These outliers may cause an underestimation

of inactivation. Therefore, MLR was reapplied to survival data excluding these 5 outlier observations. STATA 7™ output of stepwise regression is given in Appendix C (Table C.1.c). When the outlier observations were discarded from the survival data, the significant predictors in the MLR model changed, however survival was still independent of initial microbial density. The predictors of survival of *B. subtilis* at exponential growth phase were ln*CT, CT* and time. The MLR model that provided a superior fit is given in Table 6.9. The regression residuals were normally distributed and symmetrical. There was no statistically significant ($P < 0.05$) correlation between regression residuals and any of the independent variables (Table 6.10).

Table 6.9: MLR model developed using stepwise regression for *B. subtilis* at exponential growth phase experiments without outlier observations.

Experiment	Adjusted r^2	MLR Model
B. subtilis log, 84 observations	0.9044	$\ln S = 2.47439 - 2.31869 \times \ln CT - 0.06488 \times \text{time} + 0.080472 \times CT$

$\ln S = \ln(N/N_0)$

Table 6.10: Significance of pairwise correlation of MLR residuals with predictors and Shapiro-Wilk test for normal regression residuals.

	Probability of Predictors							Normality	Skewness
Experiment	Time	C_o	CT	lnCT	N_0	lnN_o	Ln^3N_o	P	P
G. muris	1.00		1.00	1.00				0.7581	0.854

The histogram of the residuals and the regression plot of the *B. subtilis* at logarithmic growth phase survival data, excluding 5 outlier observations, are given in Figure 6.23 and Figure 6.32, respectively.

Multiple linear regression analyses of inactivation data show that there was a significant effect of initial microbial density on inactivation efficiencies of monochloramine on stationary phase *E. coli*, except *E. coli* DMS control data set. For the rest of the inactivation data, survival ratio was a function of disinfectant dose and contact time only.

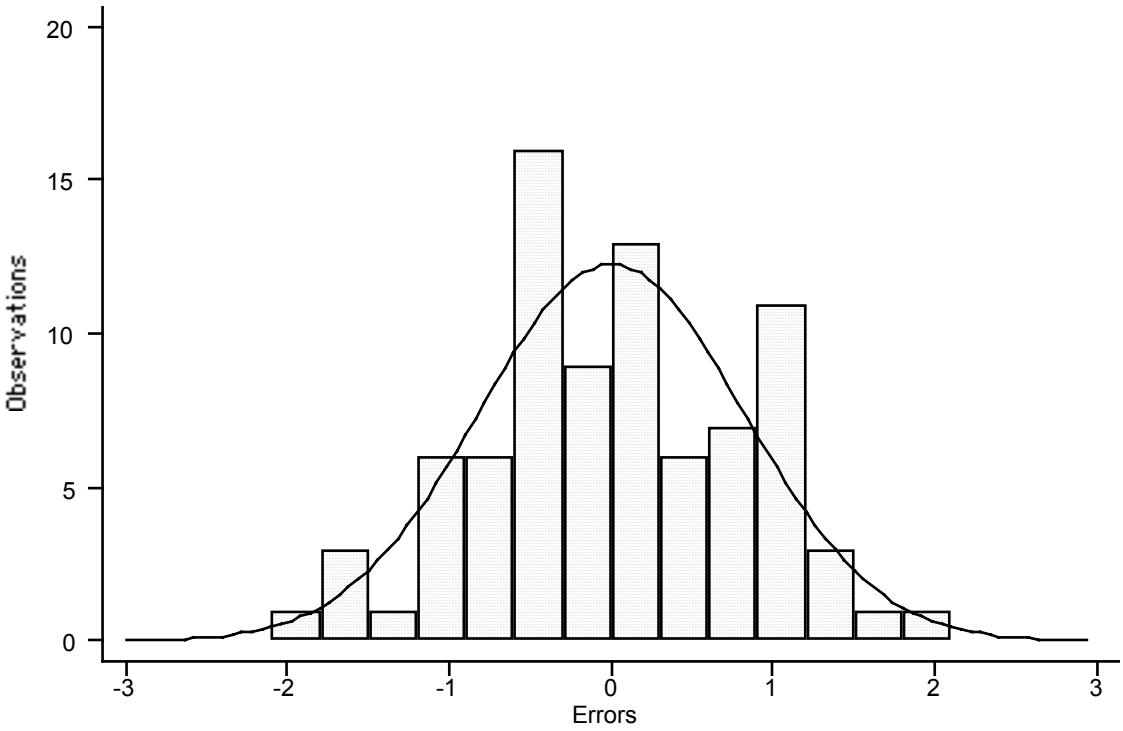

Figure 6.23: Distribution of MLR residuals of *B. subtilis* log experiments without outliers.

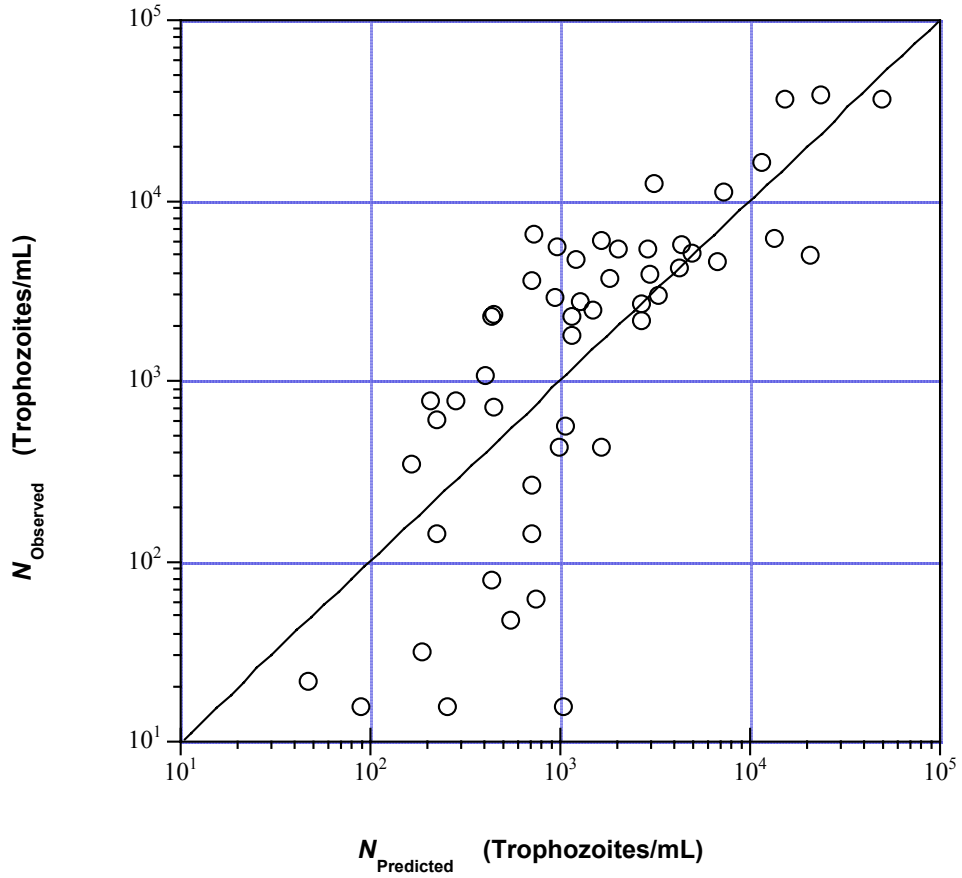

Figure 6.24: Observed surviving organism density versus surviving organism density predicted by MLR in *G. muris* experiments.

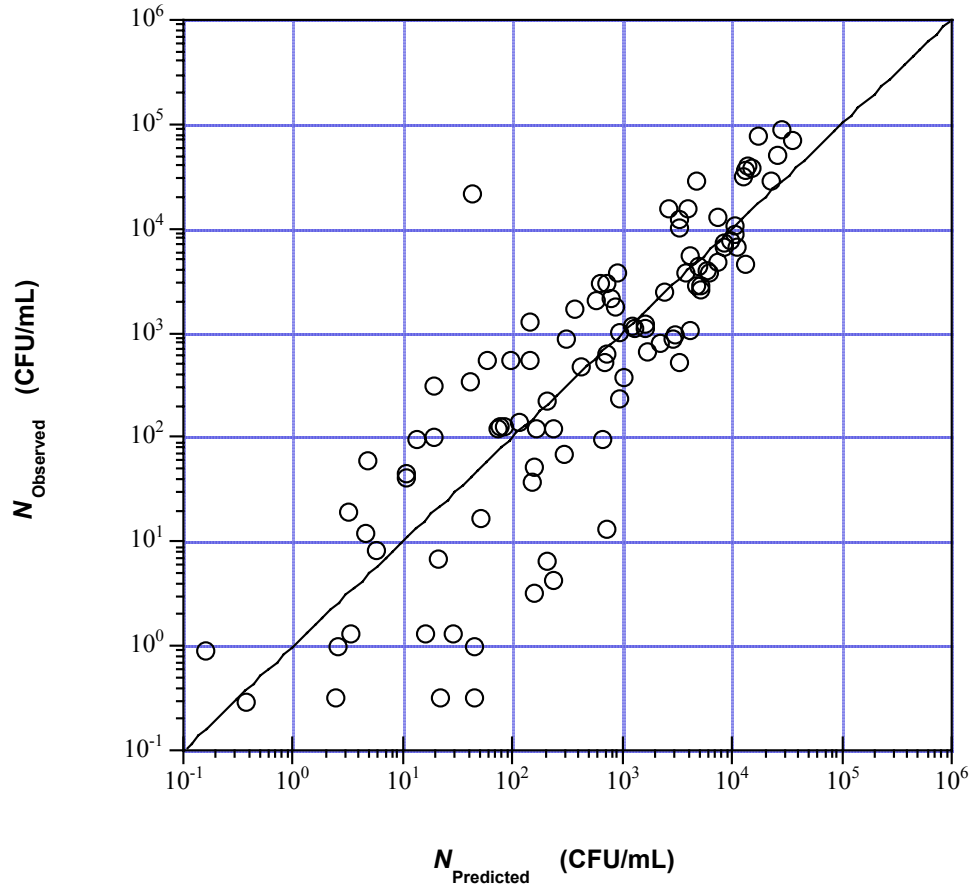

Figure 6.25: Observed surviving organism density versus surviving organism density predicted by MLR in *E. coli* batch experiments.

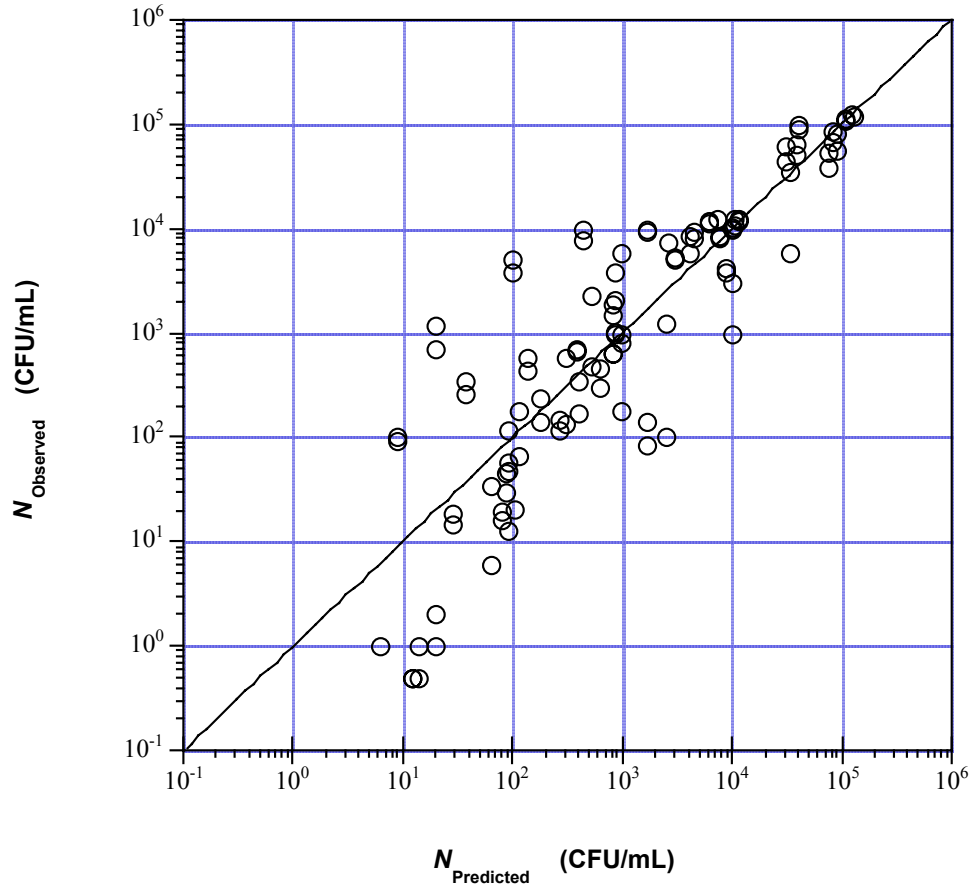

Figure 6.26: Observed surviving organism density versus surviving organism density predicted by MLR in *E. coli* log experiments.

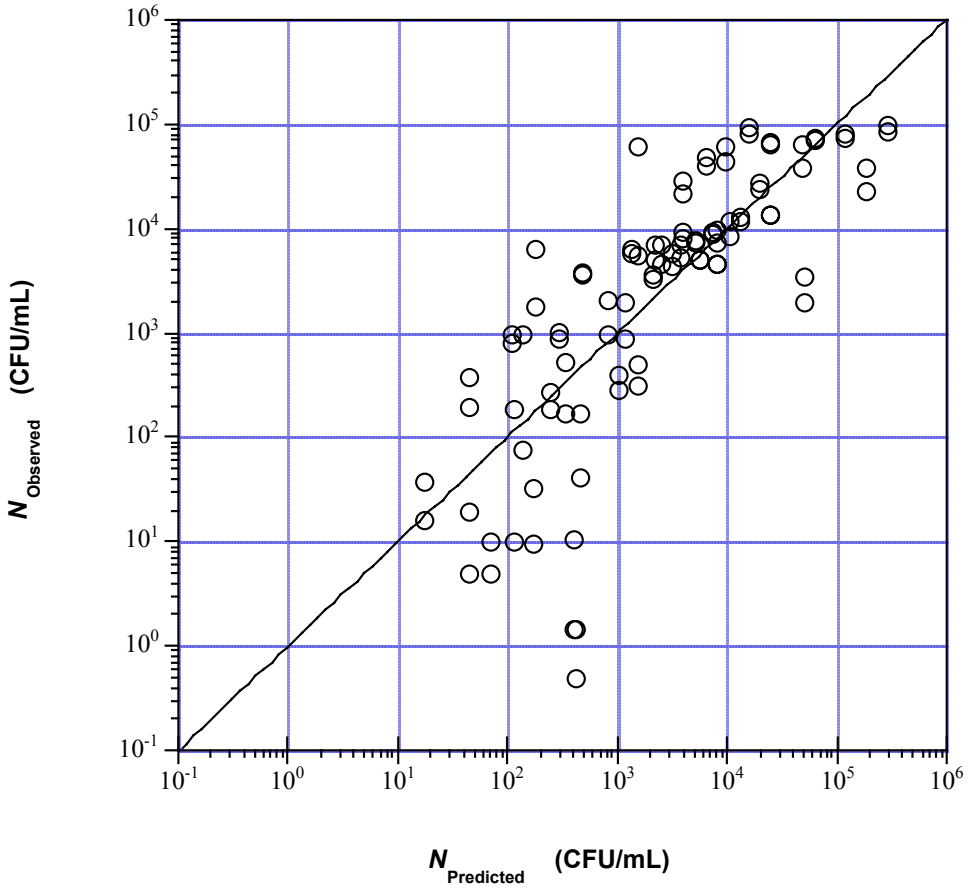

Figure 6.27: Observed surviving organism density versus surviving organism density predicted by MLR in *E. coli* DMS experiments.

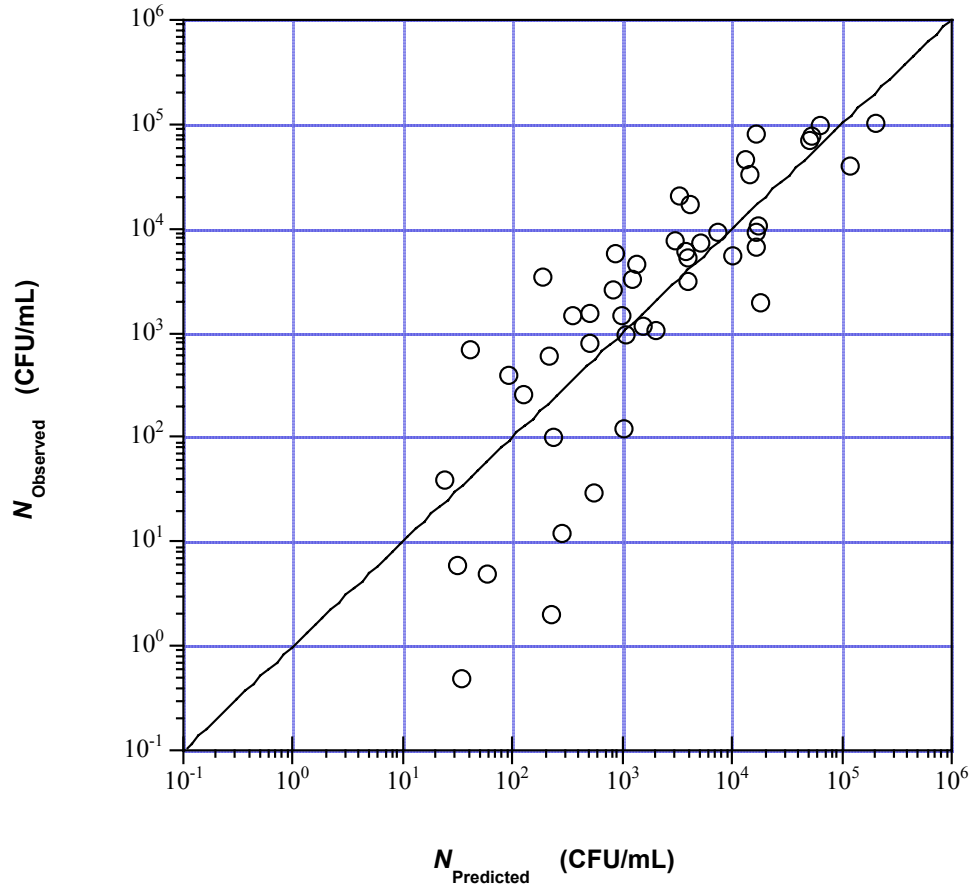

Figure 6.28: Observed surviving organism density versus surviving organism density predicted by MLR in *E. coli* DMS Control experiments.

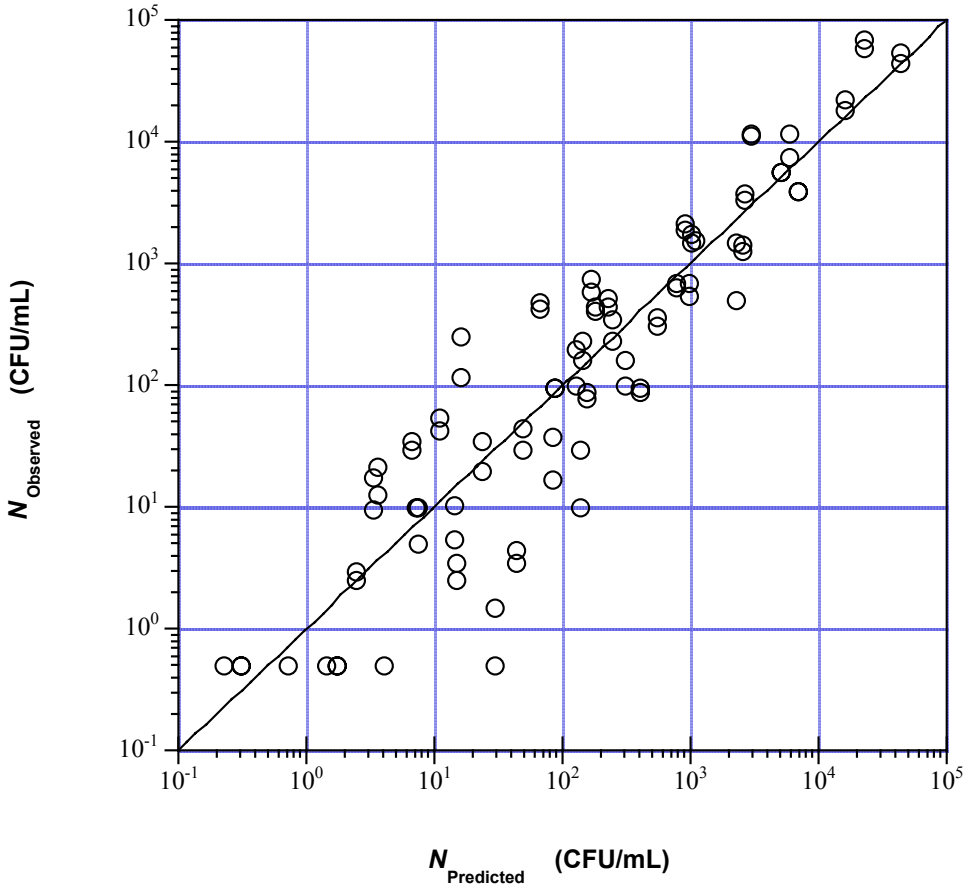

Figure 6.29: Observed surviving organism density versus surviving organism density predicted by MLR in *E. coli* chemostat experiments.

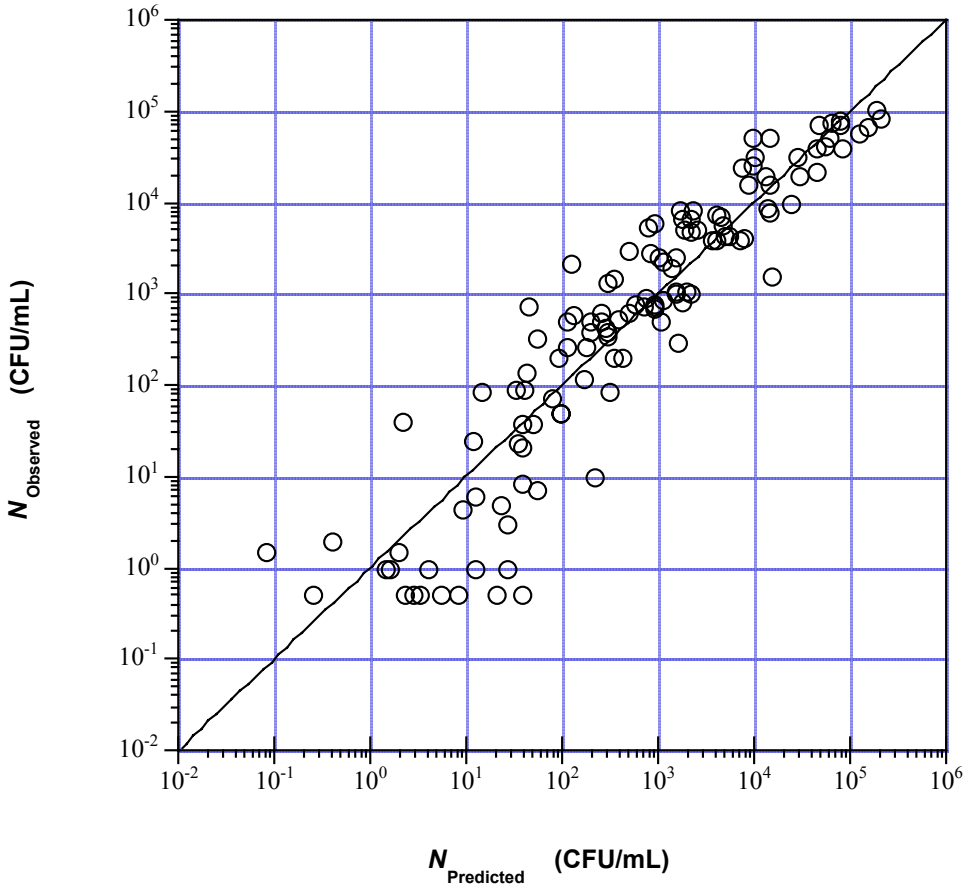

Figure 6.30: Observed surviving organism density versus surviving organism density predicted by MLR in *B. subtilis* spores experiments.

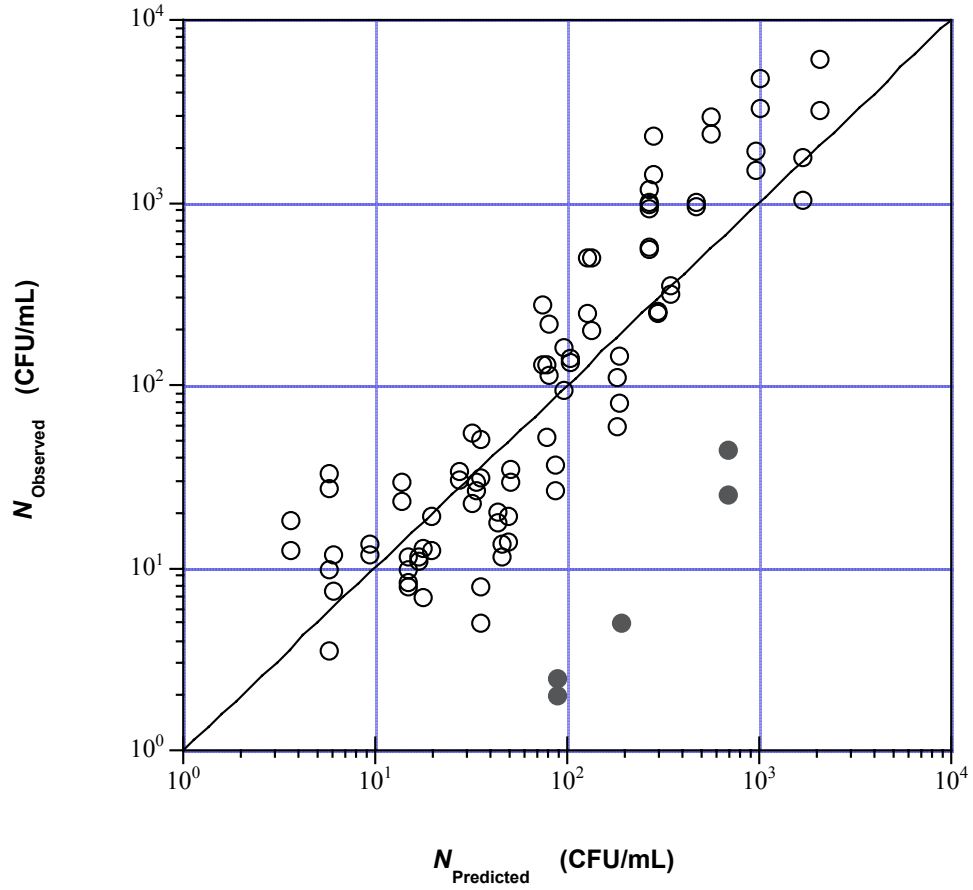

Figure 6.31: Observed surviving organism density versus surviving organism density predicted by MLR in *B. subtilis* log experiments (the full circles represent the possible outlier observations, see appropriate text for details).

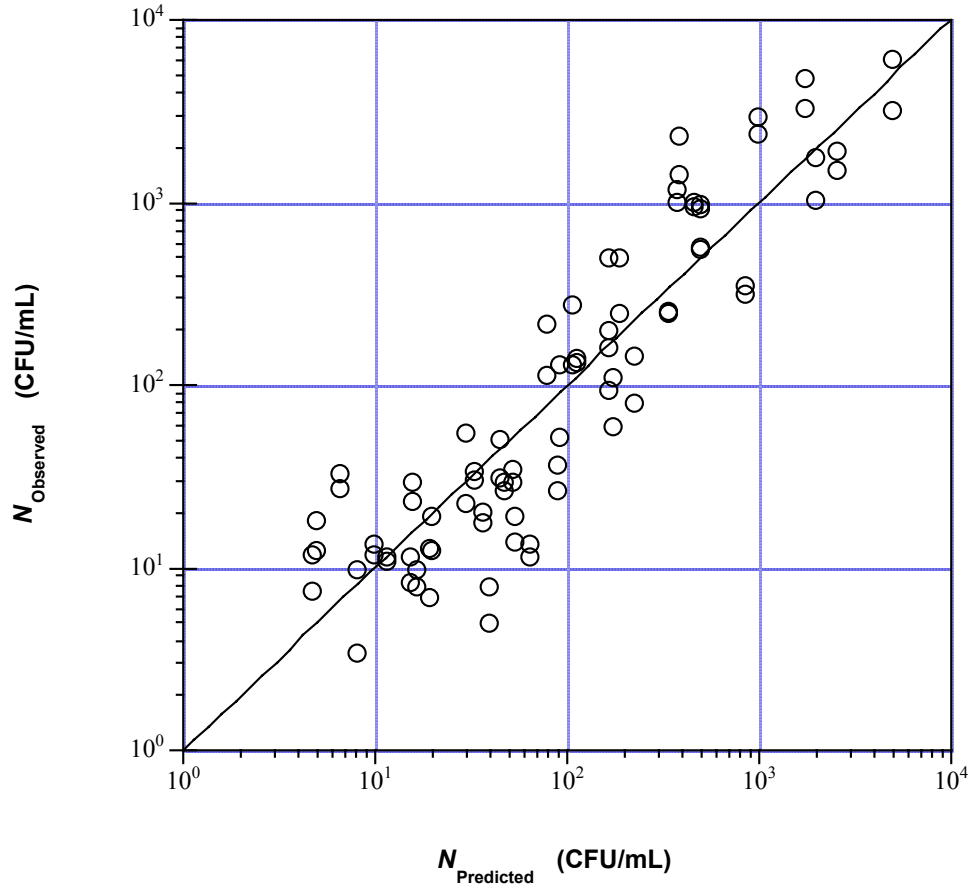

Figure 6.32: Observed surviving organism density versus surviving organism density predicted by MLR in *B. subtilis* log experiments where 5 outlier observations are discarded.

6.3.2. Nonlinear Least-squares Regression

The inactivation model analyses of experiments were conducted by fitting the experimental data to the previously described inactivation models using ordinary nonlinear least-squares (NLLS) regression. Survival data from each data set were fit to all of the previously described inactivation models one at a time. The best-fit inactivation model incorporated explicit dependence on the independent variables that had significant effects on disinfection efficiency. The results showed in which of the experimental series inactivation was cell density dependent. In addition, the best-fit model and its estimated parameters showed the type of dependency on microbial density, whether it is direct, inverse or none.

Before proceeding to nonlinear regression analysis, the kinetic inactivation models described in Section 3.5 were modified. The models so far discussed, except the Series-event Model, were derived from differential rate laws assuming a batch reactor and a disinfectant concentration that remained constant throughout the reactor. The disinfectant concentration was, however, decreasing during the contact time. Disinfectant demand-free conditions were unlikely for most oxidants (Haas and Finch, 1999). Although the cultures were washed with sterile buffered Milli-Q™ water twice, a significant amount of demand and decay was observed. The disinfectant demand and decay was estimated for each experiment using first-order decay kinetics previously in Section 6.2. Using the same first order decay kinetic model,

$$C=(C_a\text{-}D)\ exp\ (-k*t) \qquad (6.1)$$

it is possible to modify the kinetic inactivation models to include disinfectant demand and decay.

The process of performing this modification first involved noting that, for a batch system, the instantaneous reaction rate can be written as:

$$\frac{dN}{dt} = r_d$$

where, N is the volumetric concentration of microorganisms, t is disinfectant contact time and r_d

is the instantaneous reaction rate of disinfection. The instantaneous reaction rate of disinfection, r_d, for the kinetic models (Chick, Chick-Watson, Hom, Rational and Hom-Power Law) were defined in Section 3.5. During the integration of these differential rate equations, the disinfectant concentration was not treated as a constant. The first order decay kinetic model (Equation 6.1) was used to describe the disinfectant concentration during integration. The integrated forms of these kinetic models are given in Table 6.11 (Haas and Finch, 1999). Since the full derivations of these kinetic models and integration methods used were available elsewhere (Anotai, 1996; Haas and Finch, 1999; Haas and Joffe, 1994), the details are not discussed here. Only the final integrated forms of these models are given in Table 6.11.

Multiple-target and Modified Multiple-target models were also be modified to take disinfectant demand and decay into account. The Equation 6.1 was used in this case to describe disinfectant concentration in the rate expression of the inactivation of particles, rather than treating disinfectant concentration as constant. The detailed derivation of Multiple-target and Modified Multiple-target models under disinfectant demand and decay are given in Appendix D. The final integrated forms of these two statistical inactivation models are given in Table 6.11.

The Series Event Model was the only inactivation model that was not derived from differential rate laws. The Series-event model assumes random collision between oxidant molecules and microorganisms, expressed as a Poisson probability (Gyürèk and Finch, 1998; Severin *et al*., 1984). This model was used as defined in Section 3.5.6 without any modification.

The values of the first order decay rate (k^*) and the instantaneous demand (D) were already calculated in Section 6.2.

Table 6.11: Disinfection kinetic models with first-order decay and instantantenuous demand.

Model Name	Model	Kinetic Parameters
Chick;	$\ln\left(\frac{N}{N_0}\right) = -\frac{k(C_a - D)}{k^*}\left[1 - \exp\left(-k^* t\right)\right]$	*k*
Chick-Watson;	$\ln\left(\frac{N}{N_0}\right) = -\frac{k(C_a - D)^n}{nk^*}\left[1 - \exp\left(-nk^* t\right)\right]$	*k, n*
Hom Model;	$\ln\left(\frac{N}{No}\right) = -\frac{mk(C_a - D)^n}{(nk*)^m}\gamma(m, nk*t)$	*k, n, m*
Power Law;	$\ln\left(\frac{N}{N_0}\right) = -\frac{1}{x-1}\ln\left\{1 + \frac{(x-1)k(C_a - D)^n}{nk^*}\underline{N_0}^{x-1}\left[1 - \exp\left(-nk^* t\right)\right]\right\}$	*k, n, x*
Hom Power Law;	$\ln\left(\frac{N}{N_0}\right) = -\frac{1}{x-1}\ln\left\{1 + (x-1)\frac{mk(C_a - D)^n}{(nk^*)^m}\gamma(m, nk^* t)\underline{N_o}^{x-}\right.$	*k, n, m, x*
Multiple-target	$\ln\frac{N}{N_o} = \ln(P_i) = \ln\left[1 - \left(1 - \mathrm{e}^{\frac{k((C_a - D)(e^{-k*t} - 1))}{k*}}\right)^{\mathrm{n_C}}\right]$	*k, n_c*
Modified Multiple-target	$\ln\frac{N}{N_o} = \ln(P_i) = \ln\left[1 - \left(1 - \mathrm{e}^{\frac{k(C_a - D)^{\mathrm{n}}}{nk*}(e^{-nk*t} - 1)}\right)^{\mathrm{n_C}}\right]$	*k, n, n_c*

C_a : Applied disinfectant dose (mg/L)
D : Instantaneous disinfectant demand (mg/L)
k^* : First order disinfectant decay rate (minutes^{-1}).
t : Time (minutes)
N : Viable microorganism concentration at time t
N_0 : Initial viable microorganism concentration
n_c : Number of critical targets
k, n, m, x: Rate parameters
γ : Incomplete gamma function

In non-linear regression analysis of microbial inactivation, the microbial decay data from each inactivation experiment set along with the disinfectant decay rates and instantaneous demands were fit into each of the 8 inactivation models described above. The parameters for each of the inactivation models were estimated by NLLS regression. In this case, the best-fit parameters were the ones that resulted in minimum sum of squares of differences in predicted and observed log survival;

$$\text{RSS} = \text{minimum} \sum \left[\ln(N/N_o)_{predicted} - \ln(N/N_o)_{observed} \right]^2$$

where, $\ln(N/N_0)_{\text{observed}}$ is the actual survival ratio of organisms and $\ln(N/N_0)_{\text{predicted}}$ is the survival ratio predicted using the equations in Table 6.11.

This approach has been outlined and described elsewhere (Haas, 1988; Haas and Heller, 1989) and applied to disinfection data for virus, protozoa and bacteria by chlorine, chloramines and ozone (Haas *et al*., 1995). The objective for estimating the kinetic parameters was to determine the values in the most applicable rate expression that described disinfection performance. By comparing the goodness of fit of each model, the best-fit model representing disinfection kinetics was found for that specific experimental series. The microbial density effects were seen more clearly in the resulting best-fit model and parameters. A statistically significant improvement in the model fit with a model that incorporated initial microbial density as a predictor showed the effect of initial microbial density on response variables. For example, if the Hom Power Law was the best-fit, there was an effect of microbial density on disinfection efficiency, because the parameter "x" is the power of initial microbial density (N_o) on the right hand side of the differential equation (Equation 1.7). When "x" is equal to 1, there was no effect of initial microbial density and the Hom Power Law reduced to the Hom Model. Any significant improvement in the fit with the addition of this extra parameter, "x", which added microbial density as an independent variable, showed a significant effect of initial microbial density on disinfection kinetics. Otherwise, the Hom model would describe the data to the same degree. Also, a similar relation existed between the Power Law and the Chick-Watson Model. The Power Law was identical to Chick-Watson Model when the empirical parameter "x" was equal to 1.

The first part of parameter estimation of inactivation models was done for one model and data set at a time. Each data set consisted of initial microbial density (N_o), density of surviving organisms (N), disinfectant contact time (t), applied disinfectant dose (C_a) and the

corresponding disinfectant decay rate (k^*) and instantaneous demand (D, this value is set to zero for monochloramine experiments) obtained from the kinetic analysis of disinfectant residual data. Only observations with non-zero values of surviving organism were used in the analysis. Therefore, the non-linear regression of the inactivation data for each model was done using ordinary least squares regression. These computations were also conducted using a non-linear optimization in MATLAB®. Parameters were estimated for a single inactivation model one at a time for a single data set; hence, the overall estimation process was repeated to check all of the eight kinetic models for eight data sets. The residual sum of squares (RSS) of each fit along with the estimated parameters are given in Table 6.12 through Table 6.19. In addition, the adjusted r^2 for each model fit was calculated using Equation 6.2. As mentioned before, the Hom Power Law is a parent model for Chick, Chick-Watson, Hom and Power Law models. In the usual r^2, the value of r^2 increases with an addition of a parameter. However, the adjusted r^2 takes into account the number of predictors in the model and can decrease or increase as new parameters are added to the model (Quinn and Keough, 2002):

$$\text{Adjusted } r^2 = 1 - \frac{RSS/(n-p)}{TSS/(n-1)} \tag{6.2}$$

where, n is the number of observations, p is the number of parameters, RSS is residual sum of squares and TSS is total sum of squares.

Table 6.12: Summary of least-squares regression of *G. muris* data, 52 observations.

	Parameters					RSS	Adjusted
MODEL	k	n	m/n_c	x	κ		r^2
Chick	37.2299					175.62	0.6702
MT	10.0147		0.0872			158.27	0.6969
SE	23.2614				1.1649	293.67	0.4375
CW	72.2464	1.3979				151.69	0.7095
Hom	23.7029	0.8771	0.5509			113.00	0.7792
PL	5.4885	1.7066		1.4032		103.77	0.7972
MMT	25.2283	0.0492	2.0962			139.89	0.7266
HPL	7.8273	1.2182	0.6833	1.2186		100.95	0.7986

Table 6.13: Summary of least-squares regression of *B. subtilis* spores data, 124 observations.

	Parameters					RSS	Adjusted
MODEL	k	n	m/n_c	x	κ		r^2
Chick	1.2005					340.87	0.8555
MT	1.7873		11.2306			239.07	0.8978
SE	0.7167				1.8078	251.12	0.8927
CW	0.9644	0.4200				291.20	0.8755
Hom	0.6627	0.6861	1.2755			261.42	0.8873
PL	1.2932	0.4201		0.9553		271.37	0.8830
MMT	1.5449	0.6992	8.4567			220.04	0.9052
HPL	0.7993	0.6249	1.2116	0.9842		260.24	0.8869

Table 6.14: Summary of least-squares regression of *B. subtilis* log data, 89 observations.

	Parameters					RSS	Adjusted
MODEL	k	n	m/n_c	x	κ		r^2
Chick	0.1770					225.36	0.8345
MT	0.1020		0.1510			156.25	0.8839
SE	0.1765				1.2926	225.24	0.8327
CW	0.1800	0.5585				210.51	0.8436
Hom	0.8031	0.2009	0.5414			136.05	0.8977
PL	0.0484	0.8827		1.2585		144.24	0.8916
MMT	0.1062	0.3865	0.1591			145.19	0.8909
HPL	0.4364	0.3553	0.6218	1.0649		133.38	0.8986

Table 6.15: Summary of least-squares regression of *E. coli* batch data, 98 observations.

	Parameters					RSS	Adjusted
MODEL	k	n	m/n_c	x	κ		r^2
Chick	0.7829					453.53	0.8018
MT	1.3388		31.2862			350.62	0.8452
SE	1.6469				4.1521	337.72	0.8509
CW	0.7823	0.8999				443.02	0.8044
Hom	0.1827	1.5843	1.7735			356.39	0.8410
PL	0.6729	0.8569		1.0206		430.55	0.8079
MMT	1.3606	0.9895	34.4469			326.37	0.8544
HPL	0.0048	2.4737	2.9479	1.2180		274.99	0.8760

Table 6.16: Summary of least-squares regression of *E. coli* DMS data, 96 observations.

	Parameters					RSS	Adjusted
MODEL	k	n	m/n_c	x	κ		r^2
Chick	0.5171					374.76	0.6246
MT	0.7008		2.8459			365.02	0.6305
SE	0.5126				0.7405	376.16	0.6192
CW	0.5086	1.2451				371.14	0.6243
Hom	0.2784	1.4828	1.3434			363.71	0.6279
PL	1.1283	1.3291		0.9063		356.28	0.6355
MMT	0.6787	1.1237	2.5852			363.55	0.6280
HPL	0.7491	1.4416		0.9173		353.79	0.6341

Table 6.17: Summary of least-squares regression of *E. coli* DMS control data, 46 observations.

	Parameters					RSS	Adjusted
MODEL	k	n	m/n_c	x	κ		r^2
Chick	0.6286					151.70	0.7565
MT	1.1569		22.4415			119.09	0.8045
SE	0.6236				1.9795	152.18	0.7502
CW	0.6320	0.8808				151.07	0.7520
Hom	0.0753	1.7450	2.1646			108.40	0.8179
PL	1.2022	1.0309		0.9220		143.87	0.7583
MMT	1.2659	0.7975	41.3201			113.35	0.8096
HPL	0.0798	7.7399	2.1485	0.9964		108.39	0.8136

Table 6.18: Summary of least-squares regression of *E. coli* log data, 106 observations.

	Parameters					RSS	Adjusted
MODEL	k	n	m/n_c	x	κ		r^2
Chick	0.8452					387.19	0.7186
MT	2.1286		210.69			248.93	0.8174
SE	0.8427				0.0368	385.73	0.7170
CW	0.8381	0.7872				383.31	0.7188
Hom	0.0780	2.3796	2.5989			237.35	0.8242
PL	0.8461	0.8668		1.0000		380.11	0.7184
MMT	2.1167	0.9651	203.001			248.38	0.8160
HPL	0.1029	2.3502	2.5744	0.9670		233.90	0.8250

Table 6.19: Summary of least-squares regression of *E. coli* chemostat data, 92 observations.

MODEL	Parameters					RSS	Adjusted r^2
	k	n	m/n_c	x	κ		
Chick	1.0048					218.60	0.9140
MT	1.4353		11.1532			155.02	0.9383
SE	1.0032				1.3168	217.85	0.9133
CW	0.9953	1.3242				204.08	0.9188
Hom	0.3750	1.8554	1.5428			137.94	0.9445
PL	0.9059	1.3201		1.0144		202.38	0.9186
MMT	1.4295	1.2223	11.3455			141.52	0.9431
HPL	0.2125	1.9980	1.6910	1.0492		126.30	0.9486

After fitting the inactivation data, the best-fit models were decided for each data set. The main criteria was to protect against "overfitting", where the addition of an extra parameter may cause lower RSS, however, this extra parameter may add very little to the explanatory power (Quinn and Keough, 2002). For sake of simplicity, first models were divided into subgroups according to the number of parameters they had (Figure 6.33). Then the models with the lowest RSS in each subgroup were compared with each other.

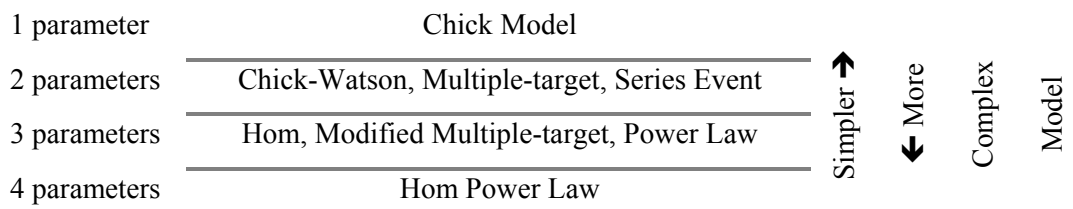

Figure 6.33: Illustration of hierarchy of models.

Next, starting from the simplest model, the relatively simpler model was compared with a relatively more complex model (with an additional parameter) to test whether the extra parameter improves the fit significantly. Models with more parameters usually have lower RSS, however, the improvement in the fit may not be significant. Therefore, the statistical

significance of improvement in fit was checked by partial F-test, where the F value was calculated as follows;

$$F = \frac{(\mathrm{RSS}_{\text{Simple Model}} - \mathrm{RSS}_{\text{Complex Model}})/(\mathrm{df}_{\text{Simple Model}} - \mathrm{df}_{\text{Complex Model}})}{\mathrm{RSS}_{\text{Complex Model}} / \mathrm{df}_{\text{Complex Model}}}$$

The corresponding probability was calculated using the inverse F distribution function in Microsoft Excel 98®, where the null hypothesis (H_o) was that the partial slope {*F(Model with added parameter| Previous model*)} equaled zero.

$$\text{Probability} = P = Fdist\,(F, \mathrm{df}_{\text{Simple Model}} - \mathrm{df}_{\text{Complex Model}}, \mathrm{df}_{\text{Complex Model}})$$

where, *df* is degrees of freedom.

The significance level selected in this process was 0.05. Simply, probability, *P*, below the significance level indicates the statistical significance of improvement in fit of the more complex model over the simpler model. In this way, statistical significance after the addition of parameter was tested. The pairwise F-test comparisons are given in Table 6.20. For example, in *G. muris* experiments, there was a statistically significant improvement in fit to the Chick-Watson model over the Chick Model. When Chick-Watson Model was compared with the Power Law, the fit of the Power Law was statistically significantly better. Addition of a parameter in the kinetic model provided a significantly better fit. However, the comparison of the Power Law against the Hom Power Law, which is a relatively more complex model, showed that there was no statistically significant improvement in the fit of the Hom Power Law even though the regression of Hom Power Law had lower RSS. Therefore, it was concluded that the Power Law provided superior fit compared to other inactivation models. The Power Law was the best-fit model for *G. muris* experiments. As discussed before, Power Law can be reduced to Chick-Watson Model when the parameter "*x*" is set to 1. The "*x*" parameter in the Power Law was different from 1 (x = 1.4032) and there was a statistically significant improvement in the fit by adding the initial microbial density as an independent variable into the model. Otherwise, the Chick-Watson Model would describe the inactivation data to same degree. Kinetic analysis of

the inactivation of *G. muris* with ozone showed that the Power Law was the best-fit model and there was a statistically significant effect of initial microbial density on disinfection efficiency. An "x" parameter greater than 1 (x = 1.4032), showed that the disinfection efficiency of ozone increased as initial *G. muris* cysts density increased.

Table 6.20: Probabilities for pairwise comparison of model fits with partial F-test.

a. Probabilities for pairwise comparison of kinetic models for *G. muris* experiments.

Simpler Model		More Complex Model	Probability
Chick Model	vs.	Chick-Watson Model	7.10×10^{-3}
Chick-Watson Model	vs.	Power Law	1.80×10^{-5}
Power Law	vs.	Hom Power Law	2.53×10^{-1}

b. Probabilities for pairwise comparison of kinetic models for *E coli* batch experiments.

Simpler Model		More Complex Model	Probability
Chick Model	vs.	Series-event	2.15×10^{-9}
Series-event	vs.	Modified Multiple-target	4.60×10^{-2}
Modified Multiple-target	vs.	Hom Power Law	6.05×10^{-6}

c. Probabilities for pairwise comparison of kinetic models for *E. coli* log experiments.

Simpler Model		More Complex Model	Probability
Chick Model	vs.	Multiple-target	1.35×10^{-11}
Multiple-target	vs.	Hom Model	2.72×10^{-2}
Hom Model	vs.	Hom Power Law	2.23×10^{-1}

d. Probabilities for pairwise comparison of kinetic models for *E. coli* DMS experiments.

Simpler Model		More Complex Model	Probability
Chick Model	vs.	Multiple-target	1.17×10^{-1}
Multiple-target	vs.	Power Law	1.32×10^{-1}
Power Law	vs.	Hom Power Law	4.24×10^{-1}

e. Probabilities for pairwise comparison of kinetic models for *E. coli* chemostat experiments.

Simpler Model		More Complex Model	Probability
Chick Model	vs.	Multiple-target	2.92×10^{-8}
Multiple-target	vs.	Hom Model	1.30×10^{-3}
Hom Model	vs.	Hom Power Law	5.48×10^{-3}

(continued)

Table 6.20: (continued)

f. Probabilities for pairwise comparison of kinetic models for *B. subtilis* spores experiments.

Simpler Model		More Complex Model	Probability
Chick Model	vs.	Multiple-target	2.09×10^{-12}
Multiple-target	vs.	Modified Multiple-target	1.57×10^{-3}
Modified Multiple-target	vs.	Hom Power Law	N/A

g. Probabilities for pairwise comparison of kinetic models for *B. subtilis* log experiments

Simpler Model		More Complex Model	Probability
Chick Model	vs.	Multiple-target	1.50×10^{-8}
Multiple-target	vs.	Hom Model	5.40×10^{-4}
Hom Model	vs.	Hom Power Law	1.93×10^{-1}

N/A: Not Applicable

The same pairwise comparison processes were carried out for each of the data sets to determine the best-fit models. In a pairwise comparison of *B. subtilis* spore experiments, the Hom Power Law did not show any improvement in the fit over the Modified Multiple-target Model. In other words, the *RSS* from the Hom Power Law fit was greater than that of the Modified Multiple-target Model. Therefore, the application of the partial F-test to determine the significance of improvement was not applicable in this case. However, the improvement of the Hom Power Law over the Hom model in this case was insignificant ($P = 0.463$) showing that there was no statistically significant effect of initial spore density on inactivation efficiency. The models that provided a superior fit according to pairwise comparison are given in Table 6.21. The main problem in improving the fit by adding parameters is that high numbers of parameters in the model may cause over-parameterization and may result in highly correlated parameter estimates (Bates and Watts, 1988). Therefore, the significance of the correlation between regression residuals of the models in Table 6.21 and the independent variables (applied disinfectant dose, contact time and initial microbial density) was checked. The probabilities of

correlation are given in Table 6.22 for each data set, where 0.05 was chosen as the significance level.

Table 6.21: The models that provided superior fit to survival data.

Experiments	Disinfectant	Inactivation Model
G. muris	Ozone	Power Law
E. coli batch	Monochloramine	Hom Power Law
E. coli log	Monochloramine	Hom Model
E. coli DMS	Monochloramine	Chick Model
E. coli DMS Control	Monochloramine	Hom Model
E. coli chemostat	Monochloramine	Hom Power Law
B. subtilis spores	Ozone	Modified Multiple-target
B. subtilis log	Monochloramine	Hom Model

There must be no significant correlation ($P < 0.05$) between errors of non-linear regression and any of the independent variables. The errors in prediction of *B. subtilis* spores inactivation by Modified Multiple-target were significantly correlated with initial disinfectant concentration. However, there were 24 independent significance tests at the level of 0.05. The probability of getting no significant differences in all these tests was simply the product of individual probabilities: $(1-0.05)^{24} = 0.29$. This is the probability of making no type I errors in any of the 24 tests. In other words, there was a 71% chance that at least one of these 24 tests would turn out significant, despite each individual test was only at the 5% level (Sokal and Rohlf, 1995). In order to guarantee that the overall significance test was still at the 0.05 level, the significance level $\alpha`$ of the individual test was adapted using the Dunn-Sidàk method. In this approach, the probability values of tests are ordered from smallest to largest. The corresponding significance levels,$\alpha`$, for the test with the lowest probability were calculated using Dunn-Sidàk method:

$$\alpha` = 1 - (1 - \alpha)^{1/k}$$

where, k is the number of independent significance tests, α is the significance level, it is 5% in this case and $\alpha`$ is the corresponding significance level.

Table 6.22: Pairwise correlation coefficient of regression residuals with C_o, N_o and time.

Experiment-Model		C_o	Time	N_o
G. muris - *PL*	Correlation Coefficient	0.0681	0.1130	0.1113
	Probability	0.6314	0.4249	0.4321
E. coli Batch- HPL	Correlation Coefficient	-0.1015	0.0309	-0.0125
	Probability	0.320	0.7628	0.9031
E. coli Log - Hom	Correlation Coefficient	0.1675	-0.0759	-0.0057
	Probability	0.4392	0.4392	0.9539
E. coli DMS - Chick	Correlation Coefficient	0.0407	0.1929	-0.0957
	Probability	0.6937	0.0597	0.3538
E. coli DMS Control - Hom	Correlation Coefficient	-0.0150	-0.0386	-0.0166
	Probability	0.9211	0.7987	0.9129
E. coli Chemostat - HPL	Correlation Coefficient	0.0709	0.0316	-0.0130
	Probability	0.5020	0.7649	0.9021
B. subtilis Spores - MMT	Correlation Coefficient	0.2036	0.0163	-0.0516
	Probability	0.0233	0.8574	0.5690
B. subtilis Log - Hom	Correlation Coefficient	0.0189	0.0130	-0.0940
	Probability	0.8605	0.9041	0.3809

The corresponding significance levels,$\alpha`$, for the test with the second lowest probability were also calculated as follows:

$$\alpha` = 1 - (1 - \alpha)^{1/(k-1)}$$

The corresponding significance levels, $\alpha`$, for the rest of the tests were calculated using the same approach. This approach has been described in detail in Sokal and Rohlf (1995). The probability values of correlation of each test and the corresponding significance levels are given in Table 6.23.

The comparison of probabilities with associated α ($\alpha`$) starts with the smallest probability. For a 5% significance level, the calculated associated significance level,

$\alpha` = (1 - 1 - 0.05)^{1/24} = 0.0021$. Since P_1 (P_1 = 0.0233) is greater than the critical value ($\alpha' = 0.0021$), it was declared that all tests were not significant, meaning that there was no correlation between regression residuals and any of the independent variables.

The best-fit inactivation models and Shapiro-Wilk test for normal regression residuals for each data set are given in Table 6.24. According to the Shapiro-Wilk test, only the hypothesis of a normal distribution of the regression residuals of *G. muris* and *E. coli* chemostat experiments could not be rejected. In the rest of the regressions, the hypothesis of normally distributed regression residuals was rejected. The skewness test measured the significance of the asymmetry of the regression residuals around the sample mean. Based on the skewness alone, one could not reject the hypothesis of normally distributed regression residuals except for *E. coli* DMS, *E. coli* chemostat and *B. subtilis* log data sets. The assumption of normally distributed errors is almost always arbitrary. Nevertheless, the central-limit theorem assured that under broad conditions, inference based on the least-squares estimators was approximately valid in all as long the sample size was not small. The validity of least-squares estimation is robust. The levels of tests and confidence intervals are approximately correct in large samples even when the assumption of normality is violated (Fox, 1991). In a study by Driscoll (1996), the effects of departures from normality on the analysis of variance was investigated via simulation. The results supported the contention that this procedure was “robust” in the sense that it yielded insignificant differences from the nominal type I errors when used on a wide range of nonnormal populations and designs of experiments.

Table 6.23: Probability of pairwise correlation of regression residual with C_0, N_0, and time and the corresponding significance levels calculated using Dunn-Sidàk method.

Experiment and Model	Correlation	Probability, P_i	α`
B. subtilis spores- MMT	Regression Residuals vs. C_0	0.0233	0.0021
E. coli DMS – Chick	Regression Residuals vs. Time	0.0597	0.0022
E. coli batch- HPL	Regression Residuals vs.C_0	0.3200	0.0023
E. coli DMS- Chick	Regression Residuals vs. N_0	0.3538	0.0024
B. subtilis log – Hom	Regression Residuals vs. N_0	0.3809	0.0026
G. muris – PL	Regression Residuals vs. Time	0.4249	0.0027
G. muris – PL	Regression Residuals vs. N_0	0.4321	0.0028
E coli log – Hom	Regression Residuals vs. C_0	0.4392	0.0030
E coli log – Hom	Regression Residuals vs. Time	0.4392	0.0032
E. coli chemostat – HPL	Regression Residuals vs.C_2	0.5020	0.0034
B. subtilis spores- MMT	Regression Residuals vs. N_0	0.5690	0.0037
G. muris- PL	Regression Residuals vs. C_0	0.6314	0.0039
E. coli DMS – Chick	Regression Residuals vs.C_0	0.6937	0.0043
E. coli batch- HPL	Regression Residuals vs. Time	0.7628	0.0047
E. coli chemostat – HPL	Regression Residuals vs. Time	0.7649	0.0051
E. coli DMS control – Hom	Regression Residuals vs. Time	0.7987	0.0057
B. subtilis spores- MMT	Regression Residuals vs. Time	0.8574	0.0064
B. subtilis log – Hom	Regression Residuals vs.C_0	0.8605	0.0073
E. coli chemostat – HPL	Regression Residuals vs. N_0	0.9021	0.0085
E. coli batch- HPL	Regression Residuals vs. N_0	0.9031	0.0102
B. subtilis log – Hom	Regression Residuals vs. Time	0.9041	0.0127
E. coli DMS control – Hom	Regression Residuals vs. N_0	0.9129	0.0170
E. coli DMS control – Hom	Regression Residuals vs. C_0	0.9211	0.0253
E coli log – Hom	Regression Residuals vs. N_0	0.9539	0.0500

The histograms of errors are given in Figure 6.34 through Figure 6.41. In a perfect fit the errors would be zero. These histograms give visual distributional information. The deviations from normal distribution can be seen in these figures. Also, one should note that even the errors are not normally distributed, they are relatively small.

Table 6.24: Best-fit inactivation models and Shapiro-Wilk test for normal regression residuals.

Experiment	Best-fit Model	Normality, *P*	Skewness, *P*
G. muris	Power Law	0.1654	0.128
E. coli batch	Hom Power Law	0.0002	0.157
E. coli log	Hom Model	0.0141	0.627
E. coli DMS	Chick Model	<0.0001	<0.001
E. coli DMS control	Hom Model	0.0004	0.073
E. coli chemostat	Hom Power Law	0.0713	0.040
B. subtilis spores	Modified Multiple-target	<0.0001	0.082
B. subtilis log	Hom Model	<0.0001	<0.001

Based on the best-fit inactivation models, inactivation efficiencies of *G. muris* with ozone, batch and continuous cultures of *E. coli* with monochloramine were dependent on initial microbial density in addition to disinfectant contact time and disinfectant concentration. Cell density dependent inactivation was observed in neither *E. coli* nor *B. subtilis* at exponential growth phases. The inactivation efficiency of *B. subtilis* spores and stationary phase *E. coli* in the presence of DMS was also independent of microbial density.

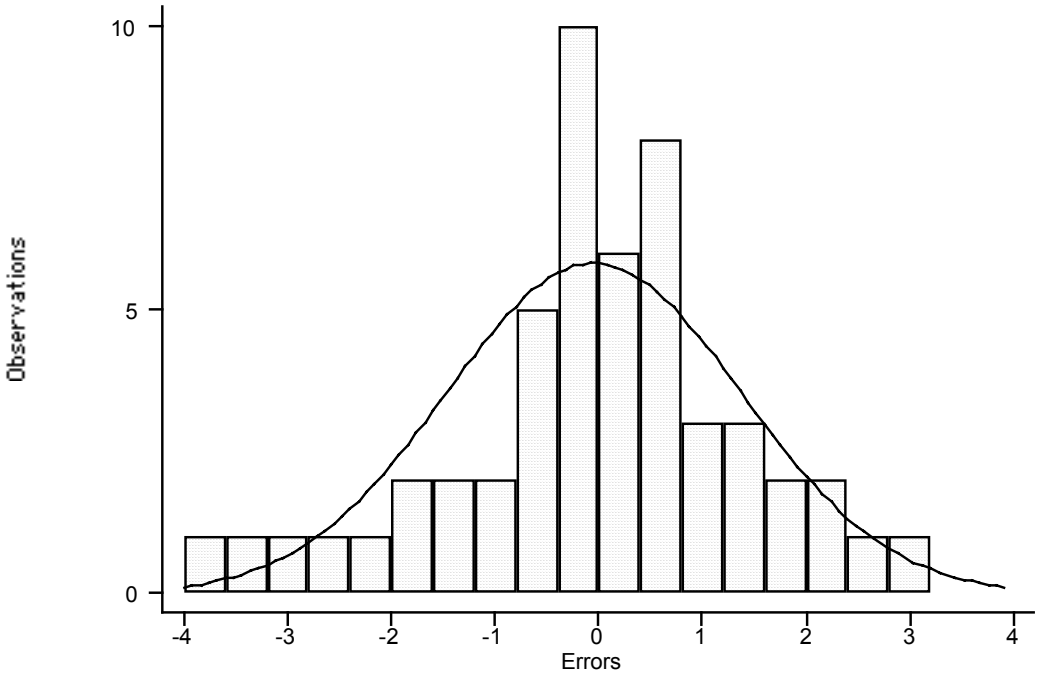

Figure 6.34: Distribution of regression residuals of *G. muris* experiments.

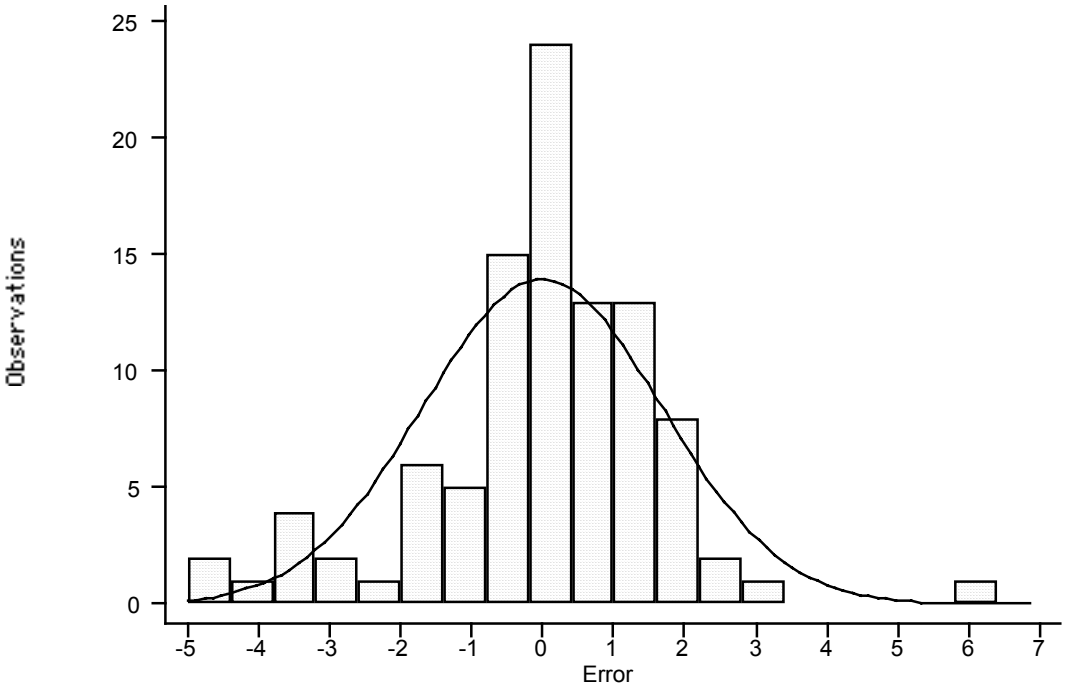

Figure 6.35: Distribution of regression residuals of *E. coli* batch experiments.

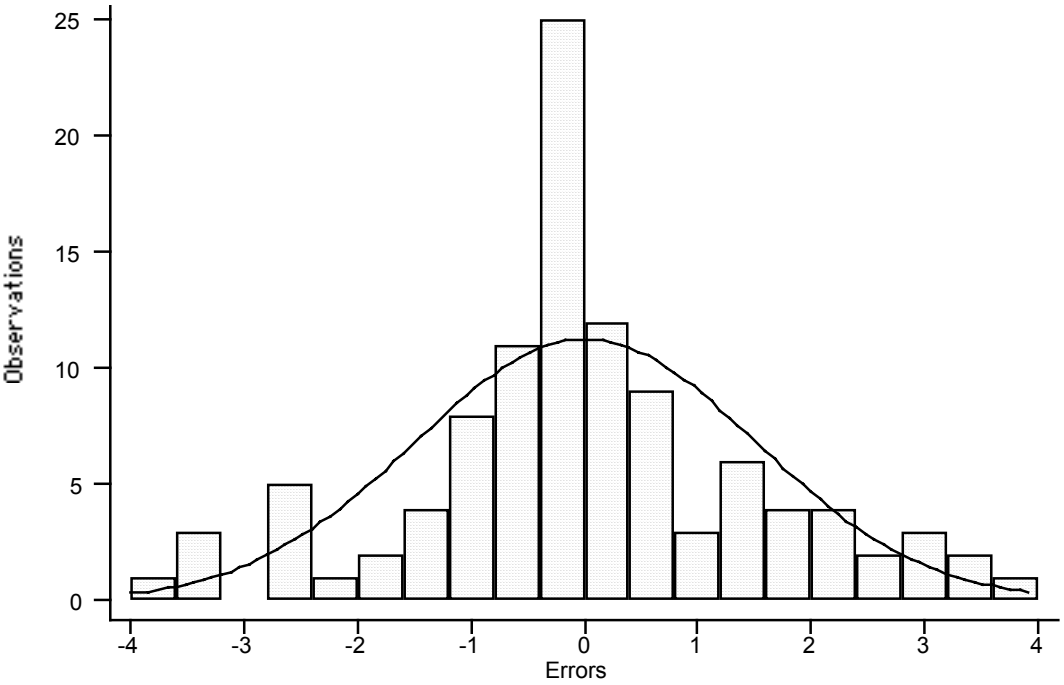

Figure 6.36: Distribution of regression residuals of *E. coli* log experiments.

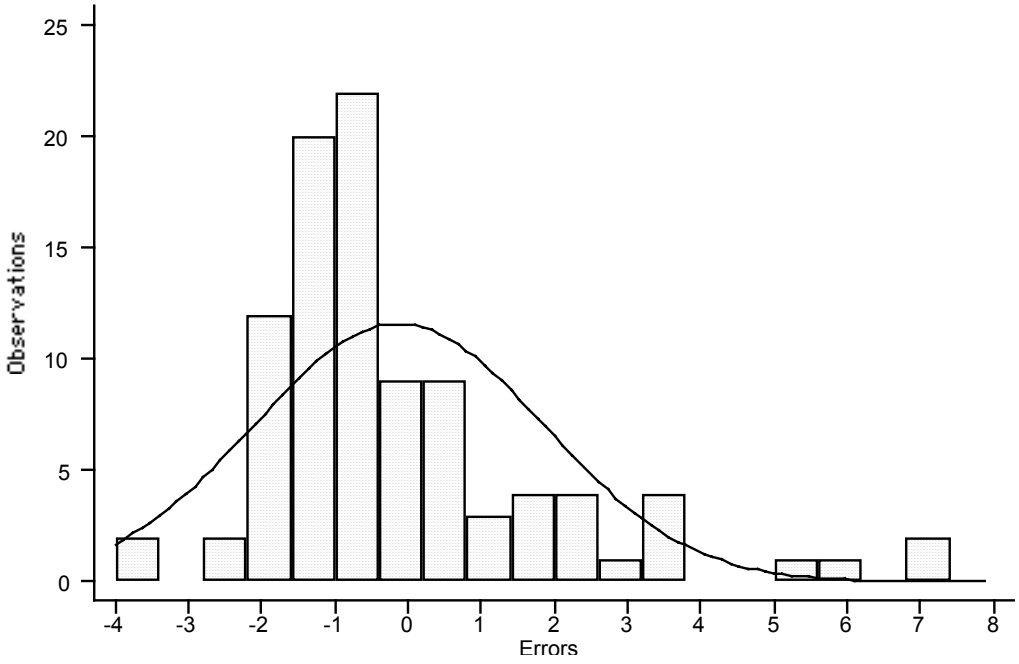

Figure 6.37: Distribution of regression residuals of *E. coli* DMS experiments.

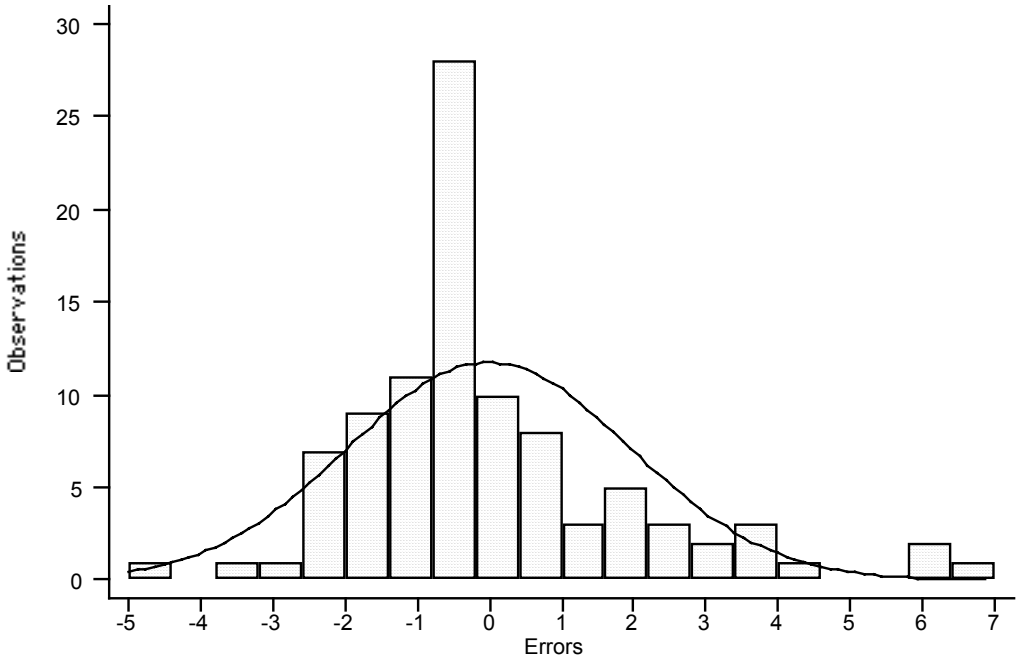

Figure 6.38: Distribution of regression residuals of *E. coli* DMS control experiments.

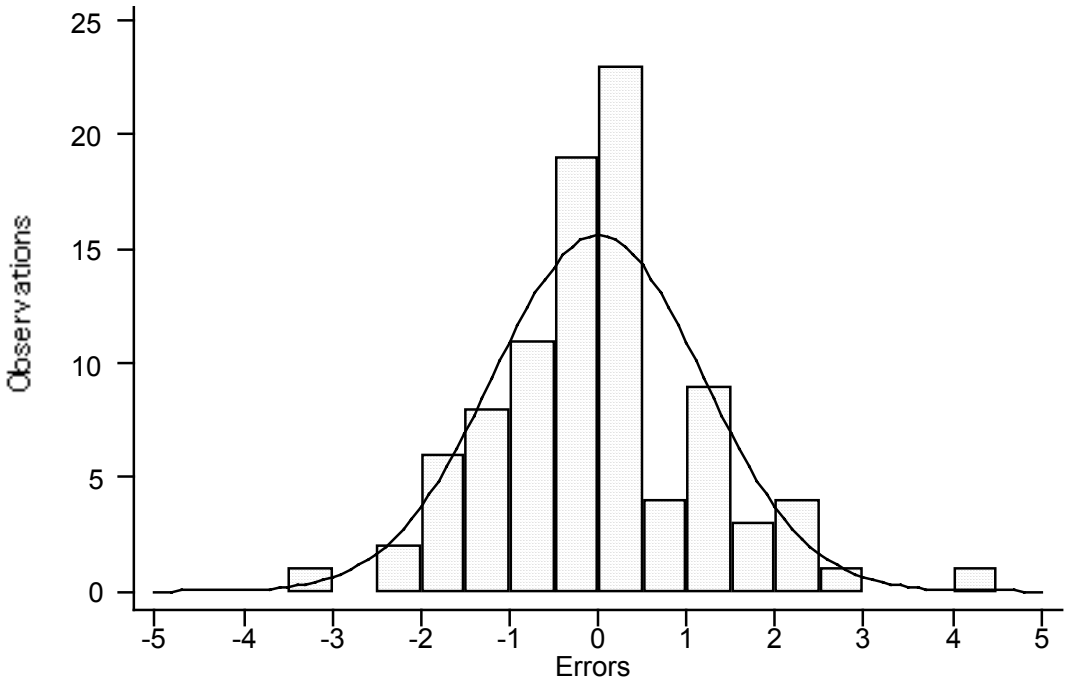

Figure 6.39: Distribution of regression residuals of *E. coli* chemostat experiments.

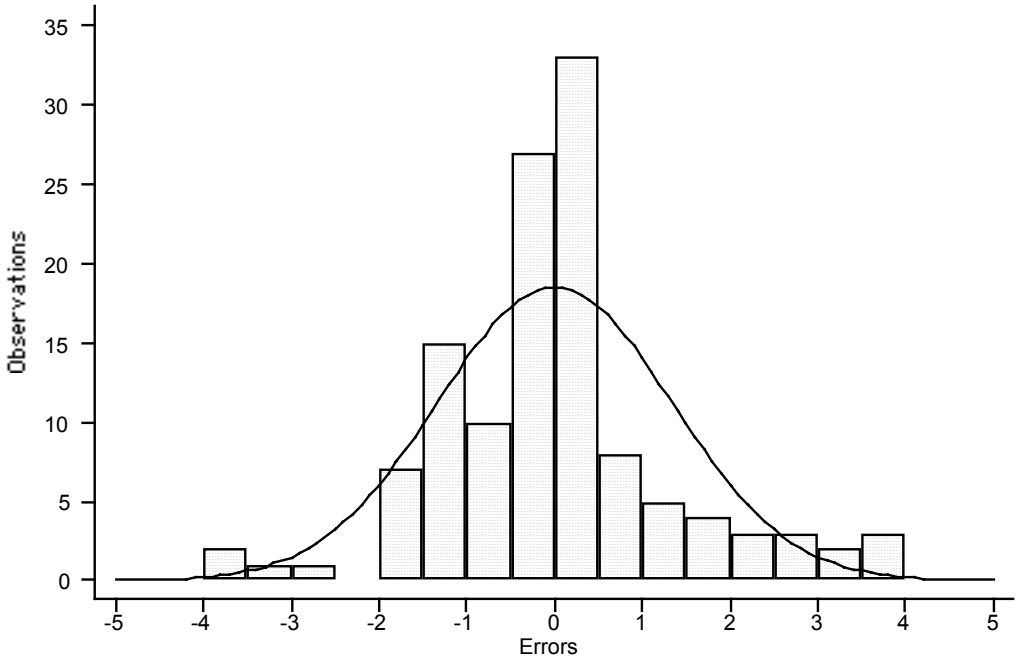

Figure 6.40: Distribution of regression residuals of *B. subtilis* spores experiments.

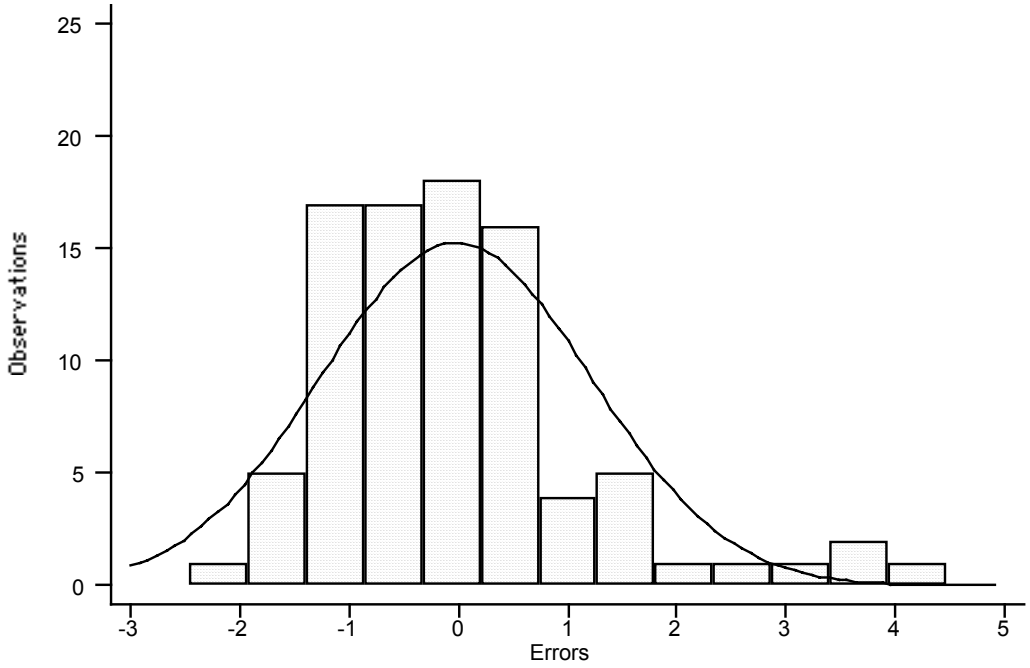

Figure 6.41: Distribution of regression residuals of *B. subtilis* log experiments.

The 95% confidence intervals for each parameter of the best-fit models were computed using the following F ratio test (Bates and Watts, 1988):

$$\frac{RSS(\theta_z)/(n-df)}{RSS_0/(n-df)} \le (1 + \underset{n-z(1-\alpha)}{\overset{df}{F}} \frac{z}{n-z})$$

or

$$RSS(\theta_z) = RSS_0(1 + \underset{n-z(1-\alpha)}{\overset{df}{F}} \frac{z}{n-z})$$

where θ_z is the vector of parameters for the bound of confidence region, *df* is the degrees of freedom, *n* is the number of observations, and *z* is the number of parameters. F is the F statistic computed using the inverse F probability distribution function in Microsoft Excel 98. For 95% confidence interval, α is 5%, with a numerator degrees of freedom of *z*, and denominator degrees of freedom of (*n* - *z*). The above equation was solved by varying one parameter at a time. This equation had at least two solutions for each parameter, and the upper and lower solutions closest to the optimum parameter were found by using "Goal Seek" add-in in Microsoft Excel 98. The computed 95% confidence intervals for each parameter in each best-fit model are given in Table 6.25.

Table 6.25: 95% confidence intervals for each parameter of each best-fit model.

Experiment	Model	Parameter	Optimum	Lower Limit	Upper Limit
G. muris	Power Law	k	5.4881	4.5810	6.5243
		n	1.7066	1.5997	1.8210
		x	1.4032	1.3809	1.4257
E. coli batch	Hom Power Law	k	0.0048	0.0043	0.0055
		n	2.4737	2.0207	2.8265
		m	2.9479	2.8868	3.0149
		x	1.2180	1.2010	1.2377
E. coli log	Hom Model	k	0.0780	0.0729	0.0831
		n	2.3796	2.1549	2.6101
		m	2.5989	2.5595	2.6356
E. coli DMS	Chick Model	k	0.5171	0.4823	0.5518
E. coli DMS control	Hom Model	k	0.0753	0.0682	0.0824
		n	1.7449	1.4378	2.0456
		m	2.1645	2.1131	2.2112
E. coli chemostat	Hom Power Law	k	29.2543	0.2021	0.2230
		n	4.1685	1.7959	2.1949
		m	0.5957	1.6637	1.7172
		x	0.0876	1.0414	1.0570
B. subtilis spores	Modified Multiple-target	k	1.5449	1.4263	1.6631
		n	0.6992	0.5523	0.8734
		n_c	8.4567	5.0372	14.5374
B. subtilis log	Hom Model	k	0.8031	0.7612	0.8450
		n	0.2009	0.0020	0.3967
		m	0.5414	0.5243	0.5576

The main objective of regression analysis was to determine the values of parameters in the most applicable inactivation model that provided the best prediction of observed surviving organisms. Regression plots can give visual information on how well the model fits the observed data and the presence of any unusual observations that might be outliers. The regression plots of the best-fit models for each of the data set are given in Figure 6.42 through Figure 6.49. In these regression plots, the predicted and observed surviving organisms were graphed to see how well the predictions came true. The solid line shows equally predicted and observed surviving organisms. The smaller the spread around this line, the better the fit is. In most of the regression plots, the data points are grouped around this line. However, in residual plots of *B. subtilis* log and *E. coli* DMS experiments, 5 and 4 data points were observed, respectively, that seem to have

unusually large residuals. These observations were also noticed on histograms of regression residuals (Figure 6.37 and Figure 6.41, respectively). The outliers in the inactivation experiments of *B. subtilis* at exponential growth phase were observed in experiments 411 and 412, where these 5 observations had unusually larger errors in MLR. These experiments were conducted the same day using the same batch of microbial suspension. The outlier observations in the *E. coli* DMS experiments were in experiments 501, 502, 505 and 506. Experiments 501 and 505 were conducted on the same day, with the same microbial suspension as experiments 502 and 506, respectively. These four observations were at lower surviving microbial densities (0.5, 1.5, 10.6 and 1.5 CFU/mL, respectively). These outliers may cause underestimation of inactivation. The inactivation data of both of the experimental series was re-evaluated without these outliers. The same non-linear regression process was followed for *B. subtilis* log and *E. coli* DMS data sets where 5 and 4 of the outliers were dropped from the inactivation data, respectively. The summaries of the non-linear regression analyses of these two inactivation data sets without the outliers are given in Table 6.26 and Table 6.27. A slight improvement in adjusted r^2 in fit of *B. subtilis* log data and *E. coli* DMS data sets were observed. The regression plots of the best-fit models for these two data sets without outliers are presented in Figure 6.52 and Figure 6.53. In these plots, one can see that the observations are closer to the regression line this time.

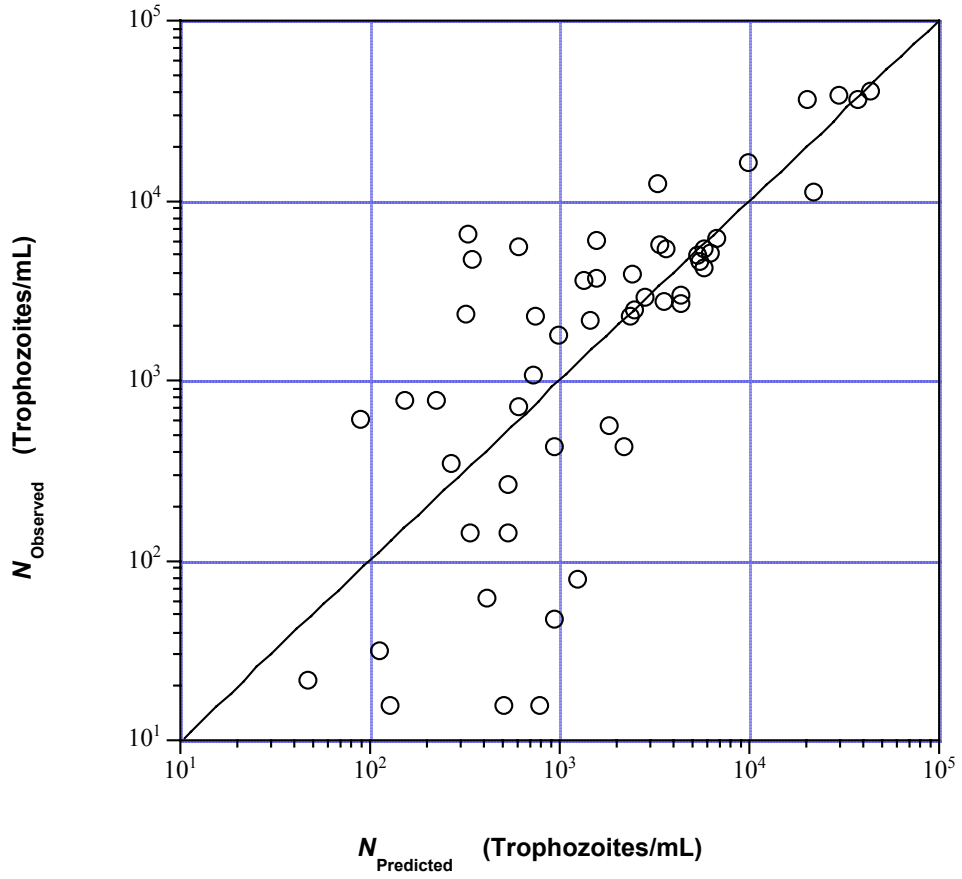

Figure 6.42: Observed surviving organism density versus surviving organism density predicted by PL in *G. muris* experiments.

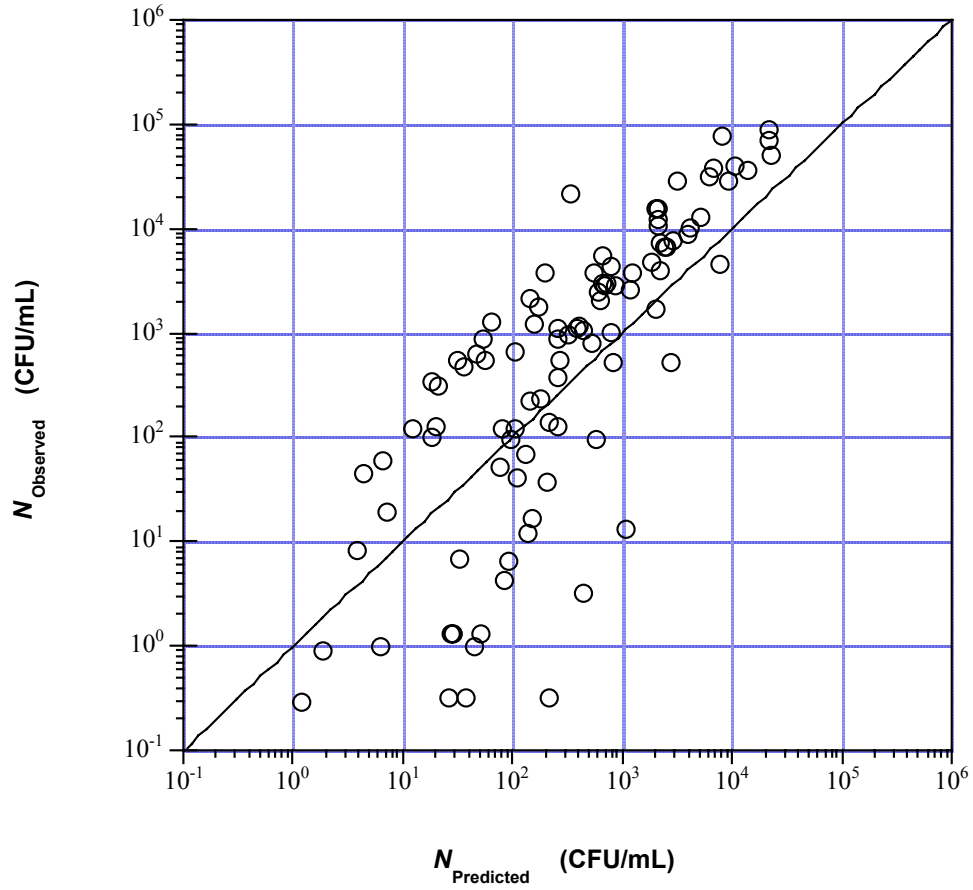

Figure 6.43: Observed surviving organism density versus surviving organism density predicted by HPL in *E. coli* batch experiments.

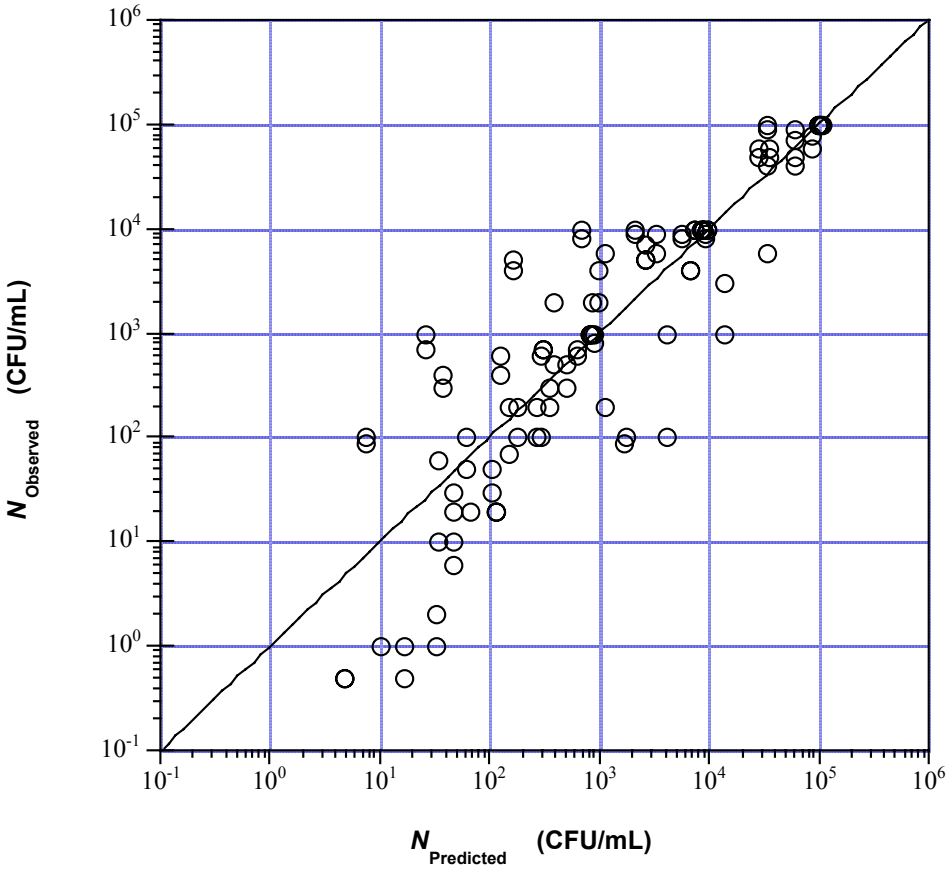

Figure 6.44: Observed surviving organism density versus surviving organism density predicted by Hom model in *E. coli* log experiments.

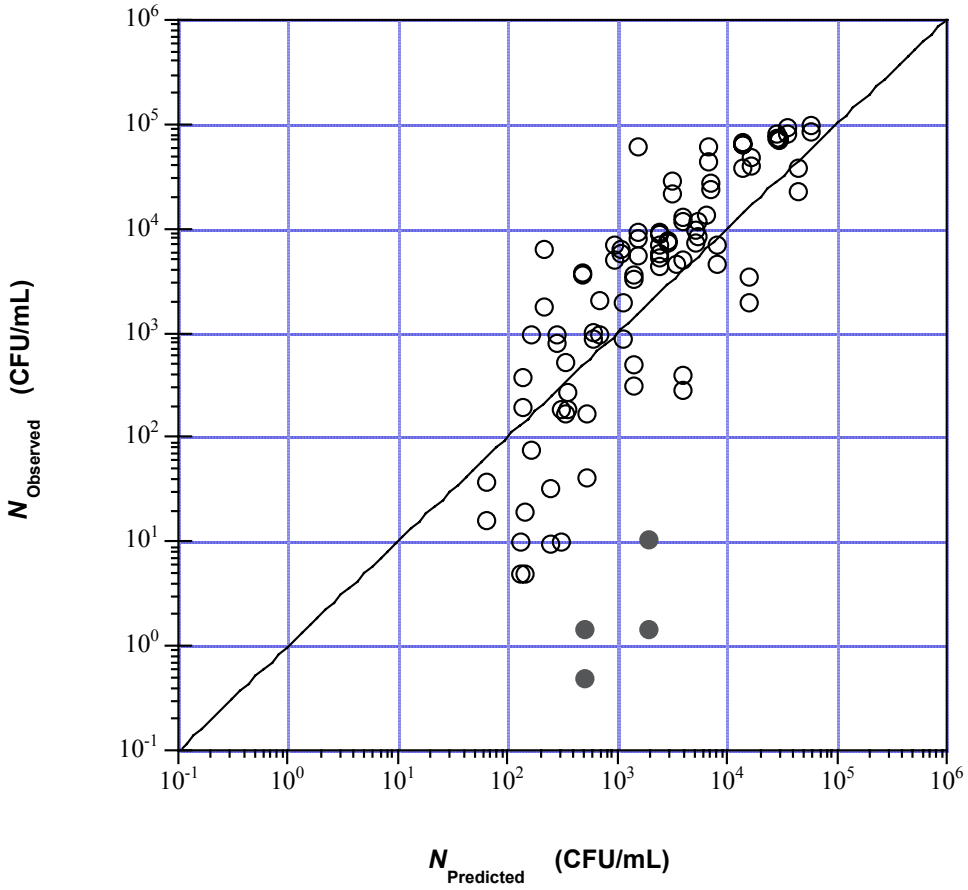

Figure 6.45: Observed surviving organism density versus surviving organism density predicted by Chick model in *E. coli* DMS experiments (the full circles represent possible outlier observations, see appropriate text for details).

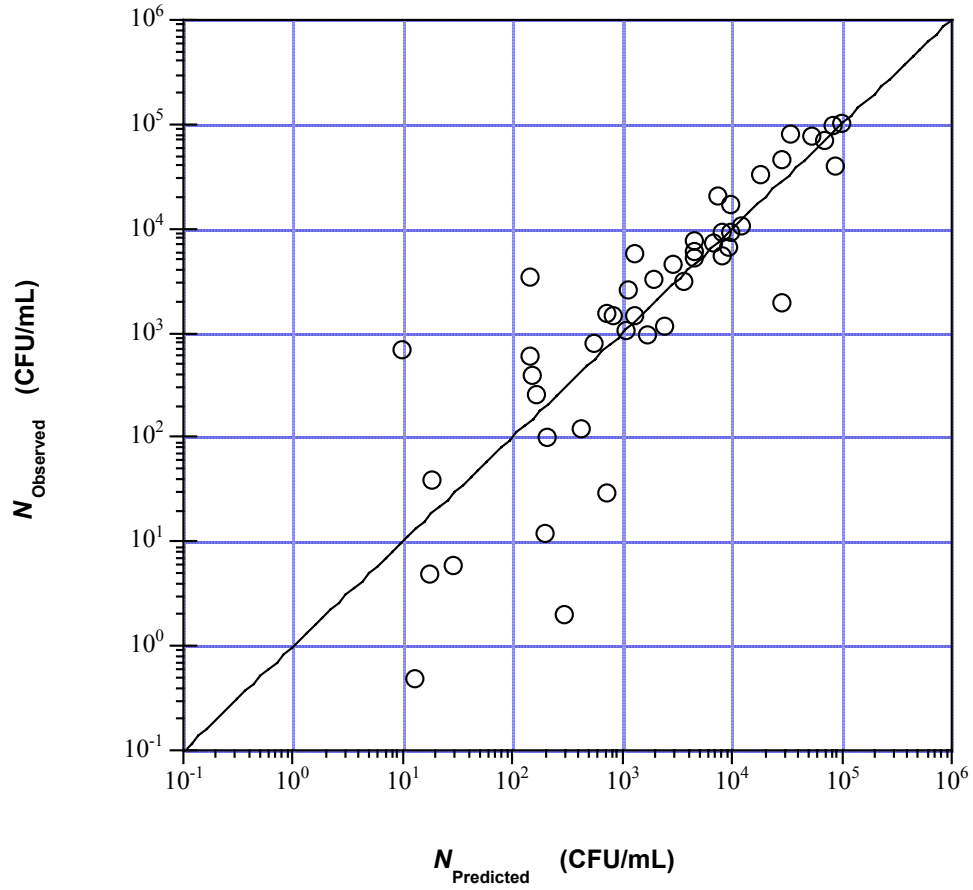

Figure 6.46: Observed surviving organism density versus surviving organism density predicted by Hom model in *E. coli* DMS control experiments.

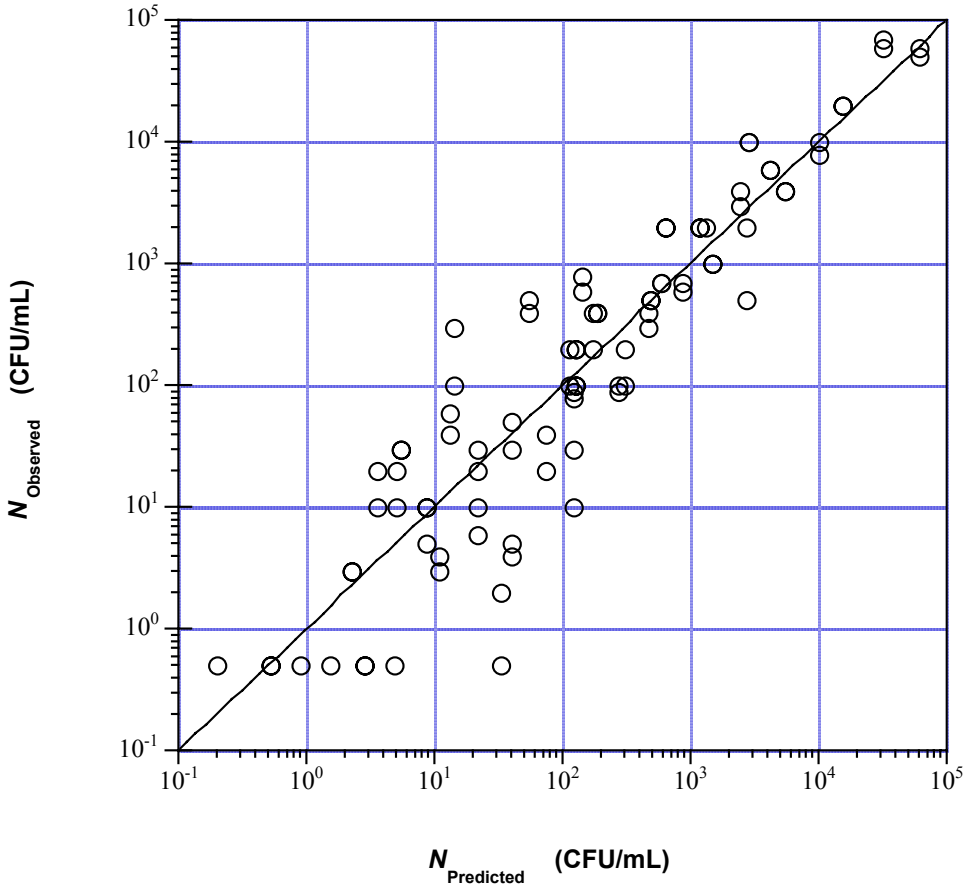

Figure 6.47: Observed surviving organism density versus surviving organism density predicted by HPL in *E. coli* chemostat experiments.

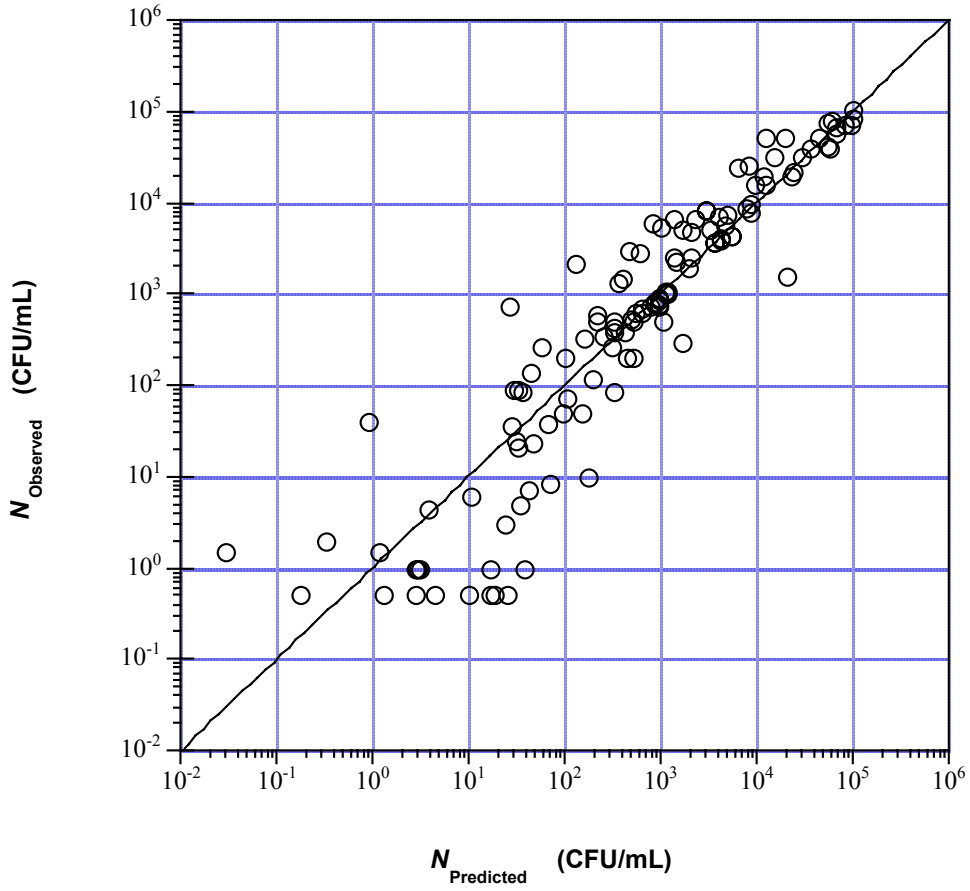

Figure 6.48: Observed surviving organism density versus surviving organism density predicted by Modified Multiple-target model in *B. subtilis* spore experiments.

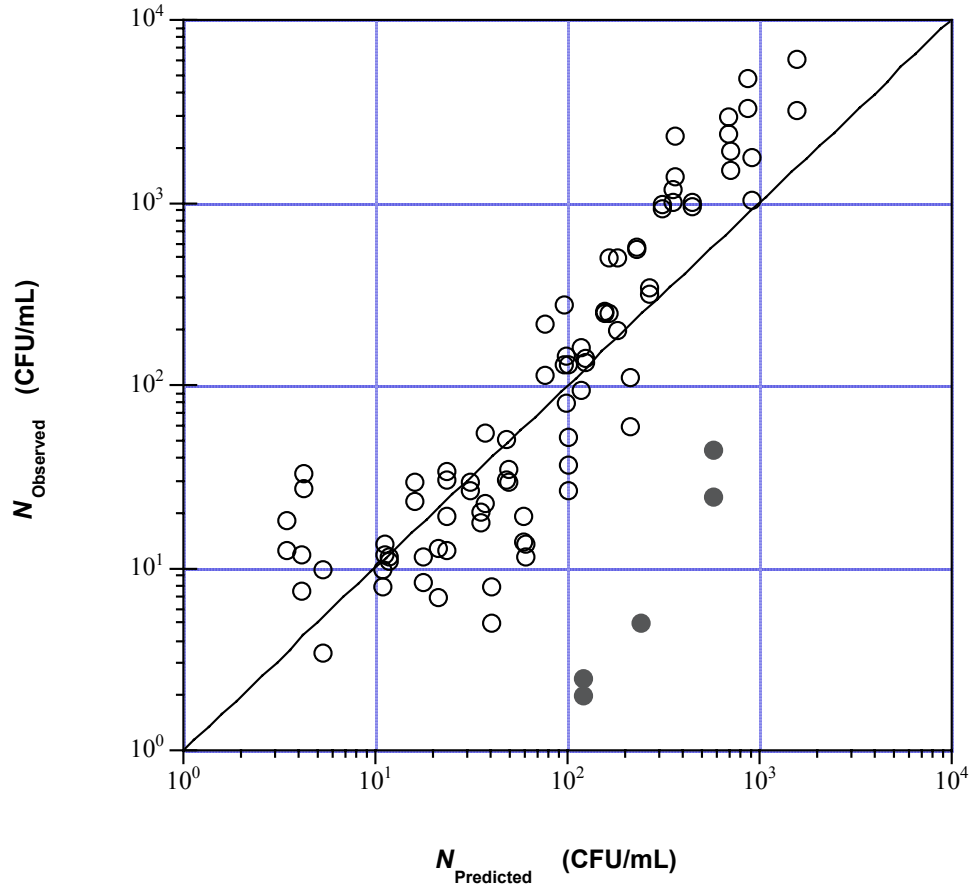

Figure 6.49: Observed surviving organism density versus surviving organism density predicted by Hom model in *B. subtilis* log experiments (the full circles represent possible outlier observations, see appropriate text for details).

Table 6.26: Summary of least-squares regression of *E. coli* DMS data without outliers, 92 observations.

	Parameters					RSS	Adjusted
MODEL	k	n	m/n_c	x	κ		r^2
Chick	0.4319					200.86	0.6629
MT	0.4688		1.2327			200.51	0.6597
SE	0.4283				0.8940	201.02	0.6589
CW	0.4320	0.9982				200.86	0.6591
Hom	0.3932	1.0337	1.0548			200.71	0.6556
PL	1.7579	1.2426		0.8346		176.21	0.6976
MMT	0.4711	0.9780	1.2466			200.49	0.6559
HPL	2.2202	1.1845	0.8885	0.8297		175.22	0.6959

Table 6.27: Summary of least-squares regression of *B. subtilis* Log data without outliers, 84 observations.

	Parameters					RSS	Adjusted
MODEL	k	n	m/n_c	x	κ		r^2
Chick	0.1707					121.80	0.8951
MT	0.1146		0.2389			85.58	0.9254
SE	0.1702				0.9941	121.59	0.8940
CW	0.1735	0.5708				109.23	0.9048
Hom	0.5946	0.2786	0.6249			67.99	0.9400
PL	0.0669	0.8210		1.1843		73.55	0.9351
MMT	0.1188	0.4555	0.2506			75.46	0.9334
HPL	0.3572	0.4104	0.6965	1.0511		66.38	0.9407

Table 6.28: Probabilities for pairwise comparison with partial F-test.

a. Probabilities for pairwise comparison of kinetic models for *E. coli* DMS data without outliers.

Simpler Model		More Complex Model	Probability
Chick Model	vs.	Multiple-target	6.94×10^{-1}
Chick Model	vs.	Power Law	2.95×10^{-3}
Power Law	vs.	Hom Power Law	4.82×10^{-1}

b. Probabilities for pairwise comparison of kinetic models for *B. subtilis* log data without outliers.

Simpler Model		More Complex Model	Probability
Chick Model	vs.	Multiple-target	8.17×10^{-8}
Multiple-target	vs.	Hom Model	1.67×10^{-5}
Hom Model	vs.	Hom Power Law	1.68×10^{-1}

The pairwise comparison of the model fit by the partial F-test shows that (Table 6.28) the Power Law provided superior fit for the inactivation data of *E. coli* DMS experiments with 92 observations. In the case of *B. subtilis* log experiments, the Hom Model provided the best-fit for the inactivation data again. The histograms of the distribution of the errors are given in Figure 6.50 and Figure 6.51, and they are still not normally distributed. The residuals of both of the best-fit model were independent of any of the predictors (Table 6.29).

Table 6.29: Pairwise correlation coefficient of regression residuals with C_0, N_0 and time and Shapiro-Wilk normality test results for regression residuals.

					Normality	
	Best-fit	Significance Level			Test	Skewness
Experiment	Model	C_o	Time	N_o	*P*	*P*
E. coli DMS (n = 92)	Power Law	0.6358	0.6552	0.0845	<0.0001	<0.001
B. subtilis log (n = 84)	Hom Model	0.4474	0.7133	0.1991	0.6125	0.309

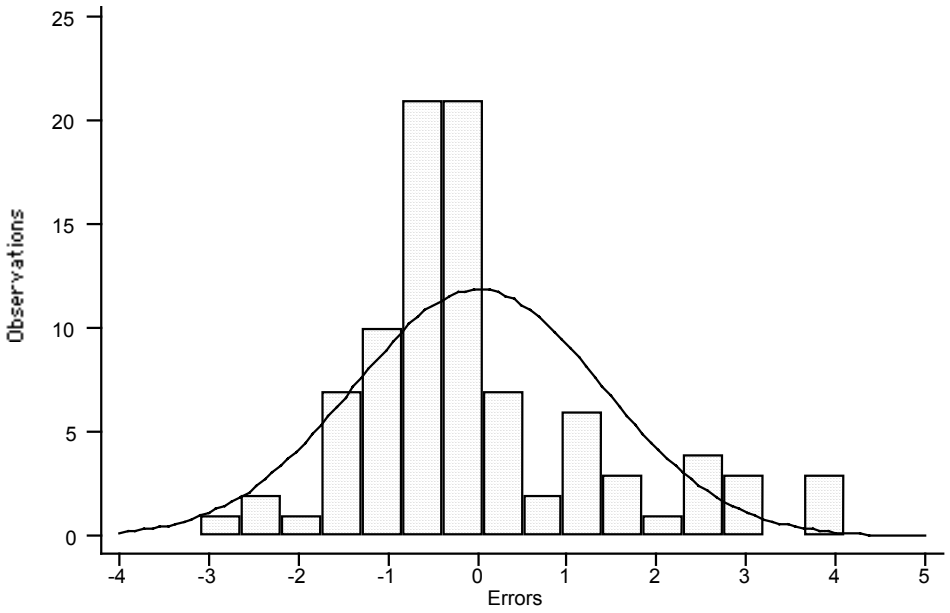

Figure 6.50: Distribution of regression residuals of *E. coli* DMS experiments without outliers.

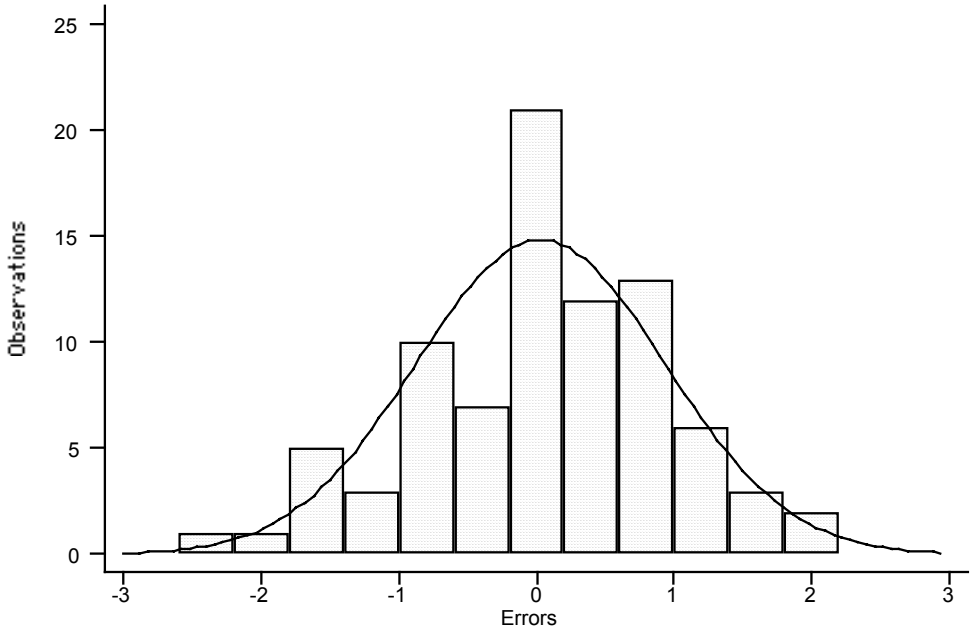

Figure 6.51: Distribution of regression residuals of *B. subtilis* log experiments without outliers.

The 95% confidence intervals of each parameter of the best-fit models of the data sets without outliers were computed using the same process as described above (Table 6.30).

Table 6.30: 95% confidence intervals for each parameter of each best-fit models.

Experiment	Model	Parameter	Optimum	Lower Limit	Upper Limit
E. coli DMS (n = 92)	Power Law	k	1.7579	1.6215	1.8870
		n	1.2426	0.9926	1.4780
		x	0.8346	0.8246	0.8437
B. subtilis Log (n = 84)	Hom Law	k	0.5946	0.5717	0.6174
		n	0.2786	0.1305	0.4248
		m	0.6249	0.6126	0.6366

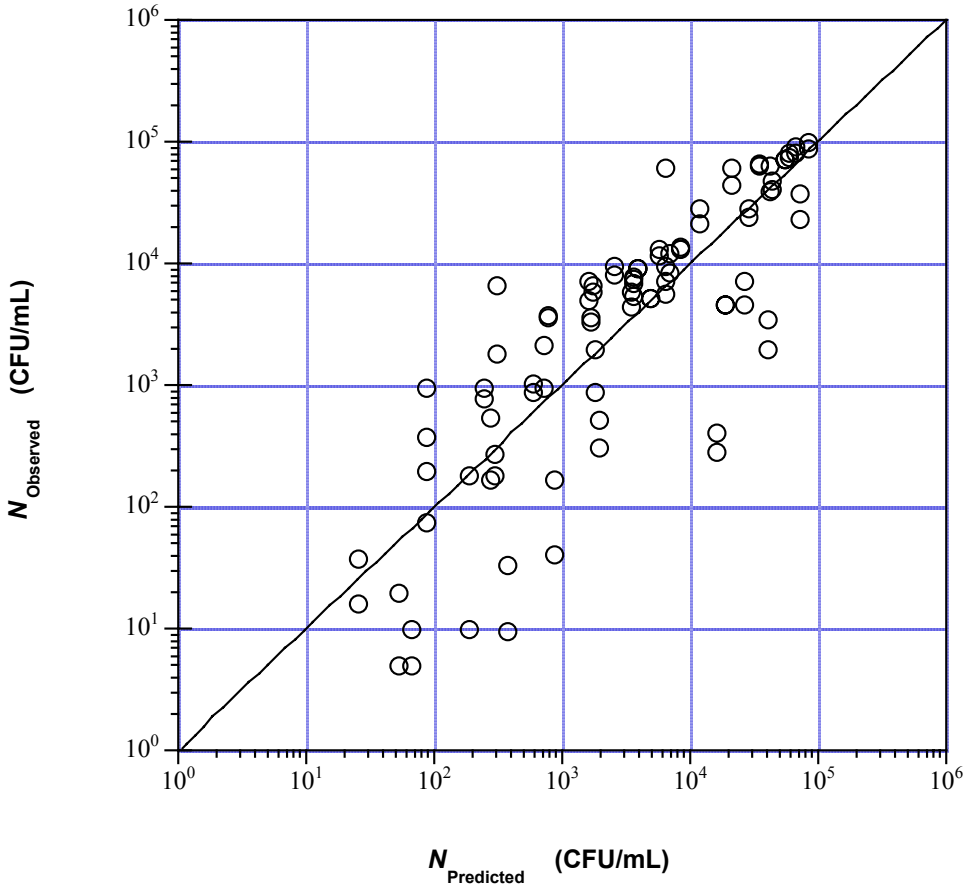

Figure 6.52: Observed surviving organism density versus surviving organism density predicted by Chick model in *E. coli* DMS experiments without outliers.

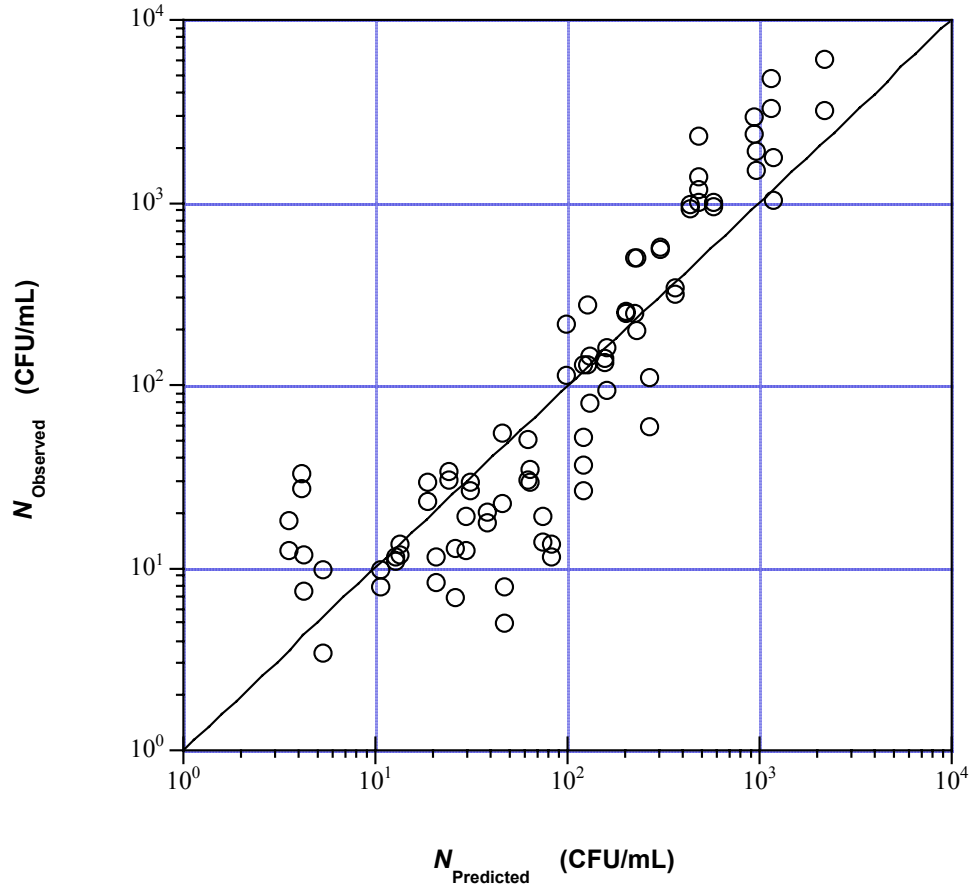

Figure 6.53: Observed surviving organism density versus surviving organism density predicted by Chick model in *B. subtilis* log experiments without outliers.

6.4. Comparison of Inactivation Kinetics

The objective of conducting *E. coli* DMS experiments was to investigate whether the cell density dependent activities in bacteria had any effects on disinfectant resistance or sensitivity. As described in the previous sections, the quorum sensing mechanism in bacteria is driven by extra-cellular molecules. By conducting inactivation experiments of *E. coli* in the presence of DMS, a high microbial density environment was simulated. The underlying basic

assumption was that, adding excess amount of DMS would result in a high concentration of autoinducers and the cells would act as if the microbial density surrounding them was higher than the actual density.

To verify if this assumption was satisfied, the inactivation kinetics of batch cultures of *E. coli* at stationary growth phase in the presence and absence of DMS was compared using two different methods.

In the first method, inactivation data sets of *E. coli* batch, *E. coli* DMS and *E. coli* DMS control were pooled together and then, the best multiple linear model was developed using stepwise regression for the pooled inactivation data. In the next step, the pooled data were categorized according to the survival data set. In other words, data sets pooled (*E. coli* batch, *E. coli* DMS and *E. coli* DMS Control) were added as a categorical variable. The significance of this categorical variable showed the significant difference in inactivation efficiency. The STATA 7™ output of stepwise regression results with the subset of predictors are given in Table 6.31.

Table 6.31: STATA 7™ output of stepwise MLR results for pooled *E. coli* batch, *E. coli* DMS and *E. coli* DMS control data.

```
  Source |       SS       df       MS          Number of obs =     240
---------+------------------------------       F(  2,   237) =  138.48
   Model |  1077.10376     2  538.551882        Prob > F      =  0.0000
Residual |  921.691027   237  3.88899168        R-squared     =  0.5389
---------+------------------------------       Adj R-squared =  0.5350
   Total |  1998.79479   239  8.36315812        Root MSE      =  1.9721

------------------------------------------------------------------------------
     lns |      Coef.   Std. Err.      t    P>|t|     [95% Conf. Interval]
---------+--------------------------------------------------------------------
      CT |   -1.57863    .229196    -6.89   0.000    -2.030152   -1.127108
    lnCT |   2.619838   .9509613     2.75   0.006    0.7464216    4.493255
   _cons |  0.8925847  0.4393809     2.03   0.043    0.0269937    1.758176
------------------------------------------------------------------------------
```

In the next step, analysis of variance (ANOVA) was conducted with this additional categorical variable. According to ANOVA results (Table 6.32), the experiment type was a statistically significant ($P < 0.05$) predictor of survival ratio.

Table 6.32: STATA 7™ output of ANOVA for pooled *E. coli* batch, *E. coli* DMS and *E. coli* DMS control data.

```
      Number of obs =     240     R-squared     =  0.5548
      Root MSE      = 1.94591     Adj R-squared =  0.5472

    Source |  Partial SS    df       MS           F     Prob > F
-----------+----------------------------------------------------
     Model |  1108.95082     4  277.237705      73.22     0.0000
           |
        ct |  168.569654     1  168.569654      44.52     0.0000
      lnCT |  25.2660452     1  25.2660452       6.67     0.0104
       Exp |  31.8470579     2  15.9235289       4.21     0.0161
           |
  Residual |  889.843969   235  3.78657008
-----------+----------------------------------------------------
     Total |  1998.79479   239  8.36315812
```

In computing ANOVA, a value was a given to each level of the categorical variable ("effects"). During this process, the value of effect for one of the factors was set to zero, i.e., it was dropped. The values for the effect of other factors were calculated relative to the dropped factor. These values associated with each factor (data set) and coefficients for the other predictors were given in Table 6.33, along with the estimated standard errors and 95% confidence intervals. In the ANOVA computation of the pooled data, the effects of *E. coli* batch experiments were set to zero. The calculated effects for *E. coli* DMS Control experiments was 0.5484, but the value of this effect was not statistically significantly different than zero based on a 95% confidence interval, which means that the inactivation efficiency of monochloramine in *E. coli* DMS Control experiments was not significantly different from *E. coli* batch experiments.

The ANOVA results showed that the addition of DMS into the experimental water had a statistically significant effect on inactivation efficiency.

Table 6.33: STATA 7™ output for effects of categorical variable and regression coefficients estimated in ANOVA.

```
------------------------------------------------------------------------------
  lns       Coef.   Std. Err.      t    P>|t|     [95% Conf. Interval]
------------------------------------------------------------------------------
_cons     .4401392   .4622995     0.95   0.342    -.4706417    1.35092
CT       -1.515875   .2271939    -6.67   0.000    -1.963472   -1.068278
lnCT      2.429822   .9406515     2.58   0.010    0.5766346    4.283008
Exp
  Ctrl   0.5484399   0.3487417    1.57   0.117   -0.1386197    1.235499
  DMS    0.8066676   0.2816927    2.86   0.005    0.251702     1.361633
 Batch   0
------------------------------------------------------------------------------
```

In the second method of comparison, it was assumed that under both conditions, the inactivation kinetics were identical. Based on this assumption, inactivation data sets of *E. coli* batch, *E. coli* DMS and *E. coli* DMS Control were pooled together as pairs in different combinations again. The pooled data were fit to inactivation models using NLLS regression using the same process as before. The summaries of least squares regression for each combination of pooled inactivation data and the pairwise F-test comparisons are given in Table 6.34 through Table 6.36 and Table 6.37, respectively. The errors of regressions were also tested for normality and any correlation with independent variables (Table 6.38).

Table 6.34: Summary of least-squares regression of pooled *E. coli* batch and *E. coli* DMS Control data, 144 observations.

	Parameters					RSS	Adjusted
MODEL	k	n	m/n_c	x	κ		r^2
Chick	0.7389					625.56	0.7851
MT	1.3048		31.6972			482.86	0.8330
SE	1.0664				2.8439	528.88	0.8171
CW	0.7436	0.9058				612.67	0.7881
Hom	0.1429	1.6217	1.8806			476.77	0.8339
PL	0.6460	0.8925	1.0180			610.96	0.7872
MMT	1.0304	0.9423	7.0448			479.54	0.8330
HPL	0.0169	2.0287	2.55	1.1256		422.73	0.8517

Table 6.35: Summary of least-squares regression of pooled *E. coli* batch and *E. coli* DMS data, 194 observations.

	Parameters					RSS	Adjusted
MODEL	k	n	m/n_c	x	κ		r^2
Chick	0.6665					920.96	0.7198
MT	1.0986		13.1111			809.19	0.7525
SE	0.9860				2.5343	831.91	0.7456
CW	0.6669	0.9951				916.47	0.7197
Hom	0.1598	1.6324	1.7746			802.27	0.7534
PL	0.5865	1.0009		1.0159		911.09	0.7199
MMT	0.9155	0.9061	5.7874			801.56	0.7536
HPL	0.0715	1.7562	1.9941	1.0532		787.35	0.7567

Table 6.36: Summary of least-squares regression of pooled *E. coli* DMS and *E. coli* DMS Control data, 142 observations.

	Parameters					RSS	Adjusted
MODEL	k	n	m/n_c	x	κ		r^2
Chick	0.5548					536.27	0.6692
MT	0.8431		5.2252			501.74	0.6883
SE	0.5502				0.9984	538.22	0.6657
CW	0.5514	1.1056				535.11	0.6676
Hom	0.1796	1.5524	1.6294			498.30	0.6882
PL	0.5702	1.0014		1.0000		524.32	0.6720
MMT	0.8479	0.9788	5.3448			501.64	0.6861
HPL	0.3886	1.5106	1.4710	0.9414		490.65	0.6908

As discussed before, 4 outlier points were observed in *E. coli* DMS experiments and the Power-Law provided a superior fit for this data set without outliers. Although the fit to the data set without outliers was slightly better than the full data set, all the pooled data analyses were conducted again without the 4 outlier observations. The summary of the regression analysis, F-test statistics, pairwise correlation results and the Shapiro-Wilk test for the normal distribution of regression residuals are given in Table 6.39 through Table 6.40, Table 6.41 and Table 6.42, respectively.

Table 6.37: Probabilities for pairwise comparison model fits with partial F-test.

a. Probabilities for pairwise comparison of kinetic models for pooled *E. coli* batch and *E. coli* DMS Control data.

Simpler Model		More Complex Model	Probability
Chick Model	vs.	Multiple-target	1.42×10^{-9}
Multiple-target	vs.	Modified Multiple-target	3.25×10^{-1}
Multiple-target	vs.	Hom Power Law	9.06×10^{-5}

b. Probabilities for pairwise comparison of kinetic models for pooled *E. coli* batch and *E. coli* DMS data.

Simpler Model		More Complex Model	Probability
Chick Model	vs.	Multiple-target	6.44×10^{-7}
Multiple-target	vs.	Hom Model	4.77×10^{-7}
Hom Model	vs.	Hom Power Law	5.95×10^{-2}

c. Probabilities for pairwise comparison of kinetic models for pooled *E. coli* DMS and *E. coli* DMS Control data.

Simpler Model		More Complex Model	Probability
Chick Model	vs.	Multiple-target	2.31×10^{-3}
Multiple-target	vs.	Hom Model	3.29×10^{-1}
Hom Model	vs.	Hom Power Law	1.45×10^{-1}

Table 6.38: Pairwise correlation coefficient of residuals of best-fit models with *Co*, *No* and time and Shapiro-Wilk test results for normal distribution of residuals.

		Significance Level			Normality Test
	Best-fit				
Pooled Data Sets	Model	C_o	Time	N_o	*P*
E. coli batch and *E. coli* DMS Control	HPL	0.2770	0.5928	0.7103	<0.0001
E. coli batch and *E. coli* DMS	Hom	0.3625	0.7627	0.4041	<0.0001
E. coli DMS and *E. coli* DMS Control	Hom	0.8661	0.8461	0.3716	<0.0001

Table 6.39: Summary of least-squares regression of pooled *E. coli* batch and *E. coli* DMS data without outliers, 190 observations.

	Parameters					RSS	Adjusted
MODEL	k	n	m/n_c	x	κ		r^2
Chick	0.6375					807.17	0.7202
MT	1.0386		10.7055			715.08	0.7508
SE	1.4712				4.4659	692.94	0.7585
CW	0.6383	0.9024				792.55	0.7238
Hom	0.1534	1.5662	1.7763			703.60	0.7535
PL	0.6356	0.8395		1.0000		791.08	0.7228
MMT	1.0368	0.8750	10.8280			698.66	0.7552
HPL	0.0784	1.6639	1.9550	1.0449		791.08	0.7213

Table 6.40: Summary of least-squares regression of pooled *E. coli* DMS and *E. coli* DMS Control data without outliers, 138 observations.

	Parameters					RSS	Adjusted
MODEL	k	n	m/n_c	x	κ		r^2
Chick	0.5028					382.06	0.6865
MT	0.7089		3.2215			365.38	0.6980
SE	1.0562				3.3285	368.83	0.6952
CW	0.5037	0.9575				381.92	0.6843
Hom	0.2082	1.3113	1.5008			362.31	0.6983
PL	1.3180	1.1357		0.8865		356.20	0.7034
MMT	0.7264	0.8942	3.5020			363.70	0.6972
HPL	0.6646	13102	1.2977	0.9050		347.50	0.7085

Table 6.41: Probabilities for pairwise comparison of model fits with partial F-test.

a. Probabilities for pairwise comparison of kinetic models for pooled *E. coli* batch and *E. coli* DMS data without outliers.

Simpler Model		More Complex Model	Probability
Chick Model	vs.	Series-Event	8.85×10^{-8}
Series-Event	vs.	Modified Multiple-target	N/A
Modified Multiple-target	vs.	Hom Power Law	N/A

b. Probabilities for pairwise comparison of kinetic models for pooled *E. coli* DMS and *E. coli* DMS Control data without outliers.

Simpler Model		More Complex Model	Probability
Chick Model	vs.	Multiple-target	1.39×10^{-2}
Multiple-target	vs.	Power Law	6.32×10^{-2}
Multiple-target	vs.	Hom Power Law	3.46×10^{-2}

Table 6.42: Pairwise correlation coefficient of residuals of best-fit models with Co, No and time and Shapiro-Wilk test results for normal distribution of residuals.

		Significance Level			Normality Test
Pooled Data Sets	Best-fit Model	C_o	Time	N_o	P
E. coli batch and *E. coli* DMS	SE	0.8075	0.7673	0.6321	<0.0001
E. coli DMS and *E. coli* DMS Control	HPL	0.6640	0.7983	0.3135	<0.0001

In the next step, the basic assumption of identical inactivation kinetics was checked. If the inactivation kinetics were identical, there would be no significant ($P < 0.05$) difference in the fit whether NLLS regression was conducted for all the data all at once or to subgroups separately. The Partial F-test was used again to test the significance of improvement in goodness of fit for subgrouped data over pooled data. When the data were divided into subgroups, more than one model was used to describe the whole data, whereas, the pooled data was described by one model. Therefore, by conducting the nonlinear regression separately for each subgroup, one decreased the overall degrees of freedom as seen in Table 6.43. The partial F-test results for comparison of the full data sets and data sets without outliers are given in Table 6.43 and Table 6.44 respectively, where F was calculated as follows,

$$F = \frac{(\mathrm{RSS}_{\mathrm{Pooled}} - \mathrm{RSS}_{\mathrm{Total\ Subgroups}})/(\mathrm{df}_{\mathrm{Pooled}} - \mathrm{df}_{\mathrm{Total\ Subgroups}})}{\mathrm{RSS}_{\mathrm{Total\ Subgroups}} / \mathrm{df}_{\mathrm{Total\ Subgroups}}}$$

The probability was calculated using inverse F distribution function in Microsoft Excel 1998®.

$$P = F_{distribution}(\mathrm{df}_{\mathrm{Pooled}} - \mathrm{df}_{\mathrm{Total\ Subgroup}}, \mathrm{df}_{\mathrm{Total\ Subgroup}}, \mathrm{F})$$

Table 6.43: Pairwise comparison of pooled data fit with individual fits using partial F-test.

a. Comparison of *E. coli* Batch and *E. coli* DMS Control data.

	Model	RSS	n	df	F	Probability
Subgroups of						
E. coli Batch,	HPL	274.99	98	94	4.6856	3.79×10^{-3}
E. coli DMS Control	Hom	108.40	46	43		
Total		383.39	144	137		
Pooled Data	HPL	422.73	144	140		

b. Comparison of *E. coli* Batch and *E. coli* DMS data.

	Model	RSS	n	df	F	Probability
Subgroups of						
E. coli Batch,	HPL	274.99	98	94	22.1183	2.22×10^{-9}
E. coli DMS,	Chick	374.76	96	95		
Total		649.75	194	189		
Pooled Data	Hom	802.27	194	191		

c. Comparison of *E. coli* DMS and *E. coli* DMS Control data.

	Model	RSS	n	df	F	Probability
Subgroups of						
E. coli DMS,	Chick	374.76	96	95	4.3243	3.94×10^{-2}
E. coli DMS Control	Hom	108.40	46	43		
Total		483.16	142	138		
Pooled Data	Hom	498.30	142	139		

n : Number of observations
df: Degrees of freedom

Table 6.44: Pairwise comparison of pooled data fit with individual fits using partial F-test.

a. Comparison of *E. coli* Batch and *E. coli* DMS without outliers data.

	Model	RSS	n	df	F	Probability
Subgroups of						
E. coli Batch,	HPL	274.99	98	94	19.6093	1.27×10^{-15}
E. coli DMS,	PL	176.21	92	89		
Total		451.20	190	183		
Pooled Data	SE	692.94	190	188		

b. Comparison of *E. coli* DMS without outliers and *E. coli* DMS Control data.

	Model	RSS	n	df	F	Probability
Subgroups of						
E. coli DMS,	PL	176.21	92	89	3.3818	5.29×10^{-9}
E. coli DMS Control	Hom	108.40	46	43		
Total		284.61	138	132		
Pooled Data	SE	692.94	138	188		

n : Number of observations
df: Degrees of freedom

When all the experimental inactivation data of batch cultures of *E. coli* (*E. coli* Batch, *E. coli* DMS and *E. coli* DMS Control) were fit to the inactivation models separately as subgroups, the total sum of RSS of all three data sets was significantly lower than the RSS of pooled data fit. This statistically significant difference showed that the inactivation of each data had different kinetics and should be described with different models and corresponding kinetic parameters. The results of the second method partially agreed with the first method. According to the second method, significantly different inactivation kinetics were observed in each data set, *E. coli* Batch, *E. coli* DMS (with or without outliers) and *E. coli* DMS Control. According to the first method, there was no statistically significant difference in inactivation kinetics between *E. coli* batch and DMS Control experiments; however, statistically significant different kinetics were observed between *E. coli* batch and DMS experiments according to the second method.

6.5. Discussion

Two different methods were used to analyze the 8 sets of inactivation data. Overall, except for two of the data sets (*G. muris* and *E. coli* DMS), the conclusions of both of the methods were in agreement. The inactivation of *B. subtilis* in either spore form or at exponential growth phase was a function of disinfectant dose and contact time only. In stationary phase, *E. coli* whether grown in batch or continuous cultures, the inactivation efficiency was dependent on disinfectant dose and contact time as well as the initial microbial density. In *E. coli* at exponential growth phase and in the inactivation data from the control reactor in the *E. coli* DMS experiments, the survival was only dependent on disinfectant dose and contact time.

The results of MLR and NLLS regressions for *Giardia* and *E. coli* DMS data did not agree with each other. According to the model developed by MLR, inactivation of *G. muris* was independent of initial microbial density and *E. coli* DMS survival data was dependent on initial microbial density, whereas it was vice versa according to best-fit models in NLLS regression. The findings of regression analysis are compared in Table 6.45. The determination coefficient represents the proportion of the total variation in survival ratio represented by the regression model. However, the sampling distribution of the determination coefficient is not normally distributed (Sokal and Rohlf, 1995). The difference between determination coefficients of 0.3 and 0.4 is not the same as the difference between 0.7 and 0.8. Therefore, Fisher's Z' transformation was used to convert adjusted r^2 to the normally distributed variable Z'. The formula for the transformation is:

$$Z' = 0.5\ \left[\ln(1+\text{Adj. r}^2) - \ln(1-\text{Adj. r}^2)\right]$$

where, ln is the natural logarithm. The standard error of Z' was calculated by this formula:

$$\sigma_{Z'} = \frac{1}{\sqrt{N-3}}$$

where, N is the sample size.

After each determination coefficient was transformed to Z′, the significance of difference in success of model fits was compared using a normal distribution, where the null hypothesis was that there was no significant difference between determination coefficients. According to the comparison of transformed Z′ of each determination coefficient, NLLS regression provided a statistically significantly better ($P < 0.05$) fit than MLR in all data sets except *B. subtilis* log. In the regression analysis of *B. subtilis* exponential growth phase survival, there was no statistically significant difference in fit. One of the main disadvantages of MLR is that, MLR models fail to predict survival when dose and/or time are equal to zero. Therefore, MLR provides poor fit at lower time and/or disinfectant dose. In addition, the MLR models cannot describe nonlinear relations. To reduce the effects of non-linear relations, transformations of some of the predictors were also added in the model. However, MLR models still have a limited capability of describing the inactivation data. In a regression analysis of survival of *B. subtilis* exponential growth phase organisms without outliers, there was no significant difference in the determination coefficient; however, the NLLS regression model had only 3 parameters where the MLR model had 5 parameters. Therefore, the Hom model provided superior fit for this survival data set.

According to the best-fit inactivation models, inactivation of *G. muris* with ozone and *E. coli* at stationary growth phase with monochloramine were dependent on initial microbial density as well as disinfectant dose and contact time. In the rest of the experiments conducted in this study, inactivation was only dependent on disinfectant dose and contact time.

The CT plots for each inactivation data set were plotted using NLLS regression models, since these models provided superior fit (Figure 6.54 through Figure 6.61). A CT plot of *B. subtilis* log experiments was made using both the MLR model and NLLS regression models, since there was no significant difference in fit of both models. The CT plots were plotted for demand-free conditions with average disinfectant decay rates given in Table 6.3 and Table 6.4.

The CT plots for *E. coli* DMS and *B. subtilis* log experiments using best-fit models of data without outliers are plotted together with the full data sets (Figure 6.55 and Figure 6.60).

Table 6.45: Adjusted coefficients of determination for multiple linear and ordinary least squares regression analyses.

Experiment	MLR Adj r^2	NLLS Adj r^2	MLR Fisher's Z′	MLR STD	NLLS Fisher's Z′	*P*
G. muris	0.5402	0.7972	0.1429	1.2195	1.4359	2.56×10^{-4}
E. coli batch	0.7182	0.8760	0.1026	1.4482	1.7043	4.17×10^{-6}
E. coli log	0.6575	0.8242	0.0985	1.3227	1.5152	4.54×10^{-5}
E. coli DMS	0.4060	0.6246	0.1037	0.9567	1.0723	1.05×10^{-3}
E. coli DMS control	0.5869	0.8179	0.1525	1.3097	1.4958	7.36×10^{-4}
E. coli chemostat	0.8467	0.9486	0.1060	1.7978	2.1641	3.07×10^{-8}
B. subtilis spores	0.8275	0.8978	0.0909	1.7038	1.8070	9.84×10^{-4}
B. subtilis log	0.9040	0.8977	0.1078	2.0513	1.8065	6.22×10^{-1}
B. subtilis log, n=84	0.9502	0.9400	2.1803	0.1111	2.0845	8.06×10^{-1}

In the overall regression analysis, only the regression residuals of the Hom Power Law fit and MLR in continuous cultures of *E. coli* experiments and Power Law fit in *G. muris* experiments were distributed normally. Normality is one of the basic assumptions of linear regression, but it is not required for the ordinary least squares estimation of the model parameters (Quinn and Keough, 2002). The central-limit theorem assures that under broad conditions, inference based on the least-squares estimators is approximately valid in all as long the sample size is not small. The validity of least-squares estimation is robust. The levels of test and confidence intervals of least-squares regression are approximately correct in large samples even when the assumption of normality is violated (Fox, 1991).

In the *E. coli* experiments, initial microbial density effects were observed only in stationary phases (in both continuous and batch cultures). As discussed in Section 3.4, batch culture techniques contain a heterogeneous population of cells with different physiological ages. In batch cultures, the metabolic activities of the bacterial population is dependent on the amount of nutrient remaining. However, in this study, the consistency of the best-fit models by

regression analysis proved the reliability and reproducibility of the results. If the observed cell density dependency were due to dynamic conditions and heterogeneity in the batch cultures, the same results would not be obtained in the homogeneous continuous cultures of *E. coli*. As seen in Figure 6.57 and Figure 6.59, the efficiency of inactivation by monochloramine was higher at higher initial microbial density. In a reactor with constant hydraulic residence time, a lower monochloramine residual was required to achieve 99% inactivation in a suspension of 1×10^5 CFU/mL compared to a suspension of 1×10^5 CFU/mL of either chemostat or batch culture grown *E. coli*. The effect of initial microbial density was lower in continuous cultures. In other words, the range of required contact time increases for a ten-fold increase in initial microbial density was less for continuous cultures of *E. coli*. The difference in humidity and oxygen concentration during growth can be the reason for this. In continuous cultures, the organisms were grown in nutrient broth and air was bubbled continuously in to the chemostat.

The inactivation data obtained from the control reactor in *E. coli* DMS experiments did not have any dependency on initial microbial density. Although preparation of organisms and experimental methods of *E. coli* DMS control were the same as for *E. coli* batch, the kinetics of inactivation for the DMS reactor was distinct from the *E. coli* batch data set according to a comparison using NLLS regression. The size of the data sets might be the reason for this difference. The size of the *E. coli* DMS control was less than half the *E. coli* batch data set (46 versus 98). When the CT curves for 99% inactivation were compared (Figure 6.63), the curves were found to be close to each other.

Although cell density played an important role in the efficiency of disinfection of *E. coli* at stationary phase, its effect in the exponential growth phase was insignificant. This result agrees with previous studies on acid sensitivity (Cui *et al*., 2001; Datta and Benjamin, 1999), where cell density dependent acid sensitivity was observed in some species of bacteria only during the stationary growth phase. It has been known that exponentially growing cells are morphologically and physiologically distinct from stationary phase cells. Besides, quorum

sensing and starvation sensing co-regulate each other. In *Vibrio fischeri, Ralstonia solanacearum* and *Myxococcus xanthus*, the production of quorum signaling molecules requires a sigma factor that is maximally active under conditions of starvation (Lazazzera, 2000). However, the results of stationary and exponential growth phase *E. coli* inactivation experiments were not enough to provide a conclusion on the mechanisms causing cell density dependent inactivation. Therefore, *E. coli* DMS experiments were conducted.

The main objective of *E. coli* DMS experiments was to supply an excess amount of extra-cellular material, which may be the cause of cell density dependent inactivation kinetics. The microbial suspension was also treated with monochloramine, in case the cell density dependent inactivation kinetics were due to synergistic effects of byproducts of disinfectant and cell density related chemicals. At an excess concentration of these chemicals, either the cells would act as if microbial density surrounding them was higher than the actual density or the byproducts would be high. Based on this assumption, it was expected to observe cell density independent inactivation kinetics. The regression analysis results agreed with this expectation. The Chick model was the best-fit model and this model incorporated only disinfectant dose and time as independent variables. According to the experimental results of *E. coli* batch series, the cells were more sensitive to monochloramine at higher initial microbial densities. The purpose of adding DMS was to simulate a high microbial density environment. The difference in the resistance of *E. coli* under both of the conditions (presence or absence of DMS) can be clearly seen, when the CT curves are plotted for 99% inactivation in the same graph (Figure 6.62). In Figure 6.62, if the basic assumption of adding DMS was satisfied, the CT curve of *E. coli* DMS would place just below the CT curve of *E. coli* batch at initial microbial density of 1.0×10^5.

Similar results were also observed by ANOVA of survival in each inactivation of *E. coli* experimental series. A statistically significant difference in inactivation efficiency of monochloramine was observed on *E. coli* in the presence and absence of DMS. During ANOVA computation, the value of the effects associated with *E. coli* DMS experiments was greater than

E. coli batch experiments (Table 6.33). In the ANOVA model, the dependent variable is natural logarithm of survival ratio. Therefore, when the independent variables are kept constant (C_o and lnCT), the survival ratio of *E. coli* would be higher in the presence of DMS relative to absence of it. However, if the initial hypothesis that imitation of a high cell density environment was satisfied *E. coli* would be more sensitive to monochloramine in the presence of DMS.

During NLLS regression analysis, 4 outliers were observed in the *E. coli* DMS data set. When the data set was analyzed without these 4 observations, the inactivation efficiency was cell density dependent. However, in this case, the inactivation efficiency increased as microbial density decreased. To make a detailed explanation of this effect of DMS, the exact chemistry of this conditioned media should be known. The variances of monochloramine decay in each series of experiments were analyzed using one-way ANOVA to investigate whether the addition of DMS affected the decay rate of monochloramine. No significant effect of experimental series was observed (Table 6.46). The addition of DMS and the type of the organism (*E. coli* or *B. subtilis*), growth phase (exponential or stationary) did not have any significant effect on the decay rate of monochloramine.

Table 6.46: ANOVA of decay rate of monochloramine.

	Partial SS	df	MS	F	Prob > F
Model	2.82×10^{-5}	4	5.60×10^{-8}	2.37	6.24×10^{-2}
Experimental series	2.82×10^{-5}	4	5.60×10^{-8}	2.37	6.24×10^{-2}
Residual	1.82×10^{-4}	61	2.98×10^{-6}		
Total	2.10×10^{-4}	65	3.23×10^{-5}		

From the kinetic analysis of monochloramine, it is known that the addition of DMS did not have any significant effect on the decay rate of monochloramine. In any microbial suspension, there exists a large number of different bacterial products. Adding disinfectant for pretreatment of the organisms in such a suspension would change the chemistry of the

suspension. All the bacterial products and disinfection byproducts in DMS and their lifetimes were unknown. Any material responsible for cell density dependent inactivation might have been destroyed during handling. Without knowing the detailed chemical composition of DMS, it is not feasible to explain the reasons and mechanisms of the effect of DMS on the inactivation kinetics. The question about the relation between a quorum sensing system and cell density dependent disinfectant resistance was unanswered.

The other organism that had cell density dependent inactivation kinetics was *G. muris.* The effect of initial microbial density was similar for *G. muris* cysts. Higher inactivation of *G. muris* cysts was observed at a higher initial microbial density at constant ozone dose and contact time (Figure 6.56). There are studies suggesting cell density dependent activities in protozoan ciliates (Christensen *et al*., 2001; Ekelund *et al*., 2002), however, these studies had no information on detailed mechanisms of any cell density dependent activity. Also, there does not appear to be any previous work done with respect to protozoa density effects on response to disinfectants.

Initial microbial density of *B. subtilis* did not have any effects on survival ratio whether the cells were at exponential growth phase or in the spore form. It is known that with *B. subtilis*, cell density dependent activities take place during sporulation. Spores of *B. subtilis* are extremely dormant and they survive under environmental stress. It is not known whether cell density dependent activities still take place after sporulation is completed. Therefore, the results of the *B. subtilis* disinfection experiments can only suggest cell density independent inactivation kinetics when they are in spore form and at exponential growth phase, but no more information exists on other stages of gram-positive bacteria.

Other than the quorum sensing mechanism, it is possible that higher densities of organisms result in formation of higher concentration of byproducts, which may have synergistic effects on inactivation. No significant correlation was observed between initial microbial density and the disinfectant decay rates (Table 6.5). The correlation between ozone demand and initial

microbial density was consistent with cell density dependency of inactivation kinetics. Ozone demand had a significant correlation with initial density of *G. muris*, where it was not significant with initial density of *B. subtilis* spores. Monochloramine was a more stable oxidant and no significant demand was observed in monochloramine experiments. Therefore, it was not feasible to investigate any correlation between monochloramine demand and initial microbial density.

It is not clear whether the cell density dependent inactivation was due to quorum sensing mechanisms or not. However, the experimental results suggest that it may have been direct or indirect outcome of change in cellular morphology and/or physiology and/or growth stage. There was a significant effect of initial microbial density on monochloramine inactivation of *E. coli* in stationary phase and on ozone inactivation of *G. muris* cysts.

The log-linear kinetic model, Chick-Watson model, used in the development of CT tables in the SWTR Guidance Manual (Clark *et al*., 2002) does not consider this effect in the calculation of required CT values. The consideration of initial microbial density effects in the disinfection process is of a major significance for utilities in terms of optimization of the process and balancing the risks associated with exposure to pathogens and DBPs.

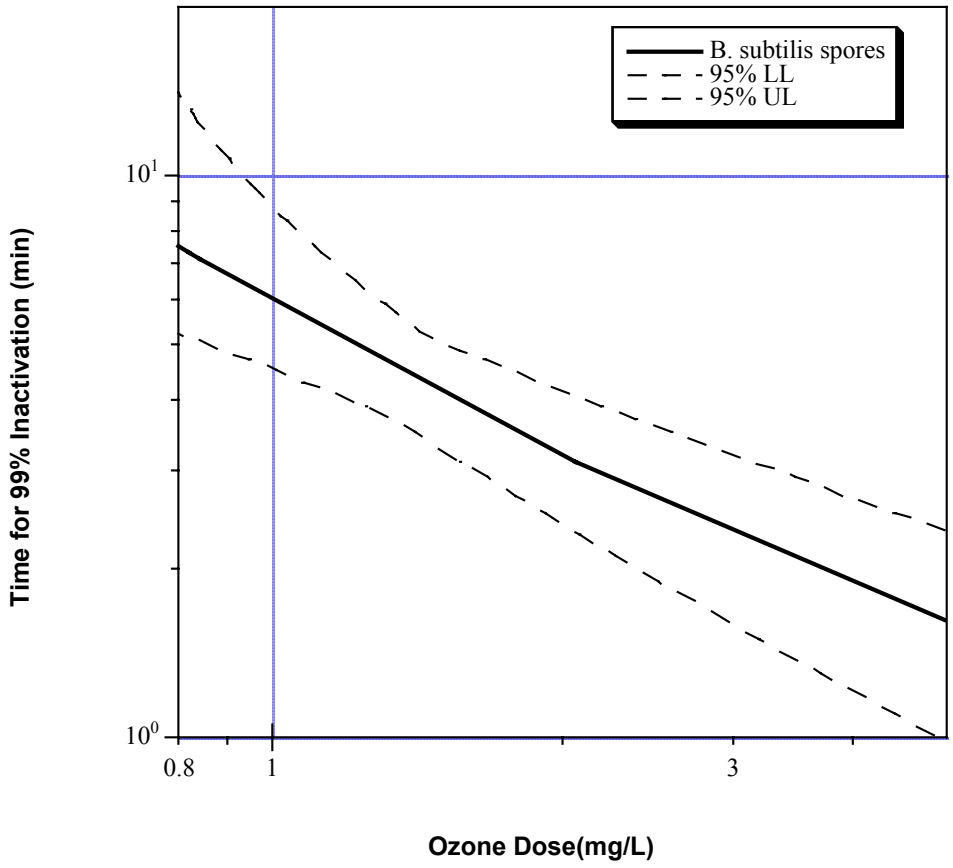

Figure 6.54: *CT* for 99% inactivation of *B. subtilis* spores predicted by Multiple-target Model.

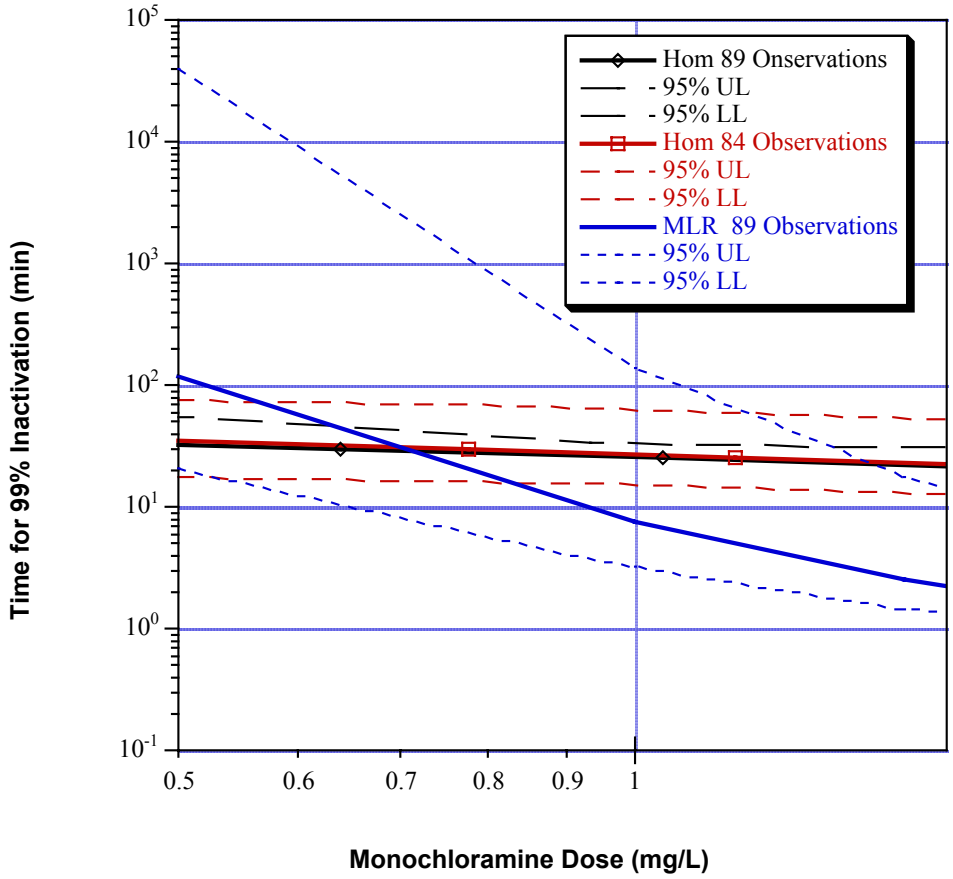

Figure 6.55: *CT* for 99% inactivation of vegetative cells of *B. subtilis* at exponential growth phase predicted by MLR for full data set and Hom model for data set without outliers.

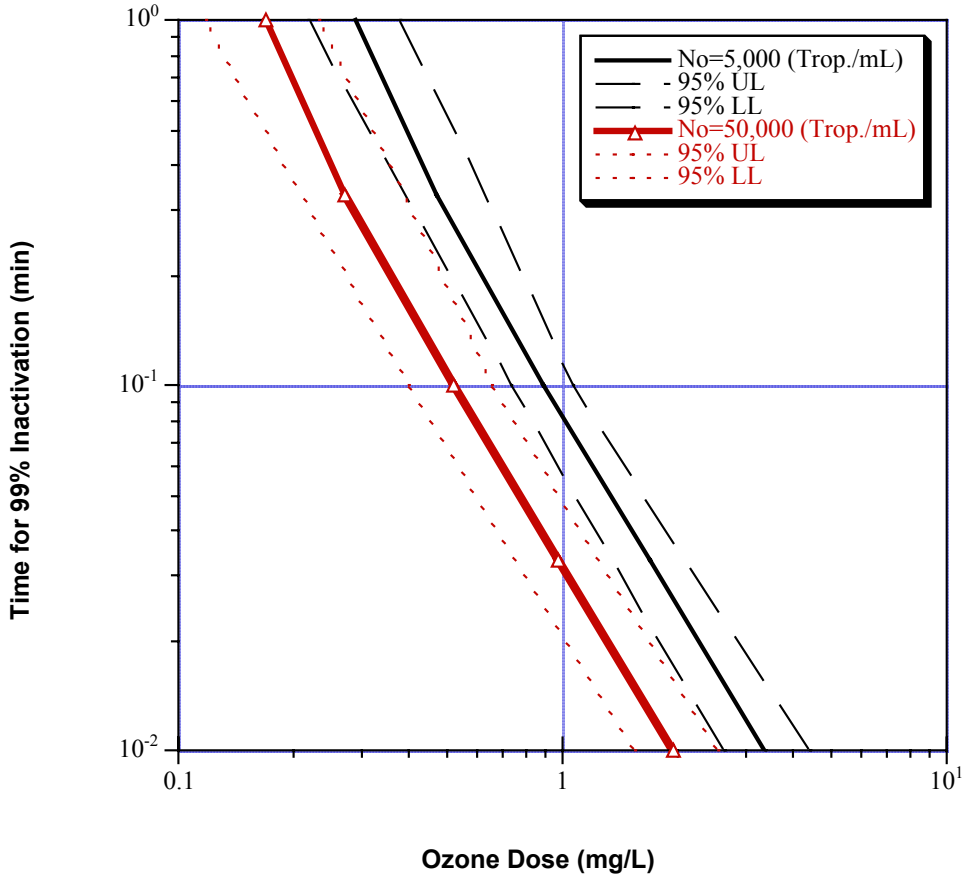

Figure 6.56: *CT* for 99% inactivation of *G. muris* predicted by Power Law.

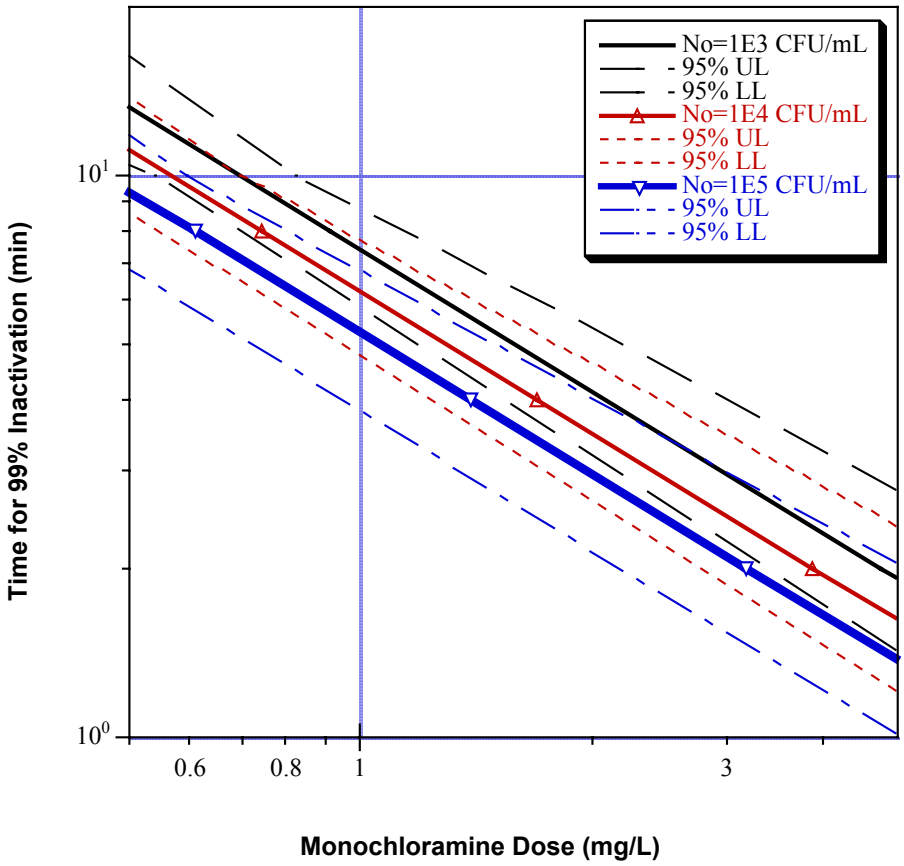

Figure 6.57: *CT* for 99% inactivation of *E. coli* predicted by Hom Power Law.

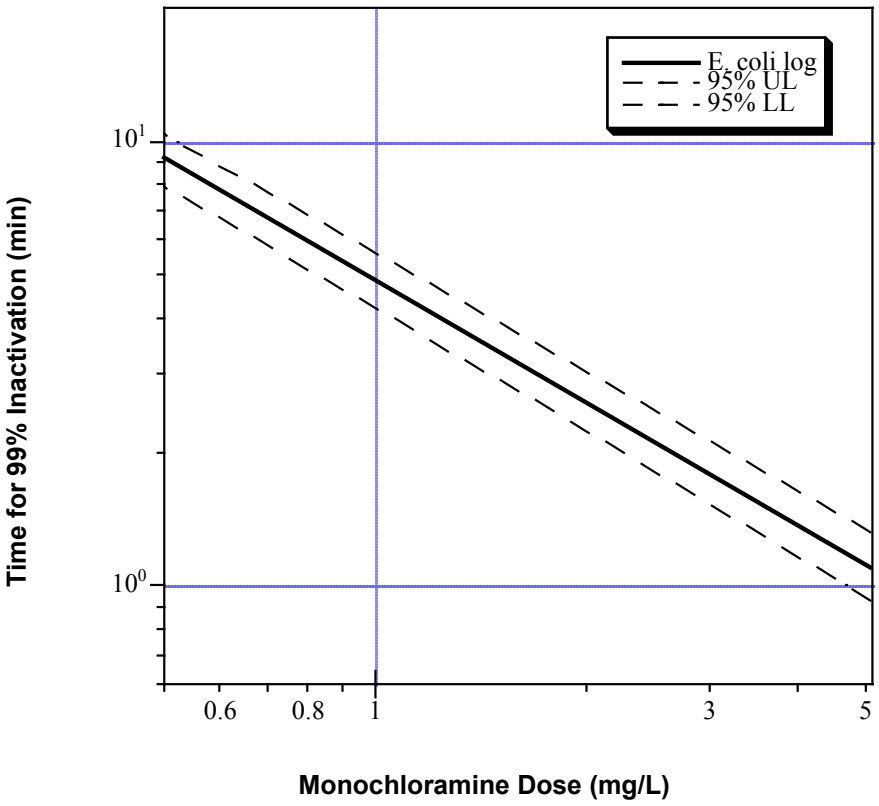

Figure 6.58: *CT* for 99% inactivation of *E. coli* at exponential growth phase predicted by Hom model.

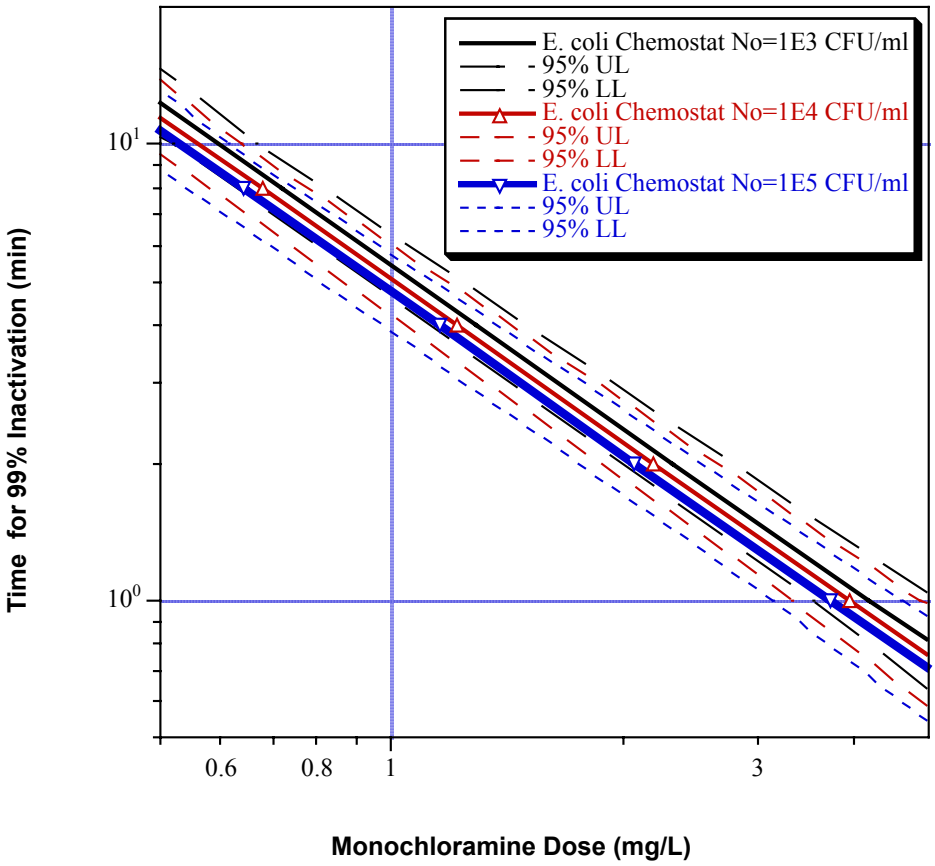

Figure 6.59: *CT* for 99% inactivation of continuous cultures of *E. coli* predicted by Hom Power Law.

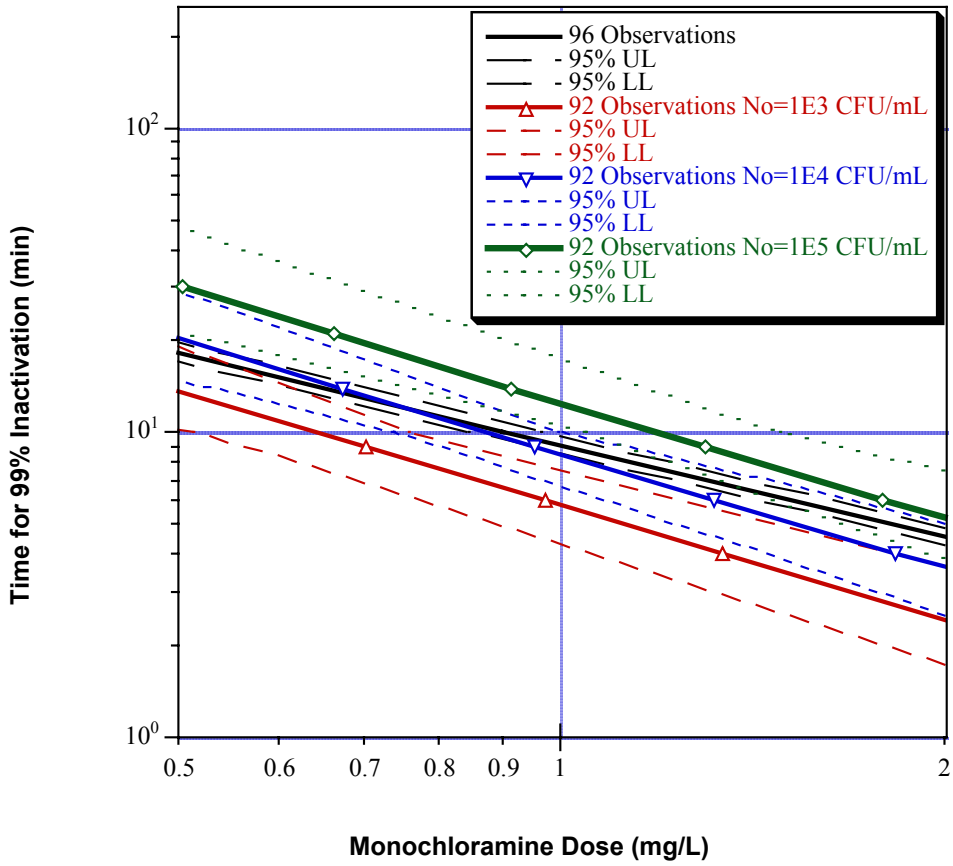

Figure 6.60: *CT* for 99% inactivation of *E. coli* in the presence of DMS of full data set and data set without outliers predicted by Chick model and Power Law, respectively.

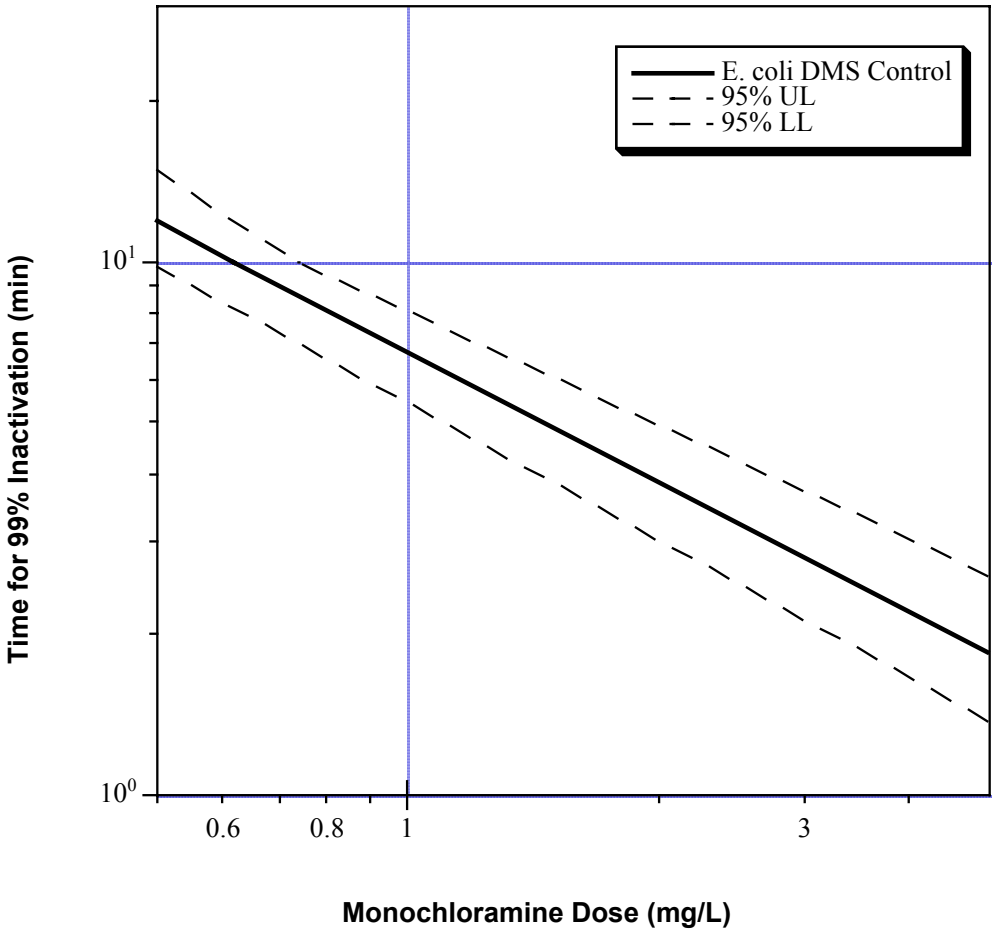

Figure 6.61: *CT* for 99% inactivation of *E. coli* DMS control data set predicted by Hom model.

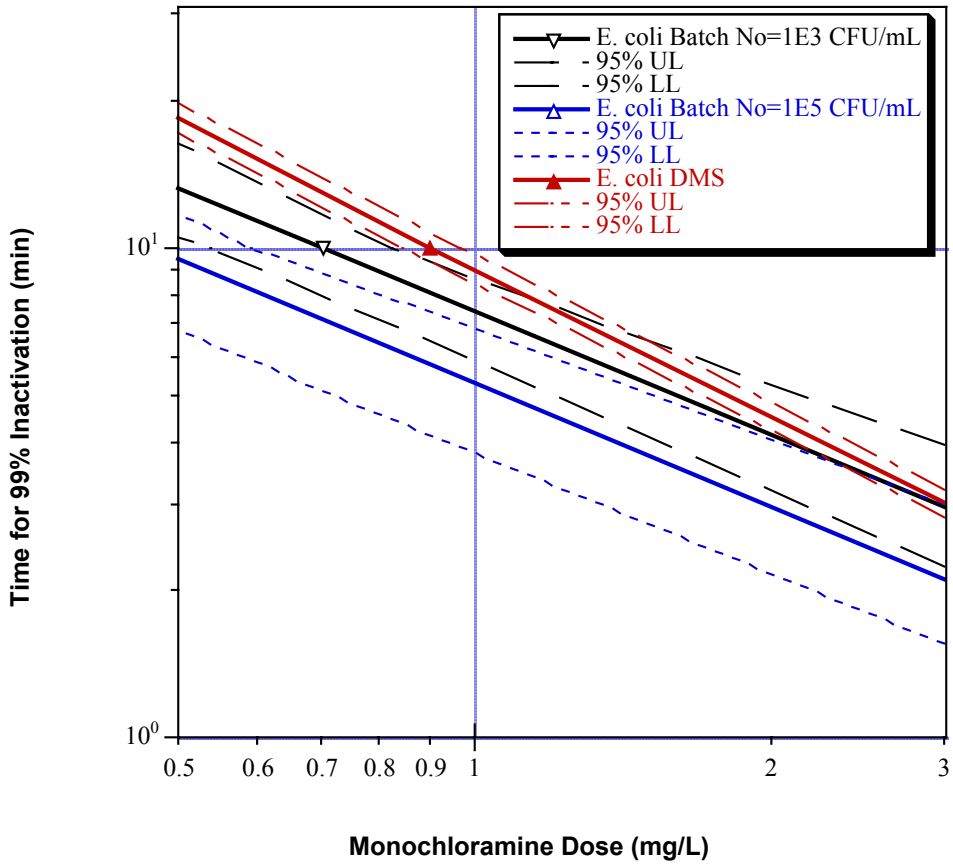

Figure 6.62: *CT* for 99% inactivation of *E. coli* batch cultures in presence and absence of DMS.

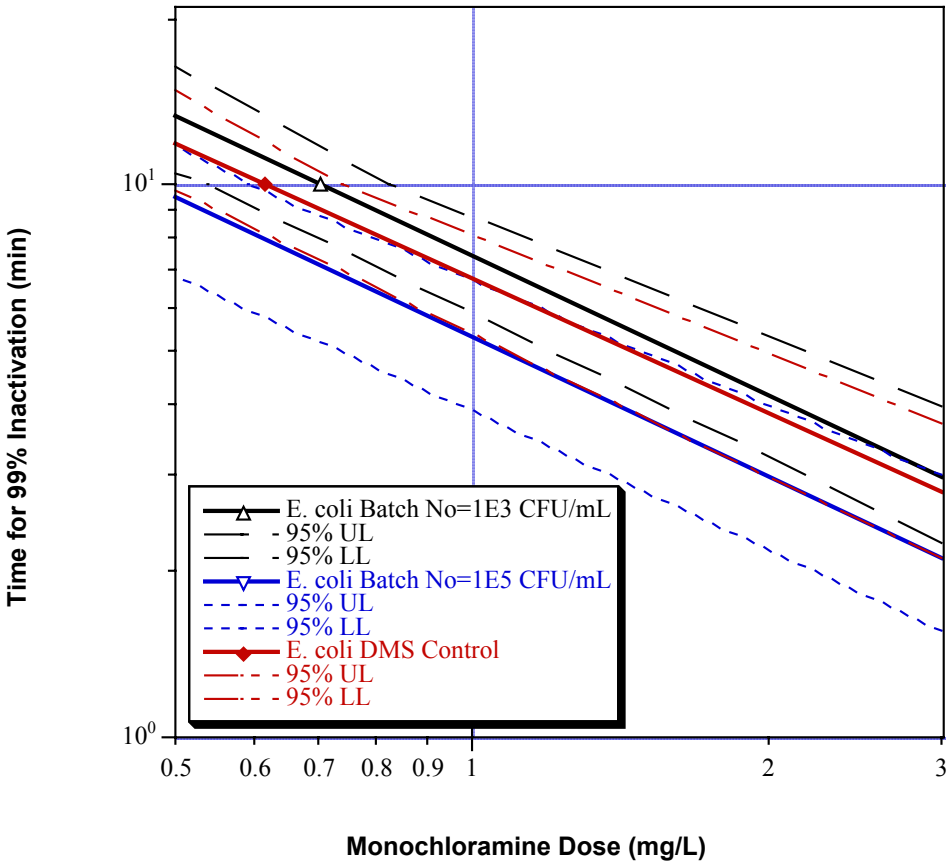

Figure 6.63: *CT* for 99% inactivation of *E. coli* batch and *E. coli* DMS Control data set.

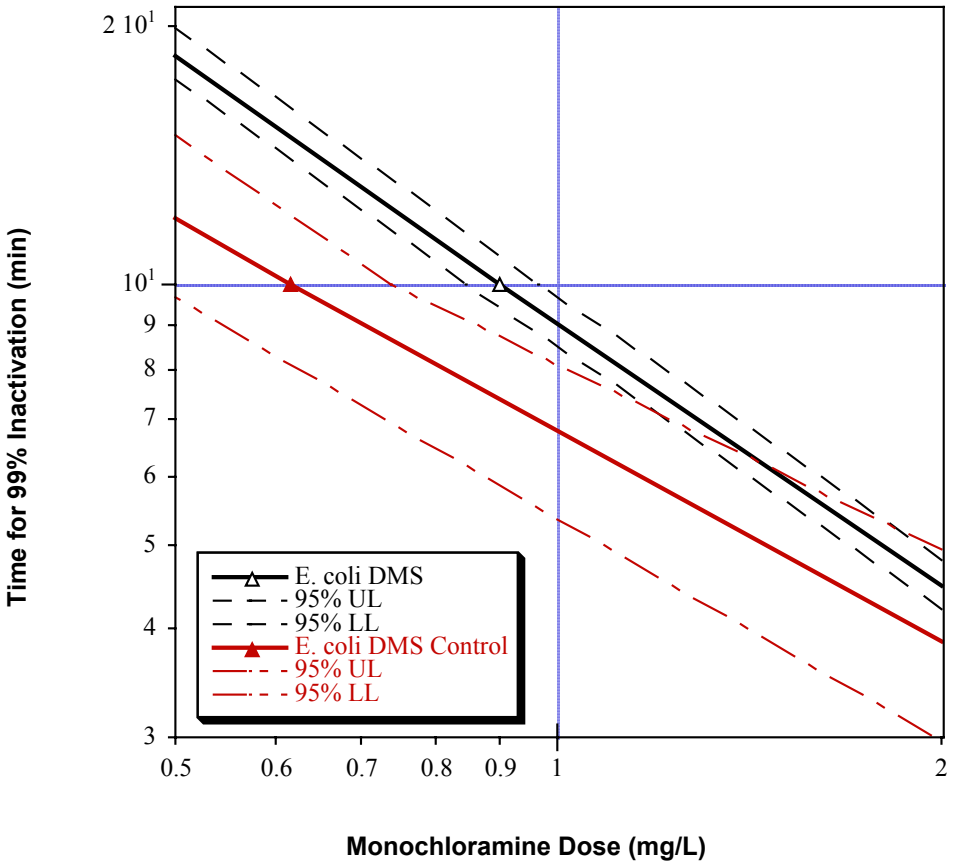

Figure 6.64: *CT* for 99% inactivation of *E. coli* DMS and *E. coli* DMS Control data set.

7. EXPERIMENTAL INVESTIGATION OF EFFECT OF GROWTH CONDITIONS ON DISINFECTION EFFICIENCY

It has been known that environmental conditions may cause substantial differences in the cellular physiology and morphology of bacteria. Therefore, inactivation of *E. coli* and *B. subtilis* was studied under two different growth stages. It is important to investigate the outcomes of changes in growth phase and its effect on the resistance or sensitivity of cells to disinfectants since they would exist in the source water at different growth stages.

In the case of *B. subtilis*, it was not feasible to compare quantitatively the kinetics of inactivation of spores and exponentially growing cells. *B. subtilis* spores were too resistant to inactivate with monochloramine within an acceptable time and dose. On the other hand, vegetative cells of *B. subtilis* at exponential growth phase were too sensitive to ozone to obtain reliable inactivation data. Under these circumstances the inactivation experiments of *B. subtilis* spores and vegetative cells in exponential growth phase had to be conducted with different disinfectants. Therefore, it was not feasible to compare the kinetics quantitatively.

E. coli was cultured using three different methods and the inactivation kinetics were analyzed with multiple linear and nonlinear regression for each condition separately. Inactivation of *E. coli* under each condition was best described by NLLS regression models. Therefore, the inactivation kinetics of *E. coli* batch, *E. coli* chemostat and *E. coli* log survival data were compared with each other using the ordinary least squares regression method as described in Section 6.3.2.

In this method of comparison, it was assumed that the inactivation kinetics of *E. coli* cultures, whether at exponential growth phase or stationary growth phase and grown in either batch or continuous cultures, were identical. Based on this assumption, inactivation data sets of *E. coli* batch, *E. coli* log and *E. coli* chemostat were pooled together as pairs in different combinations. The pooled data were fit to inactivation models using NLLS regression. The summaries of least squares regression for each combination of pooled inactivation data and the

pairwise F-test comparisons are given in Table 7.1 through Table 7.3 and Table 7.4, respectively.

Table 7.1: Summary of least-squares regression of pooled *E. coli* batch and *E. coli* chemostat data, 190 observations.

	Parameters					RSS	Adjusted
MODEL	k	n	m/n_c	x	κ		r^2
Chick	0.8789					735.85	0.8477
MT	1.3239		13.7862			594.89	0.8762
SE	0.8759				0.8575	726.37	0.8488
CW	0.8867	0.8858				726.63	0.8488
Hom	0.3081	1.5582	1.5686			601.91	0.8741
PL	0.7175	0.8890		1.0306		710.85	0.8513
MMT	1.2477	0.9925	8.6793			572.48	0.8802
HPL	0.0653	1.9520	2.0309	1.1087		521.37	0.8903

Table 7.2: Summary of least-squares regression of pooled *E. coli* batch and *E. coli* log data, 204 observations.

	Parameters					RSS	Adjusted
MODEL	k	n	m/n_c	x	κ		r^2
Chick	0.8030					844.46	0.7696
MT	1.2673		11.5457			701.17	0.8077
SE	0.7999				1.1492	832.94	0.7716
CW	0.7898	1.1053				840.10	0.7696
Hom	0.3020	1.3274		1.5612		718.61	0.8020
PL	0.6833	1.1334			1.0205	834.92	0.7699
MMT	1.2611	0.8750	11.7325			694.29	0.8087
HPL	0.0488	1.7293		2.1072	1.1244	640.22	0.8227

Table 7.3: Summary of least-squares regression of pooled *E. coli* chemostat and *E. coli* log data, 198 observations.

	Parameters					RSS	Adjusted
MODEL	k	n	m/n_c	x	κ		r^2
Chick	0.9436					628.05	0.8397
MT	1.5787		22.7324			426.27	0.8906
SE	0.9415				0.8639	626.26	0.8393
CW	0.9433	1.1202				624.73	0.8397
Hom	0.3142	1.7305	1.6569			441.83	0.8861
PL	0.9580	1.1204		0.9978		624.76	0.8389
MMT	1.5796	1.0718	22.8606			423.20	0.8909
HPL	0.1673	1.9119	1.8438	1.0476		423.47	0.8902

Table 7.4: Probabilities for pairwise comparison of model fits with partial F-test.

a. Probabilities for pairwise comparison of kinetic models for pooled *E. coli* batch and *E. coli* chemostat data.

Simpler Model		More Complex Model	Probability
Chick Model	vs.	Multiple-target	2.71×10^{-10}
Multiple-target	vs.	Modified Multiple-target	7.45×10^{-3}
Modified Multiple-target	vs.	Hom Power Law	3.11×10^{-5}

b. Probabilities for pairwise comparison of kinetic models for pooled *E. coli* batch and *E. coli* log data.

Simpler Model		More Complex Model	Probability
Chick Model	vs.	Multiple-target	3.21×10^{-9}
Multiple-target	vs.	Modified Multiple-target	1.74×10^{-1}
Multiple-target	vs.	Hom Power Law	2.03×10^{-4}

c. Probabilities for pairwise comparison of kinetic models for pooled *E. coli* chemostat and *E. coli* log data.

Simpler Model		More Complex Model	Probability
Chick Model	vs.	Multiple-target	1.53×10^{-7}
Multiple-target	vs.	Modified Multiple-target	2.45×10^{-1}
Multiple-target	vs.	Hom Power Law	5.41×10^{-1}

In the next step, each of the three survival data sets of *E.* coli examined for identical inactivation kinetics. If the inactivation kinetics were identical, any subgroup of this data set would represent the pooled data and there would be no significant ($P < 0.05$) difference in the fit

whether NLLS regression was conducted for all the data all at once or to subgroups separately. To check whether there was an improvement in fit for subgrouped data over the pooled data, the partial F-test was used. When the data were divided into subgroups, more than one model was used to describe the whole data set, whereas, the pooled data was described by one model. Use of more models result less degrees of freedom. The partial F-test results for comparison of the pooled and subgrouped data sets are given in Table 7.5, where F was calculated as follows,

$$F = \frac{(\mathrm{RSS}_{\mathrm{Pooled}} - \mathrm{RSS}_{\mathrm{Total\ Subgroups}})/(\mathrm{df}_{\mathrm{Pooled}} - \mathrm{df}_{\mathrm{Total\ Subgroups}})}{\mathrm{RSS}_{\mathrm{Total\ Subgroups}} / \mathrm{df}_{\mathrm{Total\ Subgroups}}}$$

The probability was calculated using the inverse F distribution function in Microsoft Excel 1998®.

$$P = F_{distribution}(\mathrm{df}_{\mathrm{Pooled}} - \mathrm{df}_{\mathrm{Total\ Subgroup}}, \mathrm{df}_{\mathrm{Total\ Subgroup}}, \mathrm{F})$$

When *E. coli* batch and *E. coli* chemostat data were pooled, higher residuals were obtained. This shows that the fit was statistically significantly poorer ($P < 0.05$). If these two data sets had the same kinetics, there would be no statistically significant difference in the fit. Therefore, it was concluded that the inactivation efficiency of continuous and batch cultures of *E. coli* with monochloramine can be described using the same model, however, not with the same parameters. They both have different inactivation kinetics. Also, the same conclusion was obtained for *E. coli* batch versus *E. coli* log and *E. coli* chemostat versus *E. coli* log.

Table 7.5: Pairwise comparison of pooled data fit with individual fits using partial F-test.

a. Comparison of *E. coli* Batch and *E. coli* chemostat data.

	Model	RSS	n	df	F	Probability
Subgroups of						
E. coli Batch,	HPL	274.99	98	94	13.6152	9.91×10^{-10}
E. coli Chemostat	HPL	126.30	92	88		
Total		401.29	190	182		
Pooled Data	HPL	521.37	190	186		

b. Comparison of *E. coli* Batch and *E. coli* log data.

	Model	RSS	n	df	F	Probability
Subgroups of						
E. coli Batch,	HPL	274.99	98	94	16.9039	1.51×10^{-9}
E. coli Log	Hom	237.35	106	103		
Total		512.34	204	197		
Pooled Data	HPL	640.22	204	200		

c. Comparison of *E. coli* chemostat and *E. coli* log data.

	Model	RSS	n	df	F	Probability
Subgroups of						
E. coli Chemostat	HPL	126.30	92	88	10.9633	1.12×10^{-6}
E. coli Log	Hom	237.35	106	103		
Total		363.65	198	191		
Pooled Data	MT	426.27	198	196		

n : Number of observations
df : Degrees of freedom

7.1. Discussion

Studies have shown that growth conditions lead to structural and morphological changes in cells (Hengge-Aronis, 2000; Ishihama, 1997; Russell *et al*., 1999; Sterkenurg *et al*., 1984). It is important to investigate whether any of these changes also change the disinfectant resistance of the cell. To investigate the effect of growth phase on disinfectant resistance, both *E. coli* and *B. subtilis* were studied at two different growth stages.

B. subtilis was studied as exponentially growing vegetative cells and spores. There was a significant difference in disinfectant resistance of vegetative cells and spores. Spores were too resistant against monochloramine and vegetative cells were too sensitive against ozone to obtain

reliable inactivation data with acceptable disinfectant dose and contact time. Since each series of *B. subtilis* inactivation experiments was conducted with different disinfectants, it was not feasible to compare the inactivation kinetics quantitatively. However, when the same dose of ozone as in *B. subtilis* spore experiments was applied to inactivate vegetative cells of *B. subtilis*, the inactivation was too rapid to reliably measure. *B. subtilis* spores were more resistant to disinfection than vegetative cells of *B. subtilis* at exponential growth phase.

E. coli was studied in stationary and exponential growth phases. The exponentially growing cells were obtained by incubating the cells in continuously shaking bottles containing nutrient broth. The stationary growth organisms were obtained using batch and continuous culture techniques. The batch culture technique is predominantly used in inactivation studies. It is a simple and inexpensive method, however, it has been criticized for resulting in heterogeneous populations of cells at different physiological ages. In continuous cultures the growth rate of organisms can be adjusted by dilution rate and kept constant under steady state conditions. In addition, the dissolved oxygen level and humidity would be constant in a chemostat under steady state conditions. In the previous chapter, different models were used to describe the inactivation of *E. coli* under each of these conditions, however, these models were not enough to make a conclusion if any of these conditions lead to any change in disinfection kinetics. Therefore, the inactivation kinetics of *E. coli* under three different conditions were compared with each other quantitatively.

The comparison of the inactivation kinetics of continuous cultures of *E. coli* and batch cultures of *E. coli* showed that they have different resistance against monochloramine. Allthough both continuous cultures and batch cultures of *E. coli* were at stationary growth phase, the growth conditions were not exactly the same. Continuous cultures where grown in nutrient broth, where the batch cultures were grown on nutrient agar. In addition, the continuous cultures were continuously fed with air to maintain a steady state oxygen concentration. The differences in availability of water and oxygen might be the reason for different

monochloramine resistance in batch and continuous cultures of stationary phase *E. coli*. However, these differences did not affect the cell density dependent inactivation kinetics in *E. coli* at stationary growth phase.

The inactivation kinetics of *E. coli* at exponential growth phase was significantly different than both batch and continuous cultures of *E. coli*. As mentioned in Section 3.4, growth conditions have significant effects on cellular morphology and physiology. Similar results have been observed in previous studies (Cui *et al*., 2001; Datta and Benjamin, 1999).

To visually see the difference in monochloramine resistance, the CT values for 99% kill are plotted again for each experimental series as pairs in Figure 7.1 through Figure 7.3. The difference in resistance of continuous and batch cultures of *E. coli* can be clearly seen in Figure 7.1. As seen in Figure 7.2, the batch cultures of *E. coli* in stationary growth phase are more resistant to monochloramine than the ones in exponential growth phase. When continuous cultures and cells at exponential growth phase are compared, the resistance difference depends on the disinfectant dose and initial microbial density. At lower doses, continuous cultures of *E. coli* are more resistant, however at higher doses exponentially growing cells are more resistant. These results clearly show that the growth conditions have a significant effect on resistance of bacteria against disinfectants.

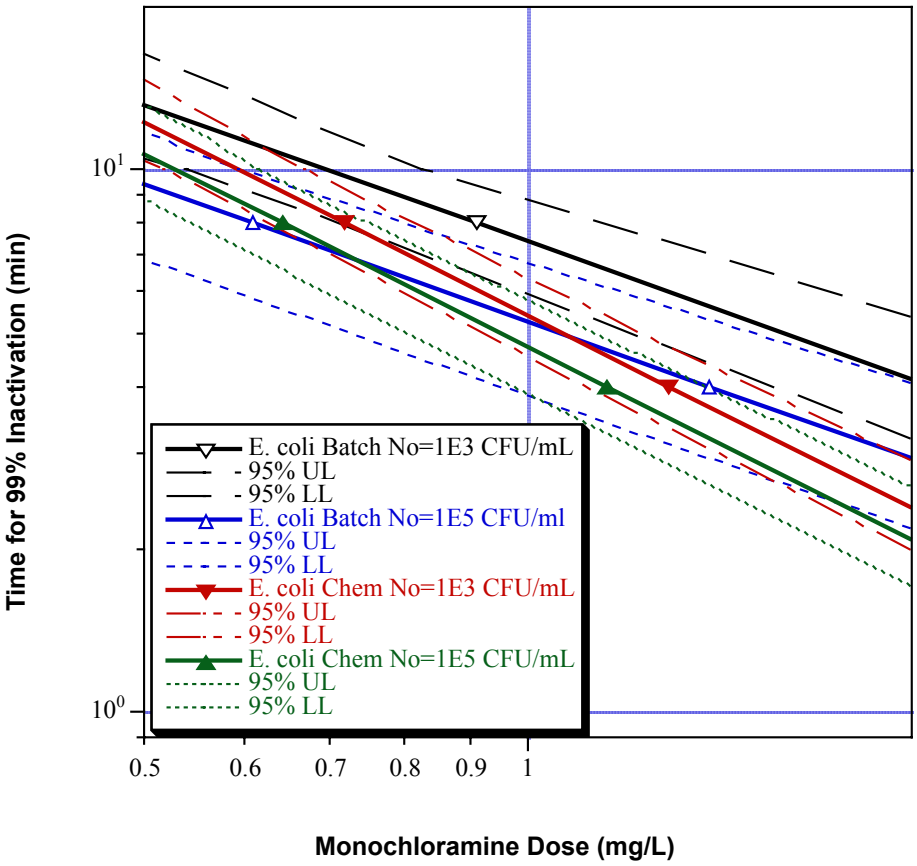

Figure 7.1: CT plot for 99% kill of batch and chemostat grown *E. coli* at stationary growth phase with monochloramine.

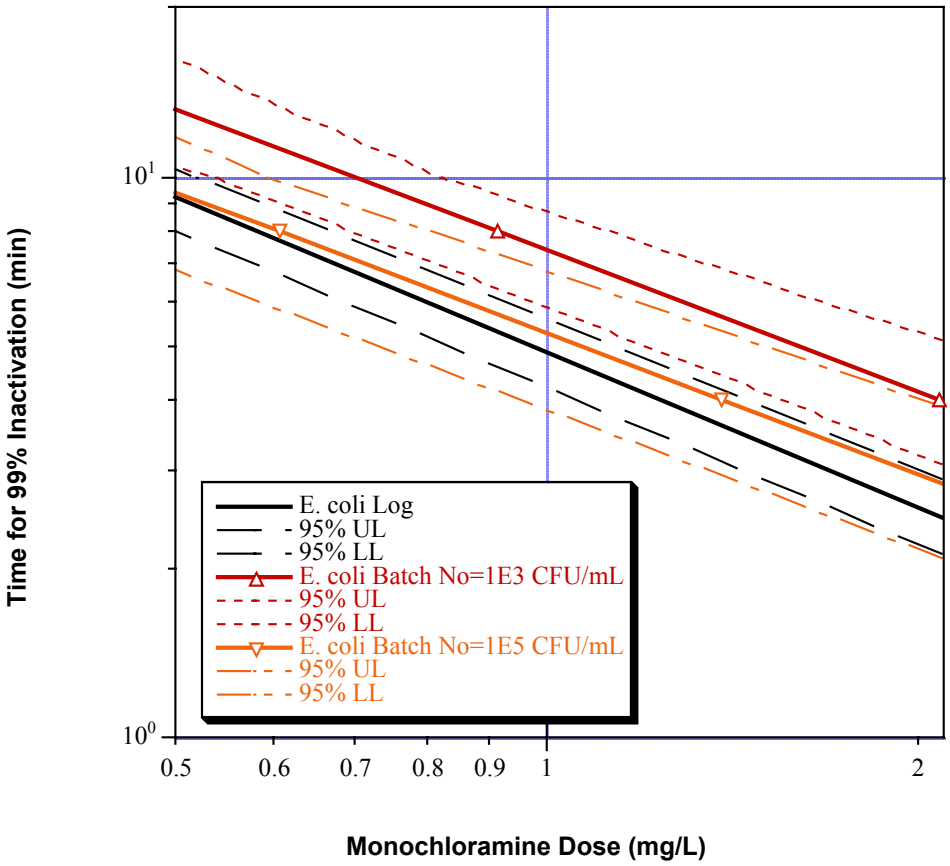

Figure 7.2: CT plot for 99% kill of batch grown *E. coli* at stationary growth phase and *E. coli* at exponential growth phase with monochloramine.

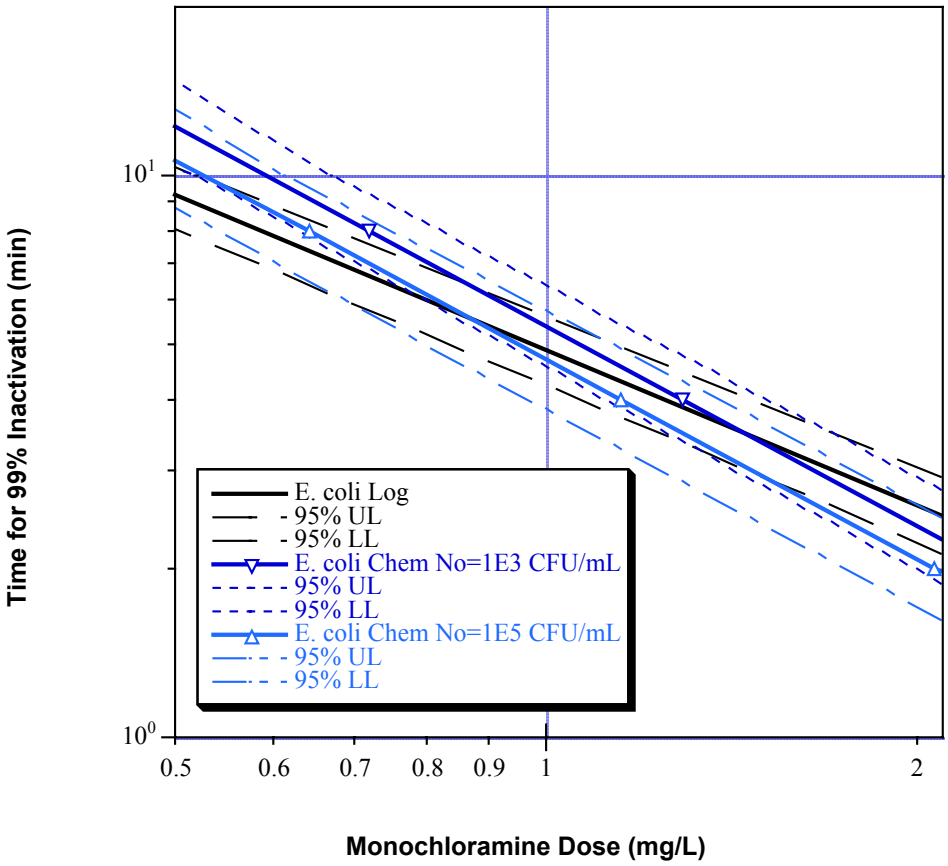

Figure 7.3: CT plot for 99% kill of chemostat grown *E. coli* at stationary growth phase and *E. coli* at exponential growth phase with monochloramine.

8. SURROGATE STUDIES FOR PROTOZOA

Protozoan cysts are one of the most disinfectant resistant forms of organisms in drinking water. Other than being resistant to disinfection processes, the limitations of direct detection had made them one of the major challenges for water treatment utilities. Their concentration in raw water may vary over a wide range and the current detection methods mainly have poor recovery and sensitivity. In addition, these methods are cumbersome, expensive and time consuming. Therefore, current direct detection methods are not appropriate for routine monitoring in most water treatment utilities (Radziminski *et al*., 2002).

The densities of protozoa in raw water are generally too low to directly measure the inactivation capacity of the treatment plant. Since they are pathogens, seeding studies in the treatment plant would cause a health risk to consumers (Craik *et al*., 2002). Therefore, in some utilities, other parameters such as turbidity, or cyst size particle count are used to predict removal efficiency of *Cryptosporidium.* However, both of the methods cannot reliably distinguish between oocysts that are viable or infective and those that are not (Rice *et al*., 1996).

There is published research on the inactivation of *Cryptosporidium* starting from the late 1980s. However, in large-scale disinfectant contacting equipment, non-ideal mixing and deviation from lab-scale reactors are likely to have a significant impact on efficiency of the disinfection process (Craik *et al*., 2002). Under these circumstances, the investigation of a surrogate organism for inactivation of protozoa that has similar or preferably somewhat higher resistance to disinfection is crucial for on-site verification of disinfection performance.

Bacterial spores are good candidate surrogates for protozoa for inactivation. They already exist in most of the source water at relatively high concentration. In addition, they are nonpathogenic and do not pose a public health risk (Nieminski *et al*., 2000).

The experimental results and kinetic analysis of inactivation of *B. subtilis* spores and *G. muris* cysts had been discussed in detail in Chapter 6. In this chapter, the survival data of *B.*

subtilis spores was compared with survival data of *G. muris* from this study and survival data of *Cryptosporidium* from the literature.

8.1. Comparison of Disinfectant Resistance of *B. subtilis* spores with *G. muris* and *C. parvum*

In the current regulatory framework, *Cryptosporidium* oocysts and *Giardia* cysts are the only protozoa whose removals are regulated for surface water treatment utilities (USEPA, 2001). It is suggested that ozone is one of the most effective chemical disinfectants for control of protozoa (Gyurék *et al*., 1999; Rennecker *et al*., 1999). Therefore, this surrogate study will focus on the inactivation of these two organisms with ozone.

During the comparison of ozone disinfection studies of *Cryptosporidium* oocysts and *Giardia* cysts, extra precaution should be taken, because of (Finch *et al*., 2001):

- different strains of organisms used
- different methods used to reproduce the organisms
- different storage conditions of organisms
- different methods of measuring viability
- different disinfection protocols
- different kinetic models used for inactivation kinetics.

8.1.1. Surrogate Analysis for *Giardia muris*

As a part of this study, inactivation kinetics of *G. muris* with ozone were studied. Both inactivation experiments of *G. muris* and the candidate surrogate organism (*B. subtilis* spores) were conducted at the same temperature and pH, using the same reactor type, reactor size and buffered water. Furthermore, the ozone generation, application and measurement techniques were identical in both inactivation experiments. In addition, the same process was followed for kinetic analysis of inactivation of both of the organisms.

In Figure 8.1, the survival ratios observed are plotted against integrated ozone concentration and time product (*CT*) for organisms in log-log scale. Both sets of survival data in this plot represent identical conditions (temperature, pH, experimental water, reactor, etc.). In this plot, there is a clear difference in kill ratio of *G. muris* and *B. subtilis* spore. As explained in detail in Chapter 6, cell density dependent inactivation was observed in inactivation of *G. muris*. For the initial microbial density range covered in *G. muris* experiments (N_o = 5,683 – 64,778 trophozoites/mL), the *CT* required to kill the same percent of *B. subtilis* spore was over one order of magnitude higher than that of *G. muris*.

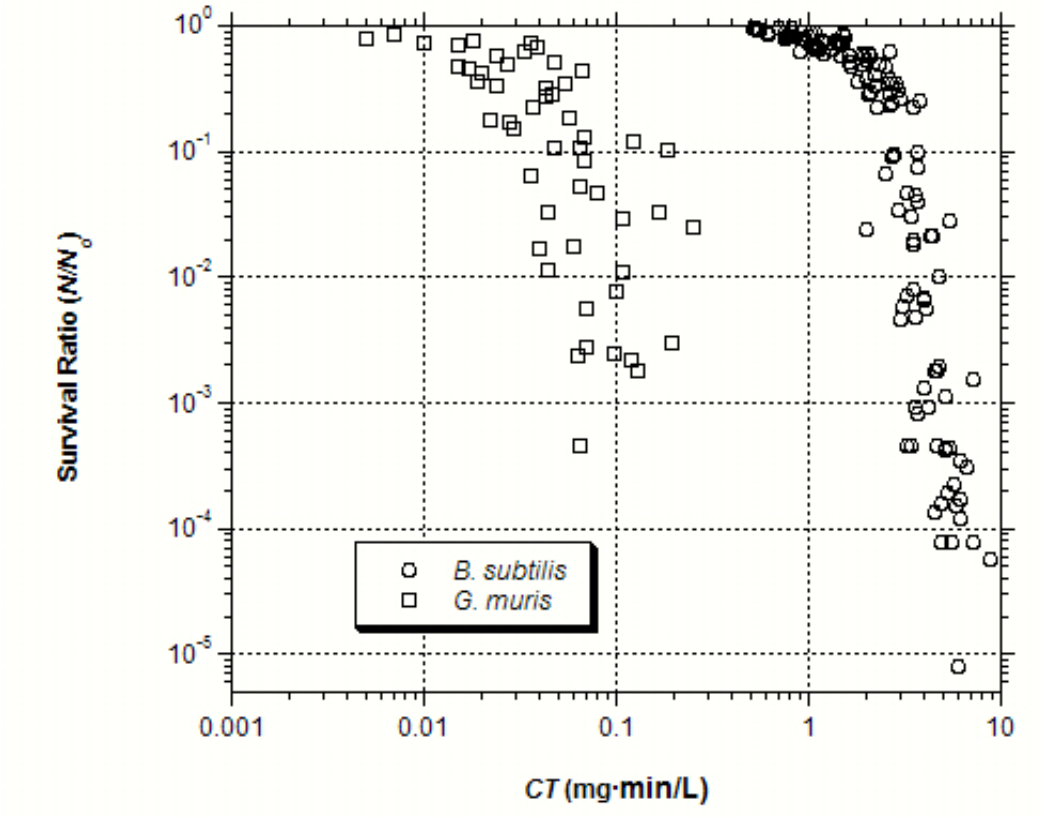

Figure 8.1: Survival data for *G. muris* cysts and *B. subtilis* spores with ozone at pH 8, and 15ºC.

The maximum initial microbial density in the *B. subtilis* spore experiments was approximately three times more than the one with *G. muris*, but maximum kill detected was

almost 2-log more than that of *G. muris*. This shows that by using *B. subtilis* spores, higher disinfection efficiencies can be detected.

The predicted *CT* values for 90%, 99% and 99.9% inactivation of both organisms at an initial ozone concentration of 0.5 mg/L are given in Table 8.1. In survival plots of both of the organisms, "shoulder" behavior was observed. After the initial lag period, the slope was higher in survival curve of the *B. subtilis* spores. This difference can be seen quantitatively in Table 8.1. The *CT* difference was higher for lower inactivation rates.

Table 8.1: Average ozone concentration and time product to achieve 1-log, 2-log and 3-log kill of *G. muris* and *B. subtilis* spores at initial ozone concentration of 0.5 mg/L.

	CT Product of Ozone (mg.minute/L)		
	G. muris		*B. subtilis*
Inactivation Ratio	$N_0=5\times10^3$	$N_0=5\times10^4$	
1-log	3.69×10^{-2}	1.45×10^{-2}	3.35
2-log	1.36×10^{-1}	5.18×10^{-2}	3.93
3-log	4.41×10^{-1}	1.52×10^{-1}	6.56

The survival data for *B. subtilis* spores and *G. muris* in this study covers distinct *CT* ranges. As shown in Figure 8.1, the inactivation data of *G. muris* was in the range of 0.001 to 0.3 mg·minutes/L *CT*, whereas the *B. subtilis* spore inactivation data was in the *CT* range of 0.4 to 10 mg . minutes/L. The models developed for each organism was applicable for different *CT* ranges. Therefore, it was not applicable to develop a quantitative correlation in between them.

Both the visual (Figure 8.1) and quantitative comparison (Table 8.1) of ozone inactivation of *G. muris* cysts and *B. subtilis* spores show that *B. subtilis* spores were relatively more resistant to ozone.

8.1.2. Surrogate Analysis for *Cryptosporidium*

Before comparing ozone inactivation efficiencies of *B. subtilis* spores and *Cryptosporidium*, the literature was critically analyzed for ozone inactivation studies of

Cryptosporidium. Due to the disparities, only the studies given in Table 8.2 were used for the evaluations, to have consistency in inactivation data. The basic characteristics of these studies are also given in Table 8.2. The reader is referred to appropriate reference for more specific information. Only the inactivation data of *C. parvum* with ozone was evaluated. No other species of *Cryptosporidium* was evaluated.

The main differences in these studies were the temperature and pH. Li *et al*. (2001) reported that pH affects the ozone chemistry, however, its effect on *C. parvum* inactivation kinetics was insignificant for pH range of 6 to 8. Similar result was also observed by Gyurék *et al*. (1999). Therefore, the *C. parvum* inactivation data collected was not categorized for pH. All the studies evaluated were in the pH range of 6 to 8. Unlike pH, temperature has a significant effect on disinfection kinetics (Finch *et al*., 1993; Li *et al*., 2001; Oppenheimer *et al*., 1999; Rennecker *et al*., 1999). The reported effect of temperature in the literature is an approximately 2 to 3 times increase in *CT* requirement for a 10°C drop in the temperature (Finch *et al*., 1993; Li *et al*., 2001; Oppenheimer *et al*., 1999; Rennecker *et al*., 1999). Therefore, the data evaluated were narrowed down to temperatures in the range of 10°C to 25°C.

Table 8.2: Characteristics of ozone inactivation studies of *C. parvum* evaluated in this study.

Study	Viability Assay	Reactor Type	Crypto Source	Water Type and pH	Temp. (°C)	Ozonation Method	Ozone Conc. Value
Rennecker et al., 2000; Rennecker et al., 2001; Rennecker et al., 1999	*In vitro* excystation	Semi batch reactor with constant ozone flow	EPA, NRMRL OH, Iowa Strain, from University of Arizona and Waterborne New Orleans LA	Phosphate buffer at pH 7	5, 10, 20, 22, 25, 30	Ozone bubbled in reactor. C= 0.36-2.2 mg/L	Constant ozone concentration
Finch et al., 1993	*In vitro* excystation and animal infectivity	Batch reactor	EPA, NRMRL, OH	Phosphate buffered at pH6.9	3, 5, 7, 8, 10, 21, 22, 24	Ozone applied as aqueous solution C= 0.7 - 2.9 mg/L	Log average C as constant
Li et al., 2001	Animal infectivity	Batch reactor	Iowa Strain, from University of Arizona	Phosphate buffered at pH6-8	1, 13, 37	Ozone applied as aqueous solution C=0.3-2.8 mg/L	First order ozone decay
Gyurék et al., 1999	Animal infectivity	Batch reactor	Iowa strain from Harley Moon, NADC, Ames, IA	Phosphate buffered at pH6-7-8	22	Ozone applied as aqueous solution	First order ozone decay
Owens et al., 2000	Animal infectivity	Pilot-scale ozone contactor	Osaka Univ. and Harley Moon, NADC, Ames, IA	Raw or filtered natural water at pH8.4 – 8.24	23.6 - 24.5	Ozone bubbled in reactor.	Integrated average ozone concentration
Driedger et al., 2000	*In vitro* excystation	Semi batch reactor with constant ozone flow	Iowa Strain, from University of Arizona	Phosphate buffered water at pH 7	20	Ozone bubbled in reactor.	Constant ozone concentration

(continued)

Table VIII-2: (continued)

Study	Viability Assay	Reactor Type	Crypto Source	Water Type and pH	Temp. (°C)	Ozonation Method	Ozone Conc. Value
Corona-Vasquez et al., In Press	*In vitro* excystation	Semi batch reactor with constant ozone flow	Iowa Strain, from University of Arizona	Phosphate buffered water at pH 7	20	Ozone bubbled in reactor.	Constant ozone concentration
Somiya et al., 2000	*In vitro* excystation	Batch reactor	Osaka City Medical School, Osaka, Japan	Milli-Q™ water at pH 5.9 –6.7	20	Ozone bubbled in reactor prior to experiment	First order decay
Hirata et al., 2000	*In vitro* excystation and animal infectivity	Semi batch reactor with constant ozone flow	Osaka Medical School, Osaka, Japan	Phosphate buffered water at pH 7	20	Ozone bubbled in reactor.	Constant ozone concentration

In the first step, the inactivation data found in the literature were plotted together in the same graph to visually see the range of observed survival at certain *CT* products for ozone. None of these studies had actual data at 15ºC. Since, temperature has significant effect, only the data at temperature in between 10°C and 25°C was selected and plotted. Therefore, in comparison of the actual observed data, the temperature differences should be considered. At 15ºC, *C. parvum*, should be less resistant to ozone than the data at 10^0C and more resistant than the data at 25°C.

A viability assay is another important aspect of the measurement of inactivation of *Cryptosporidium* oocysts. The *in vitro* excystation and animal infectivity are the most commonly used methods. *In vitro* excystation method is quick and relatively less expensive, however, this method underestimates the infectivity of oocysts (Bukhari *et al*., 2000; Chauret *et al*., 2001; Finch *et al*., 1993). Therefore, the inactivation data obtained using *in vitro* excystation and animal infectivity were plotted separately.

In Figure 8.2, the inactivation data obtained at 10°C - 20°C and at pH 5.9 - 7 using *in vitro* excystation are plotted along with predicted survival of *B. subtilis* spores using the model developed in this study at 15ºC and pH 8.

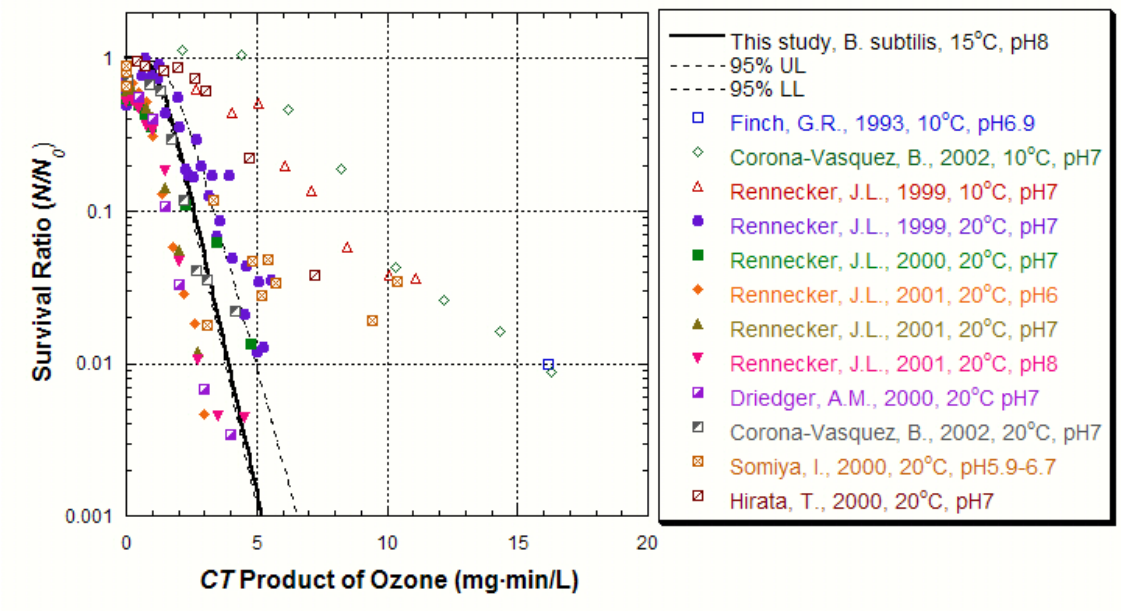

Figure 8.2: Ozone inactivation data for *C. parvum* from the literature determined using *in vitro* excystation method at pH 6-7 and at 10 - 20°C.

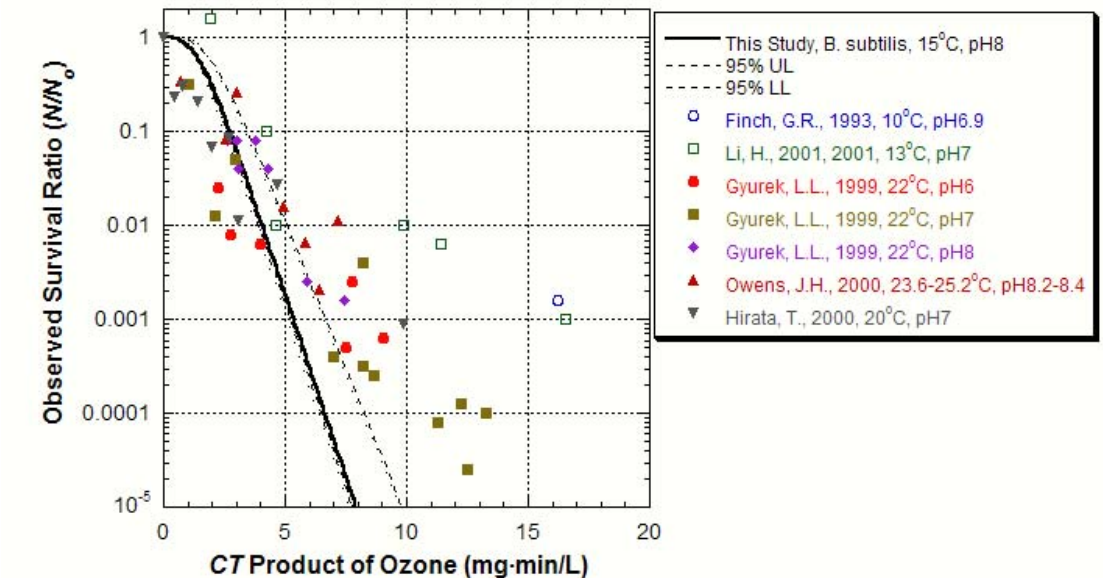

Figure 8.3: Ozone inactivation data for *C. parvum* from the literature determined using animal infectivity method at pH 6-8 and at 10 - 25°C.

In Figure 8.3, the survival data of *C. parvum* obtained at pH 6 to 8 and 10°C to 25°C using animal infectivity are plotted. In this plot, the survival data for *C. parvum* are relatively closer to the predicted survival of *B. subtilis* spores at lower *CT* products of ozone.

In both of the comparison plots (Figure 8.2 and Figure 8.3), the survival data for *C. parvum* lay mostly above the estimated survival of *B. subtilis* spores, showing that *Cryptosporidium* is more resistant to ozone than *B. subtilis* spores. Unlike *G. muris*, the data under a relatively wider range of temperatures made it more difficult to draw a conclusion on the use of *B. subtilis* spores as a surrogate. There is no actual inactivation data of *C. parvum* at 15ºC from any of these studies. Hence, it is not possible to make a direct comparison using the available survival data of *Cryptosporidium*. However, theoretically, the survival data for *Cryptosporidium* at 15ºC should be within the range covered by these scatter plots. These plots show that the resistance of *B. subtilis* spore is comparable with *C. parvum*. In addition, in these survival plots, a shoulder in the curve was observed in *B. subtilis* spore, whereas there was a slight tailing-off with the *C. parvum* inactivation. Therefore, more of a difference was observed in the ozone resistance of *Cryptosporidium* and *B. subtilis* spores at higher *CT* products of ozone.

Figure 8.2 and Figure 8.3 give visual information on the ozone resistance of both organisms, however, they do not give any quantitative information. In order to get more of a quantitative comparison, the models developed in these studies were analyzed. Li *et al*. (2001), Rennecker *et al*. (1999) and Oppenheimer *et al*. (1999) had studied ozone inactivation of *C. parvum* at different temperatures and had developed a model that incorporates temperature effects. Oppenheimer *et al*. (1999) had studied *C. parvum* inactivation in natural waters using one or more CSTRs in series. It was not be applicable to use the inactivation model developed by Oppenheimer *et al*. (1999) during this study's comparison since the other parameters in the natural water would have an effect on the inactivation of *C. parvum.* Both Li *et al*. (2001) and Rennecker *et al*. (1999) had used the same strain of *C. parvum* (Iowa strain) in phosphate buffered water. In each study, survival data were collected under tightly controlled laboratory

conditions, and their temperature range included 15ºC. The models developed in these two studies were closer to experimental conditions for the ozone inactivation of *B. subtilis* spores in this study. The main difference between these two studies was the viability assay used. The inactivation was measured using the animal infectivity method by Li *et al*. (2001), whereas the *in vitro* excystation method was used by Rennecker *et al*. (1999).

Rennecker *et al*. (1999) used a pseudo-first order kinetic model, which is also known as the delayed Chick-Watson Model, to describe the kinetics of inactivation:

$$\frac{N}{N_0} = \begin{cases} 1 & \text{if } Ct \le Ct_{lag} = \frac{1}{k}\ln\left(\frac{N_1}{N_0}\right) \\ \frac{N_1}{N_0}\exp(-kCt) = \exp\left[-k(Ct - Ct_{lag})\right] & \text{if } Ct > Ct_{lag} = \frac{1}{k}\ln\left(\frac{N_1}{N_0}\right) \end{cases}$$

$$k = A\ \exp\left(-\frac{E_a}{RT}\right)$$

where k is the post-shoulder, second order inactivation rate constant in l/(mg . minutes), C, is the dissolved ozone concentration in mg/L, t is the contact time in minute, N_1/N_0 is the intercept with the ordinate axis resulting from extrapolation of the pseudo-first order line, A is the frequency factor in l/(mg . minutes), E_a is the apparent activation energy in J/mol, R = 8.314 J/(mol.K) is the ideal gas constant and T is absolute temperature in K (Rennecker *et al*., 1999). This model did not incorporate disinfectant decay since a semi-batch reactor at constant ozone residual was used. The values of the parameters calculated for inactivation of *C. parvum* in the Rennecker *et al*., (1999) study were as follows; k = 0.80 l/(mg . minutes), N_1/N_0 = 1.8, A = 3.00x10^{14} l/(mg . minutes) and E_a = 81,200J/mole (Rennecker *et al*., 1999). The confidence intervals around these parameters were not reported by Rennecker *et al*., (1999).

Li *et al*., (2001) used a relatively more complex model (Hom model, Table 6.11) to predict inactivation.

$$\log\left(\frac{N}{No}\right) = -\frac{mk_T C_0^{\,n}}{(nk^*)^m}\,\gamma(m, nk^* t)$$

$$k_T = A\ \exp\left(-\frac{E_a}{RT}\right) \quad \text{or for narrow temperature range} \quad k_T = k_{22}\theta^{(T-273)-22}$$

where k, n and m are empirical constants, k_{22} rate constant at 22°C, k_T rate constant at water temperature T (°C), k^* is first order disinfectant decay rate in minutes^{-1}, A is the frequency factor, E_a is the apparent activation energy in J/mol, R = 8.314 J/(mol . K) is the ideal gas constant and T is absolute temperature in K (Li *et al*., 2001). The symbol γ represents the incomplete gamma function. The value of the parameters and 90% confidence intervals calculated in this study are given in Table 8.3.

Table 8.3: Kinetic parameters for Hom Model and 90% confidence intervals obtained by Li *et al*. (2001) to predict the inactivation of *C. parvum* with Hom model.

	θ	k_{22}	m	n	T (°C)	pH	MSE	Model Constraint
Mean	1.080	0.68	0.71	0.73	1-37	6,7,8	0.39	$0.1 \le C \le 2.4$
90% LL	1.076	0.65	0.70	0.65				$3 \le t \le 30$
90% UL	1.084	0.70	0.73	0.81				

It should be recalled from Chapter 6 that the Modified Multiple-target Model was used to predict the inactivation of *B. subtilis* spores with ozone at pH 8 and 15ºC:

$$\ln\frac{N}{N_0} = \ln\left\{1-\left[1-\left(Exp\left[\frac{k(C_a-D)^n}{nk^*}\left(e^{-nk^*t}-1\right)\right]\right)\right]^{n_c}\right\}$$

where k = 1.5449, n = 0.6992 and n_c = 8.4567.

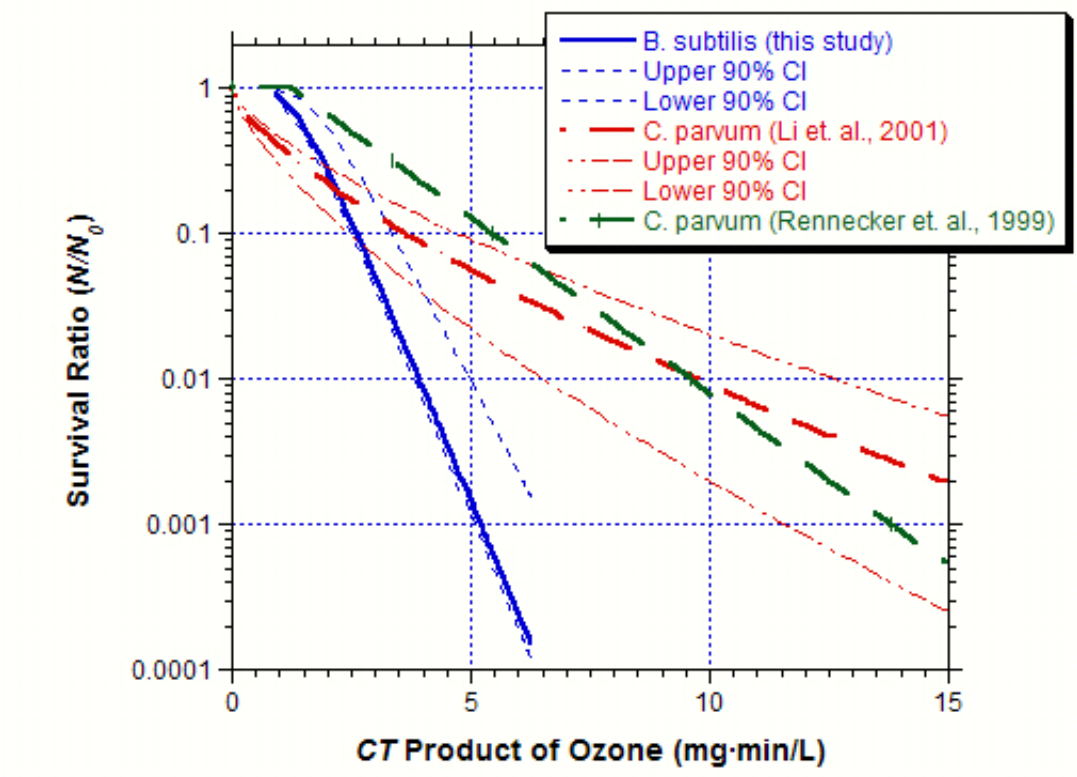

Figure 8.4: Model predicted survival curves for *B subtilis* and *C. parvum* at 15ºC.

In Figure 8.4, the model predicted survivals of both organisms at 15ºC are plotted. In this plot, the ozone resistance can be directly compared. The model plots clearly show that *C. parvum* is more resistant to ozone than spores of *B. subtilis*. The difference in survival increases gradually as CT increases. Similar results were also observed by Craik *et al*. (2002). As mentioned before, *in vitro* excystation underestimates inactivation. This can also be seen in Figure 8.4. *In vitro* excystation underestimates inactivation when it is less than 2-log. It should be considered that Rennecker *et al*. (1999) observed less than 2.5-log of inactivation and inactivation above 2.5-log was extrapolated using the developed model. Li *et al*. (2001) had detected over 4-log inactivation of *C. parvum*.

To investigate any relation between the inactivation characteristics of *B. subtilis* spores and *Cryptosporidium,* the survivals were predicted under the same conditions (ozone dose, contact time, ozone decay rate and temperature) for both organisms using the developed models.

The initial conditions chosen for predictions were 1.0 mg/L of applied ozone dose with a decay rate of 1×10^{-3} minutes^{-1} and no instantaneous demand. Next the survival was predicted from time zero to 11 minutes with 0.2 minute increments. Next the estimated survivals for *B. subtilis* spores and *C. parvum* were plotted as pairs (Figure 8.5 and Figure 8.6).

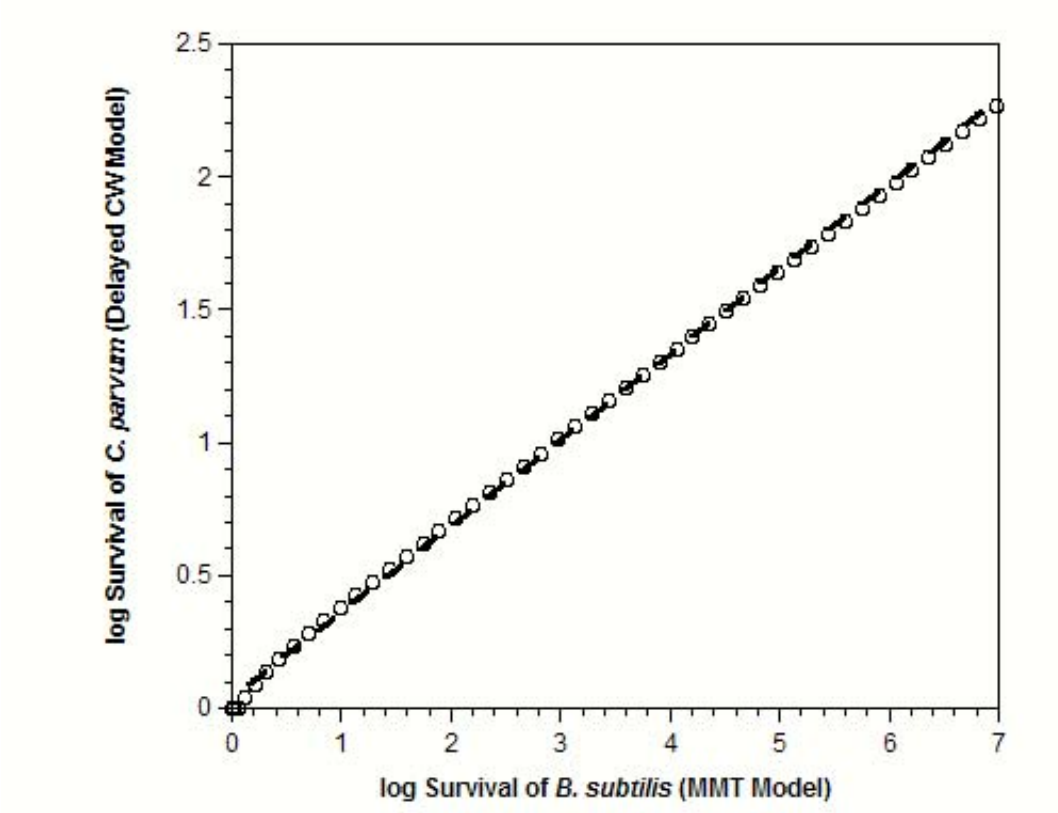

Figure 8.5: Log inactivation of *B. subtilis* spores predicted by MMT versus log inactivation *C. parvum* predicted by the delayed Chick-Watson Model (Rennecker *et al*., 1999). The dashed line represents log-linear function fit.

Rennecker *et al*. (1999) used a relatively simple pseudo-first order kinetic model to predict the inactivation of *C. parvum*. This model was valid under a steady state ozone concentration, therefore, the survival of *B. subtilis* spore was estimated for no disinfectant decay conditions using the Modified Multiple-target model (Equation 1.8). As seen in Figure 8.5, the relation between predicted log survival of *B. subtilis* spores and *C. parvum* was almost linear. A

simple linear model describes this relation successfully. The removal rate of *C. parvum* was predicted from the inactivation data of *B. subtilis* spores using the following equation:

$$S_{C.parvum} = 10^{0.3833 Log(S_{B.subtilis})}$$

where, *S* is the survival ratio.

Li *et al*. (2001) used a relatively more complex model to describe the inactivation kinetics of *C. parvum*. In addition, animal infectivity, which is considered da more reliable viability assay, was used in this study.

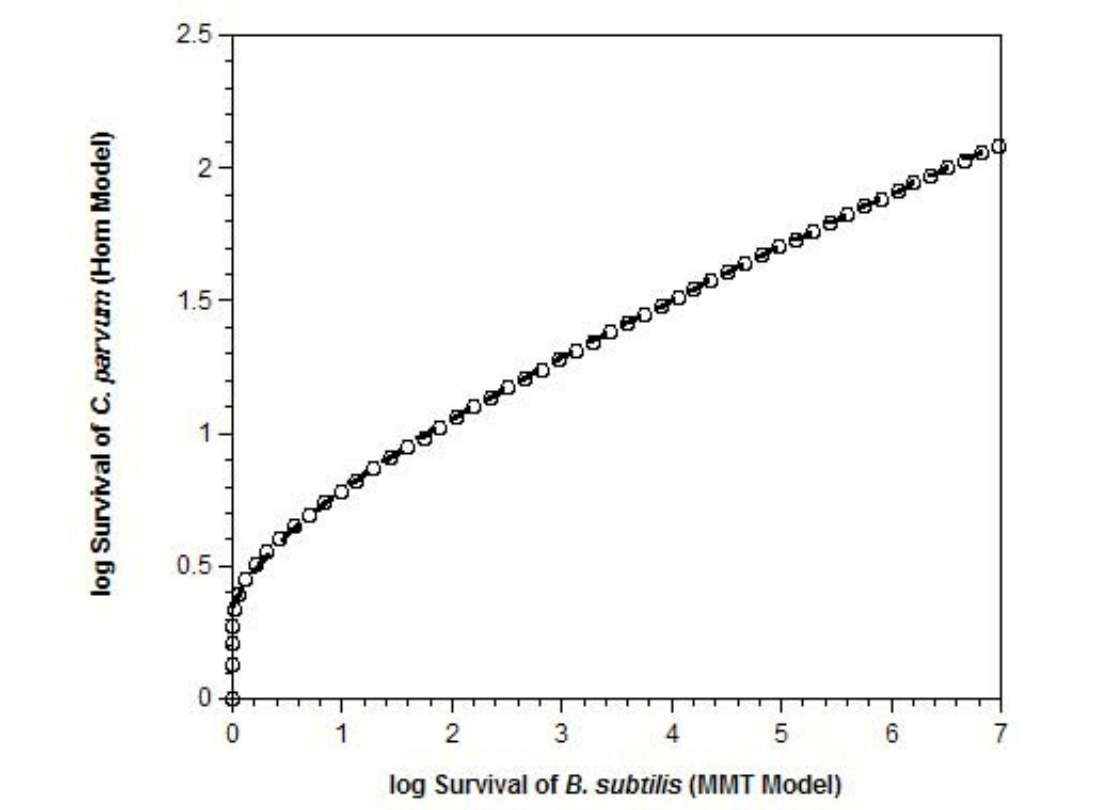

Figure 8.6: Log inactivation of *B. subtilis* spores predicted by MMT versus log inactivation *C. parvum* predicted by the Hom Model (Li *et al*., 2001). The dashed line represents third order polynomial function fit.

In the log-log scale plot of survival ratios, the relation between the survival of two organisms was non-linear in this case (Figure 8.6). A third order polynomial equation

successfully describe this relation. The removal rate of *C. parvum* was predicted from inactivation data of *B. subtilis* spores using the following equation:

$$S_{C.parvum} = 10^{0.0094 Log^3(S_{B.subtilis}) - 0.1072 Log^2(S_{B.subtilis}) + 0.6107 Log(S_{B.subtilis}) + 0.2923}$$

where, S is the survival ratio.

8.2. Discussion

Giardia and *Cryptosporidium* are two major concerns for the water industry. Waterborne diarrhea caused by these persistent pathogenic protozoan is one of the most frequently identified waterborne diseases in developed countries. They occur without predictability in the source water and the current detection methods have limitations, which were discussed in Section 3.7 in more detail.

The Surface Water Treatment Rule (SWTR) and the Interim Enhanced Surface Water Treatment Rule (IESWTR), requires that a surface water system should reduce 99.9 percent of the *Giardia* and 99 percent of the *Cryptosporidium* in the source water. In these rules, the MCLGs are set to zero for *Cryptosporidium* and *Giardia* since any exposure to these contaminants presents some level of health risk. Currently, *Giardia* and *Cryptosporidium* are the only protozoa that are regulated. Therefore, this study focused on surrogate analysis for disinfection efficiencies of only *Cryptosporidium* and *Giardia*.

As a part of this study, a series of inactivation experiments were conducted using *G. muris* and ozone under identical conditions along with a candidate surrogate organism (*B. subtilis* spores).

The inactivation kinetics of *G. muris* were cyst density dependent, whereas the inactivation kinetics of *B. subtilis* spores were independent of initial cell density. When the observed survival of each of the organisms was plotted together, a significant difference was observed in resistance against ozone. Within the initial microbial density covered in *G. muris*

experiments, in order to obtain same inactivation ratio, over an order of magnitude higher *CT* product of ozone was required for *B. subtilis* spores relative to *G. muris*.

Both organism's experimental data covered distinct *CT* ranges. Therefore, the models developed for inactivation of each organism was valid for different *CT* ranges. The inactivation data for *G. muris* was in the range of 0.001 to 0.3 mg·minutes/L *CT* product, whereas the inactivation data of *B. subtilis* spores were in the *CT* product range of 0.4 to 10 mg . minutes/L. A direct investigation of the relation between the inactivation of the two organisms using a MLR model was not applicable. However, a comparison of the actual data showed that *B. subtilis* spore was significantly more resistant to ozone than *G. muris*. This difference will assure removal efficiency of cysts, when *B. subtilis* spore is used as a surrogate to verify the removal efficiency of *G. muris* since it would underestimate inactivation of *Giardia* during the ozonation process. However, more disinfection system specific studies should be conducted to optimize the removal of *G. muris* and formation of DBPs.

In order to investigate whether *B. subtilis* spores can be used as an indicator of *Cryptosporidium* inactivation, the literature was critically analyzed for ozone inactivation studies of *Cryptosporidium*. Extra precaution was taken on the strain of *Cryptosporidium* used and its source, the methods of measuring viability, the disinfection protocols such as disinfectant used, temperature, pH, source of experimental water and reactor geometry. Only the literature on inactivation of *C. parvum* with ozone at a pH range of 5.9 to 8 and at temperature range of 10°C to 25°C were evaluated in this study.

When all the data collected from the literature were plotted along with the survival of *B. subtilis* spores predicted using Modified Multiple-target Model, the predicted survival of *B. subtilis* spore was between the scattered *C. parvum* survival data. Since a significant difference was reported between the animal infectivity and *in vitro* excystation methods (Bukhari *et al*., 2000; Chauret *et al*., 2001; Finch *et al*., 1993), the survival data were evaluated in two groups. It should be noted that none of the survival data of *C. parvum* from the literature was obtained at

15ºC. However, the temperature range of the scattered survival data covered 15ºC. Theoretically, at 25°C, *C. parvum* should be less resistant and at 10ºC, *C. parvum* should be more resistant against ozone than at 15ºC.

Based on the survival data plots, the resistance of *B. subtilis* spore against ozone was comparable with that of *C. parvum*. Especially at a lower *CT* product of ozone, the survival of *B. subtilis* spore was quite close to the survival of *C. parvum.* As mentioned before, *in vitro* excystation overestimates the infectivity of the cells, and this can be seen more clearly when two of the scattered survival plots are compared (Figure 8.2 and Figure 8.3). In Figure 8.3, the survival of *C. parvum* and *B. subtilis* spore were closer to each other especially at lower *CT* products of ozone. For *CT* products of ozone greater than 5 mg·minutes/L the difference in survival of both organisms increased. A "shoulder" behavior was observed for the inactivation of *B. subtilis* spore when the survival was plotted against the *CT* product of ozone on a semi-log scale. In the scattered plots of survival of *C. parvum* (Figure 8.2 and Figure 8.3), "tailing-off" was observed. Therefore, the difference in survival start to increase after a certain *CT* value. This effect can be clearly seen in Figure 8.4 through Figure 8.6.

Only three of the studies that were evaluated (Li *et al*., 2001; Oppenheimer *et al*., 1999; Rennecker *et al*., 1999) developed a temperature dependent model. Since Oppenheimer *et al*. (1999) had used natural water, their model was not used in this study. Laboratory grade water was used by Li *et al*., (2001), Rennecker *et al*., (1999) and in this study. In the plot of survival of *C. parvum* predicted by Hom and delayed Chick-Watson models and survival of *B. subtilis* spore predicted by Modified Multiple-target Model at 15ºC, the difference in inactivation kinetics was more clear (Figure 8.4). When the model predicted survival of *B. subtilis* spore was compared with the survival of *C. parvum* as predicted by the model developed by Rennecker *et al*. (1999), *C. parvum* was more resistant at any *CT* product. The model developed by Rennecker *et al*. (1999) overestimates the survival with respect to the study of Li *et al*. (2001). It should be noted that the maximum kill observed by Rennecker *et al*. (1999), was 2.5-log and the model they used

was a linear model which cannot describe the "tailing-off" behavior at higher *CT* products. Therefore, the delayed Chick-Watson model underestimates the kill at lower *CT* products whereas it overestimates the kill at higher *CT* products of ozone. The inactivation model (Hom Model) and the viability assay (animal infectivity) used by Li *et al*. (2001) are more advanced and they are considered to be more reliable. Based on the model developed by Li *et al*. (2001), *B. subtilis* spore was more resistant at lower *CT* products of ozone. However, *C. parvum* was more resistant to higher *CT* products and the difference increased as the *CT* product increased. This was an expected result since "shoulder" behavior was observed in kill studies of *B. subtilis* spores, whereas "tailing off" was observed in kill studies of *C. parvum*.

These plots showed that *B. subtilis* spore was significantly more sensitive to ozone than *C. parvum* oocysts. In the predicted survival plots of both organisms under the same conditions (disinfectant dose, contact time, disinfectant decay rate and temperature), the relation can be seen more clearly. In the survival plots of *C. parvum* using the delayed Chick-Watson Model by Rennecker *et al*. (1999), and *B. subtilis* spore using the Multiple-Target Model in this study, there was almost a log-linear relation. This relation can be described by a power model. Likewise, the relation between predicted logarithmic survival of *C. parvum* using the Hom Model in the study of Li *et al*., (2001) study and *B. subtilis* spore using the Multiple-Target Model in this study, can be described successfully using a third order polynomial model. The success of prediction of *C. parvum* survival using survival data of *B. subtilis* spore depends on how well the models predict survival of *C. parvum* and *B. subtilis* spore.

The main limitation to this prediction is the detection limit of the survival ratio of *B. subtilis* spores. In this study, the highest observed kill was approximately 5-log. Detection of an over 6-log removal of *B. subtilis* spore may not be practical for water utilities. Theoretically, an ozone contactor that achieves a 6-log removal of *B. subtilis* spore will also remove approximately 99% of *C. parvum* oocysts. The IESWTR established a requirement for 99% removal of *Cryptosporidium* for systems that must filter under the SWTR (USEPA, 2001). Some portion of

removal of *Cryptosporidium* would be achieved in filtration and other processes in the treatment plant. The results of this study verify the removal efficiency of *Cryptosporidium* only in the ozonation process using *B. subtilis* spore. Based on the regulations, the requirement for ozonation efficiency of *C. parvum* would not be over 2-log. *B. subtilis* spores can be used as a potential indicator of on-site *Cryptosporidium* removal efficiency of the ozonation process. Use of spores to indicate performance of the disinfection process is a simple and inexpensive method.

9. SUMMARY AND CONCLUSION

In this research, the cell density effects on disinfection efficiency and other related aspects of inactivation kinetics were investigated. The significant findings can be categorized into three major groups.

Cell density effects: Cell density dependent inactivation kinetics were observed in *G. muris* cysts and *E. coli* at stationary growth phase. The effect of initial microbial density was similar in *G. muris* cysts and *E. coli* at stationary growth phase. The efficiency of inactivation increased with increasing initial microbial density. The effect of initial microbial density was more drastic for the inactivation of *G. muris* than *E. coli*. Also, it was observed that this effect on *E. coli* inactivation efficiency was higher in organisms grown in batch cultures than the ones grown in continuous cultures. For example, in a batch reactor with an initial ozone concentration of 0.50 mg/L and first order ozone decay rate of 0.5 $minutes^{-1}$, a 10-fold increase in the initial microbial density of *G. muris* (1,000 to 10,000 cysts/mL) resulted in approximately 1-log more kill after 1 minute, under the experimental conditions studied. In *E. coli,* a 10-fold increase in initial microbial density (1,000 to 10,000 mL^{-1}) resulted in a 0.25-log and 0.12-log increase in log kill of batch grown cultures and chemostat grown cultures, respectively, in a batch reactor with an initial monochloramine concentration of 0.75 mg/L and a decay rate of 2×10^{-3} $minutes^{-1}$ after 5 minutes.

The disinfection kinetics of *E. coli* in an exponential growth phase was only a function of disinfectant dose and contact time. This showed that the cell density dependency was either a direct or indirect result of changes in the growth phase. It is known that cellular physiology and/or morphology changes occur when bacteria enter stationary growth phase and that some cell density dependent activities are coregulated with stationary phase sigma factor in some bacteria. However, the mechanisms responsible for cell density effects on disinfection efficiency were not able to be identified in this study.

The effect of the presence of extra-cellular material in inactivation efficiency of *E. coli* was studied by supplying disinfected microbial suspension (DMS) externally, however, due to the unknown chemistry of DMS, the results were not sufficient to draw a conclusion. In *E. coli*, the mechanisms responsible for the cell density effects on inactivation efficiency could not be investigated in this study, however, the data revealed that the mechanism was active during the stationary growth phase whether the organisms were grown in batch cultures on nutrient agar or in a chemostat on nutrient broth cell density effects were inactive in exponentially growing cells.

There was a significant ($P < 0.05$) positive correlation between the logarithmic transformation of initial microbial density ($\ln N_o$) and instantaneous ozone demand in *G. muris* experiments, showing an increase in ozone consumption with an increase in initial microbial density. This result agrees with a previous study (Labutiak *et al*., 1992), where the loss of infectivity was observed as a function of ozone dose and ozone consumed. This raises the question of whether the higher consumption of disinfectant at higher initial microbial density leads to increased inactivation efficiency. However, since the demand for monochloramine was not detectable, a test of any correlation in monochloramine experiments was not applicable. Therefore, this hypothesis cannot be confirmed using monochloramine inactivation data.

The inactivation kinetics of *B. subtilis* spores or vegetative cells at exponential growth phase were independent of initial microbial density. The results of both *B. subtilis* and *E. coli* at exponential growth phase agreed with each other. The spore form and stationary growth phase organisms have distinct cellular activities and structures. In spore from, the cellular activities are minimized whereas in stationary phase, most of them are suppressed. Therefore, it is hard to conclude that cell density dependent inactivation is only valid for gram-negative organisms without studying other non-sporulating gram-positive bacteria.

Growth condition: Statistically significant effects of growth phase and culture growth technique on inactivation efficiency was observed in the *E. coli* experiments. Exponentially growing cells of *E. coli* were more sensitive to monochloramine than stationary phase cells. Also,

there was a significant difference in resistance to monochloramine between batch culture grown and chemostat grown *E. coli*. Most importantly, the growth phase had direct or indirect effect on the occurrence of cell density dependent inactivation kinetics in *E. coli*. Similarly, vegetative cells of *B. subtilis* at exponential growth phase were more sensitive to disinfectant than the spores.

Surrogate study: B. subtilis spores can be used as a conservative surrogate for the disinfection efficiency of *G. muris* as they underestimate inactivation during the ozonation process. The *CT* product required to obtain the same removal rate of *G. muris* was over one order of magnitude less than that of *B. subtilis* spore. The *C. parvum* data in the literature revealed that the resistance of *C. parvum* was close to *B. subtilis* spores, especially at lower *CT* products of ozone. Comparison of the survival of *C. parvum* using the models from the literature with the survival of *B. subtilis* spore using the Modified Multiple-target model from this study gave the same results. At lower *CT* products, *B. subtilis* spore was more resistant. However, at higher *CT* products *Cryptosporidium* was more resistant against ozone. Using MLR, the nature of the relation between survival of *C. parvum* and *B. subtilis* spores can be expressed precisely. Using inactivation data of *B. subtilis* spore, an approximate 2-log reduction of *C. parvum* by the ozonation process was verified. This would be a simple and inexpensive method for the indication of on-site disinfection process performance. Since other methods, such as turbidity or particle counting, are required for verification of removal in other processes, the water utilities can verify whether the regulatory requirements (2-log removal of *Cryptosporidium*, IESWTR) are met or not by using *B. subtilis* spore as a surrogate for disinfection performance of *C. parvum*.

10. ENGINEERING SIGNIFICANCE AND FUTURE WORK

10.1. Engineering Significance

The results of this study have major significance for water treatment processes. Disinfection is one of the major advances in the drinking water industry as well as other public health related applications. However, due to health risks associated with harmful Disinfection/Disinfectant By-products (DBPs), it is essential to understand the complex effects of environmental factors on the inactivation efficiency to balance the risks associated with exposure to both pathogens and DBPs. In current regulations, the disinfection efficiency is estimated using the CT product and the corresponding inactivation credit given in CT tables provided by Surface water Treatment Rule (SWTR). The experiments used to develop these tables were conducted at relatively high (> 1,000 organisms/mL) initial microbial concentrations. In these tables, the effect of initial microbial density was not taken into account. In this study, it was observed that at least in the case of *G. muris* with ozone and *E. coli* at stationary growth phase with monochloramine, there was a statistically significant effect of initial microbial density. This result suggests that a significant change in disinfection conditions must be accounted to achieve the required inactivation. For example, in the case of *G. muris,* a decrease of N_o from 50,000 to 100 organisms/mL results in 330% increase in ozone dose to achieve a 2-log kill at a given contact time. The effect is less for *E. coli* at stationary growth phase, however, the same change in initial microbial density would require 17% to 73% increase in monochloramine dose to achieve a 2-log kill in a given contact time depending on the growth conditions. This obviously has major potential impacts on maintaining either desired pathogen removal or minimal DBPs in the drinking water.

The comparison of inactivation kinetics of *E. coli* under different growth conditions showed that the growth condition is an important factor in resistance against disinfectants. This result suggests that the utilities should consider the potential difference in resistance of organisms grown in controlled laboratory conditions and the ones in the source water.

The surrogate studies showed that *B. subtilis* spore could be used as a conservative surrogate to evaluate the disinfection efficiency of the removal of *G. muris*, as they would underestimate its removal during ozonation process. *B. subtilis* spores could also be used to verify the on-site removal efficiency of *C. parvum* in an ozone contactor. *B. subtilis* spore was not as resistant as *C. parvum* against ozone, however, the correlation can be described by simple polynomial models. For example, under the conditions studied here, whenever *B. subtilis* spores are inactivated to 6-log, approximately 2-log of *C. parvum* was inactivated. Once the water treatment utilities investigated the relation between disinfection efficiencies of *B. subtilis* spores and *C. parvum,* under their operation conditions in their ozone contactor, they could use *B. subtilis* spores as a potential indicator of on-site *Cryptosporidium* removal efficiency by the ozonation process. This will help utilities save time and resources.

10.2. Future Work

The use of appropriate design and operation criteria is important to balance the risks associated with microbial pathogens and DBPs. The main objective of this study was to investigate whether the disinfection efficiency of waterborne microorganisms was dependent on the microbial population. In this study, cell density dependent inactivation was observed in *E. coli* cells at stationary growth phase and in *G. muris* cysts. The effect of initial microbial density should also be investigated using other organisms especially *Cryptosporidium*, which is currently the major challenge of the drinking water utilities in developed countries. Since cell density dependent inactivation in bacteria was observed only at stationary growth phase, future studies should focus on other bacteria at stationary growth phase.

As seen in this study the mechanisms of cell density dependent inactivation was too complicated to investigate without investigating the detailed chemistry of the microbial suspension. The further studies on cell density dependent inactivation should consider the complexity of the mechanisms and carry out detailed analyzes of the chemistry of the microbial suspension they use.

In this study, the cell density effect on inactivation efficiency was studied in laboratory grade phosphate buffered water. In raw water, there are natural organic matter, inorganic chemicals, metals, other chemicals and a variety of microorganisms. Therefore, it is also important to investigate the cell density effects in the presence of other chemicals and organisms.

Since there exists a variety of microorganisms such as *Legionella, Mycobacterium* spp., coliforms, aerobic spores and protozoa in source waters (Maier *et al*., 2000), it is important to investigate interactions between them. A secondary sensor and a cognate autoinducer-2 system have been observed in some organisms. The structure of an autoinducer-2 is not clearly known, however it is known that it is a unique universal signal that can be used by a variety of bacteria in cell density related activities. The role of quorum sensing in cell-density dependent inactivation was not clear, however, further investigations of total cell density effects on inactivation efficiency of individual strains in the presence of other strains will provide valuable information for utilities.

B. subtilis was sporulated at 35ºC for 10 days on R2A agar and they were less resistant to ozone than *Cryptosporidium*. In some studies, it was observed that more resistant spores can be produced by changing the growth conditions, such as higher temperature (Russell *et al*., 1999). It is important to study, if more resistant spores can be produced under different sporulation conditions to use as a surrogate of *Cryptosporidium* inactivation during seeding studies in pilot plants.

LIST OF REFERENCES

Abee, T. and J.A. Wouters. 1999. Microbial Stress Response in Minimal Processing. *International Journal of Food Microbiology*, 50(1-2):65-91.

Anand, S.K. and M.W. Griffiths. 2002. Quorum Sensing and Expression of Virulence in *Escherichia coli* O157:H7. *International Journal of Food Microbiology*, 2646:1-9.

Anmangandla, U. 1993. Nonlinear Regression Analysis of Bench-Scale Microbial Disinfection Kinetics. Masters Thesis, Drexel University.

Anotai, J. 1996. Effect of Calcium Ion on Chemistry and Disinfection of Free Chlorine at pH 10. Doctoral Dissertation, Drexel University.

APHA, AWWA and A.P.H.A. WEF, American Water Works Association and Water Environment Federation). 1995. Standard Methods for the Examination of Water and Wastewater. In Edited by Washington, DC: APHA, AWWA, WEF.

Arnold, K.W. and C.W. Kasper. 1995. Starvation- and Stationary-phase Induced Acid Tolerance in *Escherichia coli* O157:H7. *Applied and Environmental Microbiology*, 61:2037-2039.

Atrih, A. and S.J. Foster. 2002. Bacterial endospores the ultimate survivors. *International Dairy Journal*, 12:217-223.

Barbeau, B., L. Boulos, R. Desjardins, J. Coallier and M. Prévost. 1999. Examining the Use of Aerobic Spore-forming Bacteria to Assess the Efficiency of Chlorination. *Water Research*, 33(13):2941-2948.

Barbeau, B., L. Boulos, R. Desjardins, J. Coallier, M. Prévost and D. Duchesne. 1996. A Modified Method For the Enumeration of Aerobic Spore-forming Bacteria. *Canadian Journal of Microbiology*, 43:976-980.

Bassler, L.B. 1999. How Bacteria Talk to Each Other: Regulation of Gene Expression by Quorum Sensing. *Current Opinion in Microbiology*, 2(6):582-587.

Bates, M.D. and D.G. Watts. 1988. *Nonlinear Regression Analysis and its Applications*. New York, N.Y.: John Wiley & Sons.

Benjamin, M.M. and A.R. Datta. 1995. Acid Tolerance of Enterohemorrhagic *Escherichia coli*. *Applied and Environmental Microbiology*, 61:1669-1672.

Berg, J.D., A. Matin and P.V. Roberts. 1982. Effects of Antecedent Growth Conditions on Sensitivity of *Escherichia coli* to Chlorine Dioxide. *Applied and Environmental Microbiology*, 44(4):814-819.

Booth, I.R. 2002. Stress and the Single Cell: Intrapopulation Diversity is a Mechanism to Ensure Survival upon Exposure to Stress. *International Journal of Food Microbiology*, 78(1-2):19-30.

Bower, C.K. and M.A. Daeschel. 1999. Resistance Responses of Microorganisms in Food Environments. *International Journal of Food Microbiology*, 50:33-44.

Bukhari, Z., M.M. Marshall, D.G. Korich, C.R. Fricker, H.V. Smith, J. Rosen and J.L. Clancy. 2000. Comparison of *Cryptosporidium parvum* Viability and Infectivity Assays Following Ozone Treatment of Oocysts. *Applied and Environmental Microbiology*, 66(7):2972-2980.

Carson, L.A., M.S. Favero, W.W. Bond and N.J. Peterson. 1972. Factors Affecting Coperative Resistance of Naturally Occurring and Subcultured *Pseudomonas aeruginosa* to Disinfectants. *Applied Microbiology*, 23:863-869.

Chapman, J.S. 1998. Characterizing Bacterial Resistance to Preservatives and Disinfectants. *International Biodeterioration and Biodegradation*, 41:241-245.

Chauret, C.P., C.Z. Redzinminski, M. Lepuil, R. Creason and R.C. Andrews. 2001. Chlorine Dioxide Inactivation of *Cryptosporidium parvum* Oocysts and Bacterial Spore Indicators. *Applied and Environmental Microbiology*, 67(7):2993-3001.

Chick, H. 1908. An Investigation of the Laws of Disinfection. *Journal of Hygiene*, 8:92-157.

Christensen, S.T., H. Sørensen, N.H. Beyer, K. Kristiansen, L. Rasmussen and M.I. Rasmussen. 2001. Cell Death in *Tetrahymena thermophila*: New Observations on Culture Conditions. *Cell Biology International*, 25(6):509-519.

Clark, R.M., M. Sivagenesan, E.W. Rice and J. Chen. 2002. Development of a *Ct* Equation for the Inactivation of *Cryptosporidium* oocysts with Ozone. *Water Research*, 36(12):3141-3149.

Corona-Vasquez, B., A. Samuelson, J.L. Rennecker and B.J. Mariñas. In Press. Inactivation of *Cryptosporidium parvum* Oocysts with Ozone and Free Chlorine. *Water Research*,

Coulthurst, S.J., N.A. Whitehead, M. Welch and G.P.C. Salmond. 2002. Can Boron Get Bacteria Talking? *Trends in Biochemical Sciences*, 27(5):217-219.

Craik, S.A., D.W. Smith, M. Belosevic and M. Chandrakanth. 2002. Use of *Bacillus subtilis* Spores as Model Microorganisms for Ozonation of *Cryptosporidium parvum* in Drinking Water. *Journal of Environmental Engineering and Science*, 1:173-186.

Craun, G.F., S.A. Hubbs, F. Frost, R.L. Calderon and S.H. Via. 1998. Waterborne Outbreaks of Cryptosporidiosis. *Journal AWWA*, 90(9):81-91.

Cui, S., J. Meng and A.A. Bhagwat. 2001. Availability of Glutamate and Arginine during Acid Challenge Determines Cell Density-Dependent Survival Phenotype of *Escherichia coli* Strains. *Applied and Environmental Microbiology*, 67(10):4914-4918.

Datta, A.R. and M.M. Benjamin. 1999. Cell Density Dependent Acid Sensitivity in Stationary Phase Cultures of Enterohemorrhagic *E. coli* O157:H7. *FEMS Microbiology Letters*, 181:289-295.

Davies, D.G., M.R. Parsek, J.P. Pearson, B.H. Iglewski, J.W. Costerton and E.P. Greenberg. 1998. The Involvement of Cell-to-Cell Signals in the Development of Bacterial Biofilm. *Science*, 280:295-298.

Decho, A.W. 1999. Chemical Communication Within Microbial Biofilms: Chemotaxis and Quorum Sensing in Bacterial Cells. In *Microbial Extra-cellular Polymeric Substances.* Edited by Wingender, J., T.R. Neu and H.C. Flemming. Berlin: Springer.

Denyer, S.P. and G.S.A.B. Stewart. 1998. Mechanisms of Action of Disinfectants. *International Biodeterioration and Biodegradation*, 41:261-268.

Driedger, A., S. Ernö, U. Pinkernell, B. Mariñas, W. Köster and U.V. Gunten. 2001. Inactivation of *Bacillus subtilis* Spores and Formation of Bromate During Ozonation. *Water Research*, 35(12):2950-2960.

Driedger, A.M., J.L. Rennecker and B.J. Mariñas. 2000. Sequential Inactivation of *Cryptosporidium parvum* Oocysts with Ozone and Free Chlorine. *Water Research*, 34(14):3591-3597.

Driscoll, W.C. 1996. Robustness of the ANOVA and Tukey-Kramer Statistical Tests. *Computer Industrial Engineering*, 31(1/2):265-268.

Dukan, S., S. Dadon, D.R. Smulski and S. Belkin. 1996. Hypochlorous Acid Activates the Heat Shock and *soxRS* Systems of *Escherichia coli*. *Applied and Environmental Microbiology*, 62(11):4003-4008.

Edward, A.I. 2001. *Fundamentals of Microbiology*. 6th. Sudbury, Mass: Jones and Barlett Publishers.

Eisenstark, A. 1998. Bacterial Gene Products in Response to Near-ultraviolet Radiation. *Mutation Research*, 422:85-95.

Ekelund, F., H.B. Frederiksen and R. Rønn. 2002. Population Dynamics of Active and Total Ciliate Populations in Arable Soil Amended with Wheat. *Applied and Environmental Microbiology*, 68(3):1096-1101.

Engebrecht, J.K., K. Nealson and M. Silverman. 1983. Bacterial Bioluminescence: Isolation and Genetic Analysis of Functions from *Vibrio fischeri*. *Cell*, 32:773-781.

Facile, N., B. Barbeau, M. Prévost and B. Koudjonou. 2000. Evaluating Bacterial Aerobic Spores as a Surrogate for *Giardia* and *Cryptosporidium* Inactivation by Ozone. *Water Research*, 34(12):3238-3246.

Fair, G., J.C. Morris, S.L. Chang, I. Weil and R.P. Burden. 1948. The Behavior of Chlorine as a Water Disinfectant. *Journal AWWA*, 40:1051-1061.

Finch, G.R., E.K. Black, L.L. Gyurék and M. Belosevic. 1993. Ozone Inactivation of *Cryptosporidium parvum* in Demand-Free Phosphate Buffer Determined *in vitro* Excystation and Animal Infectivity. *Applied and Environmental Microbiology*, 59(12):4203-4210.

Finch, G.R., C.N. Haas, J.A. Oppenheimer, G. Gordon and R.R. Trussell. 2001. Design criteria for inactivation of *Cryptosporidium* by ozone in drinking water. *Ozone Science and Technology*, 23:259-284.

Fox, J. 1991. *Regression Diagnostics*. Newbury Park, Ca.: SAGE Publications Inc.

Garcia, L.S. 2001. *Diagnostic Medical Parasitology*. 4th. Washington, D.C.: ASM Pres.

Gilbert, P. and M.R.W. Brown. 1980. Cell Wall-mediated Changes in Sensitivity of *Bacillus megaterium* to Chlorhexidine and 2-Phenoxyethanol, Associated With Growth Rate and Nutrient Limitation. *Journal of Applied Bacteriology*, 48:223-230.

Givskov, M., L. Eberl, S. Møller, L.K. Poulsen and S. Molin. 1994. Responses to Nutrient Starvation in *Pseudomonas putida* KT2442: Analysis of Cross-protection, Cell Shape and Macromolecular Content. *Journal of Bacteriology*, 176:7-14.

Gray, K.M. 1997. Intercellular Communication and Group Behavior in Bacteria. *Trends in Microbiology*, 5(5):184-188.

Gruenheid, S. and B.F. Finlay. 2000. Crowd Control: Quorum Sensing in Pathogenic *E. coli*. *Trends in Microbiology*, 8(10):442-443.

Gyürèk, L.L. and G.R. Finch. 1998. Modeling Water Treatment Chemical Disinfection Kinetics. *Journal of Environmental Engineering*, 124(9):783-793.

Gyurék, L.L., H. Li, M. Belosevic and G.R. Finch. 1999. Ozone Inactivation Kinetics of *Cryptosporidium* In Phosphate Buffer. *Journal of Environmental Engineering*, 125(10):913-924.

Gyürèk, L.L., H. Li, M. Belosevic and G.R. Finch. 1999. Ozone Inactivation Kinetics of *Cryptosporidium* in Phosphate Buffer. *Journal of Environmental Engineering*, 125(10):913-924.

Haas, C.N. 1988. Maximum Likelihood Analysis of Disinfection Kinetics. *Water Research*, 22(6):669-677.

Haas, C.N. and G.R. Finch. 1999. *Methodologies For the Determination of Disinfection Effectiveness*. AWWA Research Foundation.

Haas, C.N., M.S. Heath, J. Jacangelo, U. Anmangandla, J.C. Hornberger and J. Glicker. 1995. *Development and Validation of Rational Design Methods of Disinfection*. Denver: AWWARF.

Haas, C.N. and B. Heller. 1989. Statistics of Microbial Disinfection. *Water Science and Technology*, 21(3):197-201.

Haas, C.N., J.C. Hornberger, U. Anmangandla, M. Heath and J.G. Jacangelo. 1994. A Volumetric Method for Assessing *Giardia* Inactivation. *Journal AWWA*, 86(2):115-120.

Haas, C.N. and J. Joffe. 1994. Disinfection under Dynamic Conditions: Modifications of Hom Model for Decay. *Environmental Science and Technology*, 28(7):1367-1369.

Haas, C.N. and S.B. Karra. 1984. Kinetics of Microbial Inactivation by Chlorine-1. *Water Research*, 18(11):1443-1449.

Hengge-Aronis, R. 2000. The General Stress Response in *Escherichia coli*. In *Bacterial Stress Responses.* Edited by Storz, G. Washington D.C.: ASM Press.

Hijnen, W.A.M., J. Willemsen-Zwaagstra, P. Hiemstra, G.J. Medema and D.v.d. Kooij. 2000. Removal of Sulphite-reducing *Clostridia* Spores by Full-scale Water Treatment Processes as a Surrogate for Protozoan (Oo)cysts Removal. *Water Science and Technology*, 41(7):165-171.

Hirata, T., D. Chikuma, A. Shimura, A. Hashimoto, N. Motoyama, K. Takahashi, T. Moniwa, M. Kaneko, S. Saito and S. Maede. 2000. Effects of Ozonation and Chlorination on Viability of *Cryptosporidium parvum* Oocysts. *Water Science and Technology*, 41(7):39-46.

Hom, L.W. 1972. Kinetics of Chlorine Disinfection of an Ecosystem. *Journal of the Sanitary Engineering Division, ASCE*, 98(SA1):183-194.

Huisman, G.W. and R. Kolter. 1994. Sensing Starvation: A Homeserine Lactone-dependent Signaling Pathway in *Escherichia coli*. *Science*, 265(5171):537-539.

Hunt, N.K. and B.J. Mariñas. 1999. Inactivation of *Escherichia coli* with Ozone Chemical and Inactivation Kinetics. *Water Research*, 33(11):2633-2641.

Ishihama, A. 1997. Adaptation of Gene Expression in Stationary Phase Bacteria. *Current Opinion in Genetics and Development*, 7:582-588.

Jørgensen, F., M. Bally, V.C. Herve, G. Michel, A. Lazdunski, P. Williams and G.S.A.B. Stewart`. 1999. RpoS-dependent Stress Tolerance in *Pseudomonas aeruginosa*. *Microbiology*, 145:835-844.

Kaprelyants, A.S. and D.B. Kell. 1996. Do Bacteria Need to Communicate With Each Other for Growth. *Trends in Microbiology*, 4(6):237-242.

Klotz, M.G. and S.W. Hutcheson. 1992. Multiple Periplasmic Catalases in Phytopathogenic Strains of *Pseudomonas syringae*. *Applied and Environmental Microbiology*, 58:2468-2473.

Kouame, Y. and C.N. Haas. 1991. Inactivation of *E. coli* by Combined Action of Free Chlorine and Monochloramine. *Water Research*, 25(9):1027-1032.

Labutiak, C.W., M. Belosevic and G.R. Finch. 1992. Factors Influencing the Infectivity of *Giardia muris* Cysts Following Ozone Inactivation in Laboratory and Natural Waters. *Water Research*, 26(6):733-743.

Lazazzera, B.A. 2000. Quorum Sensing and Starvation: Signals for Entry into Stationary Phase. *Current Opinion in Microbiology*, 3:177-182.

Li, H., L.L. Gyurék, G.R. Finch, D.W. Smith and M. Belosevic. 2001. Effect of Temperature on Ozone Inactivation of *Cryptosporidium parvum* in Oxidant Demand-Free Phosphate Buffer. *Journal of Environmental Engineering*, 127(5):456-466.

Mah, T.-F.C. and G.A. O'Toole. 2001. Mechanisms of Biofilm Resistance to Antimicrobial Agents. *Trends in Microbiology*, 9(1):34-39.

Maier, R.M., I.L. Pepper and C.P. Gerba. 2000. *Environmental Microbiology*. San Diego, CA: Academic Press.

Majumdar, S.B., W.H. Ceckler and O.J. Sproul. 1973. Inactivation of Poliovirus in Water by Ozonation. *Journal Water Pollution Control Federation*, 45(12):2433-2443.

Nieminski, E.C., W.D. Bellamy and L.R. Moss. 2000. Using Surrogates to Improve Plant Performance. *Journal AWWA*, 92(3):67-78.

O'Driscoll, B., C.G.M. Gahan and C. Hill. 1996. Adaptive Acid Tolerance response in *Listeria monocytogenes:* Isolation of an Acid-tolerant Mutant Which Domenstrates Increased Virulence. *Applied and Environmental Microbiology*, 62:1693-1698.

Oppenheimer, J.A., E.M. Aleta, R.R. Trussell, J.G. Jacangelo and I.N. Najm. 1999. *Evaluation of Cryptosporidium Inactivation in Natural Waters*. Denver, CO: AWWA Research Foundation and American Water Works Association.

Owens, J.H., R.J. Miltner, E.W. Rice, C.H. Johnson, D.R. Dahling, F.W.S. III and H.M. Shukairy. 2000. Pilot-Sclae Ozone Inactivation of *Cryptosporidium* and Other Microorganisms in Natural Water. *Ozone Science and Engineering*, 22:501-517.

Payment, P. and E. Franco. 1993. *Clostridium perfringens* and Somatic Coliphages as Indicators of the Efficiency of Drinking Water Treatment for Viruses and Protozoan Cysts. *Applied and Environmental Microbiology*, 59(8):2418-2424.

Pernitsky, D.J., G.R. Finch and P.M. Huck. 1995. Disinfection Kinetics of Heterotrophic Plate Count Bacteria in Biologically Treated Potable Water. *Water Research*, 29(5):1235-1241.

Quinn, G.P. and M.J. Keough. 2002. *Experimental design and Data Analysis for Biologists*. Cambridge, UK: Cambridge University Press.

Radziminski, C., L. Ballantyne, J. Hodson, R. Creason, R.C. Andrews and C. Chauret. 2002. Disinfection of *Bacillus subtilis* spores with chlorine dioxide: a bench-scale and pilot-scale study. *Water Research*, 36:1629-1639.

Rennecker, J.L., B. Corona-Vasquez, A.M. Driedger and B.J. Mariñas. 2000. Synergism in Sequential Disinfection of *Cryptosporidium parvum*. *Water Science and Technology*, 41(7):47-52.

Rennecker, J.L., J.H. Kim, B. Corona-Vasquez and B.J. Mariñas. 2001. Role of disinfectant concentration and pH in the inactivation kinetics of *Cryptosporidium parvum* oocysts with ozone and monochloramine. *Environmental Science and Technology*, 35:2752-2757.

Rennecker, J.L., B.J. Mariñas, J.H. Owens and E.W. Rice. 1999. Inacitvation of *Cryptosporidium parvum* Oocysts with Ozone. *Water Research*, 33(11):2481-2488.

Rice, E.W., K.R. Fox, R.J. Miltner, D.A. Lytle and C.H. Johnson. 1996. Evaluating Plant Performance with Endospores. *Journal AWWA*, 88(9):122-130.

Roy, D.E., E. Chian, R. Engelbrecht. 1981. Kinetics of Enteroviral Inactivation by Ozone. *ASCE Journal of Environmental Engineering*, 107:887-889.

Russell, A.D. 1995. Mechanisms of Bacterial Resistance to Biocides. *International Biodeterioration and Biodegradation*, 36:247-265.

Russell, A.D. 1999. Factors Influencing the Efficacy of Antimicrobial Agents. In *Principles and Practice of Disinfection, Preservation and Sterilization.* Edited by Hugo, W.B. and G.A.J. Ayliffe. Malden, MA: Blackwell Science.

Russell, A.D., W.B. Hugo and G.A.J. Ayliffe. 1999. *Principles and Practice of Disinfection, Preservation and Sterilization*. 3rd. Oxon, OX: Blackwell Science.

Saby, S., P. Leroy and J.C. Block. 1999. *Escherichia coli* Resistance to Chlorine and Gluththione Synthesis in Response to Oxygenation and Starvation. *Applied and Environmental Microbiology*, 65(12):5600-5603.

Sauch, J.F. 1988. A New Method for Excystation of *Giardia*. In *Advances in Giardia Research.* Edited by Calgary: University of Calgary.

Severin, B.F., M.T. Suidan and R.S. Engelbrecht. 1983. Kinetic Modeling of U.V. Disinfection of Water. *Water Research*, 17(11):1669-1678.

Severin, F.B., M.T. Suidan and R.S. Engelbrecht. 1984. Series Event Kinetic Model For Chemical Disinfection. *Journal of Environmental Engineering, ASCE*, 110(2):430-439.

Sokal, R.R. and F.J. Rohlf. 1995. *Biometry*. 3rd. New York: W. H. Freeman and Company.

Somiya, I., S. Fujii, N. Kishimato and R.-H. Kim. 2000. Development of MAthematical Model of *Cryptosporidium* Inactivation by Ozonation. *Water Science and Technology*, 41(7):173-180.

Sommer, R., A. Cabaj, D. Schoenen, J. Gebel, A. Kolch, A.H. Havelaar and F.M. Schets. 1995. Comparison of Three Laboratory Devices for UV-Inactivation of Microorganisms. *Water Science and Technology*, 31(5-6):147-156.

Sonenshein, A.L., J.A. Hoch and R. Losick. 1993. *Bacillus subtilis and Other Gram-Positive Bacteria*. Washington, D.C.: American Society for Microbiology.

Spellman, F.R. 1999. *Choosing Disinfection Alternatives for Water/Wastewater Treatment*. Lancaster, PA: Technomic Publishing Co., Inc.

Sterkenurg, A., E. Vlegels and J.T.M. Wouters. 1984. Influence of Nutrient Limitations and Growth Rate on the Outer Membrane Proteins of *Klebsiella aerogenes* NCTC 418. *Journal of General Microbiology*, 130:2347-2355.

Stewart, M.A. and B.H. Olson. 1996. Bacterial Resistance to Potable Water Disinfectants. In *Modeling Disease Transmission and Its Prevention by Disinfection.* Edited by Hurst, C.J. Cambridge: Cambridge University Press.

Storz, G. 2000. *Bacterial Stress Response*. Washington, D.C.: ASM Press.

Surette, M.G. and B.L. Bassler. 1998. Quorum Sensing in *Escherichia coli* and *Salmonella typhimurium*. *Proc. Natl. Acad. Sci.*, 95:7046-7050.

Sussman, M. 1985. *Escherichia coli* in Human and Animal Disease. In *The Virulance of Escherichia coli.* Edited by Sussman, M. Society for General Microbiology.

Taylor, R.H., J.O.F. III, C.D. Norton and M.W. LeChevallier. 2000. Chlorine, Chloramine, Chlorine Dioxide, and Ozone Susceptibility of *Mycobacterium avium*. *Applied and Environmental Microbiology*, 66(4):1702-1705.

Tuomanen, E., R. Cozens, W. Tosch, O. Zak and A. Tomasz. 1986. The Rate of Killing of *Escherichia coli* by β–Lactam is Strictly Proportional to the Rate of Bacterial Growth. *Journal of General Microbiology*, 132:1297-1304.

USEPA. 2001. *Implementation Guidance for the Interim Enhanced Surface Water Treatment Rule*. United States Environmental Protection Agency.

USEPA, C.a.S.D. 1990. *Guidance Manual for Compliance with the Filtration and Disinfection Requirements for Public Water Systems Using Surface Water Sources*. Washington D.C.: USEPA.

Venczel, L.V., M. Arrowood, M. Hurd and M.D. Sobsey. 1997. Inactivation of *Cryptosporidium parvum* Oocysts and *Clostridium perfringens* Spores by a Mixed-Oxidant Disinfectant and by Free Chlorine. *Applied and Environmental Microbiology*, 63(4):1598-1601.

Walker, M.W., M.T. Kinter, R.J. Roberts and D.R. Spitz. 1995. Nitric Oxide-Induced Cytotoxicity: Involvement of Cellular Resistance to Oxidative Stress and the Role of Glutathione in Protection. *Pediatric Research*, 37(1):41-49.

Watson, H.E. 1908. A Note on the Variation of the Rate of Disinfection with Change in Concentration of the Disinfectant. *Journal of Hygiene*, 8:536-542.

Whiteley, M., E. Brown and R.J.C. McLean. 1997. An inexpensive chemostat apparatus for the study of microbial biofilms. *Journal of Microbiological Methods*, 30:125-132.

Whiteley, M., M.R. Parsek and E.P. Greenberg. 2000. Regulation of Quorum Sensing by RpoS in *Pseudomonas aeruginosa*. *Journal of Bacteriology*, 182(15):4356-4360.

Winans, C.S. and J. Zhu. 2000. Roles of Cell-cell Communication in Confronting the Limitations and Opportunities of High Population Densities. In *Bacterial Stress Responses.* Edited by Storz, G. Washington, D. C.: ASM Press.

Xiong, R., G. Xie, A.E. Edmondson and M.A. Sheard. 1999. Mathematical Model for Bacterial Inactivation. *International Journal of Food Microbiology*, 46:45-55.

Yamada, M., A.A. Taluker and T. Nitta. 1999. Characterization of the *ssnA* Gene, Which is Involved in the Decline of Cell Viability at the Beginning of Stationary Phase in *Escherichia coli*. *Journal of Bacteriology*, 181(6):1838-1846.

Zambrano, M.M. and R. Kolter. 1996. GASPing for Life in Stationary Phase. *Cell*, 86:181-184.

APPENDIX A: DISINFECTANT RESIDUAL, PH, TEMPERATURE AND SURVIVAL DATA OF INACTIVATION EXPERIMENTS

Table A.1: Disinfectant residual, pH and temperature in inactivation experiments of batch cultures of *E. coli.*

Experiment Date	Experiment No.	Time (min)	Monochl. Dose, C_a (mg/L)	Monochl. Residual, C (mg/L)	Initial Density, N_o (CFU/mL)	pH	Temp. (˚C)
17-Dec-99	1	2	0.70	0.70	78,700	6.99	15
17-Dec-99	1	6	0.70	0.67	78,700	6.98	
17-Dec-99	1	10	0.70	0.70	78,700	6.97	
21-Dec-99	2	2	0.97	0.97	15,700	6.98	15
21-Dec-99	2	6	0.97	1.01	15,700	6.97	
21-Dec-99	2	10	0.97	1.01	15,700	6.94	
22-Dec-99	3	2	1.45	1.45	10,500	7.07	16
22-Dec-99	3	4	1.45	1.45	10,500	7.06	
22-Dec-99	3	6	1.45	1.42	10,500	7.07	
23-Dec-99	4	2	0.98	0.98	159,000	6.93	15
23-Dec-99	4	6	0.98	0.98	159,000	6.96	
23-Dec-99	4	10	0.98	0.98	159,000	6.96	
30-Dec-99	5	2	1.64	1.64	86,600	7.03	16
30-Dec-99	5	4	1.64	1.60	86,600	7.04	
30-Dec-99	5	6	1.64	0.57	86,600	7.02	
4-Jan-00	6	2	0.70	0.70	12,900	7.10	14
4-Jan-00	6	6	0.70	0.70	12,900	7.10	
4-Jan-00	6	10	0.70	0.69	12,900	7.10	
7-Jan-00	7	2	0.75	0.75	10,100	7.06	14
7-Jan-00	7	6	0.75	0.72	10,100	7.06	
7-Jan-00	7	10	0.75	0.74	10,100	7.07	
14-Jan-00	8	2	1.46	1.46	6,950	7.01	13
14-Jan-00	8	4	1.46	1.48	6,950	7.00	
14-Jan-00	8	6	1.46	1.47	6,950	7.02	
18-Jan-00	9	2	0.93	0.93	64,100	7.04	15
18-Jan-00	9	6	0.93	0.95	64,100	7.05	
18-Jan-00	9	10	0.93	0.94	64,100	7.03	
21-Jan-00	10	2	0.98	0.98	13,800	7.07	16
21-Jan-00	10	6	0.98	0.99	13,800	7.08	
21-Jan-00	10	10	0.98	0.99	13,800	7.08	
27-Jan-00	11	2	1.43	1.43	74,000	7.11	15
27-Jan-00	11	4	1.43	1.45	74,000	7.11	
27-Jan-00	11	6	1.43	1.45	74,000	7.10	
4-Feb-00	12	2	0.68	0.68	92,900	7.02	16
4-Feb-00	12	6	0.68	0.70	92,900	7.01	

(continued)

Table A.1: (continued)

Date	Experiment No.	Time (min)	Monochl. Dose (mg/L), C_a	Monochl. Residual, C (mg/L)	Initial Density, N_o (CFU/mL)	pH	Temp. (˚C)
4-Feb-00	12	10	0.68	0.69	92,900	7.03	
8-Feb-00	13	2	0.70	0.70	9,460	6.91	15
8-Feb-00	13	6	0.70	0.71	9,460	6.91	
8-Feb-00	13	10	0.70	0.69	9,460	6.93	
16-Feb-00	14	2	0.76	0.76	7,790	7.07	15
16-Feb-00	14	6	0.76	0.68	7,790	7.06	
16-Feb-00	14	10	0.76	0.75	7,790	7.00	
17-Feb-00	15	2	1.39	1.39	55,400	6.95	15
17-Feb-00	15	4	1.40	1.39	55,400	6.97	
17-Feb-00	15	6	1.40	1.40	55,400	6.95	
21-Feb-00	16	2	0.74	0.74	6,170	7.10	15
21-Feb-00	16	6	0.74	0.73	6,170	7.07	
21-Feb-00	16	10	0.74	0.72	6,170	7.07	
23-Feb-00	17	2	1.54	1.54	97,900	6.97	15
23-Feb-00	17	4	1.54	1.54	97,900	7.02	
23-Feb-00	17	6	1.54	1.54	97,900	7.02	
28-Feb-00	18	2	1.08	1.08	3,720	7.00	15
28-Feb-00	18	6	1.08	1.01	3,720	7.02	
28-Feb-00	18	10	1.08	1.01	3,720	6.99	
3-Mar-00	19	2	1.58	1.58	1,520	7.06	16
3-Mar-00	19	5	1.58	1.54	1,520	7.05	
6-Mar-00	20	2	0.94	0.94	983	6.98	15
6-Mar-00	20	6	0.94	0.94	983	6.97	
6-Mar-00	20	10	0.94	0.95	983	6.97	
8-Mar-00	21	2	0.71	0.71	1,020	6.98	14
8-Mar-00	21	6	0.71	0.72	1,020	6.98	
8-Mar-00	21	10	0.71	0.70	1,020	7.01	

Table A.2: Disinfectant residual, pH and temperature in inactivation experiments of *G. muris* cysts.

Experiment Date	Experiment No.	Time (min)	Ozone. Dose, C_a (mg/L)	Ozone Residual, C (mg/L)	Initial Density, N_o (Trop./mL)	pH	Temp. (˚C)
21-Jul-00	1	0.33	0.75	0.55	7,500	8.05	15.0
21-Jul-00	1	0.67	0.75	0.47	7,500		
21-Jul-00	1	1.17	0.75	0.35	7,500		
23-Jul-00	2	0.25	0.50	0.19	13,524	7.98	15.0
23-Jul-00	2	0.50	0.50	0.18	13,524		
23-Jul-00	2	1.00	0.50	0.15	13,524		
23-Jul-00	3	0.25	0.75	0.47	13,524	7.97	15.0
23-Jul-00	3	0.50	0.75	0.44	13,524		
23-Jul-00	3	1.00	0.75	0.40	13,524		
29-Jul-00	4	0.25	0.50	0.18	36,111	8.17	15.0
29-Jul-00	4	0.67	0.50	0.04	36,111		
29-Jul-00	4	1.08	0.50	0.08	36,111		
29-Jul-00	5	0.25	0.75	0.31	36,111	8.16	15.0
29-Jul-00	5	0.67	0.75	0.23	36,111		
29-Jul-00	5	1.08	0.75	0.17	36,111		
11-Aug-00	6	0.33	0.50	0.27	26,167	7.94	15.0
11-Aug-00	6	0.58	0.50	0.20	26,167		
11-Aug-00	6	1.08	0.50	0.19	26,167		
11-Aug-00	7	0.33	0.75	0.38	26,167	7.96	15.0
11-Aug-00	7	0.58	0.75	0.36	26,167		
11-Aug-00	7	1.17	0.75	0.32	26,167		
12-Aug-00	8	0.25	0.40	0.17	17,222	8.04	15.0
12-Aug-00	8	0.67	0.40	0.10	17,222		
12-Aug-00	8	1.25	0.40	0.09	17,222		
16-Aug-00	9	0.33	0.40	0.16	7,079	8.06	15.0
16-Aug-00	9	0.67	0.40	0.15	7,079		
16-Aug-00	9	1.17	0.40	0.12	7,079		
19-Aug-00	10	0.33	0.25	0.02	7,730	8.00	15.0
19-Aug-00	10	2.00	0.25	0.01	7,730		
19-Aug-00	10	4.00	0.25	0.00	7,730		
24-Aug-00	11	0.33	0.25	0.04	5,937	8.07	14.0
24-Aug-00	11	2.00	0.25	0.02	5,937		
24-Aug-00	11	4.00	0.25	0.00	5,937		
1-Sep-00	12	0.33	0.25	0.01	9,472	7.97	15.5
1-Sep-00	12	2.00	0.25	0.00	9,472		
1-Sep-00	12	4.00	0.25	0.00	9,472		
7-Sep-00	13	0.25	0.40	0.17	25,467	8.04	15.0
7-Sep-00	13	0.75	0.40	0.17	25,467		
7-Sep-00	13	1.50	0.40	0.16	25,467		

(continued)

Table A.2: (continued)

Experiment Date	Experiment No.	Time (min)	Ozone. Dose, C_a (mg/L)	Ozone Residual, C (mg/L)	Initial Density, N_o (Trop./mL)	pH	Temp. (˚C)
8-Sep-00	14	0.33	0.25	0.00	25,867	8.02	15.0
8-Sep-00	14	2.00	0.25	0.02	25,867		
8-Sep-00	14	4.00	0.25	0.01	25,867		
13-Sep-00	15	0.25	0.40	0.03	51,667	8.02	15.0
13-Sep-00	15	0.75	0.40	0.02	51,667		
13-Sep-00	15	1.50	0.40	0.02	51,667		
14-Sep-00	16	0.33	0.25	0.00	65,500	8.03	14.5
14-Sep-00	16	2.00	0.25	0.02	65,500		
14-Sep-00	16	4.00	0.25	0.00	65,500		
15-Sep-00	17	0.25	0.40	0.14	47,833	8.00	15.0
15-Sep-00	17	1.00	0.40	0.09	47,833		
15-Sep-00	17	2.00	0.40	0.04	47,833		

Table A.3: Disinfectant residual, pH and temperature in inactivation experiments of *E. coli* at exponential growth phase.

Experiment Date	Experiment No.	Time (min)	Monochl. Dose, C_a (mg/L)	Monochl. Residual, C (mg/L)	Initial Density, N_o (CFU/mL)	pH	Temp. (˚C)
20-Mar-02	1	1.0	0.94	0.93	9,820	15.0	7.00
20-Mar-02	1	8.0	0.94	0.94	9,820		
20-Mar-02	2	1.0	0.94	0.93	9,820	15.0	7.00
20-Mar-02	2	4.0	0.94	0.93	9,820		
20-Mar-02	2	8.0	0.94	0.94	9,820		
23-Mar-02	3	1.0	1.44	1.43	102,027	15.0	7.00
23-Mar-02	3	2.0	1.44	1.43	102,027		
23-Mar-02	3	3.0	1.44	1.44	102,027		
23-Mar-02	4	1.0	1.44	1.43	102,027	15.0	7.00
23-Mar-02	4	2.0	1.44	1.43	102,027		
23-Mar-02	4	3.0	1.44	1.44	102,027		
25-Mar-02	5	1.0	0.75	0.74	10,890	15.0	7.00
25-Mar-02	5	3.0	0.75	0.75	10,890		
25-Mar-02	5	6.0	0.75	0.75	10,890		
25-Mar-02	6	1.0	0.75	0.74	10,890	15.0	7.00
25-Mar-02	6	3.0	0.75	0.75	10,890		
25-Mar-02	6	6.0	0.75	0.75	10,890		
27-Mar-02	7	1.5	0.97	0.95	119,820	15.0	6.98
27-Mar-02	7	3.0	0.97	0.95	119,820		
27-Mar-02	7	6.0	0.97	0.97	119,820		
27-Mar-02	8	1.5	0.97	0.95	119,820	15.0	6.98
27-Mar-02	8	3.0	0.97	0.95	119,820		
27-Mar-02	8	6.0	0.97	0.97	119,820		
29-Mar-02	9	1.0	1.42	1.41	1,059	15.0	6.82
29-Mar-02	9	3.0	1.42	1.41	1,059		
29-Mar-02	9	5.0	1.42	1.42	1,059		
29-Mar-02	10	1.0	1.42	1.41	1,059	15.0	6.82
29-Mar-02	10	3.0	1.42	1.41	1,059		
29-Mar-02	10	5.0	1.42	1.42	1,059		
30-Mar-02	11	2.0	0.69	0.67	973	14.0	6.99
30-Mar-02	11	5.0	0.69	0.69	973		
30-Mar-02	11	8.0	0.69	0.68	973		
30-Mar-02	12	2.0	0.69	0.67	973	14.0	6.99
30-Mar-02	12	5.0	0.69	0.69	973		
30-Mar-02	12	8.0	0.69	0.68	973		
31-Mar-02	13	1.0	1.39	1.39	13,435	15.0	7.09
31-Mar-02	13	3.0	1.39	1.39	13,435		
31-Mar-02	13	5.0	1.39	1.39	13,435		
31-Mar-02	14	1.0	1.39	1.39	13,435	15.0	7.09
31-Mar-02	14	3.0	1.39	1.39	13,435		
31-Mar-02	14	5.0	1.39	1.39	13,435		

(continued)

Table A.3: (continued)

Experiment Date	Experiment No.	Time (min)	Monochl. Dose, C_a (mg/L)	Monochl. Residual, C (mg/L)	Initial Density, N_o (CFU/mL)	pH	Temp. (˚C)
1-Apr-02	15	2.0	0.74	0.74	136,712	15.0	6.94
1-Apr-02	15	6.0	0.74	0.72	136,712		
1-Apr-02	15	10.0	0.74	0.73	136,712		
1-Apr-02	16	2.0	0.74	0.74	136,712	15.0	6.94
1-Apr-02	16	6.0	0.74	0.72	136,712		
1-Apr-02	16	10.0	0.74	0.73	136,712		
2-Apr-02	17	1.0	0.94	0.94	1,087	14.5	6.96
2-Apr-02	17	3.0	0.94	0.89	1,087		
2-Apr-02	17	6.0	0.94	0.92	1,087		
2-Apr-02	18	1.0	0.94	0.94	1,087	14.5	6.96
2-Apr-02	18	3.0	0.94	0.89	1,087		
2-Apr-02	18	6.0	0.94	0.92	1,087		
4-Apr-02	19	2.0	0.72	0.71	12,162	15.0	7.05
4-Apr-02	19	5.0	0.72	0.72	12,162		
4-Apr-02	19	8.0	0.72	0.72	12,162		
4-Apr-02	20	2.0	0.72	0.71	12,162	15.0	7.05
4-Apr-02	20	5.0	0.72	0.72	12,162		
4-Apr-02	20	8.0	0.72	0.72	12,162		
5-Apr-02	21	2.0	0.96	0.95	92,793	14.5	7.04
5-Apr-02	21	4.0	0.96	0.96	92,793		
5-Apr-02	21	6.0	0.96	0.95	92,793		
5-Apr-02	22	2.0	0.96	0.95	92,793	14.5	7.04
5-Apr-02	22	4.0	0.96	0.96	92,793		
5-Apr-02	22	6.0	0.96	0.95	92,793		
6-Apr-02	23	1.0	1.45	1.45	837	14.5	7.05
6-Apr-02	23	2.5	1.45	1.43	837		
6-Apr-02	23	4.0	1.45	1.44	837		
6-Apr-02	24	1.0	1.45	1.45	837	14.5	7.05
6-Apr-02	24	2.5	1.45	1.43	837		
6-Apr-02	24	4.0	1.45	1.44	837		

Table A.4: Disinfectant residual, pH and temperature in inactivation experiments of *E. coli* DMS.

Experiment Date	Experiment No.	Time (min)	Monochl. Dose, C_a (mg/L)	Monochl. Residual, C (mg/L)	Initial Density, N_o (CFU/mL)	pH	Temp. (˚C)
28-Jan-02	501	2.0	1.00	0.98	10,901	15.0	7.01
28-Jan-02	501	6.0	1.00	1.00	10,901		
28-Jan-02	501	10.0	1.00	1.00	10,901		
28-Jan-02	502	2.0	1.00	0.98	10,901	15.0	7.01
28-Jan-02	502	6.0	1.00	1.00	10,901		
28-Jan-02	502	10.0	1.00	1.00	10,901		
4-Feb-02	503	2.0	0.73	0.73	1,261	15.0	7.01
4-Feb-02	503	6.0	0.73	0.71	1,261		
4-Feb-02	503	10.0	0.73	0.71	1,261		
4-Feb-02	504	2.0	0.73	0.73	1,261	15.0	7.01
4-Feb-02	504	6.0	0.73	0.71	1,261		
4-Feb-02	504	10.0	0.73	0.71	1,261		
7-Feb-02	505	2.0	1.42	1.41	149,662	15.0	7.02
7-Feb-02	505	4.0	1.42	1.41	149,662		
7-Feb-02	505	6.0	1.42	1.42	149,662		
7-Feb-02	506	2.0	1.42	1.41	149,662	15.0	7.02
7-Feb-02	506	4.0	1.42	1.41	149,662		
7-Feb-02	506	6.0	1.42	1.42	149,662		
12-Feb-02	507	2.0	0.98	0.97	118,243	15.0	6.99
12-Feb-02	507	6.0	0.98	0.97	118,243		
12-Feb-02	507	10.0	0.98	0.98	118,243		
12-Feb-02	508	2.0	0.98	0.97	118,243	15.0	6.99
12-Feb-02	508	6.0	0.98	0.97	118,243		
12-Feb-02	508	10.0	0.98	0.98	118,243		
14-Feb-02	509	2.0	0.75	0.73	10,980	15.0	7.03
14-Feb-02	509	6.0	0.75	0.71	10,980		
14-Feb-02	509	10.0	0.75	0.75	10,980		
14-Feb-02	510	2.0	0.75	0.73	10,980	15.0	7.03
14-Feb-02	510	6.0	0.75	0.71	10,980		
14-Feb-02	510	10.0	0.75	0.75	10,980		
15-Feb-02	511	2.0	0.97	0.95	962	14.5	7.00
15-Feb-02	511	6.0	0.97	0.96	962		
15-Feb-02	511	10.0	0.97	0.97	962		
15-Feb-02	512	2.0	0.97	0.95	962	14.5	7.00
15-Feb-02	512	6.0	0.97	0.96	962		
15-Feb-02	512	10.0	0.97	0.97	962		
16-Feb-02	513	2.0	1.43	1.42	1,310	14.5	7.04
16-Feb-02	513	4.0	1.43	1.41	1,310		
16-Feb-02	513	6.0	1.43	1.43	1,310		

(continued)

Table A.4: (continued)

Experiment Date	Experiment No.	Time (min)	Monochl. Dose, C_a (mg/L)	Monochl. Residual, C (mg/L)	Initial Density, N_o (CFU/mL)	pH	Temp. (˚C)
16-Feb-02	514	2.0	1.43	1.42	1,310	14.5	7.04
16-Feb-02	514	4.0	1.43	1.41	1,310		
16-Feb-02	514	6.0	1.43	1.43	1,310		
5-Sep-02	515	2.0	0.93	0.93	16,318	15.0	7.12
5-Sep-02	515	4.0	0.93	0.92	16,318		
5-Sep-02	515	6.0	0.93	0.92	16,318		
5-Sep-02	516	2.0	0.93	0.93	16,318	15.0	7.12
5-Sep-02	516	4.0	0.93	0.92	16,318		
5-Sep-02	516	6.0	0.93	0.92	16,318		
6-Sep-02	517	2.0	0.69	0.69	117,005	14.5	7.07
6-Sep-02	517	6.0	0.69	0.69	117,005		
6-Sep-02	517	10.0	0.69	0.68	117,005		
6-Sep-02	518	2.0	0.69	0.69	117,005	14.5	7.07
6-Sep-02	518	6.0	0.69	0.69	117,005		
6-Sep-02	518	10.0	0.69	0.68	117,005		
11-Sep-02	519	2.0	1.44	1.44	12,579	14.5	7.09
11-Sep-02	519	4.0	1.44	1.41	12,579		
11-Sep-02	519	6.0	1.44	1.37	12,579		
11-Sep-02	520	2.0	1.44	1.44	12,579	14.5	7.09
11-Sep-02	520	4.0	1.44	1.41	12,579		
11-Sep-02	520	6.0	1.44	1.37	12,579		
13-Sep-02	521	2.0	1.44	1.44	126,914	15.0	7.08
13-Sep-02	521	4.0	1.44	1.42	126,914		
13-Sep-02	521	6.0	1.44	1.43	126,914		
13-Sep-02	522	2.0	1.44	1.44	126,914	15.0	7.08
13-Sep-02	522	4.0	1.44	1.42	126,914		
13-Sep-02	522	6.0	1.44	1.43	126,914		
15-Sep-02	523	2.0	0.80	0.80	12,061	15.0	7.04
15-Sep-02	523	6.0	0.80	0.78	12,061		
15-Sep-02	523	10.0	0.80	0.77	12,061		
15-Sep-02	524	2.0	0.80	0.80	12,061	15.0	7.04
15-Sep-02	524	6.0	0.80	0.78	12,061		
15-Sep-02	524	10.0	0.80	0.77	12,061		

Table A.5: Disinfectant residual, pH and temperature in inactivation experiments of continuous cultures of *E coli*.

Experiment Date	Experiment No.	Time (min)	Monochl. Dose, Ca (mg/L)	Monochl. Residual, C (mg/L)	Initial Density, N_o (CFU/mL)	pH	Temp. (˚C)
2-Aug-02	201	2.0	1.00	1.00	2,241	14.0	7.10
2-Aug-02	201	6.0	1.00	1.00	2,241		
2-Aug-02	201	10.0	1.00	0.99	2,241		
2-Aug-02	202	2.0	1.00	1.00	2,241	14.0	7.10
2-Aug-02	202	6.0	1.00	1.00	2,241		
2-Aug-02	202	10.0	1.00	0.99	2,241		
3-Aug-02	203	1.0	1.46	1.45	26,914	14.5	7.07
3-Aug-02	203	4.0	1.46	1.46	26,914		
3-Aug-02	203	7.0	1.46	1.44	26,914		
3-Aug-02	204	1.0	1.46	1.45	26,914	14.5	7.07
3-Aug-02	204	4.0	1.46	1.46	26,914		
3-Aug-02	204	7.0	1.46	1.44	26,914		
4-Aug-02	205	2.0	0.78	0.77	207	14.0	7.15
4-Aug-02	205	6.0	0.78	0.78	207		
4-Aug-02	205	10.0	0.78	0.77	207		
4-Aug-02	206	2.0	0.78	0.77	207	14.0	7.15
4-Aug-02	206	6.0	0.78	0.78	207		
4-Aug-02	206	10.0	0.78	0.77	207		
6-Aug-02	207	2.0	1.00	1.00	103,829	14.5	6.94
6-Aug-02	207	6.0	1.00	1.00	103,829		
6-Aug-02	207	10.0	1.00	1.00	103,829		
6-Aug-02	208	2.0	1.00	1.00	103,829	14.5	6.94
6-Aug-02	208	6.0	1.00	1.00	103,829		
6-Aug-02	208	10.0	1.00	1.00	103,829		
7-Aug-02	209	1.0	1.47	1.46	904	15.0	6.89
7-Aug-02	209	3.0	1.47	1.47	904		
7-Aug-02	209	5.0	1.47	1.47	904		
7-Aug-02	210	1.0	1.47	1.46	904	15.0	6.89
7-Aug-02	210	3.0	1.47	1.47	904		
7-Aug-02	210	5.0	1.47	1.47	904		
8-Aug-02	211	2.0	0.75	0.74	9,730	15.0	6.96
8-Aug-02	211	6.0	0.75	0.75	9,730		
8-Aug-02	211	10.0	0.75	0.75	9,730		
8-Aug-02	212	2.0	0.75	0.74	9,730	15.0	6.96
8-Aug-02	212	6.0	0.75	0.75	9,730		
8-Aug-02	212	10.0	0.75	0.75	9,730		
10-Aug-02	214	2.0	1.43	1.43	9,550	15.0	6.96
10-Aug-02	214	4.0	1.43	1.43	9,550		
10-Aug-02	214	6.0	1.43	1.43	9,550		

(continued)

Table A.5: (continued)

Experiment Date	Experiment No.	Time (min)	Monochl. Dose, C_a (mg/L)	Monochl. Residual, C (mg/L)	Initial Density, N_o (CFU/mL)	pH	Temp. (˚C)
11-Aug-02	215	2.0	0.97	0.95	1,139	15.0	6.98
11-Aug-02	215	6.0	0.97	0.97	1,139		
11-Aug-02	215	10.0	0.97	0.96	1,139		
11-Aug-02	216	2.0	0.97	0.95	1,139	15.0	6.98
11-Aug-02	216	6.0	0.97	0.97	1,139		
11-Aug-02	216	10.0	0.97	0.96	1,139		
13-Aug-02	217	2.0	0.74	0.73	117,568	15.0	6.99
13-Aug-02	217	6.0	0.74	0.73	117,568		
13-Aug-02	217	10.0	0.74	0.74	117,568		
13-Aug-02	218	2.0	0.74	0.73	117,568	15.0	6.99
13-Aug-02	218	6.0	0.74	0.73	117,568		
13-Aug-02	218	10.0	0.74	0.74	117,568		
14-Aug-02	219	2.0	1.43	1.43	102,477	15.0	6.98
14-Aug-02	219	4.0	1.43	1.41	102,477		
14-Aug-02	219	6.0	1.43	1.43	102,477		
14-Aug-02	220	2.0	1.43	1.43	102,477	15.0	6.98
14-Aug-02	220	4.0	1.43	1.41	102,477		
14-Aug-02	220	6.0	1.43	1.43	102,477		
16-Aug-02	221	2.0	0.93	0.93	10,541	15.0	6.97
16-Aug-02	221	6.0	0.93	0.93	10,541		
16-Aug-02	221	10.0	0.93	0.93	10,541		
16-Aug-02	222	2.0	0.93	0.93	10,541	15.0	6.97
16-Aug-02	222	6.0	0.93	0.93	10,541		
16-Aug-02	222	10.0	0.93	0.93	10,541		
17-Aug-02	223	2.0	0.78	0.77	1,061	14.5	6.98
17-Aug-02	223	6.0	0.78	0.78	1,061		
17-Aug-02	223	10.0	0.78	0.78	1,061		
17-Aug-02	224	2.0	0.78	0.77	1,061	14.5	6.98
17-Aug-02	224	6.0	0.78	0.78	1,061		
17-Aug-02	224	10.0	0.78	0.78	1,061		

Table A.6: Disinfectant residual, pH and temperature in inactivation experiments of *B subtilis* spores.

Experiment Date	Experiment No.	Time (min)	Monochl. Dose, C_a (mg/L)	Monochl. Residual, C (mg/L)	Initial Density, N_o (CFU/mL)	pH	Temp. (˚C)
10-Sep-01	1	0.5	1.50	0.97	26,351	15.0	7.91
10-Sep-01	1	3.5	1.50	0.80	26,351		
10-Sep-01	1	7.0	1.50	0.55	26,351		
10-Sep-01	1	15.5	1.50	0.30	26,351		
10-Sep-01	2	0.5	1.50	0.81	26,351	15.0	7.92
10-Sep-01	2	3.5	1.50	0.72	26,351		
10-Sep-01	2	7.0	1.50	0.51	26,351		
10-Sep-01	2	15.0	1.50	0.29	26,351		
15-Sep-01	3	0.5	2.50	1.03	8,446	14.0	7.91
15-Sep-01	3	2.5	2.50	0.75	8,446		
15-Sep-01	3	5.0	2.50	0.47	8,446		
15-Sep-01	4	0.5	2.50	0.85	8,446	14.0	7.92
15-Sep-01	4	2.0	2.50	0.48	8,446		
15-Sep-01	4	5.0	2.50	0.36	8,446		
17-Sep-01	5	1.0	2.50	1.11	112,275	14.5	8.06
17-Sep-01	5	4.0	2.50	0.57	112,275		
17-Sep-01	5	8.0	2.50	0.22	112,275		
17-Sep-01	5	12.0	2.50	0.05	112,275		
17-Sep-01	6	1.0	2.50	1.02	112,275	14.5	8.07
17-Sep-01	6	5.0	2.50	0.58	112,275		
17-Sep-01	6	8.0	2.50	0.30	112,275		
17-Sep-01	6	12.0	2.50	0.11	112,275		
21-Sep-01	7	0.5	2.00	1.04	4,257	14.5	7.93
21-Sep-01	7	2.5	2.00	0.83	4,257		
21-Sep-01	7	5.0	2.00	0.73	4,257		
21-Sep-01	7	8.0	2.00	0.49	4,257		
21-Sep-01	8	0.5	2.00	1.05	4,257	14.5	7.95
21-Sep-01	8	2.5	2.00	0.92	4,257		
21-Sep-01	8	5.0	2.00	0.69	4,257		
21-Sep-01	8	8.0	2.00	0.49	4,257		
24-Sep-01	9	0.5	2.50	1.45	874	15.0	7.98
24-Sep-01	9	3.5	2.50	0.84	874		
24-Sep-01	9	5.0	2.50	0.63	874		
24-Sep-01	10	0.5	2.50	1.00	874	15.0	8.00
24-Sep-01	10	3.5	2.50	0.68	874		
24-Sep-01	10	5.0	2.50	0.61	874		
26-Oct-01	11	0.5	2.00	1.10	6,498	14.5	8.01
26-Oct-01	11	4.0	2.00	0.70	6,498		
26-Oct-01	11	8.0	2.00	0.43	6,498		
26-Oct-01	11	12.0	2.00	0.22	6,498		

(continued)

Table A.6: (continued)

Experiment Date	Experiment No.	Time (min)	Monochl. Dose, C_a (mg/L)	Monochl. Residual, C (mg/L)	Initial Density, N_o (CFU/mL)	pH	Temp. (˚C)
26-Oct-01	12	0.5	2.00	1.09	6,498	14.5	7.99
26-Oct-01	12	4.0	2.00	0.63	6,498		
26-Oct-01	12	8.0	2.00	0.36	6,498		
26-Oct-01	12	12.0	2.00	0.26	6,498		
27-Oct-01	13	0.5	1.50	0.78	70,495	14.5	7.89
27-Oct-01	13	4.0	1.50	0.49	70,495		
27-Oct-01	13	7.5	1.50	0.27	70,495		
27-Oct-01	13	12.0	1.50	0.15	70,495		
10/27/001	14	0.5	1.50	0.71	70,495	14.5	7.87
10/27/001	14	4.0	1.50	0.29	70,495		
10/27/001	14	7.5	1.50	0.17	70,495		
10/27/001	14	12.0	1.50	0.09	70,495		
28-Oct-01	15	0.5	2.00	1.03	1,096	15.5	8.03
28-Oct-01	15	4.0	2.00	0.39	1,096		
28-Oct-01	15	8.0	2.00	0.17	1,096		
28-Oct-01	15	10.0	2.00	0.11	1,096		
28-Oct-01	16	0.5	2.00	0.95	1,096	15.5	8.02
28-Oct-01	16	4.0	2.00	0.34	1,096		
28-Oct-01	16	7.5	2.00	0.09	1,096		
28-Oct-01	16	10.0	2.00	0.03	1,096		
30-Oct-01	17	0.5	2.50	1.23	1,197	14.0	7.90
30-Oct-01	17	2.5	2.50	0.90	1,197		
30-Oct-01	17	6.0	2.50	0.66	1,197		
30-Oct-01	18	0.5	2.50	1.20	1,197	14.0	7.91
30-Oct-01	18	2.5	2.50	0.83	1,197		
30-Oct-01	18	6.0	2.50	0.57	1,197		
31-Oct-01	19	0.5	2.00	1.09	63,514	14.0	7.93
31-Oct-01	19	4.0	2.00	0.68	63,514		
31-Oct-01	19	8.0	2.00	0.45	63,514		
31-Oct-01	19	12.0	2.00	0.32	63,514		
31-Oct-01	20	0.5	2.00	0.90	63,514	14.0	7.92
31-Oct-01	20	4.0	2.00	0.45	63,514		
31-Oct-01	20	8.0	2.00	0.18	63,514		
31-Oct-01	20	12.0	2.00	0.12	63,514		
2-Nov-01	21	0.5	1.50	0.82	107,207	15.0	7.92
2-Nov-01	21	4.0	1.50	0.50	107,207		
2-Nov-01	21	7.5	1.50	0.33	107,207		
2-Nov-01	21	12.0	1.50	0.20	107,207		
2-Nov-01	22	0.5	1.50	0.76	107,207	15.0	7.90
2-Nov-01	22	4.5	1.50	0.37	107,207		
2-Nov-01	22	7.5	1.50	0.20	107,207		
2-Nov-01	22	12.0	1.50	0.11	107,207		

(continued)

Table A.6: (continued)

Experiment Date	Experiment No.	Time (min)	Monochl. Dose, C_a (mg/L)	Monochl. Residual, C (mg/L)	Initial Density, N_o (CFU/mL)	pH	Temp. (˚C)
4-Nov-01	23	0.5	1.50	0.78	1,197	14.5	8.03
4-Nov-01	23	3.5	1.50	0.53	1,197		
4-Nov-01	23	8.0	1.50	0.29	1,197		
4-Nov-01	23	12.0	1.50	0.18	1,197		
4-Nov-01	24	0.5	1.50	0.83	1,197	14.5	8.01
4-Nov-01	24	3.5	1.50	0.58	1,197		
4-Nov-01	24	8.0	1.50	0.38	1,197		
4-Nov-01	24	12.0	1.50	0.27	1,197		

Table A.7: Disinfectant residual, pH and temperature in inactivation of *B. subtilis* log.

Experiment Date	Experiment No.	Time (min)	Monochl. Dose, C_a (mg/L)	Monochl. Residual, C (mg/L)	Initial Density, N_o (CFU/mL)	pH	Temp. (˚C)
4-May-02	401	2	1.47	1.46	4,336	15.0	7.94
4-May-02	401	10	1.47	1.47	4,336		
4-May-02	401	25	1.47	1.47	4,336		
4-May-02	402	2	1.47	1.46	4,336	15.0	7.94
4-May-02	402	10	1.47	1.47	4,336		
4-May-02	402	25	1.47	1.47	4,336		
6-May-02	403	2	1.03	1.02	5,923	15.0	8.03
6-May-02	403	15	1.03	1.02	5,923		
6-May-02	403	35	1.03	1.03	5,923		
6-May-02	404	2	1.03	1.02	5,923	15.0	8.03
6-May-02	404	15	1.03	1.02	5,923		
6-May-02	404	35	1.03	1.03	5,923		
7-May-02	405	2	0.78	0.78	9,685	15.0	7.94
7-May-02	405	20	0.78	0.77	9,685		
7-May-02	405	40	0.78	0.78	9,685		
7-May-02	406	2	0.78	0.78	9,685	15.0	7.94
7-May-02	406	20	0.78	0.77	9,685		
7-May-02	406	40	0.78	0.78	9,685		
9-May-02	407	2	1.48	1.48	749	14.5	7.88
9-May-02	407	10	1.48	1.48	749		
9-May-02	407	25	1.48	1.46	749		
9-May-02	408	2	1.48	1.48	749	14.5	7.88
9-May-02	408	10	1.48	1.48	749		
9-May-02	408	25	1.48	1.46	749		
10-May-02	409	2	0.98	0.97	1,527	15.0	7.92
10-May-02	409	20	0.98	0.98	1,527		
10-May-02	409	40	0.98	0.98	1,527		
10-May-02	410	2	0.98	0.97	1,527	15.0	7.92
10-May-02	410	20	0.98	0.98	1,527		
10-May-02	410	40	0.98	0.98	1,527		
13-May-02	411	2	0.97	0.97	3,863	15.0	7.98
13-May-02	411	20	0.97	0.96	3,863		
13-May-02	411	40	0.97	0.97	3,863		
13-May-02	412	2	0.97	0.97	3,863	15.0	7.98
13-May-02	412	20	0.97	0.96	3,863		
13-May-02	412	40	0.97	0.97	3,863		
14-May-02	413	2	1.43	1.43	472	15.0	7.95
14-May-02	413	10	1.43	1.42	472		
14-May-02	413	25	1.43	1.43	472		
14-May-02	414	2	1.43	1.43	472	15.0	7.95
14-May-02	414	10	1.43	1.42	472		
14-May-02	414	25	1.43	1.43	472		

(continued)

Table A.7: (continued)

Experiment Date	Experiment No.	Time (min)	Monochl. Dose, C_a (mg/L)	Monochl. Residual, C (mg/L)	Initial Density, N_o (CFU/mL)	pH	Temp. (˚C)
18-May-02	415	2	0.78	0.78	1,654	15.0	7.98
18-May-02	415	20	0.78	0.77	1,654		
18-May-02	415	45	0.78	0.78	1,654		
18-May-02	416	2	0.78	0.78	1,654	15.0	7.98
18-May-02	416	20	0.78	0.77	1,654		
18-May-02	416	45	0.78	0.78	1,654		
20-May-02	417	2	0.71	0.68	4,170	15.0	7.95
20-May-02	417	20	0.71	0.71	4,170		
20-May-02	417	45	0.71	0.69	4,170		
20-May-02	418	2	0.71	0.68	4,170	15.0	7.95
20-May-02	418	20	0.71	0.71	4,170		
20-May-02	418	45	0.71	0.69	4,170		

Table A.8: Survival of *G. muris* in ozone experiments.

Exp. Date	Exp. No	Time (min)	Ozone Dose, C_a (mg/L)	N_o (troph./mL)	$N_{Observed}$ (troph./mL)
19-Jul-00	1	0.10	0.75	19,222	6,603
19-Jul-00	1	0.20	0.75	19,222	<16
21-Jul-00	2	0.13	0.50	7,333	2,317
21-Jul-00	2	0.25	0.50	7,333	349
21-Jul-00	2	0.38	0.50	7,333	16
21-Jul-00	2	0.65	0.50	7,333	22
21-Jul-00	3	0.10	0.75	7,333	778
21-Jul-00	3	0.23	0.75	7,333	<16
23-Jul-00	4	0.10	0.50	12,889	5,429
23-Jul-00	4	0.23	0.50	12,889	3,635
23-Jul-00	4	0.35	0.50	12,889	1,095
23-Jul-00	4	0.57	0.50	12,889	143
23-Jul-00	4	1.00	0.50	12,889	<16
23-Jul-00	5	0.12	0.75	12,889	2,392
23-Jul-00	5	0.20	0.75	12,889	32
23-Jul-00	5	0.32	0.75	12,889	<16
29-Jul-00	6	0.12	0.50	34,444	5,833
29-Jul-00	6	0.22	0.50	34,444	3,714
29-Jul-00	6	0.32	0.50	34,444	1,825
29-Jul-00	6	0.63	0.50	34,444	270
29-Jul-00	6	1.13	0.50	34,444	63
29-Jul-00	7	0.10	0.75	34,444	2,190
29-Jul-00	7	0.18	0.75	34,444	16
29-Jul-00	7	0.30	0.75	34,444	<16
11-Aug-00	8	0.10	0.50	25,444	3,921
11-Aug-00	8	0.25	0.50	25,444	143
11-Aug-00	8	0.42	0.50	25,444	<16
11-Aug-00	9	0.10	0.75	25,444	429
11-Aug-00	9	0.18	0.75	25,444	<16
12-Aug-00	10	0.12	0.40	17,028	2,984
12-Aug-00	10	0.25	0.40	17,028	571
12-Aug-00	10	0.42	0.40	17,028	48
12-Aug-00	10	0.70	0.40	17,028	<16
16-Aug-00	11	0.13	0.40	6,841	2,286
16-Aug-00	11	0.25	0.40	6,841	79
16-Aug-00	11	0.37	0.40	6,841	16
16-Aug-00	11	0.72	0.40	6,841	<16
19-Aug-00	12	0.33	0.25	7,413	6,317
19-Aug-00	12	0.72	0.25	7,413	5,175
19-Aug-00	12	1.42	0.25	7,413	4,286
19-Aug-00	12	2.50	0.25	7,413	4,643
19-Aug-00	12	4.00	0.25	7,413	5,063

(continued)

Table A.8: (continued)

Exp. Date	Exp. No	Time (min)	Ozone Dose, C_a (mg/L)	N_o (troph./mL)	$N_{Observed}$ (troph./mL)
24-Aug-00	13	0.33	0.25	5,683	2,730
24-Aug-00	13	0.67	0.25	5,683	2,786
24-Aug-00	13	1.42	0.25	5,683	2,929
24-Aug-00	13	2.50	0.25	5,683	2,524
1-Sep-00	14	0.50	0.25	9,028	7,833
1-Sep-00	14	1.00	0.25	9,028	7,056
1-Sep-00	14	2.00	0.25	9,028	5,111
1-Sep-00	14	4.00	0.25	9,028	6,000
7-Sep-00	15	0.10	0.40	24,444	11,156
7-Sep-00	15	0.22	0.40	24,444	5,429
7-Sep-00	15	0.35	0.40	24,444	429
7-Sep-00	15	0.63	0.40	24,444	730
7-Sep-00	15	1.00	0.40	24,444	794
7-Sep-00	15	1.50	0.40	24,444	619
8-Sep-00	16	0.57	0.25	24,844	19,378
8-Sep-00	16	1.00	0.25	24,844	17,689
8-Sep-00	16	2.00	0.25	24,844	17,667
8-Sep-00	16	4.00	0.25	24,844	15,667
13-Sep-00	17	0.17	0.40	50,667	40,889
13-Sep-00	17	0.33	0.40	50,667	37,000
13-Sep-00	17	0.67	0.40	50,667	38,667
13-Sep-00	17	1.50	0.40	50,667	36,800
14-Sep-00	18	0.50	0.25	64,778	22,111
14-Sep-00	18	1.00	0.25	64,778	17,333
14-Sep-00	18	2.00	0.25	64,778	9,889
14-Sep-00	18	4.00	0.25	64,778	10,000
15-Sep-00	19	0.12	0.40	46,389	16,571
15-Sep-00	19	0.28	0.40	46,389	12,730
15-Sep-00	19	0.48	0.40	46,389	6,048
15-Sep-00	19	1.00	0.40	46,389	5,587
15-Sep-00	19	2.00	0.40	46,389	4,746

Table A.9: Survival of *E. coli* in monochloramine experiments.

Exp. Date	Exp. No	Time (min)	Monochl. Dose, C_a (mg/L)	$N_{Observed}$ (CFU/mL)	N_o (CFU/mL)
17-Dec-99	1	2	0.70	51,600	78,700
17-Dec-99	1	4	0.70	39,000	78,700
17-Dec-99	1	6	0.70	15,700	78,700
17-Dec-99	1	8	0.70	3,080	78,700
17-Dec-99	1	10	0.70	143	78,700
21-Dec-99	2	2	0.97	6,670	15,700
21-Dec-99	2	4	0.97	2,550	15,700
21-Dec-99	2	6	0.97	125	15,700
21-Dec-99	2	8	0.97	1	15,700
21-Dec-99	2	10	0.97	<1	15,700
22-Dec-99	3	2	1.45	2,620	10,500
22-Dec-99	3	3	1.45	1,180	10,500
22-Dec-99	3	4	1.45	230	10,500
22-Dec-99	3	5	1.45	1	10,500
22-Dec-99	3	6	1.45	<1	10,500
23-Dec-99	4	2	0.98	72,600	159,000
23-Dec-99	4	4	0.98	13,400	159,000
23-Dec-99	4	6	0.98	541	159,000
23-Dec-99	4	8	0.98	<1	159,000
23-Dec-99	4	10	0.98	<1	159,000
30-Dec-99	5	2	1.64	4,690	86,600
30-Dec-99	5	3	1.64	535	86,600
30-Dec-99	5	4	1.64	13	86,600
30-Dec-99	5	5	1.64	3	86,600
30-Dec-99	5	6	1.64	<1	86,600
4-Jan-00	6	2	0.70	8,880	12,900
4-Jan-00	6	4	0.70	3,860	12,900
4-Jan-00	6	6	0.70	1,110	12,900
4-Jan-00	6	8	0.70	69	12,900
4-Jan-00	6	10	0.70	1	12,900
7-Jan-00	7	2	0.75	7,720	10,100
7-Jan-00	7	4	0.75	2,960	10,100
7-Jan-00	7	6	0.75	390	10,100
7-Jan-00	7	8	0.75	121	10,100
7-Jan-00	7	10	0.75	<1	10,100
14-Jan-00	8	2	1.46	1,100	6,950
14-Jan-00	8	3	1.46	234	6,950
14-Jan-00	8	4	1.46	54	6,950
14-Jan-00	8	5	1.46	7	6,950
14-Jan-00	8	6	1.46	1	6,950
18-Jan-00	9	2	0.93	28,700	64,100
18-Jan-00	9	4	0.93	4,030	64,100
18-Jan-00	9	6	0.93	99	64,100
18-Jan-00	9	8	0.93	17	64,100

(continued)

Table A.9: (continued)

Exp. Date	Exp. No	Time (min)	Monochl. Dose, C_a (mg/L)	$N_{Observed}$ (CFU/mL)	N_o (CFU/mL)
18-Jan-00	9	10	0.93	1	64,100
21-Jan-00	10	2	0.98	10,700	13,800
21-Jan-00	10	4	0.98	825	13,800
21-Jan-00	10	6	0.98	7	13,800
21-Jan-00	10	8	0.98	<1	13,800
21-Jan-00	10	10	0.98	<1	13,800
27-Jan-00	11	2	1.43	40,000	74,000
27-Jan-00	11	3	1.43	10,300	74,000
27-Jan-00	11	4	1.43	2,090	74,000
27-Jan-00	11	5	1.43	127	74,000
27-Jan-00	11	6	1.43	41	74,000
4-Feb-00	12	2	0.68	88,800	92,900
4-Feb-00	12	4	0.68	79,300	92,900
4-Feb-00	12	6	0.68	29,300	92,900
4-Feb-00	12	8	0.68	1,030	92,900
4-Feb-00	12	10	0.68	38	92,900
8-Feb-00	13	2	0.70	6,630	8,260
8-Feb-00	13	4	0.70	4,460	8,260
8-Feb-00	13	6	0.70	1,140	8,260
8-Feb-00	13	8	0.70	4	8,260
8-Feb-00	13	10	0.70	<1	8,260
16-Feb-00	14	2	0.76	7,570	7,790
16-Feb-00	14	4	0.76	5,520	7,790
16-Feb-00	14	6	0.76	3,820	7,790
16-Feb-00	14	8	0.76	1,320	7,790
16-Feb-00	14	10	0.76	324	7,790
17-Feb-00	15	2	1.39	31,800	55,400
17-Feb-00	15	3	1.39	12,700	55,400
17-Feb-00	15	4	1.39	3,030	55,400
17-Feb-00	15	5	1.39	564	55,400
17-Feb-00	15	6	1.39	97	55,400
21-Feb-00	16	2	0.74	4,800	6,170
21-Feb-00	16	4	0.74	3,810	6,170
21-Feb-00	16	6	0.74	1,780	6,170
21-Feb-00	16	8	0.74	547	6,170
21-Feb-00	16	10	0.74	104	6,170
23-Feb-00	17	2	1.54	37,200	97,900
23-Feb-00	17	3	1.54	15,900	97,900
23-Feb-00	17	4	1.54	1,770	97,900
23-Feb-00	17	5	1.54	22,500	97,900
23-Feb-00	17	6	1.54	12	97,900
28-Feb-00	18	2	1.08	2,940	3,720
28-Feb-00	18	4	1.08	2,160	3,720

(continued)

Table A.9: (continued)

Exp. Date	Exp. No	Time (min)	Monochl. Dose, C_a (mg/L)	$N_{Observed}$ (CFU/mL)	N_o (CFU/mL)
28-Feb-00	18	6	1.08	556	3,720
28-Feb-00	18	8	1.08	20	3,720
28-Feb-00	18	10	1.08	1	3,720
3-Mar-00	19	2	1.58	1,260	1,520
3-Mar-00	19	3	1.58	877	1,520
3-Mar-00	19	4	1.58	345	1,520
3-Mar-00	19	5	1.58	62	1,520
6-Mar-00	20	2	0.94	910	983
6-Mar-00	20	4	0.94	634	983
6-Mar-00	20	6	0.94	131	983
6-Mar-00	20	8	0.94	8	983
6-Mar-00	20	10	0.94	<1	983
8-Mar-00	21	2	0.71	1,000	1,020
8-Mar-00	21	4	0.71	679	1,020
8-Mar-00	21	6	0.71	474	1,020
8-Mar-00	21	8	0.71	125	1,020
8-Mar-00	21	10	0.71	46	1,020

Table A.10: Survival of *E. coli* at exponential growth phase in monochloramine experiments.

Exp. Date	Exp. No	Time (min)	Monochl. Dose, C_a (mg/L)	$N_{Observed}$ (CFU/mL)	N_o (CFU/mL)
20-Mar-02	1	1.00	0.94	8158	9,820
20-Mar-02	1	2.00	0.94	3838	9,820
20-Mar-02	1	3.50	0.94	85	9,820
20-Mar-02	1	5.50	0.94	<1	9,820
20-Mar-02	1	8.00	0.94	<1	9,820
20-Mar-02	2	1.00	0.94	9409	9,820
20-Mar-02	2	2.00	0.94	4242	9,820
20-Mar-02	2	3.50	0.94	140	9,820
20-Mar-02	2	5.50	0.94	<1	9,820
20-Mar-02	2	8.00	0.94	<1	9,820
23-Mar-02	3	1.00	1.44	56056	102,027
23-Mar-02	3	1.50	1.44	53535	102,027
23-Mar-02	3	2.00	1.44	5758	102,027
23-Mar-02	3	2.50	1.44	980	102,027
23-Mar-02	3	3.00	1.44	1222	102,027
23-Mar-02	4	1.00	1.44	81582	102,027
23-Mar-02	4	1.50	1.44	38889	102,027
23-Mar-02	4	2.00	1.44	35000	102,027
23-Mar-02	4	2.50	1.44	3111	102,027
23-Mar-02	4	3.00	1.44	100	102,027
25-Mar-02	5	2.00	0.75	9760	10,890
25-Mar-02	5	3.00	0.75	8058	10,890
25-Mar-02	5	4.00	0.75	5152	10,890
25-Mar-02	5	5.00	0.75	1485	10,890
25-Mar-02	5	6.00	0.75	242	10,890
25-Mar-02	6	2.00	0.75	10611	10,890
25-Mar-02	6	3.00	0.75	8609	10,890
25-Mar-02	6	4.00	0.75	5354	10,890
25-Mar-02	6	5.00	0.75	1884	10,890
25-Mar-02	6	6.00	0.75	143	10,890
27-Mar-02	7	1.50	0.97	113113	119,820
27-Mar-02	7	3.00	0.97	51010	119,820
27-Mar-02	7	4.00	0.97	12424	119,820
27-Mar-02	7	5.00	0.97	182	119,820
27-Mar-02	7	6.00	0.97	<1	119,820
27-Mar-02	8	1.50	0.97	110110	119,820
27-Mar-02	8	3.00	0.97	64647	119,820
27-Mar-02	8	5.00	0.97	5833	119,820
27-Mar-02	8	6.00	0.97	21	119,820
27-Mar-02	8	7.00	0.97	<1	119,820
29-Mar-02	9	1.50	1.42	651	1,059
29-Mar-02	9	2.50	1.42	177	1,059

(continued)

Table A.10: (continued)

Exp. Date	Exp. No	Time (min)	Monochl. Dose, C_a (mg/L)	$N_{Observed}$ (CFU/mL)	N_o (CFU/mL)
29-Mar-02	9	3.00	1.42	15	1,059
29-Mar-02	9	3.50	1.42	1	1,059
29-Mar-02	9	4.00	1.42	<1	1,059
29-Mar-02	10	1.50	1.42	631	1,059
29-Mar-02	10	2.50	1.42	67	1,059
29-Mar-02	10	3.00	1.42	19	1,059
29-Mar-02	10	3.50	1.42	<1	1,059
29-Mar-02	10	4.00	1.42	<1	1,059
30-Mar-02	11	2.00	0.69	976	973
30-Mar-02	11	4.00	0.69	702	973
30-Mar-02	11	5.00	0.69	444	973
30-Mar-02	11	6.00	0.69	354	973
30-Mar-02	11	7.00	0.69	100	973
30-Mar-02	12	2.00	0.69	1036	973
30-Mar-02	12	4.00	0.69	682	973
30-Mar-02	12	5.00	0.69	576	973
30-Mar-02	12	6.00	0.69	268	973
30-Mar-02	12	7.00	0.69	95	973
31-Mar-02	13	1.50	1.39	10811	13,435
31-Mar-02	13	2.50	1.39	10110	13,435
31-Mar-02	13	3.00	1.39	7879	13,435
31-Mar-02	13	3.50	1.39	5222	13,435
31-Mar-02	13	4.00	1.39	1172	13,435
31-Mar-02	14	1.50	1.39	12262	13,435
31-Mar-02	14	2.50	1.39	9409	13,435
31-Mar-02	14	3.00	1.39	9849	13,435
31-Mar-02	14	3.50	1.39	3778	13,435
31-Mar-02	14	4.00	1.39	712	13,435
1-Apr-02	15	2.17	0.74	118619	136,712
1-Apr-02	15	4.00	0.74	99600	136,712
1-Apr-02	15	6.00	0.74	7407	136,712
1-Apr-02	15	7.00	0.74	476	136,712
1-Apr-02	15	8.00	0.74	13	136,712
1-Apr-02	16	2.00	0.74	128629	136,712
1-Apr-02	16	4.00	0.74	92593	136,712
1-Apr-02	16	7.00	0.74	2323	136,712
1-Apr-02	16	8.00	0.74	58	136,712
2-Apr-02	17	1.50	0.94	796	1,087
2-Apr-02	17	3.00	0.94	175	1,087
2-Apr-02	17	4.00	0.94	30	1,087
2-Apr-02	17	5.00	0.94	1	1,087
2-Apr-02	17	6.00	0.94	<1	1,087
2-Apr-02	18	1.50	0.94	996	1,087

(continued)

Table A.10: (continued)

Exp. Date	Exp. No	Time (min)	Monochl. Dose, C_a (mg/L)	$N_{Observed}$ (CFU/mL)	N_o (CFU/mL)
2-Apr-02	18	3.00	0.94	340	1,087
2-Apr-02	18	4.00	0.94	46	1,087
2-Apr-02	18	5.00	0.94	1	1,087
2-Apr-02	18	6.00	0.94	<1	1,087
4-Apr-02	19	2.17	0.72	11762	12,162
4-Apr-02	19	4.00	0.72	5806	12,162
4-Apr-02	19	6.00	0.72	135	12,162
4-Apr-02	19	7.00	0.72	6	12,162
4-Apr-02	19	8.00	0.72	1	12,162
4-Apr-02	20	2.17	0.72	12312	12,162
4-Apr-02	20	4.00	0.72	8759	12,162
4-Apr-02	20	6.00	0.72	596	12,162
4-Apr-02	20	7.00	0.72	34	12,162
4-Apr-02	20	8.00	0.72	1	12,162
5-Apr-02	21	2.00	0.96	69570	92,793
5-Apr-02	21	3.00	0.96	45546	92,793
5-Apr-02	21	4.00	0.96	12212	92,793
5-Apr-02	21	5.00	0.96	2121	92,793
5-Apr-02	21	6.00	0.96	48	92,793
5-Apr-02	22	2.00	0.96	85586	92,793
5-Apr-02	22	3.00	0.96	62563	92,793
5-Apr-02	22	4.00	0.96	11411	92,793
5-Apr-02	22	5.00	0.96	3788	92,793
5-Apr-02	22	6.00	0.96	117	92,793
6-Apr-02	23	1.50	1.45	295	837
6-Apr-02	23	2.00	1.45	115	837
6-Apr-02	23	2.50	1.45	17	837
6-Apr-02	23	3.00	1.45	1	837
6-Apr-02	23	3.50	1.45	<1	837
6-Apr-02	24	1.50	1.45	461	837
6-Apr-02	24	2.00	1.45	150	837
6-Apr-02	24	2.50	1.45	20	837
6-Apr-02	24	3.00	1.45	2	837
6-Apr-02	24	3.50	1.45	<1	837

Table A.11: Survival of *E. coli* in DMS in monochloramine experiments.

Exp. Date	Exp. No	Time (min)	Monochl. Dose, C_a (mg/L)	$N_{Observed}$ (CFU/mL)	N_o (CFU/mL)
28-Jan-02	501	2.0	1.00	5155	10,901
28-Jan-02	501	4.0	1.00	310	10,901
28-Jan-02	501	6.0	1.00	1	10,901*
28-Jan-02	501	8.0	1.00	<1	10,901
28-Jan-02	501	10.0	1.00	<1	10,901
28-Jan-02	502	2.0	1.00	5155	10,901
28-Jan-02	502	4.0	1.00	516	10,901
28-Jan-02	502	6.0	1.00	2	10,901*
28-Jan-02	502	8.0	1.00	<1	10,901
28-Jan-02	502	10.0	1.00	<1	10,901
4-Feb-02	503	2.0	0.73	881	1,261
4-Feb-02	503	4.0	0.73	801	1,261
4-Feb-02	503	6.0	0.73	202	1,261
4-Feb-02	503	8.0	0.73	17	1,261
4-Feb-02	503	10.0	0.73	<1	1,261
4-Feb-02	504	2.0	0.73	1036	1,261
4-Feb-02	504	4.0	0.73	976	1,261
4-Feb-02	504	6.0	0.73	384	1,261
4-Feb-02	504	8.0	0.73	38	1,261
4-Feb-02	504	10.0	0.73	<1	1,261
7-Feb-02	505	2.0	1.42	94094	149,662
7-Feb-02	505	3.0	1.42	41414	149,662
7-Feb-02	505	4.0	1.42	4647	149,662
7-Feb-02	505	5.0	1.42	283	149,662
7-Feb-02	505	6.0	1.42	11	149,662*
7-Feb-02	506	2.0	1.42	80581	149,662
7-Feb-02	506	3.0	1.42	48485	149,662
7-Feb-02	506	4.0	1.42	7172	149,662
7-Feb-02	506	5.0	1.42	404	149,662
7-Feb-02	506	6.0	1.42	2	149,662*
12-Feb-02	507	2.0	0.98	23524	118,243
12-Feb-02	507	4.0	0.98	2002	118,243
12-Feb-02	507	6.0	0.98	<1	118,243
12-Feb-02	507	8.0	0.98	<1	118,243
12-Feb-02	507	10.0	0.98	<1	118,243
12-Feb-02	508	2.0	0.98	38038	118,243
12-Feb-02	508	4.0	0.98	3504	118,243
12-Feb-02	508	6.0	0.98	<1	118,243
12-Feb-02	508	8.0	0.98	<1	118,243
12-Feb-02	508	10.0	0.98	<1	118,243

(continued)

* Possible outlier observations

Table A.11: (continued)

Exp. Date	Exp. No	Time (min)	Monochl. Dose, C_a (mg/L)	$N_{Observed}$ (CFU/mL)	N_o (CFU/mL)
14-Feb-02	509	2.0	0.75	9760	10,980
14-Feb-02	509	4.0	0.75	4455	10,980
14-Feb-02	509	6.0	0.75	886	10,980
14-Feb-02	509	8.0	0.75	42	10,980
14-Feb-02	509	10.0	0.75	10	10,980
14-Feb-02	510	2.0	0.75	7374	10,980
14-Feb-02	510	4.0	0.75	5906	10,980
14-Feb-02	510	6.0	0.75	1962	10,980
14-Feb-02	510	8.0	0.75	168	10,980
14-Feb-02	510	10.0	0.75	33	10,980
15-Feb-02	511	2.0	0.97	280	962
15-Feb-02	511	4.0	0.97	5	962
15-Feb-02	511	6.0	0.97	<1	962
15-Feb-02	511	8.0	0.97	<1	962
15-Feb-02	511	10.0	0.97	<1	962
15-Feb-02	512	2.0	0.97	185	962
15-Feb-02	512	4.0	0.97	10	962
15-Feb-02	512	6.0	0.97	<1	962
15-Feb-02	512	8.0	0.97	<1	962
15-Feb-02	512	10.0	0.97	<1	962
16-Feb-02	513	2.0	1.43	10	1,310
16-Feb-02	513	3.0	1.43	20	1,310
16-Feb-02	513	4.0	1.43	<1	1,310
16-Feb-02	513	5.0	1.43	<1	1,310
16-Feb-02	513	6.0	1.43	<1	1,310
16-Feb-02	514	2.0	1.43	185	1,310
16-Feb-02	514	3.0	1.43	5	1,310
16-Feb-02	514	4.0	1.43	<1	1,310
16-Feb-02	514	5.0	1.43	<1	1,310
16-Feb-02	514	6.0	1.43	<1	1,310
5-Sep-02	515	2.0	0.93	14014	16,318
5-Sep-02	515	3.0	0.93	11712	16,318
5-Sep-02	515	4.0	0.93	9141	16,318
5-Sep-02	515	5.0	0.93	8182	16,318
5-Sep-02	515	6.0	0.93	7167	16,318
5-Sep-02	516	2.0	0.93	13514	16,318
5-Sep-02	516	3.0	0.93	13113	16,318
5-Sep-02	516	4.0	0.93	9242	16,318
5-Sep-02	516	5.0	0.93	9495	16,318
6-Sep-02	517	2.0	0.69	100601	117,005
6-Sep-02	517	4.0	0.69	81582	117,005
5-Sep-02	516	6.0	0.93	5056	16,318

(continued)

Table A.11: (continued)

Exp. Date	Exp. No	Time (min)	Monochl. Dose, C_a (mg/L)	$N_{Observed}$ (CFU/mL)	N_o (CFU/mL)
6-Sep-02	517	6.0	0.69	64647	117,005
6-Sep-02	517	8.0	0.69	23889	117,005
6-Sep-02	517	10.0	0.69	4611	117,005
6-Sep-02	518	2.0	0.69	87588	117,005
6-Sep-02	518	4.0	0.69	76577	117,005
6-Sep-02	518	6.0	0.69	38889	117,005
6-Sep-02	518	8.0	0.69	28333	117,005
6-Sep-02	518	10.0	0.69	4556	117,005
11-Sep-02	519	2.0	1.44	7508	12,579
11-Sep-02	519	3.0	1.44	3353	12,579
11-Sep-02	519	4.0	1.44	2117	12,579
11-Sep-02	519	5.0	1.44	540	12,579
11-Sep-02	519	6.0	1.44	77	12,579
11-Sep-02	520	2.0	1.44	7758	12,579
11-Sep-02	520	3.0	1.44	3687	12,579
11-Sep-02	520	4.0	1.44	970	12,579
11-Sep-02	520	5.0	1.44	172	12,579
11-Sep-02	520	6.0	1.44	970	12,579
13-Sep-02	521	2.0	1.44	71071	126,914
13-Sep-02	521	3.0	1.44	65065	126,914
13-Sep-02	521	4.0	1.44	44444	126,914
13-Sep-02	521	5.0	1.44	21768	126,914
13-Sep-02	521	6.0	1.44	5611	126,914
13-Sep-02	522	2.0	1.44	73574	126,914
13-Sep-02	522	3.0	1.44	67067	126,914
13-Sep-02	522	4.0	1.44	61616	126,914
13-Sep-02	522	5.0	1.44	28889	126,914
13-Sep-02	522	6.0	1.44	61616	126,914
15-Sep-02	523	2.0	0.80	12162	12,061
15-Sep-02	523	4.0	0.80	5355	12,061
15-Sep-02	523	6.0	0.80	6010	12,061
15-Sep-02	523	8.0	0.80	3778	12,061
15-Sep-02	523	10.0	0.80	1828	12,061
15-Sep-02	524	2.0	0.80	8659	12,061
15-Sep-02	524	4.0	0.80	7057	12,061
15-Sep-02	524	6.0	0.80	6566	12,061
15-Sep-02	524	8.0	0.80	3611	12,061
15-Sep-02	524	10.0	0.80	6566	12,061

Table A.12: Survival of *E. coli* DMS control in monochloramine experiments.

Exp. Date	Exp. No	Time (min)	Monochl. Dose, C_a (mg/L)	$N_{Observed}$ (CFU/mL)	N_o (CFU/mL)
28-Jan-02	601	2	1.00	5706	10,901
28-Jan-02	601	4	1.00	1206	10,901
28-Jan-02	601	6	1.00	2	10,901
28-Jan-02	601	8	1.00	1	10,901
28-Jan-02	601	10	1.00	<1	10,901
4-Feb-02	603	2	0.73	1076	1,261
4-Feb-02	603	4	0.73	796	1,261
4-Feb-02	603	6	0.73	263	1,261
4-Feb-02	603	8	0.73	6	1,261
4-Feb-02	603	10	0.73	<1	1,261
7-Feb-02	605	2	1.42	98098	149,662
7-Feb-02	605	3	1.42	83333	149,662
7-Feb-02	605	4	1.42	17273	149,662
7-Feb-02	605	5	1.42	991	149,662
7-Feb-02	605	6	1.42	13	149,662
12-Feb-02	607	2	0.98	41041	118,243
12-Feb-02	607	4	0.98	2002	118,243
12-Feb-02	607	6	0.98	<1	118,243
12-Feb-02	607	8	0.98	<1	118,243
12-Feb-02	607	10	0.98	<1	118,243
14-Feb-02	609	2	0.75	6857	10,980
14-Feb-02	609	4	0.75	5456	10,980
14-Feb-02	609	6	0.75	1492	10,980
14-Feb-02	609	8	0.75	104	10,980
14-Feb-02	609	10	0.75	5	10,980
15-Feb-02	613	2	1.43	30	1,310
15-Feb-02	613	3	1.43	<1	1,310
15-Feb-02	613	4	1.43	<1	1,310
15-Feb-02	613	5	1.43	<1	1,310
15-Feb-02	613	6	1.43	<1	1,310
16-Feb-02	615	2	0.93	10811	16,318
16-Feb-02	615	3	0.93	9460	16,318
16-Feb-02	615	4	0.93	7879	16,318
16-Feb-02	615	5	0.93	3384	16,318
16-Feb-02	615	6	0.93	1571	16,318
5-Sep-02	617	2	0.69	104605	117,005
5-Sep-02	617	4	0.69	79079	117,005
5-Sep-02	617	6	0.69	34343	117,005
5-Sep-02	617	8	0.69	3131	117,005
5-Sep-02	617	10	0.69	121	117,005
6-Sep-02	619	3	1.44	4655	12,579
6-Sep-02	619	4	1.44	1527	12,579
6-Sep-02	619	5	1.44	409	12,579
6-Sep-02	619	6	1.44	41	12,579

(continued)

Table A.12: (continued)

Exp. Date	Exp. No	Time (min)	Monochl. Dose, C_a (mg/L)	$N_{Observed}$ (CFU/mL)	N_o (CFU/mL)
6-Sep-02	619	2	1.44	7508	12,579
11-Sep-02	621	2	1.44	72072	126,914
11-Sep-02	621	3	1.44	47548	126,914
11-Sep-02	621	4	1.44	20707	126,914
11-Sep-02	621	5	1.44	5859	126,914
11-Sep-02	621	6	1.44	601	126,914
13-Sep-02	623	2	0.80	9460	12,061
13-Sep-02	623	4	0.80	6206	12,061
13-Sep-02	623	6	0.80	2626	12,061
13-Sep-02	623	8	0.80	3444	12,061
13-Sep-02	623	10	0.80	702	12,061

Table A.13: Survival of continuous cultures of E. coli in monochloramine experiments.

Exp. Date	Exp. No	Time (min)	Monochl. Dose, C_a (mg/L)	$N_{Observed}$ (CFU/mL)	N_o (CFU/mL)
2-Aug-02	201	2.0	1.00	551	2,241
2-Aug-02	201	4.0	1.00	100	2,241
2-Aug-02	201	6.0	1.00	10	2,241
2-Aug-02	201	8.0	1.00	1	2,241
2-Aug-02	201	10.0	1.00	<1	2,241
2-Aug-02	202	2.0	1.00	701	2,241
2-Aug-02	202	4.0	1.00	200	2,241
2-Aug-02	202	6.0	1.00	5	2,241
2-Aug-02	202	8.0	1.00	1	2,241
2-Aug-02	202	10.0	1.00	<1	2,241
3-Aug-02	203	2.0	1.46	501	26,914
3-Aug-02	203	3.5	1.46	10	26,914
3-Aug-02	203	5.0	1.46	<1	26,914
3-Aug-02	203	6.3	1.46	<1	26,914
3-Aug-02	203	7.0	1.46	<1	26,914
3-Aug-02	204	2.0	1.46	1502	26,914
3-Aug-02	204	3.5	1.46	30	26,914
3-Aug-02	204	5.0	1.46	<1	26,914
3-Aug-02	204	6.0	1.46	<1	26,914
3-Aug-02	204	7.0	1.46	<1	26,914
4-Aug-02	205	2.0	0.78	90	207
4-Aug-02	205	4.0	0.78	45	207
4-Aug-02	205	6.0	0.78	<1	207
4-Aug-02	205	8.0	0.78	<1	207
4-Aug-02	205	10.0	0.78	<1	207
4-Aug-02	206	2.0	0.78	80	207
4-Aug-02	206	4.0	0.78	30	207
4-Aug-02	206	6.0	0.78	10	207
4-Aug-02	206	8.0	0.78	1	207
4-Aug-02	206	10.0	0.78	<1	207
6-Aug-02	207	2.0	1.00	59059	103,829
6-Aug-02	207	4.0	1.00	11662	103,829
6-Aug-02	207	6.0	1.00	756	103,829
6-Aug-02	207	8.0	1.00	35	103,829
6-Aug-02	207	10.0	1.00	1	103,829
6-Aug-02	208	2.0	1.00	69069	103,829
6-Aug-02	208	4.0	1.00	11161	103,829
6-Aug-02	208	6.0	1.00	596	103,829
6-Aug-02	208	8.0	1.00	30	103,829
6-Aug-02	208	10.0	1.00	<1	103,829
7-Aug-02	209	1.0	1.47	456	904
7-Aug-02	209	3.0	1.47	11	904

(continued)

Table A.13: (continued)

Exp. Date	Exp. No	Time (min)	Monochl. Dose, C_a (mg/L)	$N_{Observed}$ (CFU/mL)	N_o (CFU/mL))
7-Aug-02	209	2.0	1.47	96	904
7-Aug-02	209	4.0	1.47	1	904
7-Aug-02	209	5.0	1.47	<1	904
7-Aug-02	210	1.0	1.47	536	904
7-Aug-02	210	2.0	1.47	98	904
7-Aug-02	210	3.0	1.47	6	904
7-Aug-02	210	4.0	1.47	1	904
7-Aug-02	210	5.0	1.47	<1	904
8-Aug-02	211	2.0	0.75	4004	9,730
8-Aug-02	211	4.0	0.75	1452	9,730
8-Aug-02	211	6.0	0.75	95	9,730
8-Aug-02	211	8.0	0.75	4	9,730
8-Aug-02	211	10.0	0.75	<1	9,730
8-Aug-02	212	2.0	0.75	3904	9,730
8-Aug-02	212	4.0	0.75	1301	9,730
8-Aug-02	212	6.0	0.75	90	9,730
8-Aug-02	212	8.0	0.75	5	9,730
8-Aug-02	212	10.0	0.75	1	9,730
10-Aug-02	213	2.0	1.43	1502	9,550
10-Aug-02	213	3.0	1.43	415	9,550
10-Aug-02	213	4.0	1.43	20	9,550
10-Aug-02	213	5.0	1.43	3	9,550
10-Aug-02	213	6.0	1.43	<1	9,550
10-Aug-02	214	2.0	1.43	1752	9,550
10-Aug-02	214	3.0	1.43	440	9,550
10-Aug-02	214	4.0	1.43	35	9,550
10-Aug-02	214	5.0	1.43	3	9,550
10-Aug-02	214	6.0	1.43	<1	9,550
11-Aug-02	215	2.0	0.97	310	1,139
11-Aug-02	215	4.0	0.97	17	1,139
11-Aug-02	215	6.0	0.97	<1	1,139
11-Aug-02	215	7.0	0.97	<1	1,139
11-Aug-02	215	8.0	0.97	<1	1,139
11-Aug-02	216	2.0	0.97	370	1,139
11-Aug-02	216	4.0	0.97	38	1,139
11-Aug-02	216	6.0	0.97	<1	1,139
11-Aug-02	216	7.0	0.97	<1	1,139
11-Aug-02	216	8.0	0.97	<1	1,139
13-Aug-02	217	2.0	0.74	45455	117,568
13-Aug-02	217	4.0	0.74	18168	117,568
13-Aug-02	217	6.0	0.74	3838	117,568
13-Aug-02	217	8.0	0.74	160	117,568
13-Aug-02	217	10.0	0.74	2	117,568
13-Aug-02	218	2.0	0.74	55556	117,568

(continued)

Table A.13: (continued)

Exp. Date	Exp. No	Time (min)	Monochl. Dose, C_a (mg/L)	$N_{Observed}$ (CFU/mL)	N_o (CFU/mL)
13-Aug-02	218	4.0	0.74	22422	117,568
13-Aug-02	218	6.0	0.74	3434	117,568
13-Aug-02	218	8.0	0.74	99	117,568
13-Aug-02	218	10.0	0.74	1	117,568
14-Aug-02	219	2.0	1.43	12012	102,477
14-Aug-02	219	4.0	1.43	165	102,477
14-Aug-02	219	5.0	1.43	3	102,477
14-Aug-02	219	6.0	1.43	<1	102,477
14-Aug-02	220	2.0	1.43	7508	102,477
14-Aug-02	220	3.0	1.43	1552	102,477
14-Aug-02	220	4.0	1.43	235	102,477
14-Aug-02	220	5.0	1.43	4	102,477
14-Aug-02	220	6.0	1.43	1	102,477
16-Aug-02	221	2.0	0.93	5656	10,541
16-Aug-02	221	4.0	0.93	1907	10,541
16-Aug-02	221	6.0	0.93	434	10,541
16-Aug-02	221	7.0	0.93	118	10,541
16-Aug-02	221	8.0	0.93	13	10,541
16-Aug-02	222	2.0	0.93	5806	10,541
16-Aug-02	222	4.0	0.93	2117	10,541
16-Aug-02	222	6.0	0.93	490	10,541
16-Aug-02	222	7.0	0.93	258	10,541
16-Aug-02	222	8.0	0.93	22	10,541
17-Aug-02	223	2.0	0.78	696	1,061
17-Aug-02	223	4.0	0.78	230	1,061
17-Aug-02	223	7.0	0.78	42	1,061
17-Aug-02	223	8.0	0.78	10	1,061
17-Aug-02	224	2.0	0.78	651	1,061
17-Aug-02	224	4.0	0.78	355	1,061
17-Aug-02	224	7.0	0.78	55	1,061
17-Aug-02	224	8.0	0.78	18	1,061

Table A.14: Survival of *B. subtilis* spore in ozone experiments.

Exp. Date	Exp. No	Time (min)	Ozone Dose, C_a (mg/L)	$N_{Observed}$ (CFU/mL)	N_o (CFU/mL)
10-Sep-01	1	1.0	1.5	20020	26,351
10-Sep-01	1	2.0	1.5	16016	26,351
10-Sep-01	1	4.0	1.5	5856	26,351
10-Sep-01	1	7.0	1.5	745	26,351
10-Sep-01	1	10.5	1.5	40	26,351
10-Sep-01	1	15.0	1.5	2	26,351
10-Sep-01	2	1.0	1.5	21522	26,351
10-Sep-01	2	2.0	1.5	15516	26,351
10-Sep-01	2	4.0	1.5	6857	26,351
10-Sep-01	2	7.0	1.5	265	26,351
10-Sep-01	2	10.0	1.5	5	26,351
10-Sep-01	2	15.0	1.5	<1	26,351
15-Sep-01	3	0.5	2.5	7851	8,446
15-Sep-01	3	1.5	2.5	7307	8,446
15-Sep-01	3	2.0	2.5	8509	8,446
15-Sep-01	3	3.0	2.5	5305	8,446
15-Sep-01	3	5.0	2.5	2121	8,446
15-Sep-01	4	0.5	2.5	9851	8,446
15-Sep-01	4	1.0	2.5	8809	8,446
15-Sep-01	4	2.2	2.5	6907	8,446
15-Sep-01	4	3.0	2.5	4905	8,446
15-Sep-01	4	5.0	2.5	2929	8,446
17-Sep-01	5	1.1	2.5	73073	112,725
17-Sep-01	5	2.3	2.5	53053	112,725
17-Sep-01	5	4.0	2.5	8509	112,725
17-Sep-01	5	6.0	2.5	200	112,725
17-Sep-01	5	8.0	2.5	50	112,725
17-Sep-01	5	12.0	2.5	25	112,725
17-Sep-01	6	1.0	2.5	72573	112,725
17-Sep-01	6	2.7	2.5	32533	112,725
17-Sep-01	6	4.0	2.5	5005	112,725
17-Sep-01	6	6.0	2.5	200	112,725
17-Sep-01	6	8.0	2.5	50	112,725
17-Sep-01	6	12.0	2.5	<1	112,725
21-Sep-01	7	0.5	2.0	4154	4,257
21-Sep-01	7	1.0	2.0	3804	4,257
21-Sep-01	7	2.0	2.0	2273	4,257
21-Sep-01	7	3.0	2.0	1462	4,257
21-Sep-01	7	5.0	2.0	90	4,257
21-Sep-01	7	8.0	2.0	1	4,257
21-Sep-01	8	0.5	2.0	4004	4,257
21-Sep-01	8	1.0	2.0	3804	4,257
21-Sep-01	8	2.0	2.0	2576	4,257
21-Sep-01	8	5.0	2.0	91	4,257

(continued)

Table A.14: (continued)

Exp. Date	Exp. No	Time (min)	Ozone Dose, C_a (mg/L)	$N_{Observed}$ (CFU/mL)	N_o (CFU/mL)
21-Sep-01	8	3.0	2.0	1321	4,257
21-Sep-01	8	8.0	2.0	2	4,257
24-Sep-01	9	0.5	2.5	786	874
24-Sep-01	9	1.0	2.5	616	874
24-Sep-01	9	1.5	2.5	511	874
24-Sep-01	9	2.0	2.5	323	874
24-Sep-01	9	3.0	2.5	87	874
24-Sep-01	9	5.0	2.5	1	874
24-Sep-01	10	0.5	2.5	841	874
24-Sep-01	10	1.0	2.5	726	874
24-Sep-01	10	1.5	2.5	641	874
24-Sep-01	10	2.0	2.5	434	874
24-Sep-01	10	3.0	2.5	202	874
24-Sep-01	10	5.0	2.5	6	874
26-Oct-01	11	1.0	2.0	4254	6,498
26-Oct-01	11	2.0	2.0	1902	6,498
26-Oct-01	11	4.0	2.0	<1	6,498
26-Oct-01	11	6.0	2.0	1	6,498
26-Oct-01	11	8.0	2.0	1	6,498
26-Oct-01	11	12.0	2.0	1	6,498
26-Oct-01	12	1.0	2.0	4404	6,498
26-Oct-01	12	2.0	2.0	2553	6,498
26-Oct-01	12	4.0	2.0	120	6,498
26-Oct-01	12	6.0	2.0	3	6,498
26-Oct-01	12	8.0	2.0	1	6,498
26-Oct-01	12	12.0	2.0	2	6,498
27-Oct-01	13	1.0	1.5	57057	70,495
27-Oct-01	13	2.0	1.5	40040	70,495
27-Oct-01	13	4.0	1.5	24748	70,495
27-Oct-01	13	7.0	1.5	2778	70,495
27-Oct-01	13	12.0	1.5	137	70,495
27-Oct-01	14	1.0	1.5	67067	70,495
27-Oct-01	14	2.0	1.5	51552	70,495
27-Oct-01	14	4.0	1.5	20020	70,495
27-Oct-01	14	7.0	1.5	6607	70,495
27-Oct-01	14	12.0	1.5	501	70,495
28-Oct-01	15	1.0	2.0	766	1,096
28-Oct-01	15	2.0	2.0	390	1,096
28-Oct-01	15	4.0	2.0	38	1,096
28-Oct-01	15	6.0	2.0	1	1,096
28-Oct-01	15	8.0	2.0	<1	1,096
28-Oct-01	15	10.0	2.0	1	1,096
28-Oct-01	16	1.0	2.0	851	1,096

(continued)

Table A.14: (continued)

Exp. Date	Exp. No	Time (min)	Ozone Dose, C_a (mg/L)	$N_{Observed}$ (CFU/mL)	N_o (CFU/mL)
28-Oct-01	16	2.0	2.0	521	1,096
28-Oct-01	16	4.0	2.0	73	1,096
28-Oct-01	16	6.0	2.0	5	1,096
28-Oct-01	16	8.0	2.0	1	1,096
28-Oct-01	16	10.0	2.0	1	1,096
30-Oct-01	17	0.5	2.5	1036	1,197
30-Oct-01	17	1.0	2.5	731	1,197
30-Oct-01	17	2.0	2.5	265	1,197
30-Oct-01	17	3.5	2.5	1	1,197
30-Oct-01	17	6.0	2.5	<1	1,197
30-Oct-01	18	0.5	2.5	1066	1,197
30-Oct-01	18	1.0	2.5	901	1,197
30-Oct-01	18	2.0	2.5	395	1,197
30-Oct-01	18	3.5	2.5	24	1,197
30-Oct-01	18	6.0	2.5	1	1,197
31-Oct-01	19	1.0	2.0	42042	63,514
31-Oct-01	19	2.0	2.0	1552	63,514
31-Oct-01	19	4.0	2.0	300	63,514
31-Oct-01	19	6.0	2.0	10	63,514
31-Oct-01	19	8.0	2.0	1	63,514
31-Oct-01	19	12.0	2.0	<1	63,514
31-Oct-01	20	1.0	2.0	40040	63,514
31-Oct-01	20	2.0	2.0	32533	63,514
31-Oct-01	20	4.0	2.0	5806	63,514
31-Oct-01	20	6.0	2.0	501	63,514
31-Oct-01	20	8.0	2.0	85	63,514
31-Oct-01	20	12.0	2.0	9	63,514
2-Nov-01	21	1.0	1.5	104605	107,207
2-Nov-01	21	2.0	1.5	77077	107,207
2-Nov-01	21	4.0	1.5	26263	107,207
2-Nov-01	21	7.0	1.5	701	107,207
2-Nov-01	21	12.0	1.5	21	107,207
2-Nov-01	22	1.0	1.5	84585	107,207
2-Nov-01	22	2.0	1.5	81081	107,207
2-Nov-01	22	4.0	1.5	52525	107,207
2-Nov-01	22	7.0	1.5	5051	107,207
2-Nov-01	22	12.0	1.5	596	107,207
4-Nov-01	23	1.0	1.5	996	1,197
4-Nov-01	23	3.0	1.5	345	1,197
4-Nov-01	23	5.0	1.5	7	1,197
4-Nov-01	23	8.0	1.5	<1	1,197
4-Nov-01	23	12.0	1.5	<1	1,197
4-Nov-01	24	1.0	1.5	1,046	1,197

(continued)

Table A.14: (continued)

Exp. Date	Exp. No	Time (min)	Ozone Dose, C_a (mg/L)	$N_{Observed}$ (CFU/mL)	N_o (CFU/mL)
4-Nov-01	24	3.0	1.5	495	1,197
4-Nov-01	24	5.0	1.5	37	1,197
4-Nov-01	24	8.0	1.5	<1	1,197
4-Nov-01	24	12.0	1.5	<1	1,197

Table A.15: Survival of exponential growth phase *B. subtilis* in monochloramine experiments.

Exp. Date	Exp. No	Time (min)	Monochl. Dose, C_a (mg/L)	$N_{Observed}$ (CFU/mL)	N_o (CFU/mL)
4-May-02	401	3.0	1.47	1,802	4,336
4-May-02	401	6.0	1.47	1,006	4,336
4-May-02	401	10.0	1.47	61	4,336
4-May-02	401	15.0	1.47	27	4,336
4-May-02	401	25.0	1.47	27	4,336
4-May-02	402	3.0	1.47	1,051	4,336
4-May-02	402	6.0	1.47	966	4,336
4-May-02	402	10.0	1.47	112	4,336
4-May-02	402	15.0	1.47	37	4,336
4-May-02	402	25.0	1.47	30	4,336
6-May-02	403	5.0	1.03	3,303	5,923
6-May-02	403	10.0	1.03	2,307	5,923
6-May-02	403	15.0	1.03	510	5,923
6-May-02	403	20.0	1.03	131	5,923
6-May-02	403	35.0	1.03	31	5,923
6-May-02	404	5.0	1.03	4,855	5,923
6-May-02	404	10.0	1.03	1,421	5,923
6-May-02	404	15.0	1.03	202	5,923
6-May-02	404	20.0	1.03	52	5,923
6-May-02	404	35.0	1.03	35	5,923
7-May-02	405	5.0	0.78	6,206	9,685
7-May-02	405	10.0	0.78	2,980	9,685
7-May-02	405	15.0	0.78	1,186	9,685
7-May-02	405	25.0	0.78	134	9,685
7-May-02	405	40.0	0.78	18	9,685
7-May-02	406	5.0	0.78	3,253	9,685
7-May-02	406	10.0	0.78	2,424	9,685
7-May-02	406	15.0	0.78	1,006	9,685
7-May-02	406	25.0	0.78	143	9,685
7-May-02	406	40.0	0.78	21	9,685
9-May-02	407	3.0	1.48	250	749
9-May-02	407	6.0	1.48	115	749
9-May-02	407	10.0	1.48	23	749
9-May-02	407	15.0	1.48	9	749
9-May-02	407	25.0	1.48	10	749
9-May-02	408	3.0	1.48	255	749
9-May-02	408	6.0	1.48	220	749
9-May-02	408	10.0	1.48	56	749
9-May-02	408	15.0	1.48	12	749
9-May-02	408	25.0	1.48	4	749
10-May-02	409	5.0	0.98	576	1,527
10-May-02	409	10.0	0.98	130	1,527

(continued)

Table A.15: (continued)

Exp. Date	Exp. No	Time (min)	Monochl. Dose, C_a (mg/L)	$N_{Observed}$ (CFU/mL)	N_o (CFU/mL)
10-May-02	409	15.0	0.98	31	1,527
10-May-02	409	25.0	0.98	30	1,527
10-May-02	409	40.0	0.98	33	1,527
10-May-02	410	5.0	0.98	566	1,527
10-May-02	410	10.0	0.98	275	1,527
10-May-02	410	15.0	0.98	52	1,527
10-May-02	410	25.0	0.98	24	1,527
10-May-02	410	40.0	0.98	28	1,527
13-May-02	411	5.0	0.97	25	3,863*
13-May-02	411	10.3	0.97	<1	3,863
13-May-02	411	15.0	0.97	2	3,863*
13-May-02	411	25.0	0.97	8	3,863
13-May-02	411	40.0	0.97	10	3,863
13-May-02	412	5.0	0.97	45	3,863*
13-May-02	412	10.0	0.97	5	3,863*
13-May-02	412	15.0	0.97	3	3,863*
13-May-02	412	25.0	0.97	5	3,863
13-May-02	412	40.0	0.97	8	3,863
14-May-02	413	3.0	1.43	80	472
14-May-02	413	6.0	1.43	30	472
14-May-02	413	10.0	1.43	20	472
14-May-02	413	15.0	1.43	12	472
14-May-02	413	25.0	1.43	13	472
14-May-02	414	3.0	1.43	145	472
14-May-02	414	6.0	1.43	35	472
14-May-02	414	10.0	1.43	13	472
14-May-02	414	15.0	1.43	14	472
14-May-02	414	25.0	1.43	19	472
18-May-02	415	5.0	0.78	320	1,654
18-May-02	415	10.0	0.78	162	1,654
18-May-02	415	15.0	0.78	14	1,654
18-May-02	415	25.0	0.78	7	1,654
18-May-02	415	45.0	0.78	8	1,654
18-May-02	416	5.0	0.78	350	1,654
18-May-02	416	10.0	0.78	94	1,654
18-May-02	416	15.0	0.78	12	1,654
18-May-02	416	25.0	0.78	13	1,654
18-May-02	416	45.0	0.78	12	1,654

(continued)

* Possible outlier observations

Table A.15: (continued)

Exp. Date	Exp. No	Time (min)	Monochl. Dose, C_a (mg/L)	$N_{Observed}$ (CFU/mL)	N_o (CFU/mL)
20-May-02	417	5.0	0.71	1502	4,167
20-May-02	417	10.0	0.71	981	4,167
20-May-02	417	15.0	0.71	510	4,167
20-May-02	417	25.0	0.71	20	4,167
20-May-02	417	45.0	0.71	11	4,167
20-May-02	418	5.0	0.71	1952	4,167
20-May-02	418	10.0	0.71	931	4,167
20-May-02	418	15.0	0.71	253	4,167
20-May-02	418	25.0	0.71	14	4,167
20-May-02	418	45.0	0.71	12	4,167

APPENDIX B: INSTANTANEOUS DISINFECTANT DEMAND AND DECAY CONSTANTS FITTED TO EXPERIMENTAL DATA

Table B.1: Instantaneous ozone demand and decay constants fitted to experimental data.

Exp Date	Organism	Demand	Decay Rate
19-Jul-00	*G. muris*	0.199	0.270
21-Jul-00	*G. muris*	0.174	0.268
21-Jul-00	*G. muris*	0.088	0.537
23-Jul-00	*G. muris*	0.292	0.318
23-Jul-00	*G. muris*	0.257	0.213
29-Jul-00	*G. muris*	0.231	1.822
29-Jul-00	*G. muris*	0.379	0.720
11-Aug-00	*G. muris*	0.202	0.469
11-Aug-00	*G. muris*	0.343	0.206
12-Aug-00	*G. muris*	0.206	0.733
16-Aug-00	*G. muris*	0.218	0.342
19-Aug-00	*G. muris*	0.225	0.556
24-Aug-00	*G. muris*	0.201	0.556
7-Sep-00	*G. muris*	0.226	0.050
13-Sep-00	*G. muris*	0.369	0.354
15-Sep-00	*G. muris*	0.233	0.671
10-Sep-01	*B. subtilis* spores	0.480	0.081
10-Sep-01	*B. subtilis* spores	0.636	0.071
15-Sep-01	*B. subtilis* spores	1.372	0.171
15-Sep-01	*B. subtilis* spores	1.602	0.221
17-Sep-01	*B. subtilis* spores	1.089	0.234
17-Sep-01	*B. subtilis* spores	1.271	0.169
21-Sep-01	*B. subtilis* spores	0.915	0.092
21-Sep-01	*B. subtilis* spores	0.871	0.099
24-Sep-01	*B. subtilis* spores	0.911	0.184
24-Sep-01	*B. subtilis* spores	1.450	0.116
26-Oct-01	*B. subtilis* spores	0.818	0.131
26-Oct-01	*B. subtilis* spores	0.848	0.140
27-Oct-01	*B. subtilis* spores	0.656	0.145
27-Oct-01	*B. subtilis* spores	0.720	0.222
28-Oct-01	*B. subtilis* spores	0.834	0.257
28-Oct-01	*B. subtilis* spores	0.892	0.308
30-Oct-01	*B. subtilis* spores	1.219	0.118
30-Oct-01	*B. subtilis* spores	1.238	0.142
31-Oct-01	*B. subtilis* spores	0.871	0.113
31-Oct-01	*B. subtilis* spores	1.013	0.198
2-Nov-01	*B. subtilis* spores	0.637	0.128
2-Nov-01	*B. subtilis* spores	0.674	0.181
4-Nov-01	*B. subtilis* spores	0.664	0.131
4-Nov-01	*B. subtilis* spores	0.635	0.102

Table B.2: Monochloramine decay constants fitted to experimental data.

Exp Date	Organism	Decay Rate (minutes^{-1})
17-Dec-99	*E. coli* batch	1.86E-03
21-Dec-99	*E. coli* batch	8.91E-23
22-Dec-99	*E. coli batch*	2.23E-03
23-Dec-99	*E. coli* batch	8.91E-23
30-Dec-99	*E. coli* batch	6.41E-03
4-Jan-00	*E. coli* batch	1.02E-03
7-Jan-00	*E. coli* batch	2.71E-03
14-Jan-00	*E. coli* batch	8.91E-23
18-Jan-00	*E. coli* batch	8.91E-23
21-Jan-00	*E. coli* batch	8.91E-23
27-Jan-00	*E. coli* batch	8.91E-23
4-Feb-00	*E. coli* batch	8.91E-23
8-Feb-00	*E. coli* batch	4.08E-04
16-Feb-00	*E. coli* batch	5.65E-03
17-Feb-00	*E. coli* batch	5.12E-04
21-Feb-00	*E. coli* batch	2.54E-03
23-Feb-00	*E. coli* batch	8.91E-23
28-Feb-00	*E. coli* batch	7.67E-03
3-Mar-00	*E. coli* batch	4.40E-03
6-Mar-00	*E. coli* batch	8.91E-23
8-Mar-00	*E. coli* batch	4.02E-04
28-Jan-02	*E. coli* DMS	3.45E-04
4-Feb-02	*E. coli* DMS	4.15E-03
7-Feb-02	*E. coli* DMS	6.57E-04
12-Feb-02	*E. coli* DMS	2.20E-04
14-Feb-02	*E. coli* DMS	2.55E-03
15-Feb-02	*E. coli* DMS	7.58E-04
16-Feb-02	*E. coli* DMS	1.18E-03
5-Sep-02	*E. coli* DMS	2.66E-03
6-Sep-02	*E. coli* DMS	1.58E-03
11-Sep-02	*E. coli* DMS	6.20E-03
13-Sep-02	*E. coli* DMS	1.72E-03
15-Sep-02	*E. coli* DMS	2.76E-03
20-Mar-02	*E. coli* Log	1.47E-04
23-Mar-02	*E. coli* Log	1.64E-03
25-Mar-02	*E. coli* Log	7.85E-04
27-Mar-02	*E. coli* Log	1.52E-03
29-Mar-02	*E. coli* Log	8.86E-04
30-Mar-02	*E. coli* Log	1.52E-03
31-Mar-02	*E. coli* Log	3.08E-04
1-Apr-02	*E. coli* Log	2.55E-03
2-Apr-02	*E. coli* Log	6.17E-03
4-Apr-02	*E. coli* Log	2.10E-04
5-Apr-02	*E. coli* Log	1.57E-03
6-Apr-02	*E. coli* Log	3.20E-03

(continued)

Table B.2: (continued)

Exp Date	Organism	Decay Rate (minutes^{-1})
4-May-02	*B. subtilis* Log	5.23E-05
6-May-02	*B. subtilis* Log	1.64E-04
7-May-02	*B. subtilis* Log	1.31E-04
9-May-02	*B. subtilis* Log	3.56E-04
10-May-02	*B. subtilis* Log	5.81E-05
13-May-02	*B. subtilis* Log	2.88E-04
14-May-02	*B. subtilis* Log	5.39E-05
18-May-02	*B. subtilis* Log	1.43E-04
20-May-02	*B. subtilis* Log	5.61E-04
2-Aug-02	*E. coli* Chemostat	6.02E-04
3-Aug-02	*E. coli* Chemostat	1.75E-03
4-Aug-02	*E. coli* Chemostat	8.49E-04
6-Aug-02	*E. coli* Chemostat	3.13E-04
7-Aug-02	*E. coli* Chemostat	2.14E-04
8-Aug-02	*E. coli* Chemostat	1.72E-04
10-Aug-02	*E. coli* Chemostat	2.00E-04
11-Aug-02	*E. coli* Chemostat	1.06E-03
13-Aug-02	*E. coli* Chemostat	1.09E-03
14-Aug-02	*E. coli* Chemostat	7.28E-04
16-Aug-02	*E. coli* Chemostat	5.98E-04
17-Aug-02	*E. coli* Chemostat	1.10E-04

APPENDIX C: STATA 7™ OUTPUT OF STEPWISE REGRESSIONS

Table C.1: STATA 7™ output of stepwise regression of *G. muris* inactivation data.

```
                     begin with empty model
p = 0.0000 <  0.0500  adding   lnCT
p = 0.0005 <  0.0500  adding   Time

  Source |       SS       df       MS              Number of obs =      52
---------+------------------------------           F(  2,    49) =   30.96
   Model |  115.406744     2  57.7033721           Prob > F      =  0.0000
Residual |  91.3307476    49  1.86389281           R-squared     =  0.5582
---------+------------------------------           Adj R-squared =  0.5402
   Total |  206.737492    51  4.05367631           Root MSE      =  1.3652

------------------------------------------------------------------------------
   lnS |      Coef.   Std. Err.      t    P>|t|     [95% Conf. Interval]
-------+----------------------------------------------------------------
  lnCT |  -1.787748   .2362375    -7.57   0.000    -2.262485   -1.313011
  Time |   .9508017   .2569527     3.70   0.000      .434436    1.467167
 _cons |  -8.593843   .7990546   -10.76   0.000     -10.1996   -6.988083
------------------------------------------------------------------------------
```

Table C.2: STATA 7™ output of stepwise regression of *B. subtilis* inactivation data.

```
                     begin with empty model
p = 0.0000 <  0.0500  adding   CT
p = 0.0001 <  0.0500  adding   Time
p = 0.0179 <  0.0500  adding   Co

      Source |       SS       df       MS              Number of obs =     124
-------------+------------------------------           F(  3,   120) =  197.69
       Model |  1048.70512     3  349.568373           Prob > F      =  0.0000
    Residual |  212.188036   120  1.76823363           R-squared     =  0.8317
-------------+------------------------------           Adj R-squared =  0.8275
       Total |  1260.89315   123  10.2511638           Root MSE      =  1.3297

------------------------------------------------------------------------------
         lnS |      Coef.   Std. Err.      t    P>|t|     [95% Conf. Interval]
-------------+----------------------------------------------------------------
          CT |  -.9284106   .1605409    -5.78   0.000     -1.24627   -.6105509
        Time |  -.3894717   .0836425    -4.66   0.000     -.555078   -.2238654
          Co |  -1.635658   .6813925    -2.40   0.018    -2.984767   -.2865479
       _cons |   3.075749   .7254502     4.24   0.000     1.639408    4.51209
------------------------------------------------------------------------------
```

Table C.3: Original STATA 7™ outputs of survival data of vegetative cells of *B. subtilis* at exponential growth phase.

a. STATA 7™ output of stepwise regression of vegetative cells of *B. subtilis* at exponential growth phase inactivation data.

```
begin with empty model
p = 0.0000 <  0.0500  adding   lnCT
p = 0.0231 <  0.0500  adding   Co

      Source |       SS       df       MS              Number of obs =      89
-------------+------------------------------           F(  2,    86) =   61.56
       Model |  181.845303     2  90.9226516           Prob > F      =  0.0000
    Residual |  127.024437    86  1.47702833           R-squared     =  0.5887
-------------+------------------------------           Adj R-squared =  0.5792
       Total |   308.86974    88  3.50988341           Root MSE      =  1.2153

------------------------------------------------------------------------------
         lnS |      Coef.   Std. Err.      t    P>|t|     [95% Conf. Interval]
-------------+----------------------------------------------------------------
        lnCT |   -1.93256   .1758278   -10.99   0.000    -2.282094   -1.583026
          Co |   1.012504   .4378005     2.31   0.023     .1421851    1.882822
       _cons |   .4522168   .6410904     0.71   0.482    -.8222288    1.726662
------------------------------------------------------------------------------
```

b. STATA 7™ output of MLR without constant.

```
      Source |       SS       df       MS              Number of obs =      89
-------------+------------------------------           F(  2,    87) =  420.07
       Model |  1233.74262     2   616.87131           Prob > F      =  0.0000
    Residual |  127.759363    87  1.46849842           R-squared     =  0.9062
-------------+------------------------------           Adj R-squared =  0.9040
       Total |  1361.50198    89  15.2977751           Root MSE      =  1.2118

------------------------------------------------------------------------------
         lns |      Coef.   Std. Err.      t    P>|t|     [95% Conf. Interval]
-------------+----------------------------------------------------------------
          Co |   1.222736   .3197638     3.82   0.000     .5871706    1.858301
        lnCT |   -1.85155   .1327534   -13.95   0.000    -2.115411   -1.587688
------------------------------------------------------------------------------
```

(continued)

Table C.3: (continued)

c. STATA 7™ output of stepwise regression of vegetative cells of *B. subtilis* at exponential growth phase inactivation data without outliers.

```
      begin with empty model
p = 0.0000 <  0.0500  adding   lnCT
p = 0.0090 <  0.0500  adding   time
p = 0.0094 <  0.0500  adding   ct

  Source |       SS       df       MS              Number of obs =      84
---------+------------------------------           F(  3,    80) =   97.85
   Model |  204.668772     3  68.2229241           Prob > F      =  0.0000
Residual |  55.7765584    80   .69720698           R-squared     =  0.7858
---------+------------------------------           Adj R-squared =  0.7778
   Total |  260.445331    83  3.13789555           Root MSE      =  .83499

------------------------------------------------------------------------------
       lns |      Coef.   Std. Err.      t    P>|t|     [95% Conf. Interval]
-----------+------------------------------------------------------------------
      lnCT |  -2.318694   .3982961    -5.82   0.000    -3.111329    -1.52606
      time |  -.0648759   .0173228    -3.75   0.000    -.0993493   -.0304025
        ct |   .0804722   .0302276     2.66   0.009     .0203174     .140627
     _cons |   2.474385   .6310398     3.92   0.000     1.218575    3.730194
------------------------------------------------------------------------------
```

Table C.4: STATA 7™ output of stepwise regression of batch cultures of *E. coli* inactivation data.

```
                     begin with empty model
p = 0.0000 <  0.0500  adding   CT
p = 0.0000 <  0.0500  adding   LnNo
p = 0.0241 <  0.0500  adding   lnCT

      Source |       SS       df       MS              Number of obs =      98
-------------+------------------------------           F(  3,    94) =   83.39
       Model |   772.21006     3  257.403353           Prob > F      =  0.0000
    Residual |  290.137171    94  3.08656565           R-squared     =  0.7269
-------------+------------------------------           Adj R-squared =  0.7182
       Total |  1062.34723    97  10.9520333           Root MSE      =  1.7569

------------------------------------------------------------------------------
         lns |      Coef.   Std. Err.      t    P>|t|     [95% Conf. Interval]
-------------+----------------------------------------------------------------
          CT |    -1.8085   .2934168    -6.16   0.000    -2.391086   -1.225914
        LnNo |   -.506256   .1146287    -4.42   0.000     -.733854    -.278658
        lnCT |   2.868479   1.251614     2.29   0.024     .3833706    5.353588
       _cons |   6.152156   1.245524     4.94   0.000      3.67914    8.625173
------------------------------------------------------------------------------
```

Table C.5: STATA 7™ output of stepwise regression of *E. coli* at exponential growth phase inactivation data.

```
                     begin with empty model
p = 0.0000 <  0.0500  adding   CT
p = 0.0004 <  0.0500  adding   lnCT

      Source |       SS       df       MS              Number of obs =     106
-------------+------------------------------           F(  2,   103) =  101.79
       Model |  482.831099     2  241.415549           Prob > F      =  0.0000
    Residual |  244.288195   103  2.37173005           R-squared     =  0.6640
-------------+------------------------------           Adj R-squared =  0.6575
       Total |  727.119294   105  6.92494566           Root MSE      =    1.54

------------------------------------------------------------------------------
         lns |      Coef.   Std. Err.      t    P>|t|     [95% Conf. Interval]
-------------+----------------------------------------------------------------
          CT |  -3.368061   .5065311    -6.65   0.000    -4.372646   -2.363475
        lnCT |     5.5364   1.498019     3.70   0.000     2.565432    8.507368
       _cons |   2.716801   .4095766     6.63   0.000     1.904502    3.529099
------------------------------------------------------------------------------
```

Table C.6: STATA 7™ output of stepwise regression of continuous cultures of *E. coli* inactivation data.

```
                     begin with empty model
p = 0.0000 <  0.0500  adding   CT
p = 0.0073 <  0.0500  adding   Co
p = 0.0033 <  0.0500  adding   lnCT
p = 0.0226 <  0.0500  adding   No

      Source |       SS       df       MS              Number of obs =      92
-------------+------------------------------           F(  4,    87) =  126.68
       Model |  763.574667     4  190.893667           Prob > F      =  0.0000
    Residual |  131.097189    87  1.50686425           R-squared     =  0.8535
-------------+------------------------------           Adj R-squared =  0.8467
       Total |  894.671856    91  9.83155886           Root MSE      =  1.2275

------------------------------------------------------------------------------
         lnS |      Coef.   Std. Err.      t    P>|t|     [95% Conf. Interval]
-------------+----------------------------------------------------------------
          CT |  -2.024963   .2584063    -7.84   0.000    -2.538573   -1.511353
          Ca |  -1.560672   .4589124    -3.40   0.001     -2.47281   -.6485336
        lnCT |   2.917124   1.019521     2.86   0.005     .8907158    4.943532
          No |  -6.47e-06   2.79e-06    -2.32   0.023     -.000012   -9.28e-07
       _cons |   2.753049   .5932354     4.64   0.000      1.57393    3.932169
------------------------------------------------------------------------------
```

Table C.7: STATA 7™ output of stepwise regression of *E. coli* DMS inactivation data.

```
                     begin with empty model
p = 0.0000 <  0.0500  adding   ct
p = 0.0479 <  0.0500  adding   LnNo
p = 0.0144 <  0.0500  adding   No
p = 0.0101 <  0.0500  adding   Ln3No

      Source |       SS       df       MS              Number of obs =      96
-------------+------------------------------           F(  4,    91) =   17.23
       Model |  231.008861     4  57.7522153           Prob > F      =  0.0000
    Residual |  304.967813    91  3.35129464           R-squared     =  0.4310
-------------+------------------------------           Adj R-squared =  0.4060
       Total |  535.976674    95  5.64185973           Root MSE      =  1.8307

------------------------------------------------------------------------------
         lnS |      Coef.   Std. Err.      t    P>|t|     [95% Conf. Interval]
-------------+----------------------------------------------------------------
          CT |  -.6515395   .0976909    -6.67   0.000    -.8455905   -.4574884
        LnNo |   -8.44915   3.539042    -2.39   0.019    -15.47902   -1.419277
          No |  -.0001522   .0000515    -2.96   0.004    -.0002546   -.0000499
       Ln3No |   .0475057   .0180802     2.63   0.010     .0115917    .0834198
       _cons |   42.68778   18.72818     2.28   0.025     5.486556      79.889
------------------------------------------------------------------------------
```

Table C.8: STATA 7™ output of stepwise regression of *E. coli* DMS control inactivation data.

```
                     begin with empty model
p = 0.0000 <  0.0500  adding   CT

      Source |       SS       df       MS              Number of obs =      46
-------------+------------------------------           F(  1,    44) =   64.92
       Model |  185.021526     1  185.021526           Prob > F      =  0.0000
    Residual |  125.393313    44  2.84984803           R-squared     =  0.5960
-------------+------------------------------           Adj R-squared =  0.5869
       Total |  310.414839    45  6.89810754           Root MSE      =  1.6881

------------------------------------------------------------------------------
         lnS |      Coef.   Std. Err.      t    P>|t|     [95% Conf. Interval]
-------------+----------------------------------------------------------------
          CT |  -.9573994   .1188209    -8.06   0.000    -1.196867   -.7179316
       _cons |   1.837306   .6050968     3.04   0.004     .6178133    3.056798
------------------------------------------------------------------------------
```

APPENDIX D: MODEL DERIVATIONS

Derivation of Multiple-target Model

Binomial probability of zero gives q/q_c, where, q is the concentration of targets surviving attack (#/mL) and q_c is the critical (total) number of targets (#/mL).

P(0) : Probability of a specific target surviving attack, q/q_c

1-P(0) : Probability of inactivating a specific target

Each particle has n_c critical targets

$[1-P(0)]^{n_c}$ is the probability of a particle to survive

$1-[1-P(0)]^{n_c}$ is the probability of a inactivating a particle

$$\frac{N}{N_0} = 1-[1-P(0)]^{n_c}$$

$$\frac{dq}{dt} = -kCq$$

Under first order decay of disinfectant and instantaneous demand conditions;

$$C = (C_a - D)e^{-k^*t}$$

where C_a is the applied disinfectant dose (mg/L), D is the instantaneous disinfectant demand (mg/L) and k^* is the first order disinfectant decay rate ($time^{-1}$).

$$\int_{qc}^{q} \frac{dq}{q} = \int_{t=0}^{t} -k(C_a - D)e^{-k^*t}dt$$

$$\ln\left(\frac{q}{q_c}\right) = \frac{-k(C_a - D)}{-k^*}\left(e^{-k^*t} - 1\right)$$

$$\frac{q}{q_c} = Exp\left[\frac{k(C_a - D)}{k^*}\left(e^{-k^*t} - 1\right)\right] = P(0)$$

$$\frac{N}{N_0} = 1 - [1 - P(0)]^{n_c} = 1 - \left[1 - \left(Exp\left[\frac{k(C_a - D)}{k^*} \left(e^{-k^* t} - 1 \right) \right] \right) \right]^{n_c}$$

$$\ln \frac{N}{N_0} = \ln \left\{ 1 - \left[1 - \left(Exp\left[\frac{k(C_a - D)}{k^*} \left(e^{-k^* t} - 1 \right) \right] \right) \right]^{n_c} \right\}$$

Derivation of Modified Multiple-target Model

Binomial probability of zero gives q/q_c, where, q is the concentration of targets surviving attack (#/mL) and q_c is the critical (total) number of targets (#/mL).

P(0) : Probability of a specific target surviving attack, q/q_c

1-P(0) : Probability of inactivating a specific target

Each particle has n_c critical targets

$[1 - P(0)]^{n_c}$ is the probability of a particle to survive

$1 - [1 - P(0)]^{n_c}$ is the probability of a inactivating a particle

$$\frac{N}{N_0} = 1 - [1 - P(0)]^{n_c}$$

In Modified Multiple-target the rate of inactivation of targets has non-first order dependency of disinfectant concentration.

$$\frac{dq}{dt} = -kC^n q$$

Under first order decay of disinfectant and instantaneous demand conditions;

$$C = (C_a - D)e^{-k^* t}$$

where C_a is the applied disinfectant dose (mg/L), D is the instantaneous disinfectant demand (mg/L) and k^* is the first order disinfectant decay rate ($time^{-1}$).

$$\int_{qc}^{q} \frac{dq}{q} = \int_{t=0}^{t} -k(C_a - D)^n e^{-nk*t} dt$$

$$\ln\left(\frac{q}{q_c}\right) = \frac{-k(C_a - D)^n}{-nk*}\left(e^{-nk*t} - 1\right)$$

$$\frac{q}{q_c} = Exp\left[\frac{k(C_a - D)^n}{nk*}\left(e^{-nk*t} - 1\right)\right] = P(0)$$

$$\frac{N}{N_0} = 1 - \left[1 - P(0)\right]^{n_c} = 1 - \left[1 - \left(Exp\left[\frac{k(C_a - D)^n}{nk*}\left(e^{-nk*t} - 1\right)\right]\right)\right]^{n_c}$$

$$\ln\frac{N}{N_0} = \ln\left\{1 - \left[1 - \left(Exp\left[\frac{k(C_a - D)^n}{nk*}\left(e^{-nk*t} - 1\right)\right]\right)\right]^{n_c}\right\}$$

APPENDIX E: NOMENCLATURE

ANOVA	Analysis Of Variance
ASF	Aerobic Spore Formers
C_0	Initial Disinfectant Concentration
C_a	Applied Disinfectant Dose
CFU	Colony Forming Unit
Chick	Chick Model
CI	Confidence Interval
CSF	Competence and Sporulation Factor
CT	Product Of Concentration And Contact Time
CW	Chick-Watson Model
D	Instantaneous Disinfectant Demand
DBPR	Disinfection/Disinfectant By-product Rule
DBPs	Disinfection/Disinfectant By-products
df	Degrees of Freedom
DMS	Disinfected Microorganism Suspension
DNA	Deoxyribonucleic Acids
EPA	Environmental Protection Agency
GWUDI	Groundwater Under Direct Influence
Hom	Hom Model
HPC	Heterotrophic Plate Count
HPL	Hom Power Law
HSL	Homoserine Lactones
IESWTR	Interim Enhanced Surface Water Treatment Rule
LL	Lower Limit
LPS	Lipopolysaccharide
MCLG	Maximum Contaminant Level Goal
MLR	Multiple Linear Regression
MMT	Modified Multiple-target Model
Monochl.	Monochloramine
MS	Mean Square
MSE	Mean Square Error
MT	Multiple-target Model
N_0	Initial Microbial Density
NADC	National Animal Disease Center
OD_{660}	Optical Density at 660 nm
OLR	Ordinary Least squares Regression
PBS	Phosphate Buffered Solution
PL	Power Law
PWS	Public Water System
r_d	Rate of Disinfection
RNA	Ribonucleic Acids
RSS	Residual Sum of Squares
S	Survival Ratio
SDS	Sodium Dodecyl Sulfate
SDWA	Safe Drinking Water Act
SE	Series Event Model

SS	Sum of Squares
SWTR	Surface Water Treatment Rule
THM	Trihalomethane
Trop.	Trophozoites
TSB	Trypticase Soy Broth
TSS	Total Sum of Squares
u.v.	Ultra Violet radiation
UL	Upper Limit

VITA

Vita	Barış Kaymak
	Birth Date: April 16, 1976
	Birth Place: Afyon, Turkey
Education	B.Sc. Environmental Engineering, Middle East Technical University, Ankara, Turkey
Professional Experience	Graduate Research Assistant, 1999 – 2003, Drexel Universtiy, Philadelphia, PA USA
Professional Affiliations	American Water Works Association, 2000 - Present